Dissertation

Controls on progressive rock failure:

environmental conditions, subcritical mechanisms and rock stress memory

Anne Voigtländer

TECHNISCHE UNIVERSITÄT MÜNCHEN
Ingenieurfakultät Bau Geo Umwelt
Professur für Hangbewegungen

Controls on progressive rock failure: environmental conditions, subcritical mechanisms and rock stress memory

Anne Voigtländer

Vollständiger Abdruck der von der Ingenieurfakultät Bau Geo Umwelt der Technischen Universität München zur Erlangung des akademischen Grades eines

Doktors der Naturwissenschaften (Dr. rer. nat.)

genehmigten Dissertation.

Vorsitzender:	Prof. Dr. Kurosch Thuro
Prüfer der Dissertation:	1. Prof. Dr. Michael Krautblatter
	2. Prof. Dr. Andreas Lang
	3. Prof. Dr. Martin Elsner

Die Dissertation wurde am 16.07.2020 bei der Technischen Universität München eingereicht und durch die Ingenieurfakultät Bau Geo Umwelt am 12.10.2020 angenommen.

Preface

With this thesis, I want to communicate two main points:

First, in all disciplines working with rocks, from rock physics, geology, engineering geology, geomorphology to physical chemistry, we need to account for the geological past, former stress fields and conditions of the geomaterial. These considerations affect the rock's present state and future behaviour.

Throughout this thesis, I will demonstrate how we can assess the memory state of rocks by using residual elastic strain. Locked-in elastic strains are a promising proxy to further infer the material state and its susceptibility to failure and the (re)distribution of elastic strains in rheology.

Secondly, we need an integrative perspective of processes and mechanisms that contribute to the deterioration of rocks. A holistic approach to these questions can present several challenges in the context of scientific research, but being open and aware of how something is seen from a different perspective might yield new insides and reactions.

One of them, for example, is applying a load to rocks. In geosciences, stressing a rock is often minimized to breaking rocks, but from engineering and architecture, we know it can also strengthen the material.

The aim of this thesis is to ask the question of how rocks break.

I investigated coupled mechanical and chemical processes at the Solid Earth's interface with the atmosphere, which affect progressive rock failure. This work is put in the context of geomorphology and progressive rock slope instabilities but is also relevant to other research areas such as material sciences, engineering geology and rock physics. The research, especially on subcritical crack growth mechanisms is at the cross-section between physics, geology and physical chemistry. The methods used include theory and laboratory experiments. Coming from primarily a geomorphological/structural geology background, I feel very lucky to have had the opportunity to expand my knowledge in these different fields.

In geological and geomorphological studies, we are faced with the end result of millions of years of coupled processes which have taken place under largely unknown conditions. Laboratory studies offer a chance to study isolated processes under controlled conditions. Theoretical studies allow us to explore the consequences of what we know, and of what we think we know, in beautiful, simple geometries with well-defined boundary conditions. I think that to fully understand how the Earth works, it is necessary to combine these and other approaches.

I have had three excellent supervisors who have helped me out through the process of conducting my doctoral research. I would like to thank Michael Krautblatter in particular, for accepting me into his newly formed landslide research group and giving me the freedom to explore and define my own field of research within the group. My unofficial principal supervisor has been Kerry Leith. He has also been a great co-worker in my laboratory studies. I would like to thank Andreas Lang for his encouragements to stay true to myself and my developing expertise and to complete this thesis.

Moreover, Jens Turowski has been an excellent mentor and provided invaluable theoretical support.

There are some other people without whom my lab activities would have been much more challenging. Matthias Graf and Christian Ihns from the TH Cologne have very patiently helped me with large and small practical issues and have dealt with my frequent frustrations over things not working. Big thanks also go to Rebecca Kühn, Thilo Pirling, and the other guys at the workshop who have made my clumsy constructions become working equipment. Lab work would also have been much more frustrating and less fun without the good company and enormous amount of help I've received from my fellow TUM landslide group members, including Sibylle Knapp and Riccardo Scandroglio. Then there are some people at the TUM, TH Cologne, KIT, Museum König Bonn who know "everything" can test "everything" and are always willing to take the time to share their wisdom. I would particularly like to thank Kurosch Thuro, Axel Dominik, Frank Schilling, and Christian Scheffzük for everything they have taught me. I am grateful for a BMBF scholarship of the Rosa-Luxemburg Foundation.

Thanks to past and present office- and flatmates: Nils, Johanna, Lizzie, Audrey, Djamil, Nima, Jens, Gunnar, Hannah and all you other GFZns. Thanks for providing an exciting research environment while I was writing and finishing my thesis, you are a fantastic bunch of talented and friendly people.

I would also like to acknowledge the support from friends and family outside of work. You're such great people, and just the fact that you're reading this means you are actually making an effort to understand my project. In particular, I want to thank 'my family' members Lena Voigtländer, Nils Hein, Lisa Voigtländer, Inki and Erich Schulte, Leoni Willnow, Gregor Weckbecker, Lina Franken and of course 'Papa'.

I want to dedicate this thesis to my grandmother Ingeborg Nissel. She always has and still does, nurture, support and question my curiosity about how the world works and maybe also sometimes break apart. She has challenged me throughout the years of this dissertation to explain my research and findings in plain language to her, so she too could expand her knowledge on how rocks break.

Potsdam, July 2020

Anne Voigtländer

Content

Figures and Tables

Abstract

How do rocks break? What makes them strong? What weakens them over time? What causes rock failure? These questions are at the core of basic and applied geoscientific research, yet our knowledge of progressive rock failure is finite. Improved knowledge on controls of progressive failure is necessary to accurately anticipate rock slope hazards or take steps to enhance infrastructure lifetimes and preserve artistic sculptures.

Nested within concepts of progressive rock failure is the notion of time. Past and present endogenic processes, which are encrypted in rock, precondition its future evolution. Rock at the surface and near-surface of Earth is affected by environmental conditions and the stresses that these conditions exert over geologic times. These external forces and conditions can deform and progressively fracture rock to different extents and rates, depending on its internal state, which is concomitantly modified by damage mechanisms.

In this thesis, I use a combination of theory and laboratory experiments to investigate progressive rock failure in geomorphological context. Specifically, I explore external and internal controls of progressive rock failure, focussing on environmental conditions and related stresses, subcritical crack growth mechanisms and inherited and conditioned rock stresses, via residual elastic strains. Due to the significance and pervasive nature of progressive rock failure in many disciplines, from engineering to structural geology, multiple concepts, models and methods coexist. I carefully selected and combined methods and approaches from rock physics, physical chemistry, material sciences, geology and geomorphology to synthesise and enhance our knowledge of progressive rock failure.

Based on these considerations, I designed two experiments which allowed me to assess how environmental conditions, subcritical mechanisms and rock stress memory affects progressive rock failure. In order to isolate the controls of progressive rock failure, Carrara marble, a near pure calcite homogeneous and isotropic metamorphic rock was used in all experiments. The simplicity and defined properties of this marble make it an ideal reference rock type for these experiments. First, I adapted standard laboratory experiments for rock mechanics to test long-term creep deformation such as subcritical crack growth and environmentally enhanced stress corrosion cracking and wet rheology. Second, I measured residual elastic strains within the Carrara marble samples with neutron diffraction, a novel approach within geomaterials, derived from engineering material science. This method enables the assessment of the internal elastic and inherited strain states of the rock, and thus the identification of the internal controls of the Carrara marble, instead of only inferring the internal rock state through the response of the rock to external stresses and conditions. The obtained insights on the environmentally altered internal states and the rock stress memory provide means to identify mechanisms and conditions which promote progressive rock failure.

The results of inverted single edge-notch bending long-term creep experiments on Carrara marble are published in:

Voigtländer, A., Leith, K., & Krautblatter, M. (2018). *Subcritical crack growth and progressive failure in Carrara marble under wet and dry conditions*. In the Journal of Geophysical Research: Solid Earth, 123, 3780–3798. https://doi.org/10.1029/2017JB014956.

Internal elastic strain states of intact and chemo-mechanically pretested Carrara marble have been assessed with neutron diffraction. The results and discussion are published in:

Voigtländer, A., Leith, K., Walter, J. M., & Krautblatter, M. (2020). *Constraining internal states in progressive rock failure of Carrara marble by measuring residual strains with neutron diffraction.* In Journal of Geophysical Research: Solid Earth, 125, e2020JB019917. https://doi.org/10.1029/2020JB019917

The result highlight the importance of (i) the preconditioning of rocks, (ii) chemo-mechanical composite fracturing mechanisms, and (iii) the mechanical effect of internal and external conditions. With this multidisciplinary approach, knowledge of progressive rock failure controls could be further extended. Based on the insights from the experiments, I developed a new theoretical framework about 'How rocks break?', and what controls progressive rock failure in a geomorphological context. The resulting paper comprises the experimental and theoretical studies of this thesis and is published in the ESEX Commentary series as

Voigtländer, A., & Krautblatter, M. (2019). *Breaking rocks made easy. Blending stress control concepts to advance geomorphology.* In the journal Earth Surface Processes and Landforms, 44(1), 381–388. https://doi.org/10.1002/esp.4506

By providing new insights, novel methodological approaches and a conceptual framework of progressive rock failure, this thesis contributes to ongoing efforts to understand and anticipate progressive rock failure in real-world settings, a challenge at the frontier of geoscience, geohazard and socioeconomic research.

Zusammenfassung

Wie brechen Steine? Was macht sie stark? Was schwächt sie im Laufe der Zeit? Was verursacht Felsversagen? Diese Fragen bilden den Kern geowissenschaftlichen Grundlagenforschung und angewandter Studien. Wenn wir das Versagen von Felshängen antizipieren, die Leistungsfähigkeit und Lebensdauer von Infrastrukturen verbessern und steinerne Kunst- und Kulturgegenstände erhalten möchten, müssen wir das progressive Versagen von Gestein besser verstehen. Aufgrund der Bedeutung des zeitabhängigen Versagens in vielen Disziplinen existieren mehrere Konzepte, Modelle und spezifische Methoden nebeneinander. Um unser Wissen über progressivem Versagen im geowissenschaftlichen Kontext zu erweitern, habe ich Methoden und Konzepte aus der Felsmechanik, den Materialwissenschaften und der Geomorphologie kombiniert.

Dem Konzept des progressiven Gesteinsversagens ist der Zeitbegriff eingeschrieben. Vergangene und gegenwärtige Zustände, die im Gestein verschlüsselt sind, bestimmen seine zukünftige Entwicklung. Gesteine an oder nahe der Erdoberfläche sind Umweltbedingungen ausgesetzt. Diese Umgebungsbedingungen und durch sie erzeugte Spannungen formen und verändern Gesteine im Laufe der Zeit. Diese Veränderungen wirken sich auf den Zustand des Gesteins, seine Rheologie und sein fortschreitendes Versagen aus.

In dieser Arbeit untersuche ich externe und interne Kontrollen des progressiven Gesteinsversagens. Dabei setzt sie einen Schwerpunkt auf Umweltbedingungen und damit verbundenen Spannungen, subkritische Risswachstumsmechanismen und inhärente und konditionierte elastische Restspannungen im Gestein. Die im Rahmen dieser Arbeit durchgeführten Studien bauen auf einer Kombination aus Theorie- und Laborexperimenten auf, um das fortschreitende Gesteinsversagen im geomorphologischen Kontext zu untersuchen. Aufgrund der Bedeutung und Verbreitung des fortschreitenden Gesteinsversagens in vielen Disziplinen, vom Ingenieurwesen bis zur Strukturgeologie, existieren mehrere Konzepte, Modelle und Methoden nebeneinander. Ich habe Methoden sorgfältig ausgewählt und Ansätze aus Felsmechanik, physikalischer Chemie, Materialwissenschaften, Geologie und Geomorphologie kombiniert um unser Wissen über progressives Gesteinsversagen zu erweitern.

Basierend auf diesen Überlegungen habe ich zwei Laborexperimente entworfen, um zu erforschen, wie sich Umweltbedingungen, subkritische Mechanismen und das Gesteinsstressgedächtnis auf das fortschreitende Gesteinsversagen auswirken. Um die Kontrolle des fortschreitenden Gesteinsversagens zu isolieren, wurde in allen Experimenten Carrara-Marmor verwendet, ein homogenes, isotropes, metamorphes und nahezu reines Calcit-haltiges Gestein. Die Einfachheit und die definierten Eigenschaften dieses Marmors machen ihn zu einem idealen Referenzgesteinstyp für diese Experimente.

Zunächst wurden Standardlaborexperimente für die Gesteinsmechanik angepasst, um langfristige Kriechverformungen wie subkritisches Risswachstum, Umwelt verstärkte Spannungskorrosion und Rheologie zu testen. Zweitens, anstatt auf den inneren Gesteinszustand durch die Reaktion des Gesteins auf äußere Spannungen und Bedingungen zu schließen, wurden Neutronenbeugungstechniken, ein immer noch neuartiger Ansatz in Geomaterialien, eingesetzt. Diese materialwissenschaftliche Methode ermöglicht die Beurteilung der inneren elastischen und vererbten Dehnungszustände des Gesteins und damit die Identifizierung der inneren Kontrollen des Carrara-Marmors. Mittels Kenntnis

umweltveränderter innerer Zustände konnten Mechanismen und Bedingungen, die ein fortschreitendes Gesteinsversagen fördern, identifiziert werden.

Die Ergebnisse der langzeitlichen invertierten Biegezugexperimente an Carrara Marmor sind veröffentlicht in:

Voigtländer, A., Leith, K., & Krautblatter, M. (2018). *Subcritical crack growth and progressive failure in Carrara marble under wet and dry conditions*. In the Journal of Geophysical Research: Solid Earth, 123, 3780–3798. https://doi.org/10.1029/2017JB014956.

Die internen elastischen Dehnungszustände von intaktem und chemo-mechanisch vorgetestetem Carrara Marmor wurden mit Neutronenbeugung untersucht. Die Ergebnisse und die Diskussion sind publiziert in:

Voigtländer, A., Leith, K., Walter, J. M., & Krautblatter, M. (2020). *Constraining internal states in progressive rock failure of Carrara marble by measuring residual strains with neutron diffraction.* In Journal of Geophysical Research: Solid Earth, 125, e2020JB019917. https://doi.org/10.1029/2020JB019917

Die Ergebnisse dieser Experimente unterstreichen die Bedeutung von (i) der Vorkonditionierung von Gesteinen, (ii) chemo-mechanischen Bruchmechanismen und (iii) der mechanischen Wirkung innerer und äußerer Bedingungen. Mit diesem multidisziplinären Ansatz konnte das Wissen über Kontrollen progressive Gesteinsversagens weiter ausgebaut werden. Diese Ergebnisse sind anschließend in die theoretische Studie darüber was das fortschreitende Versagen von Gesteinen in einem geomorphologischen Kontext kontrolliert, eingegangen. Die Überlegungen und konzeptionellen Anregungen aus den experimentellen und theoretischen Studien dieser Arbeit, sind in der ESEX Commentary-Reihe veröffentlicht:

Voigtländer, A., & Krautblatter, M. (2019). *Breaking rocks made easy. Blending stress control concepts to advance geomorphology*. In the journal Earth Surface Processes and Landforms, 44(1), 381–388. https://doi.org/10.1002/esp.4506

Durch die Bereitstellung neuer Erkenntnisse, neuartiger methodischer Ansätze und eines konzeptionellen Rahmens für progressives Gesteinsversagen trägt diese Arbeit dazu bei, progressives Gesteinsversagen in realen Umgebungen zu verstehen und zu antizipieren, eine Herausforderung an geowissenschaftlichen, Naturgefahren und sozioökonomischen Forschungsgrenzen.

1. Introduction

Rocks are the foundation of the Earth. They support and form persistent topography and contribute to both natural and human structures. We carve and shape rocks into long-lived artworks and reliable infrastructure networks. Rocks are quintessentially conceived as resistant and durable.

Rocks are also dissected by fractures on all scales. Hiking in mountains, fractures in bedrock can be observed on all slopes in all blocks, boulders and pebbles. Once queued into observing fractures one will start seeing them everywhere, in infrastructures, in art, and in food (Figure 1.1). Given that they are so pervasive, what do fractures tell us? Are they important? Where do they come from? Do they progress or are at arrest? Why did they form at this location?

In geosciences, our interest in rock fractures commonly relates to stability, especially rock slope instabilities. Important questions remain over whether fractures are structurally important and if they are simply surficial features. What caused the rock to break? Going beyond the status of the rocks, we still want to know more about what happens to these fractures. What controls fracture propagation? How concerned should we be about the rock's integrity and structure in the future? Which factors predict rock failure? Or does it fail without an obvious or incipient trigger event and pose a great danger? What efforts need to be made to ensure that the rocky structure will remain stable? Can it be fixed, anchored or restored?

To predict the timing and extent of a rock slope instability, for example, we need to know how and why rocks break. A better understanding of progressive rock failure can help anticipate potential geohazards, infrastructure collapse or preservation of objects of art.

Central to these questions is a notion of time, which has often been overlooked. Fractures and all natural and man-made systems containing them are sensitive to time. They are dynamic rather than static and change progressively both in meaning and behaviour. A fractured rock slope that has been stable can become unstable by an increment of crack growth. A small fracture in a rock can grow slowly and as it growth accelerates until it ruptures. In some cases, rock failure seems imminent, and in others, it stays in a stable state for a long time. So even though cracks, joints and discontinuities are present, they do not necessarily seem to propagate and fail in the time span we observe them. At what point in time does a rock fail? Is it when we see fractures, detect damage or all is in pieces?

Despite its importance for anticipating geohazards, progressive rock failure is one of the least understood processes in geosciences (Bjerrum & Jørstad, 1968; Krautblatter & Moore, 2014; Ventura et al., 2010). We still do not understand the controls of transient deformation of rocks that lead to dynamic rupture. The objective of my thesis is to determine the controls and enhance the theory of progressive rock failure in geomorphology.

The phenomenon of fracture and damage evolution within rock has been termed 'progressive rock failure'. Progressive rock failure is defined as an increase in the extent of microscopic damage over time that eventually leads to failure on the macroscopic scale (Atkinson, 1987; Jaeger et al., 2007; Lawn, 1993). Progressive rock failure is a widespread phenomenon and is of broad interest to the disciplines of rock physics, geology, geomorphology, physical chemistry, and material sciences (Brantut et al., 2013; Diederichs, 2003b; Eppes & Keanini, 2017; Withers, 2015).

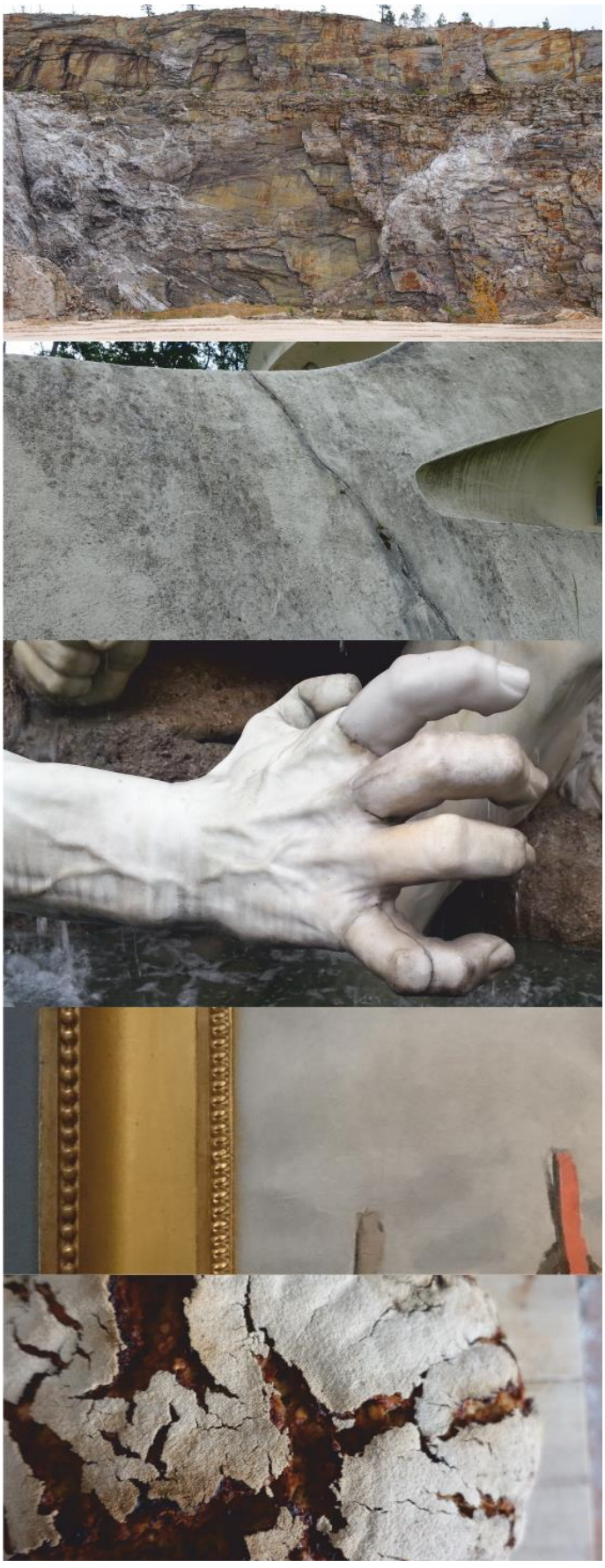

Figure 1.1 Fractures in a quartzite quarry, in concrete structures of the Einsteinturm, in sculptures of a fountain, in an oil painting and in home-made bread

In this thesis, I investigated 'How rocks break' in a geomorphological context. The spatial and temporal scale and potential controls of progressive rock failure addressed in this thesis depend on this perspective.

Exploring progressive rock failure in a geomorphological context supposes that,

- processes act over geologic time scales,
- and (inter)operate at all spatial scales,
- the Earth surface interfacing the atmosphere is subject to environmental conditions and stresses also called external or exogenic,
- material properties are inherited and conditioned by their path to or near the surface of the Earth, thus by internal or endogenic processes,
- mechanisms are likely coupled and involve feedback relations.

The geomorphological context is not exclusive and the findings of this thesis relevant to other research areas such as material science, rock physics and engineering. Time and spatial scales vary with the respective focus area in geomorphology, ranging from laboratory experiments running for days to months, in hazard anticipation of a local mountain slope failure from years to over decades, and finally to the long-term geologic evolution of landscapes (Church, 2010).

Environmental conditions at the Earth surface are ambient and, being at the interface of atmosphere and hydrosphere, predominantly wet or at least moist (Viles, 2013). The environmental forcing, as a result of fluctuations and gradients of these conditions, is commonly high in frequency and low in magnitude. Environmental conditions can facilitate both physical and chemical alteration of rocks.

The material properties, particularly rock strength, are key in progressive rock failure. Perhaps more poetically phrased by Gilbert (1877:99): "All indurated rocks and most earths are bound together by a force of cohesion which must be overcome before they can be divided and removed". Therefore, long-term strength of rocks can be seen as the inverse of progressive rock failure. Rock stress memory partly constitutes these properties. Theses inherited and internal states of rocks have been described by Emery (1964:244) as "[…] any rock, because it is a rock, must have in it more or less conserved elastic strain energy and that its present condition is a transient one and represents the sum of all that has happened to the rock". This quote refers to residual elastic strains which are induced by stressing or tempering the rocks and remain even when the traction is removed. The residual elastic strain state represents thus the encrypted past stress states in the material properties. Within the rock fabric, these locked-in elastic strain energy conceptually constitute not only an internal condition but also affects the rheology (Friedman, 1972; Holzhausen & Johnson, 1979).

Over geologic times, rocks are not only exposed to endogenic but also exogenic stresses and condition. Voight (1966:56), already including environmental conditions and geomorphic processes and characterised the stress states in rocks, as a "[…] function of rock properties, age, tectonic history, amount and degree of erosion, topography, and local boundary conditions".

Progressive rock failure is the deterioration of rock due to creep or fatigue mechanisms (Brantut et al., 2012, 2013). Creep is facilitated by subcritical crack growth, microplasticity and can be environmentally enhanced by chemical activity (Atkinson, 1984; Jaeger et al., 2007). Progressive fracturing altogether leads to the degradation of the elastic material properties

(Resende & Martin, 1984). This is expressed in terms of internal inelastic and elastic variables, defining the progressive damage state.

Progression or change of damage in rock is detected in reference to another or an initial state. In order to predict the behaviour of the rock, we need to know its internal, structural and characteristics state and how it will respond to changes in boundary conditions or simply over time. Creep is usually observed in a time-dependent framework, while subcritical mechanisms have been tested in reference to differences in environmental conditions and stress level (Atkinson, 1987; Brantut et al., 2013; Eppes & Keanini, 2017, and references within).

In a seminal publication, Bjerrum & Jørstad (1968) evaluated which factors control the progressive damage of rocks based on field observations of rock slope instabilities in Norway, and theorized which factors are needed to be monitored to understand progressive rock failures. They list the commonly addressed external factors like climate, structure and morphology, yet highlight the role of internal and stress states within the slopes. They mourn the missing variable of "time" in rock mechanical studies. But suppose that with time, methods would be developed to assess and quantify controls of progressive rock failure. What they ignored in their discussion were the 'means and ways' we observe and quantify the internal state of rocks. This study also failed to account for the interaction or feedbacks between internal and external factors, and the specific mechanisms facilitating progressive rock slope failure. In this thesis, I seek to address these issues.

Progressive rock failure has wide implications in geomorphology beyond progressive rock slope failure, as it broadly concerns the disintegration of rock. Because rock slope failures have been described systematically, they lend themselves for a reference object in discussing how rocks break. The outcomes of this thesis will be relevant for, for example, glacial or fluvial erosion, weathering or landscape evolution models.

Subjects of this thesis are therefore the interaction of internal and external controls of progressive rock failure, subcritical and environmentally enhanced mechanisms that facilitate it and how the internal transient stress states can be quantified.

The objectives of this thesis are the following:

- **(i)** Which coupled effects have of environmental conditions, in particular fluids/water, on the chemical and physical transformation of the rock?
- **(ii)** Which methods can we use to observe and quantify the internal inherited state - rock stress memory- and its effects on progressive rock failure?
- **(iii)** What is the nature of subcritical mechanisms relevant in Earth surfaces settings?
- **(iv)** And, how can geomorphological processes be imagined/visualized in a progressive fracturing framework?

In order to address these objectives, I combined conceptual approaches of progressive rock failure from geomorphology, rock mechanics, and material sciences. The methods used include theory and laboratory experiments. In geological and geomorphological studies, we are faced with the result of millions of years of processes which have taken place under largely unknown conditions (**Figure 1.2**). Laboratory studies offer an opportunity to study isolated processes in simple geometries under well-defined boundary conditions. Theoretical studies, like Alfred Wegener's' plate tectonics theory, allow us to explore the consequences of what we know, and of what we think we know of, and in the case here, progressive rock failure. To fully understand Earth surface processes, it is necessary to combine all scales of analysis.

A challenging part of working on an interdisciplinary topic, like progressive rock failure, is to determine which concepts and methods we can adapt, which are transferable, and where are the limitations? This requires to harmonize existing concepts, treating incongruent spatial and temporal scales of these models and methods appropriately, and being aware and explicit with assumptions, simplifications and context of each theory and laboratory experiment. These pre-settings need to be considered as they limit viable extrapolation in time and space and influence the robustness of possible interpretations.

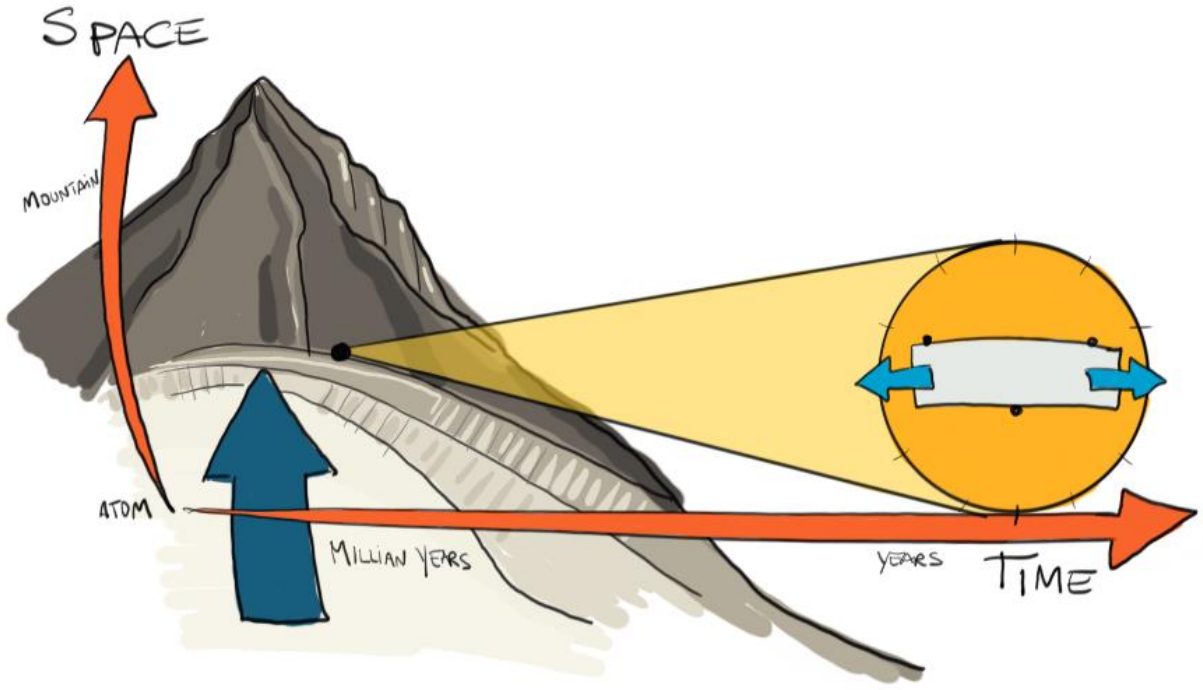

Figure 1.2 Spatial and temporal scope of the thesis

Within the scope of this thesis, I limited the spatial scale of the explorative and experimental studies to the rock sample size. Inherited and conditioned structures at a larger scale such as joint sets, discontinuities, faults are important, especially concerning rock slope stabilities, but exceed the main objective of this thesis to assess principals of controls of progressive rock failure. The limitation to intact laboratory scale rock samples provided the base to compare experiments. I focused on subcritical mechanical and chemo-mechanically initiated responses transmitted from the macroscale through the microstructure to the microscale and back (**Figure 1.3**). Starting at the macroscale of the rock sample where a far-field bending moment evokes stress gradient within the sample and tensile stress concentrations due to the geometry of it. These stresses and environmental conditions facilitate subcritical crack growth mechanisms at the microscale. Mechanical and chemical properties of the rock regulate the interaction of these subcritical mechanisms. The microscale processes and conditions then feedback into the stress field and the macroscopic response of the rock sample.

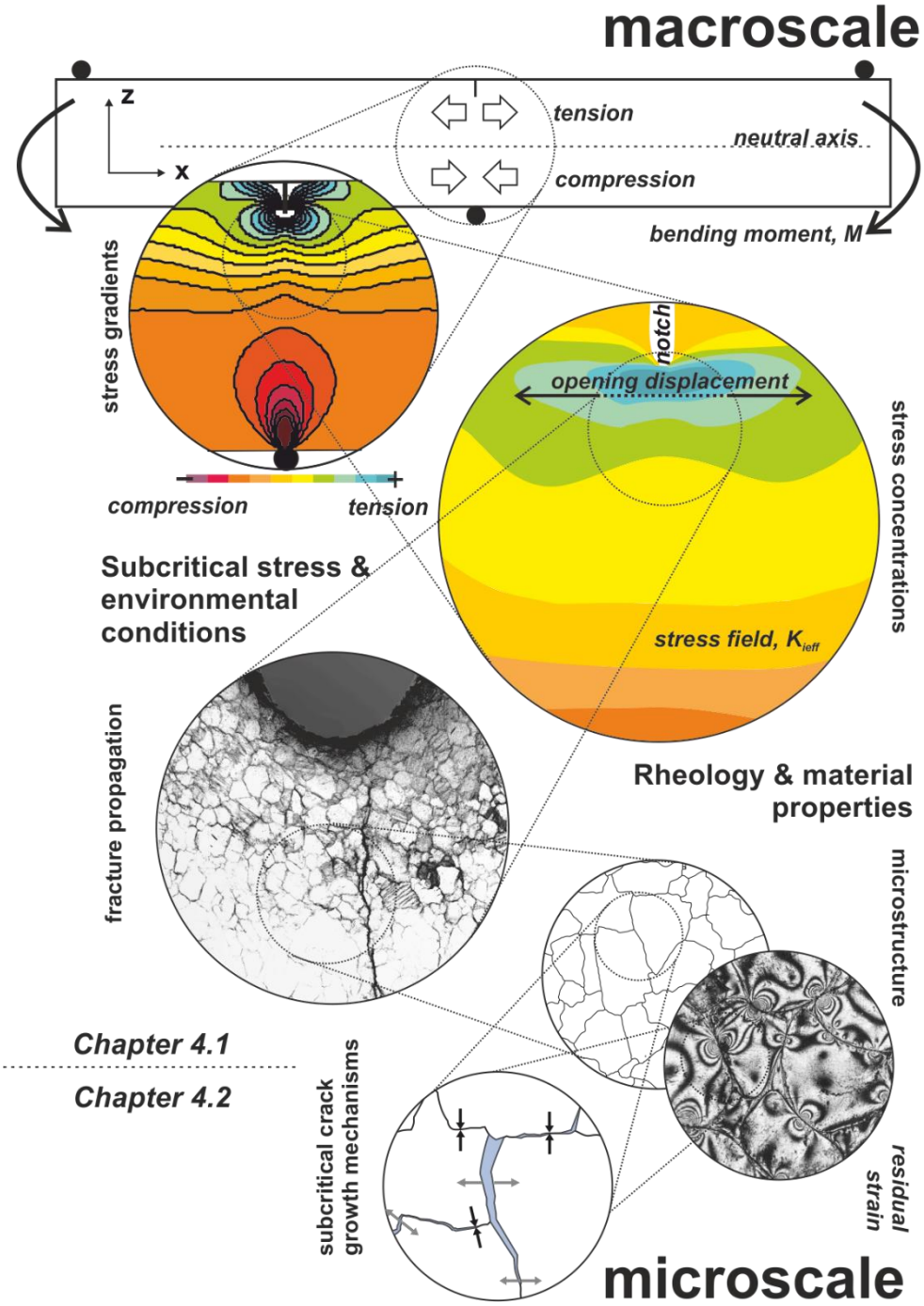

Figure 1.3 Interconnected spatial scales and objectives of laboratory studies in this thesis

Concept of thesis

This thesis is compiled in a cumulative fashion in which each of the three articles is self–contained, finite and published in an international peer-reviewed journal. Each scientific publication addresses one or more of the objectives outlined above. Two publications are based on laboratory experiments while the third comprises a theoretical approach, offering an overall conclusion of these studies.

In the study that resulted in the scientific publication in **Chapter 4.1**, I addressed the objectives **(i)** and **(iii)**, which focussed on the coupled chemical and mechanical effects of environmental conditions and resulting subcritical mechanisms on progressive rock failure. To investigate the effects and isolate the mechanisms; progressive rock failure was simplified to inverted single-edge notch three-point bending laboratory creep experiments. The setup created tensile (mode I) stress concentration at the notch, enabling the observation of single fracture initiation and propagation (**Figure 1.3**). In this way, we could test the degree of loading and progressive damage in relation to the material resistance, the fracture toughness and how this is altered by environmental conditions. Water was chosen as the environmental testing condition, as this is a ubiquitous, and more constant condition in natural rocks than fluctuating and graded thermal conditions.

The scientific publication in **Chapter 4.2** adds the internal inherited state to the objectives addressed in the first publication (**Figure 1.3**). It is based on an experimental study testing the aptitude of residual elastic strains as a proxy for rock stress memory (objectives **(ii)**). Residual elastic strains for one signifies structural preconditioning or inheritance by former tectonic or geomorphological processes, but can also be environmentally conditioned (Friedman, 1972; Holzhausen & Johnson, 1979). It can therefore play a key role in progressive fracturing as well as a way to assess the internal state of rocks. Residual elastic strain in rocks can be quantified with neutron diffraction techniques. Neutron diffraction is a standard method in material sciences to assess intended or unintended remnant strains of the production process as well as internal damage states but is still under-utilized in Geosciences.

For the study that resulted in the scientific publication in **Chapter 4.3**, I focussed on how geomorphological processes can be imagined/visualized in a progressive fracturing framework (objective **(iv)**) by combining concepts of subcritical mechanisms and rock stress memories. Progressive rock failure has been studied in laboratory and numerical experiments from rock physics and material sciences perspective and in applied field studies by geomorphologists and engineering geologists. The descriptive nature of earth surfaces processes and forms has sometimes created an apparent divide to other quantitative physical disciplines. I explored how diverse approaches can be combined to create a symbiosis to enhance our understanding of progressive rock failures. I also challenge these concepts in the application to geomorphology and (near) surface conditions. By introducing rock physics to geomorphology or vice versa, some of the pre-sets of rock physics change, especially external environmental conditions and stress magnitudes.

In order to provide a background to these studies, I review and introduce the underlying concepts of progressive rock failure in **Chapter 2**. As progressive rock failure is an interdisciplinary field and I want to evaluate it in a geomorphological context, it is necessary to outline the basic concepts of geomorphology as well as rock mechanical state of the art and the particularity of geomaterial properties.

I delineate the concept of progressive rock failure in a geomorphological context, on the basis of rock slopes instabilities. To better grasp fracturing in rock, the system is commonly simplified to driving and resisting forces which are transposed to external and internal processes (Strahler, 1952). I clarify this existing framework by addressing the effects of internal and external processes on rock slopes by describing their interaction in terms of forces and conditions imposed on rocks. Internal or endogenic means that the forces and conditions within the rock are a result of the solid Earth's geodynamic system (e.g. tectonics, structural

inheritance, residual elastic strains, Holzhausen & Johnson, 1979; McGarr & Gay, 1978; Scheidegger, 1979). External or exogenic mean that processes at the Earth's surface exert stress on rocks as a result of gravitational and climatic forcing and provides a physical environment that superimposes the condition of the rock (e.g. weathering, erosion, transport, deposition, Gregory & Lewin, 2015; Scheidegger, 1979). The internal system state is commonly assumed to be (near) critical (Byerlee, 1978; Leith et al., 2014a; Zoback, 1992). External forcing exerts high frequency but low magnitude stresses and thus promoting subcritical mechanisms (Eppes & Keanini, 2017; Wolman & Miller, 1960).

The chemical and mechanical properties of rock regulate the interaction of internal and external processes and are transposed by them. The rock responds by progressive rock failure (Brantut et al., 2013). The most intriguing fracture mechanics concept to assess 'How rocks break' in a geomorphological context is subcritical crack growth (Eppes & Keanini, 2017). The general concepts of subcritical crack growth are introduced including environmentally enhanced and coupled chemo-mechanical mechanism, like stress corrosion cracking and water-weakening effects (Atkinson, 1984, 1987). Most of these concepts are concerned with external conditions and stresses. To evaluate the role of internal controls and their interaction with external factors, the state of the art of subcritical mechanism is extended to the inducement and relaxation of residual elastic strains as drawn in material sciences (Toribio et al., 2007; Withers, 2007).

In **Chapter 3**, I outline the material and methods that were used in the experimental studies. Experimental rock deformation provides us with several ways to investigate time-dependent brittle deformation. As this is the first attempt, the long-term experimental setup is highly simplified and an exemplary rock type was chosen; a metamorphic near pure calcite Carrara marble. The experiments rely on selected methods that enabled the isolation and quantification of external and internal controls. Based on standard methods I derived and adapted a single edge-notch three-point bending experiment to observe tensile (mode I) creep in Carrara marble samples. The calcite Carrara marble enabled the collection of simple diffraction patterns to assess internal strain states. The feasibility and limits of measurements of residual elastic strains with neutron diffraction techniques are exemplified in **Chapter 3**.

The results of the theoretical and experimental studies are compiled in the scientific publications in **Chapter 4**. The scientific publications are organized by the following rational, visualized in Figure 1.4. Results of the theoretical study in **Chapter 4.3** constitute the starting point of all considerations on how rocks break at the Earth's surface, defines the setting as well as resumes the findings of the experimental studies (**Chapter 4.1** and **Chapter 4.2**). The outcomes of the experimental studies in **Chapter 4.1** and **Chapter 4.2** build upon each other.

The scientific publication in **Chapter 4.1** reported on the long-term experiments and the response of the rocks to externally applied factors. **Chapter 4.1**, *"Subcritical crack growth and progressive failure in Carrara marble under wet and dry conditions"* The publications demonstrate that environmental conditions, here the introduction and presence of water pose a strong control on subcritical crack growth and progressive rock failure. Key findings are that wet rheology matters and a conceptual challenge is identified that most stress corrosion chemo-mechanical models are phrased for silicates and not adequately adapted to carbonate rocks.

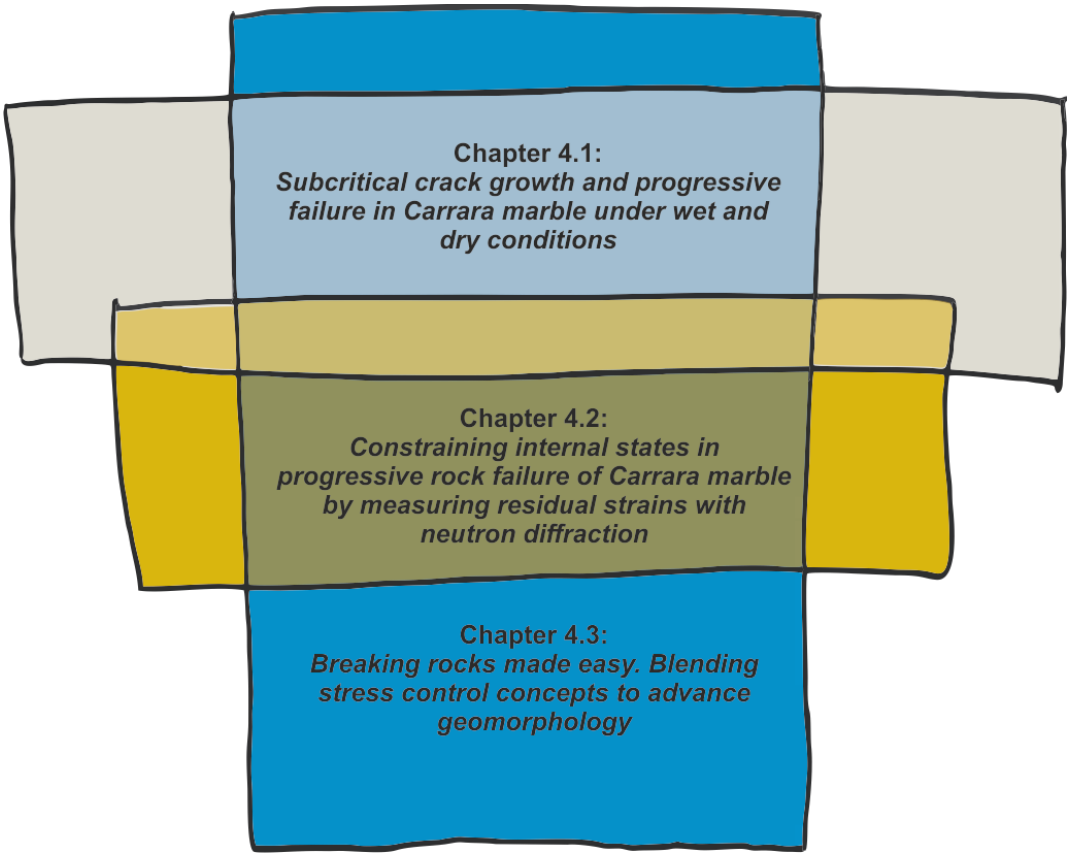

Figure 1.4 Organizational rational of the scientific publications

The publication *"Constraining internal states in progressive rock failure of Carrara marble by measuring residual strains with neutron diffraction* in **Chapter 4.2,** described the internal (residual) strain state which governs progressive rock failure and is also progressively altered by it. It is the first time the internal state and its alteration by subcritical mechanical and chemo-mechanical pretesting have been systematically assessed by using the residual elastic strain as a proxy. The findings highlight the importance of time scales, rates and tenses (past-present-future) in laboratory experiments and geological settings.

In **Chapter 4.3**, an ESEX Commentary on *"Breaking rocks made easy. Blending stress control concepts to advance geomorphology"* discussed how to include rock physics and material sciences conceptually into geomorphological research questions. The publication suggests a conceptual framework of progressive rock failure in geomorphology and defines possible applications. A key finding of these theoretical considerations is the importance of defining initial or reference states in science and the challenge to quantify especially internal states in Geosciences.

In **Chapter 5**, I discuss the main findings from the published articles. These include time in terms of time-dependency and the geological scale, the mechanical as well as chemical coupling of water with carbonate rocks and defining initial and reference rock states.

In **Chapter 6**, I conclude using the following seven themes that accompanied my research project: Methods –Theory –Rocks –Limits –Failure –Strength –Stress.

My research interest was sparked by the understudied relationship between fracture mechanics of the solid Earth with erosion and weathering processes in geomorphology. I studied which factors pose a control on progressive rock failure (long-term) and how the failure mechanisms are affected by those, both in rate (time) and extent (space). I observed the response of these rocks to external factors, such as subcritical loading and the presence of water and I assessed internal factors and their response, such as residual strain and microstructural properties. My research contributes to new conceptual and methodological approaches in geosciences.

2. State of the Art in progressive rock failure

Progressive rock failure describes the evolution of disintegration, fracturing and decohesion of rock. In the context of geomorphology and landscape evolution, it is an essential part of weathering enabling erosion. For the anticipation of natural hazards and safety of infrastructures, the state and rate of microcracking and fracture progression in the precursory phase of rock failure is crucial. Regarding the performance and preservation of artistic and engineered structures of rock, progressive failure is resembled by ageing and fatigue and the potential loss by disintegration and fracture.

In this thesis, I explored how this failure proceeds, how environmental conditions affect the response, which fracture mechanisms need to be considered and how internal and inherited strains in the rock influence progressive rock failure. To be able to better discern the controls of progressive rock failure an experimental approach was chosen. One of the prerequisites of the experiments has been that we can separate and control the factors, mechanisms and constituents of the system under investigation. Progressive rock slope failure, both as an easy to imagine analogue system and due to conceptual existing groundwork, lends itself to depict the possible controls and mechanisms of the progressive rock failure system. The chosen reference system in this thesis, are steep rock slopes in a geomorphological context.

If a steep rock slope has been observed to be progressively deforming, for example, indicated by precursory rock falls, tension cracks or tilted trees, they are often monitored to anticipated hazardous failure. Monitoring studies often report incoherent behaviour of rock slope deformation (Gischig et al., 2011; Loew et al., 2016; Moore et al., 2010, 2011; Rouyet et al., 2017). Incoherent to the assumption of the system response and limited by the physical and methodological assessability of rock slopes. These limitations have been also pointed out by Bjerrum & Jørstad (1968, cf. **Chapter 1**).

First, the basic concept of rock slope failure, which is based in an antagonistic system driving and resisting forces is introduced. Resisting forces are termed those factors and forces inhibiting failure while driving forces are those promoting failure. But because this is often done in a time-independent concept, progressive or time-dependent concepts, like the margin of stability and landscape sensitivity are presented subsequently (**Chapter 2.1**). A consequence of susceptibility and sensitivity concepts is that instead of competing of forces the interaction and response of internal and external factors control the system.

Second, external and internal controls of progressive rock slope failure are inspected in **Chapter 2.2**. The path in which progressive rock damage evolves these internal and external factors. The intrinsic factors of rock are conditioned by its geologic past. Extrinsic factors, especially at the Earth surface or near-surface are determined by high frequency, low magnitude processes of the atmosphere and its interaction at this boundary layer.

What aspects and factors of progressive rock slope stability can be assessed, observed or even be quantified is despite technological and methodological advances limited in geomorphology. To date, geomorphologists have primarily focused on either statistical or phenomenological approaches to assess rock slope instabilities on broad temporal and spatial scales (Crozier & Glade, 1999; Korup & Clague, 2009). Although there is a long tradition of considering the mechanics of dynamic geomorphic processes, the mechanical behaviour of the material is often overlooked (Brunsden & Prior, 1984; Erismann & Abele, 2001), though notable exceptions exist (Bruthans et al., 2014; Gerber & Scheidegger, 1969; Yatsu, 1966).

Engineering approaches to similar challenges generally focus on mechanical properties of the bedrock on a site- or project-specific basis (Hoek, 2007; Wyllie & Mah, 2004) and do not consider the dynamic nature of the landscape and the temporal evolution of intrinsic and extrinsic factors. The mechanisms which are involved in progressive rock failure have been assessed especially regarding the performance of materials and infrastructure lifetime. The application to natural rock slopes has been suggested for decades but is often limited by methodological constraints to observe in situ, hampered by the feasibility to extrapolate from laboratory experiments and general upscaling in terms of space and time.

Another factor which clearly distinct geomaterials from engineered materials and the mechanisms of progressive failure is the geologic history. With the geologic history, preconditions but also heterogeneities and singularities might alter the rate and extent at which the mechanisms operate. Progressive rock failure in a geomorphic context, therefore, implies two requisites about fracture mechanics: First, the involved stress magnitudes, and second, velocities of fracture propagation. Both of these are defined as 'subcritical'.

Subcritical, in the context of stress magnitudes, indicate applied far-field loads below the critical rupture stress, or the rock strength. At the microscale where subcritical stresses concentrate they can become critical and cause microcracks and fractures.

Subcritical, in the context of fracture propagation, is understood in terms of at which rate or with which velocity fractures form or extend.

Third, **Chapter 2.3** introduces the basic fracture mechanics concepts of subcritical mechanisms of progressive rock failure. Starting with brittle crack extension, as postulated by the Griffith criterion, environmental conditions are added. Mechanisms which are chemical or environmentally enhanced, like stress corrosion cracking, plasticity and embrittlement are discussed. To consider also internal conditions, a description of the mechanisms that lock-in and relax residual elastic strain follows.

2.1 Key concepts in geomorphology and rock slope failure

Driving and resisting forces

Concepts of landscape evolution and geomorphology often build upon the principle of Antagonism (Church, 2010). The division into entities of contrasting driving and resisting forces, external and internal factors enables a structured and systematic approach. When phrasing the concept into driving and resisting forces, like in limit equilibrium analysis several assumptions and ascription to external or internal factors are made. Drivers of the system are usually ascribed to external factors, while internal factors pose resistance to them. If the driving forces are equal to the resisting forces (**Figure 2.1.1**, left) the system is in a critical state. This state is assumed for the lithosphere (Sibson, 2017; Zoback, 1992). Any increase in the driver or decrease in the resisting forces results in failure, fracture or earthquake. Near the earth surface, this assumption is not constrained. And indications that near-surface the resisting forces are likely to be greater than the driving forces are given by lower stress magnitudes discussed below in **Chapter 2.2**. To initiate failure in a subcritical system (**Figure 2.1.1**, right), either the driving forces need to increase at least proportional to the resisting or the resisting need to decrease to match the driving forces.

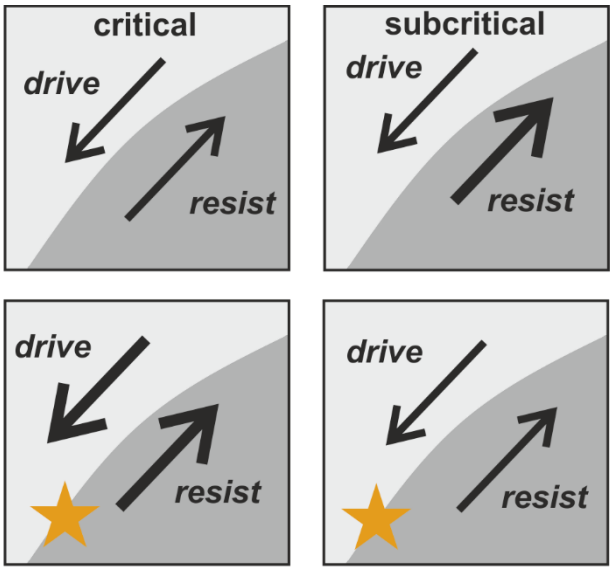

Figure 2.1.1 Causing failure by competing driving and resisting forces in a system in a critical (left) and a subcritical stress system state.

A change in the system can then be assigned to a specific state, e.g. critical state, or thresholds. Especially concepts of rock slope failure build upon the principle of Antagonism, by contrasting driving and resisting forces. In rock slope stability assessments, a threshold is assumed, controlled by an increase in external driving or a decrease of internal resisting forces. If the threshold is approached, the slope fails. Failure occurs due to relative change of driving and resisting forces in reference to a threshold (Schumm, 1979, **Figure 2.1.1**).

Systems are assumed to be dynamically linked between driving and mobilized resisting forces grounded in Newton´s laws of motion (Strahler, 1952). Strahler (1952) discerns between gravitational and molecular stress to link and order processes, forms and agents involved in geomorphic work. Classifications of driving and resisting forces, to discern the factors involved, are ample (Gregory, 2010; Gregory & Lewin, 2015; Strahler, 1952). An example is given in **Table 2.1.1**. Most resisting forces are inevitable linked to the material properties, which conversely are regularly not included or simplified to “strength”. Resisting forces in rock slope stability are for example controlled by a) mineral composition, structure, and texture, b) bedding, jointing, and anisotropy; c) water content; and d) state of stress or strain in the rock mass (Augustinus, 1991).

Geomorphic work

Overall, geomorphic work is done if either the resisting or driving forces are altered. The amount of work done by geomorphic processes is a key geomorphic concept illustrated by Wolman & Miller (1960) (**Figure 2.1.2**). From the perspective of many driving forces, or processes, geomorphologists have thrived to quantify these states, despite all obstacles of spatial and temporal extrapolation or randomness of these processes. In contrast, the resisting forces which have often been left out, subsumed to boundary conditions, and gladly assigned to structural geologists, soil and rock mechanics.

Table 2.1.1 Major categories of earth surface processes from Gregory (2010)

Category of Process	**Examples of Force and Resistance**	
Exogenetic	**Force**	**Resistance**
Weathering	Crystal growth, heating and cooling, tree roots	Physical and chemical bonding
Mass movement, hillslope processes, including processes of mass wasting	Gravity, increased water content, earthquake movements	Shear strength of materials, binding effects of vegetation, structures
Fluvial, drainage basin processes, hydrologic processes	Gravity, discharge reflecting precipitation, stream power	Friction in fluid and between water and channel margins,
Coastal processes and landforms that occur on coastal margins	Wave action, tides	Friction on coasts, strength of materials
Aeolian wind-dominated processes in hot and cold deserts and other areas such as some coastal zones	Wind action giving lift force and drag forces	Gravity, particle cohesion, friction between particles and with surface
Glacial, glaciers and ice caps, and landscapes occupied by glaciers, and those glaciated in the past	Gravity, pressure of snow and ice	Friction with bedrock
Periglacial/nival, cryonival, typify the processes in the periglacial zone, in some cases associated with permafrost, but also found in high altitude areas	Expansion of water on freezing	Strength of materials
Subsidence	Gravity following the removal of fluids or material	Strength and cohesion of materials
Soil pedogenic processes, soil erosion	Water and wind on surface	Vegetation cover
Ecosystem dynamics	Animal burrowing	Indurated soils resist plant growth
Endogenetic		
Earthquakes and tectonic	Rock uplift	Gravity, rock strength
Volcanic processes	Magma extruded	Friction with surface

Geomorphic work is generally a great concept in geomorphology as it suggests that by quantifying the amount of energy we put into the system we can expect the response. The energy or forcing which are usually considered, are external factors (stresses and conditions) because we can observe and measure them directly. The system transforms an often unknown fraction of the available energy. Part of the energy provided to the system is used to do geomorphic work, parts will be stored internally and others enter and exit without changing the external or

internal state. (This would be a geomorphological phrasing of Helmholtz free energy). In the context of progressive rock failure, this means that the expected response relies not only on the applied stress but on the initial state, the conditions and the mechanisms how the stresses are transmitted.

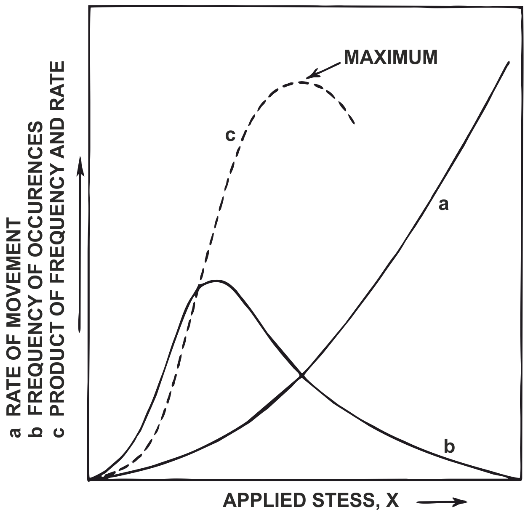

Figure 2.1.2 Relations between rate of movement, applied stress, and frequency of stress application (adapted from Wolman & Miller, 1960)

Progressive rock slope failure is embedded in the proposition of landscape or rock slope stability. The adjective "progressive" denotes its time-dependent evolution of sensitivity to respond/change or in the case of rock slopes to fail. Response/Change or failure is a function of resisting and driving forces, but a complex function. In landslide susceptibility and also the margin of stability a combination of both, a time-dependent decrease of the resisting forces due to preparatory and precondition factors as well as an increase of the driving forces, by triggering factors, is assumed.

Landscape sensitivity concept

Another key concept in geomorphology highlights the system states and its sensitivity to change, thus its response to perturbations (Brunsden & Thornes, 1979). The landscape sensitivity concept originates in physics and chemistry and is being applied to landscapes in a rather metaphorical, and yet in regard to slope failure even in a literal way (**Figure 2.1.3**).

Due to the system specification – thus in which state the slope is both due to external or internal conditions, or where on the margin of stability, the response to a perturbation- an increase in driving or decrease in resisting forces (or in this model more specific of energy), will vary. In the following sections (**Chapter 2.3**) we will see that this can also be applied to the sensitivity of breakage of material bonds. If this concept is applied to rock slope stability it is again limited as it hampered by us knowing what state the rock slope, with all its visible fractures or not, is actually in. What it though provides, is to highlight that due to different states (stable-metastable-instable) of the system or rock slope, different magnitudes of forcing are needed and that various factors condition the state – we will keep this in mind and discuss these aspects later on.

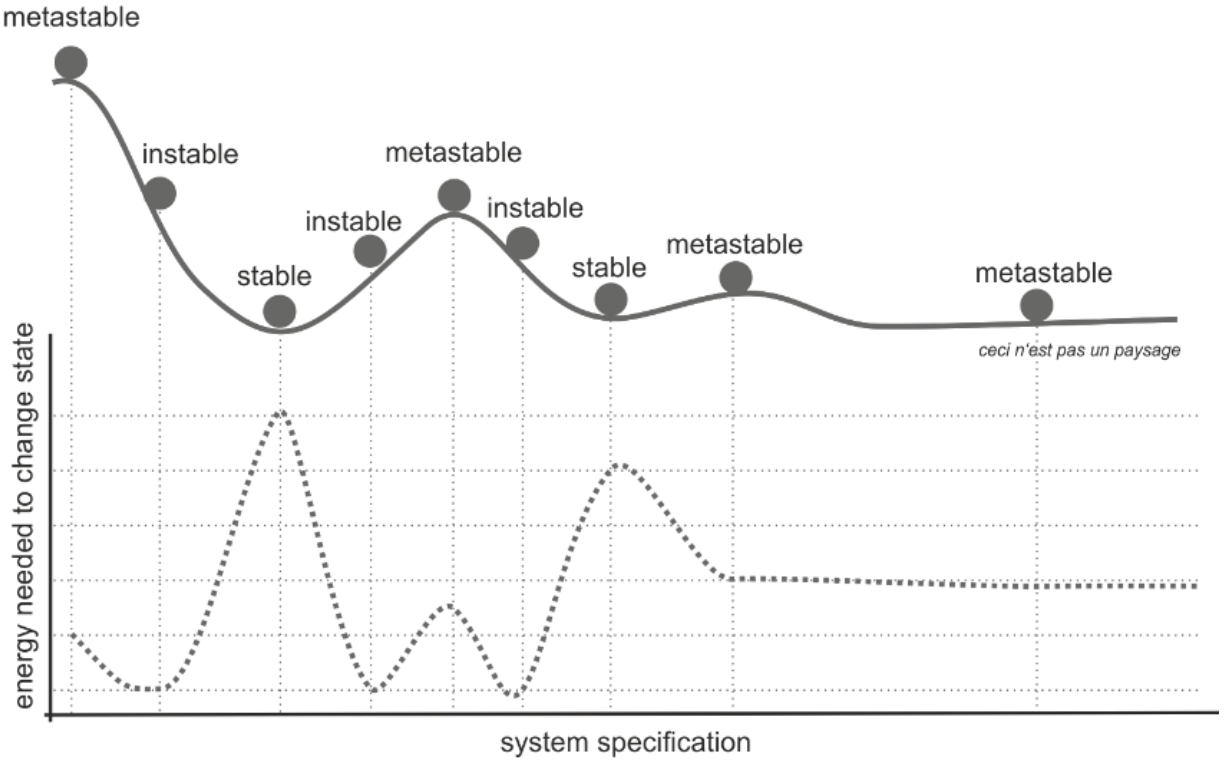

Figure 2.1.3 Illustration of the sensitivity concept of Brunsden & Thornes (1979)

Margin of stability

To include a time-dependency at least indirectly in the limit equilibrium approaches, susceptibility studies are conducted to determine the state of the system or the rock slope on the margin of stability (e.g. Crozier & Glade, 2012; Matasci, et al., 2018). Analogues with the 'margin of stability' one can describe the rock slopes system state and evolution (Crozier, 1989) (**Figure 2.1.4**) Conceptually it shows along the margin of stability – which has a suggestive, non-scaled timeline, how the rock slope evolves from a stable condition towards a marginally stable state to an actively unstable one, in which sustaining factors and triggering factors compete. It goes beyond a simple force balance approach as it includes additional factors that either have a preconditioning, preparatory or triggering role.

The precondition factors are commonly inherited and inherent features of the rock and the slope. The sustaining or resisting factors are similar to those listed in **Table 2.1.1**, some derivatives of 'rock strength'. The internal state or the manner in which the resisting forces might decrease in time as well are packed in a passive black box in these concepts. Due to limitations of assessing the internal state, most susceptibility analyses reside in reporting geometries and structural feature and monitoring triggering factors, especially precipitation. With this approach, the likelihood of where some slopes might fail is often determined. For that comparison with former slope failures- thus in hindsight ad those topographic, lithological and triggering event characteristics are statistically consulted. (Absolute) timing, prediction or the mechanisms behind these failures are disguised.

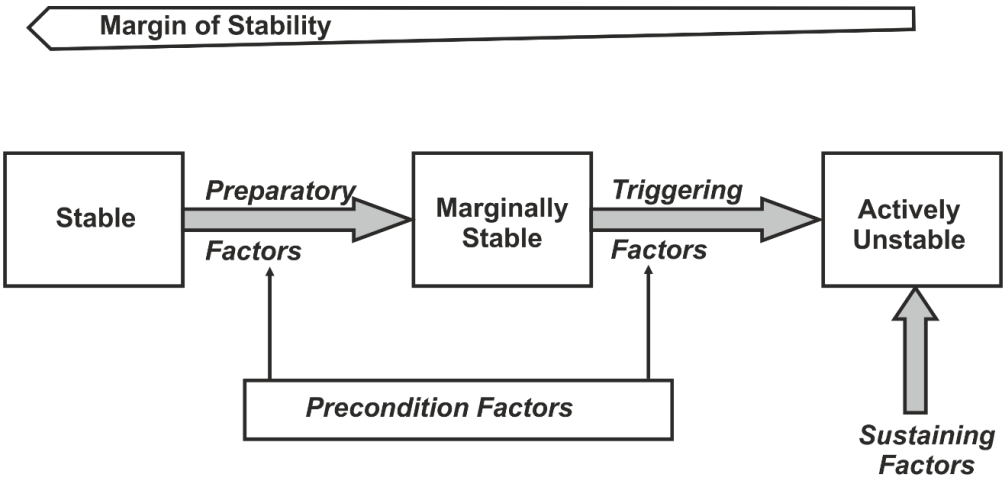

Figure 2.1.4 Margin of stability (after Crozier 1989). Note that there is no explicit time frame mentioned. External factors are driving the system influenced by precondition and only restrained by sustaining factors

Progressive rock slope failure concepts

Progressive failure of rocks has been identified as a key control of geomorphic processes ranging from landscape and slope stability evolution, to erosion and weathering (Aldred et al., 2016; Clarke & Burbank, 2010; Collins & Stock, 2016; Dühnforth et al., 2010; Gerber & Scheidegger, 1969; Gischig et al., 2016; Leith et al., 2014; Stock et al., 2012; Whalley et al., 1982). In slope stability assessments, progressive rock failure is often overlooked until of rock slopes hazardously fail without any obvious forcing event. Those have, for example, been reported for the Yosemite-Valley, California (Stock et al., 2012). General slope stability concepts expect that fractures propagate or failure occurs when the driving forces exceed the resisting forces (Jaeger et al., 2007). These limit equilibrium theories, like the factor of safety, define if a slope is stable or not, fracturing is either on or off. The applicability of these concepts to progressive rock slope failure is limited as there is no notion of time. Even though progressive rock failure is identified as key in rock slope failure, we still lack a profound and quantifiable knowledge on the precursory phase of time-dependent deformations that lead up to dynamic ruptures, and potential hazards (McColl, 2015; Ventura et al., 2010).

The adjective ‘progressive’ generally refers to the time-dependent and incremental characteristics of internal structural changes that reduce strength and stability of rock slopes and structures (Bjerrum & Jørstad, 1968; Terzaghi, 1950). Several external and internal factors and forces have been suggested to govern the mechanisms and rates of progressive rock fracturing like pre-existing structural inhomogeneity, loading and unloading by external drivers, and environmental conditions (Atkinson, 1987; Attewell & Farmer, 1973; Bjerrum & Jørstad, 1968). In addition, in engineering materials, progressive damage evolution is assessed focussing on material properties and internal strain or stress state (Lee et al., 2011; Toribio et al., 2007; Withers, 2007). This resides in the possibility to tweak, exploit and control the production of these properties and strains, which for geomaterials is spatially and temporally impossible. The geologic past of rocks is for most parts concealed or only indirectly accessible. Its role and the memory effect of those is relevant as progressive rock slope failure, erosion and

weathering, exploit preexisting structures on all spatial scales of the bedrock (Hantke & Scheidegger, 1999; Krautblatter & Moore, 2014; Whalley et al., 1982)

Mechanisms of progressive damage comprise any deformation caused by local stresses exceeding the local strength of the rock (Eberhardt et al., 1999, 2004). This introduces space and place into the study of progressive rock failure. The mechanisms act on the microscale and can evolve to (macro)fractures up to the slope scale. Where far-field stresses concentrate and localize is conditioned by geometries and structures from the slope scale to the microstructure and processes. These scale-interdependencies and possible extrapolations are still not resolved, hampering the application of laboratory experiments to mountain slopes.

Fracture propagation and damage evolution progressively weaken the rock. The rate of deformation is non-linear, non-proportional and accelerating. This often cannot be explained by classical fracture mechanics and slope stability where stress and strain, or external forcing and slope deformation are assumed to be proportional or linear related. The time-dependency, even if starting at a fully elastic state, inelastic damage accumulation leading to these offsets in response and at the same time making it more susceptible to triggering factors and ultimately lead to failure. For geomorphology and slope stability, this has been described by susceptibility concept and a so-called margin of stability (Brunsden & Thornes, 1979; Crozier, 1989). **These concepts enable us to assort investigate and quantify factors and relationships to enhance our understanding of progressive rock slope failure.**

2.2 External and internal factors

Conditions and stresses that evoke by Earth surface interfacing the atmosphere are called, external or exogenic factors. Internal or endogenic processes precondition material properties of rocks during their path to or near the surface of the Earth. Their interaction resembles geomorphologic processes, forms and materials.

Rocks are imposed by external and internal stresses and their change over time. In natural environments rock strength is thus a function of stress changes due to gravity, tectonics, exhumation, and ‘environmental stresses’ resulting from relatively low constant or cyclic loading of rock at the Earth’s surface. Extrinsic factors act on rocks at presumably subcritical stress magnitudes and are enhanced by environmental conditions (Atkinson, 1987; Brantut et al., 2013; Vann Jones et al., 2015). Intrinsic strain states of rocks are preconditioned by their geological history of a variety of deviatory thermal and mechanical stress states, especially in metamorphic rock. Residual internal strains have been shown to play a fundamental role in the elastic behaviour of engineering materials (Withers, 2007). Their effect on the behaviour of bedrock remains still unspecified (Engelder, 1993)

Driving and resisting forces are often used synonymously with external and internal factors and forces. This though misses the mark and rather stems from accessibility, reductionism and technical limitations. We still have very little quantification of inherited conditions such as rock stress memory or in-situ rock stresses due to especially methodological reasons. But also environmental stress quantifications are sparse. State changes, either internal or external, are due to internal or external conditions. These conditions basically control the rate and extent of progressive rock failure and generate any driving and resisting forces.

2.2.1 External factors

Environmental conditions

In natural environments, rocks are always subject, not only to applied stress or gravitational acceleration but also to environmental conditions. Usually, the effect of environmental conditions on rocks is discussed in terms of weathering. Weathering is commonly discretized into chemical, physical-mechanical and biological process regimes. Physical weathering, describes the breakdown of rock material due to forces, either originating within the rock or mineral or applied externally, thermally or mechanically, e.g. by environmental stresses. Chemical weathering covers all chemical kinetics that alter the material, from diffusion and dissolution, hydrolysis and leaching, to precipitation and crystallization. It has often been the focal mechanism in weathering studies (Hoke & Turcotte, 2004; Thornbush & Viles, 2007), as the chemical kinetics are closely linked to the activation energy, exerted by temperature and reactive potential by the solute, thriving to attain equilibrium with its surrounding. Due to the dependency of chemical weathering to the chemical potential, rates are limited by the access to fresh mineral bonds or reactive fluids (Attewell & Taylor, 1990; Thornbush & Viles, 2007). Chemical weathering would thus cease over time, as potentials attain equilibrium. Ongoing chemical weathering needs external processes changes, e.g. transport or erosion of material to be effective (Ferrier & Kirchner, 2008; Hilley et al., 2010).

Rock moisture measurements suggest, that there are essentially no completely dry rocks (Sass, 2005; Sass & Viles, 2010). It has been shown that a gradient, from a more or less constant moisture level in the core toward exposed rockfaces which are subject to frequent variations in moisture as well as in temperature, exists in the rock (Sass, 2005). Surrounding temperature changes by geothermal gradients (Ball et al., 2008; Batzle & Simmons, 1976; England & Wilkins, 2004), but more frequent and pronounced at exposure to radiation e.g. solar (Hall & André, 2001) or nuclear (Damjanac & Fairhurst, 2010; Dupray et al., 2013; Was et al., 2007); as well as due to the movement of fluids and air masses through fracture networks (Benedek & Molnár, 2013; Mattila & Tammisto, 2012).

One of the most important environmental conditions or factors is the presence of water, from moisture to free flow, gas, liquid and solid-state. Being ubiquitous and chemically active, we focus on the effect of water on progressive damage. This includes chemo-mechanical interactions of water at a stressed material bond, and water weakening effects (**Chapter 2.3**).

Environmental stresses

External factors that influence progressive rock failure include stresses applied on the rock by its environment and environmental conditions the rock is exposed to. Environmental stresses, as I would like to call them, are exerted constantly by gravity, periodically or stochastically by geomorphic processes. These geomorphic processes include stresses produced wind and wave loads (Müller et al., 2003; Vann Jones et al., 2015), (micro)seismicity (Arosio et al., 2009; Brain et al., 2014; Hovius et al., 2011; Mainsant et al., 2012), pore-water pressure (McColl & Davies, 2013; Simon & Collison, 2001), ice- and mineral-crystallization pressure (Gratier et al., 2012; Murton et al., 2006; Røyne, Meakin, et al., 2011), fluvial, marine and glacial shear (Hsu et al., 2008; Lamb & Fonstad, 2010; Mitchell et al., 2013) and bio-geomorphic agents (DeVries, 2012; Gabet & Mudd, 2010). The magnitude of natural processes

at the surface is generally low but high frequent (Crozier & Glade, 1999; Wolman & Miller, 1960). Yet, the delimitation of the signal and effect of the energy, stress or loads exerted on rocks slopes are still pending (Norman, 2012), as is the systematic quantification of environmental stresses. Few quantifications of those environmental stresses point to a range from a few kPa up to approximately 1-2 MPa e.g. glacial traction 20-100 kPa (Fischer et al., 2001), impact wave loads 17.5-60 kPa (Cuomo et al., 2010) or ice-crystallization pressure of up to 2MPa (Walder & Hallet, 1985). The effective temporal and spatial scale, as well as the direction/orientation of environmental stresses, vary highly (Gabriel & Kreutzwiser, 2000; Ilk et al., 2005). Besides the dynamically applied stresses, provide form and topography induced gravitational stresses near-constant low-stress states (Brunner & Scheidegger, 1973; Molnar, 2004; Scheidegger, 1976). In gravitational systems, the applied stress is actually nearly constant by 9.81 m/s-1 times the weight. Changes in the weight of a slope can arise due to wetting, snow load, but would in a rock slope be minor. Stress distribution can change and evoke stress concentrations due to undercutting, partial failure, or progressive damage.

Generally, environmental stresses can be described as high-frequency low-magnitude stresses. The high frequency, due to small fluctuations can be summed up as constant forcing.

2.2.2 Internal factors

Structural geology has been identified as an important control in rock slope failure. Lithology, faults, and joints govern where and how it might fail, the microstructure, texture and strain state determines the mechanisms (Bjerrum & Jørstad, 1968; Stead & Wolter, 2015; Zangerl et al., 2006). Material and memory properties define the rate and extent of rock damage. In regard to progressive rock slope failure, geological and geomorphological conditions, like lithology, joint sets, material properties, slope angle which predispose slopes to failure are commonly assessed. Knowledge of these conditions can help to predict the location, types, and volumes of potential failures. They constitute the basis of landslide susceptibility maps. As this thesis is based on laboratory studies of progressive rock failure I focus on material properties and rock stresses in the microstructure.

Material properties

Characterization of rocks is commonly based in physical and chemical properties. Mechanical properties like compressive or tensile strength, or toughness, and elastic properties like Young's modulus or Poisson ratio are assessed for intact bulk rock samples as well as rock constituent minerals single crystal. These physical properties are usually empirically determined. The resulting property estimates have been shown not to be independent of the tests. For example, the Young's modulus, describing the resistance of a body to deform (linear) elastically when stressed, varies by magnitudes, depending on the mode of assessment (static or dynamic), as well as in direction, scale, and environmental condition. Or marked by the difference in strength of rocks in short-term and long-term testing (see **Chapter 2.3**).

Chemical and thermal properties of rocks are commonly defined for the rock constituent minerals. For bulk rocks, they are usually poorly defined. Assessments of these chemical and

thermal properties are additionally challenged due to coupled modifying effects, like thermo-mechanical or chemo-mechanical processes (see **Chapter 2.3**).

Microstructural properties resemble shape, orientation, and distribution of rock constituting minerals and their boundaries, as well as voids, pores, flaws, grain and crystal interfaces and microcracks (Cai et al., 2004; Hoagland et al., 1973; Kranz, 1983).

Memory properties

Memory properties of rocks are the ability of rocks to accumulate, preserve and (re)produce information about the stresses and conditions which they experienced earlier. They are encrypted in the microstructure. Microstructural material properties of rocks have been shown to depend (i) on the formation conditions (temperature, pressure, presence of a fluid), (ii) deformation, its mode, direction and duration and (iii) the mineral composition (Cai et al., 2004; Hoagland et al., 1973; Kranz, 1983). The preconditions pose a control on the damage pattern in rocks, in rate and extend (Hoagland et al., 1973). Microstructural assessments are therefore essential to any rock-related study.

A well-studied way to assess deformation or inelastic strain memory in rock mechanics is known as Kaiser Effect (Holcomb, 1993; Lavrov, 2003; Yoshikawa & Mogi, 1981). The Kaiser effect is related to inelastic damage in the microstructure. During the first mechanical loading of a rock sample, this inelastic damage extends when the earlier experienced deformation load is exceeded. Because brittle crack growth produces acoustic emissions (AE), the former stress state is inferred from an increase in AE measurements. The robustness to assess the memory properties with the Kaiser Effect has been questioned (Hsieh et al., 2014, 2015).

Another rock stress memory is related to elastic strains locked-in the microstructure. Because residual elastic strains are both a condition and effectively elastic strain energy that can be mobilized it is introduced in more detail below.

Residual elastic strains and stresses

The conceptualization of residual strains originates from material sciences especially metallurgist (Holden et al., 1995). Residual in this context refers to the elastic strain energy which is locked in the material or is induced by external deformation or tempering but remains even if the traction is removed. This doesn’t contradict the general assumption that elastic strains equilibrate on the macroscale, but due to internal constraints and the scale domain of these inter- and intragranular strains, it is possible that not all strain energy is instantaneously equilibrated, once the external forces are relieved. In material science, residual strains are both anticipated and feared in term of the performance of engineered material, e.g. tempered glass, pre-stressed concrete but also disastrous structural failure. That pre-stressing of rocks and geomaterials might also make them more durable has been unintentionally been observed in any structural feature like Roman arches, or already in sandbox experiments, where pre-compaction led to a higher angle of friction (Gudehus & Touplikiotis, 2017) and in applied mechanics, has led to the development of pre-stressed single rock slabs as bridges (Hennecke & Kusser, 2014; Pinto & Fonseca, 2013).

Due to deviatory stresses in the crust rocks deform and are strained (Ramsay, 1967). Mechanical or thermal stress can cause elastic or permanent deformation along grain boundaries, crystal axis, and lattice planes. Upon the removal of the loads elastically yielding strain is relaxed, while plastic strain is preserved. However, some elastic strains may be locked-in because their strain state is confined by adjacent inelastic deformed grains or defects (Chen et al., 2011, 2015). If the deformation cannot be reversed, either by plastic deformation or the lock-in of elastic strain, the solid remains residually strained. Residual strains remain in a solid material after the original cause of stress, i.e. external stress, temperature gradient or body force, has been removed (Friedman, 1972; Holzhausen & Johnson, 1979). Residual elastic strains are locked-in the microstructure of rocks (Withers & Bhadeshia, 2001). In **Figure 2.2.1** tensile and compressive stresses that arise from the residual elastic strains in the microstructure are highlighted in an analogous experiment (Leith, 2012).

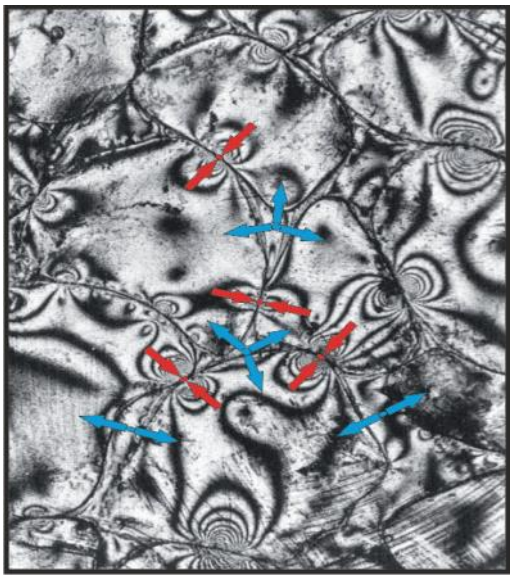

Figure 2.2.1 Converging red arrows indicate compressive, diverging blue arrows indicate tensile residual stresses (after Gallagher, 1971).

Conceptualizations of the evolution, storage and relief of residual strains in rocks by can be found by (Emery, 1964), (Kieslinger, 1958), which rely on observations but lack appropriate techniques to assess and quantify these residual strains. In the 1970s analogous experiments and geotechnical methods, like under- or overcoring could confirm their existence in rocks (Friedman, 1972; Holzhausen & Johnson, 1979). Investigations and measurements of residual strains are carried out on the microscale of the material, their implications for paleo- and in-situ stresses as well as their upscaling are still on debate and needs further research (Chen et al., 2015; Tullis, 1977; Zang & Berckhemer, 1989). Emerging techniques from material sciences like neutron or X-ray diffraction enabled to assess residual strains as a material parameter in-situ (Chen et al., 2015; Kunz et al., 2009; Scheffzük et al., 2000). A sparse dataset of residual strain measurements in geomaterial exists indicate grain-scale stress magnitudes for samples in static equilibrium ranging up to 50 MPa (Schäfer, 2002; Scheffzük et al., 2000). These and further measurements confirm that near-surface, not all locked-in strains are relieved or redistributes even over geologic time scales.

Eisbacher & Bielenstein (1971) and Friedman (1972) suggest a "storage-time" of residual strains or recoverable elastic distortions in strong quartzose quartzite rock of at least 10^7 years, up to 10^9 years. This implies that rocks have a fundamental long-term strength as well as volumetric stored strain energy which cannot be neglected (Engelder, 1993; Friedman, 1972; Xu et al., 2012). The rates and mechanisms of the time-dependent relaxation of residual strains in rocks are not in-depth understood. Inelastic micro-processes, like slip along microcracks or the migration of dislocations in individual crystals, are presumably responsible for the relaxation and thus their rates (Holzhausen & Johnson, 1979). This is discussed further in **Chapter 2.3**.

Taking into account both internal and external stresses and conditions as well as memory properties, we can gain a better understanding of relevant mechanisms and characteristic modes of response.

2.3 Mechanisms of progressive rock failure

Given the long reoccurrence time, field-based investigations of progressive rock slope damage and failure are difficult. Under such constraints, laboratory-based analogues models present a valuable tool. Experiments are also based on micromechanical models and concepts. The basic fracture mechanics concepts, which are at the core of progressive rock failure are subcritical crack growth mechanisms. Here the prefix "subcritical" refers to the velocity at which they progress.

Experimental rock deformation provides us with several ways to investigate time-dependent rock deformation. Two main types of experiments can be distinguished. First experiments that are driven by constant strain rate, in which stress or stress intensity varies as a result of deformation or fracture growth. Stress corrosion cracking experiments are commonly run with a constant strain rate. Second, are so-called creep experiments. In creep experiments, deformation and deformation rate vary over time as a result of an imposed differential constant stress (Brantut et al., 2012). Based on observed macroscopic strain-time behaviour of rocks schematic creep curves like in **Figure 2.3.1** are established. Such creep curves have commonly been described as exhibiting three phases: (i) an initial decelerating stage, termed primary creep, (ii) followed by an apparent constant strain rate stage, termed secondary or steady-state creep, and (iii) finally an accelerating tertiary creep stage, after which the sample fails. Because a distinction between primary and secondary phases is not given, they are sometimes combined in one phase, called transient creep (Cruden, 1970). It is apparent from **Figure 2.3.1** that the rock experiences a wide range of strain rates as deformation proceeds. A modification of creep experiments are fatigue experiments, in which repeated cycles of loading and unloading, at a maintained constant stress cause deformation and damage (Attewell & Farmer, 1973; Costin & Holcomb, 1981; Ko & Kemeny, 2013).

Most rocks accommodate applied stresses in a brittle manner through cracking, fracturing and faulting, depending on the stress regime and environmental conditions. Such cracks can grow at all scales from the micro scale to the crustal scale, and under different stress regimes. At and near the Earth's surface the stress regimes are both tensile and compressive. Under tensile stress, single, long cracks tend to grow at the expense of shorter ones. By contrast, under compression, deformation of rocks proceeds by the progressive growth and coalescence of many microcracks. This has been illustrated in a schematic uniaxial compression experiment

by Martin & Chandler (1994, **Figure 2.3.2**). The schematic experiment shows that under nominally dry environmental conditions and rapid stress-controlled loading, crack growth is primarily governed by the applied stresses. At the microscale, the crack growths under tensile stress and is controlled by the stress intensity at crack tips (Brantut et al., 2012, 2013). In time-dependent experiments the crack growth is primarily governed by the crack growth itself. Mechanisms and conditions that facilitated subcritical crack growth are introduced in the following section.

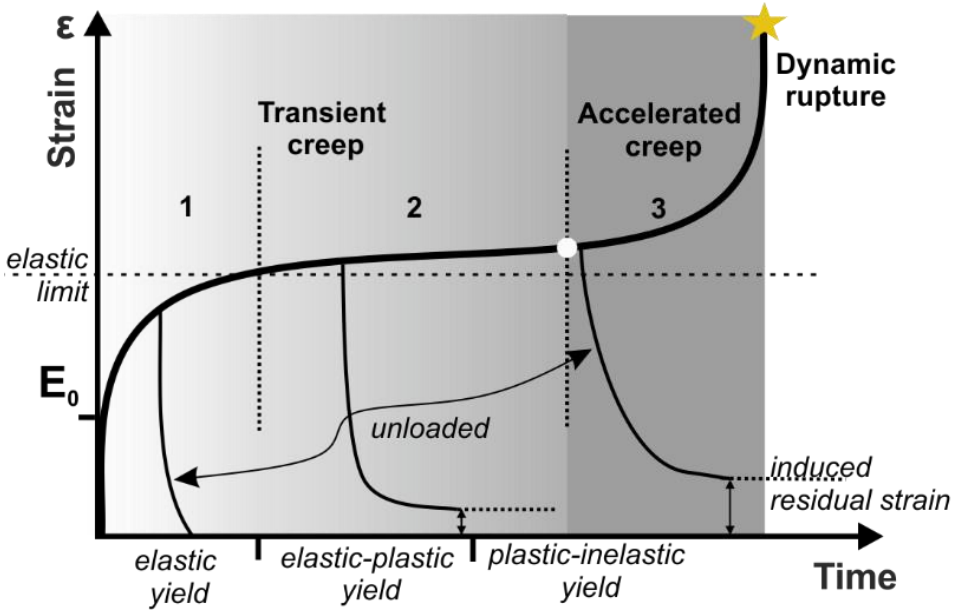

Figure 2.3.1 Schematic creep curve (after Voight, 1966)

The manner in which macroscopic fractures nucleate and propagate through intact rock is a function of its material properties and the external loading acting upon it. Usually, the fracture of brittle rocks results from the coalescence and growth of microcracks and micro-defects (Hoagland et al., 1973; Kranz, 1983; Turcotte & Shcherbakov, 2006). At the most fundamental level, the accumulation of damage through crack growth reflects the breaking of atomic bonds (Amitrano, 2006; Hatton et al., 1993; Main et al., 1994; Marder & Fineberg, 1996). Microcracks form and propagate, when local stress exceeds the local strength, and therefore result from either a local stress increase or strength decrease (Simmons & Richter, 1976). These properties that control the local strength and stress are, in turn, a result of the physics of the materials and applied stresses. They contribute to the microstructure of the rock material, which directly influence the transmission, distribution and concentration of elastic strain energy (stress) in a material (Gerber & Scheidegger, 1969; Hoagland et al., 1973; Kranz, 1983; Potyondy, 2007). This phenomenological scheme of feedbacks in **Figure 2.3.3** can be applied to all scales but the constituents that resembles stress or strength of a material vary. Laboratory experiments concerning the microscale allow us to relate stress and strain, environmental conditions and material properties to the rheological behaviour and damage pattern that progressively leads to localized macroscopic fracture.

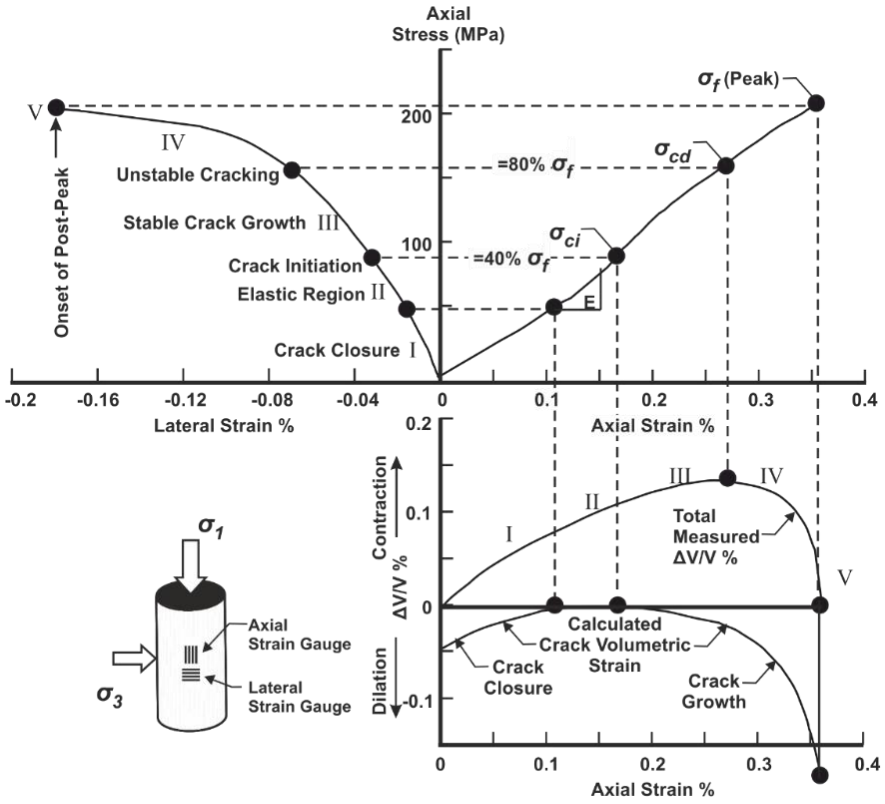

Figure 2.3.2 Stress-strain diagram obtained from a single uniaxial compression test for Lac du Bonnet granite showing the definition of crack initiation, crack damage and peak strength. Note only the axial and lateral strains are measured. The volumetric strain and crack volumetric strains are calculated (redrawn, Martin &Chandler, 1994)

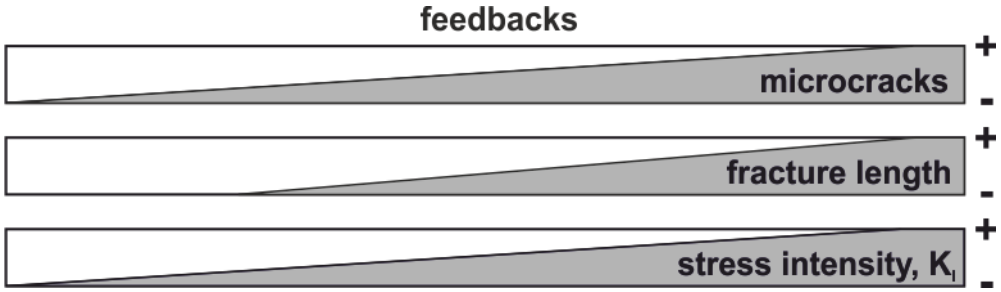

Figure 2.3.3 Feedbacks in creep experiments

2.3.1 Subcritical crack growth mechanisms

Several mechanisms have been associated with the progressive degradation of bedrock, subsumed under the term subcritical crack growth (Atkinson, 1984; Brantut et al., 2013). Subcritical refers to the velocity at which some crack extents. To establish a mechanistic model a single crack is often considered. The basis for many existing micromechanical models of fracture growth is the Griffith criterion. It has been defined in terms of energy (**Figure 2.3.4**) or stress (**Figure 2.3.5**). The Griffith criterion can be described following Parks (1984) is: the energy needed to extend a crack - an ideal brittle solid - is the energy needed to rupture the cohesive bonds between two planes of atoms in the structure. This means twice the surface

energy of the fracture plane. **More comprehensively, the energy or stress needed to extend the length of a crack decreases with the length of the crack.**

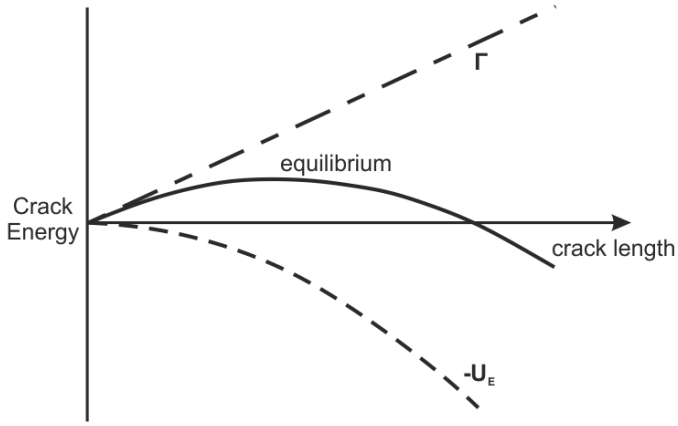

Figure 2.3.4 Griffith criterion (after Parks, 1984)

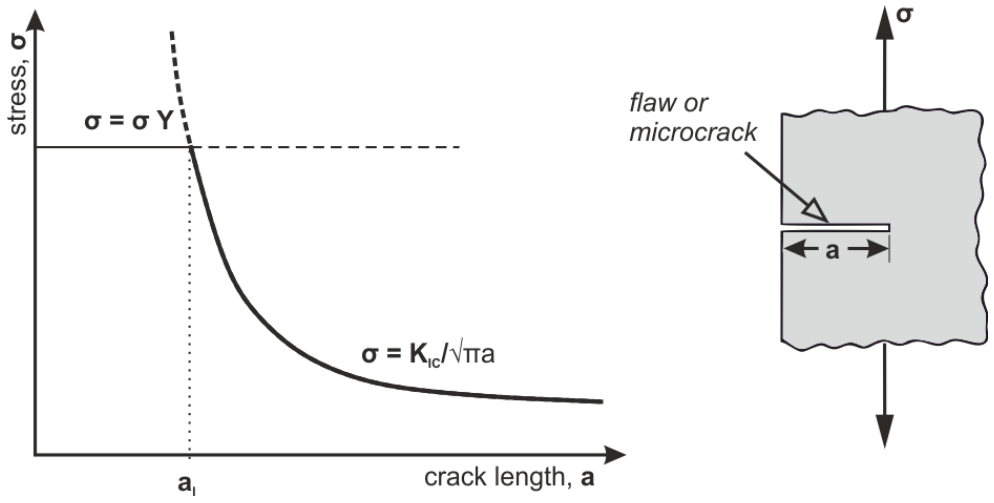

Figure 2.3.5 Griffith criterion (after Lawn, 1993)

Subcritical crack growth is influenced by several macroscopic and microscopic, internal and external factors, which vary depending on the particular mechanism involved (Atkinson & Meredith, 1987). These factors include (i) the stress intensity and concentration, (ii) temperature, (iii) chemical activity and kinetics, (iv) pressure state, (v) rock microstructure, e.g. grain size and morphology, preexisting pores, flaws and microcracks, preferred orientation and heterogeneity in structure and composition (Cai et al., 2004; Hoagland et al., 1973; Kranz, 1983), and (vi) residual strain (Atkinson & Meredith, 1987).

Enhancement of subcritical crack growth is observed if the rock or fracture is exposed to environmental conditions, especially water (Atkinson, 1980; Grgic & Giraud, 2014; Nara et al., 2011). This chemo-mechanical enhanced subcritical crack growth is termed stress corrosion cracking.

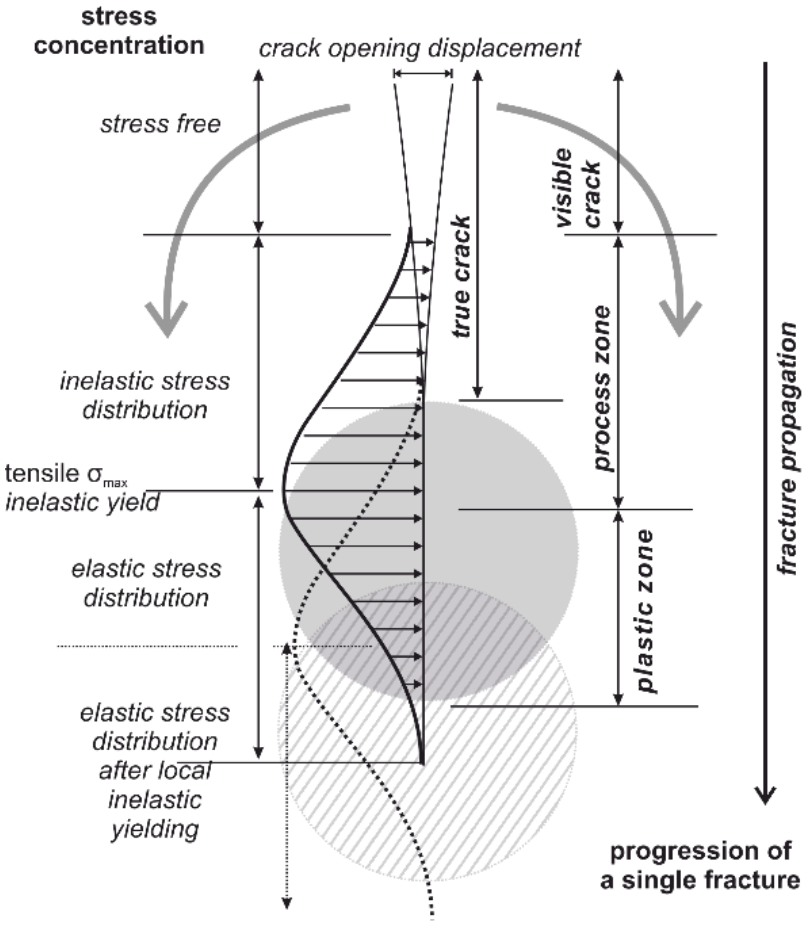

Figure 2.3.6 Schematic of crack extension under tensile stress. See text for details.

Subcritical crack growth mechanisms progressively damage and fracture rocks twofold. First, subcritical loading leads to stress concentrations and crack nucleation at microstructural flaws. If the stress concentrations exceed the local tensile strength the crack can propagate by which it self-reinforcing the stress concentration. The separation of one bond then transfers the stress concentration to the next bond, strains it, and is positively reinforced as microcrack coalescent and the fracture progresses in length (Atkinson & Rawlings, 1981; Lawn, 1993). This defines the process zone (**Figure 2.3.3**). Secondly, plastic and inelastic damage accumulation at and ahead of the actual fracture, defined as the plastic zone (**Figure 2.3.3**) progresses the material towards higher susceptibility to environmental forcing. Subcritical crack growth strongly interacts with the microstructure of rock, exploiting existing cracks, flaws, and interfaces and is thus likely influenced by the residual strain state (Goodfellow et al., 2016; Putnis, 2014; Whalley et al., 1982). It has been suggested that macroscopic fracture propagation, orientation, and arrest is controlled by residual strains (Friedman & Bur, 1974; Friedman & Logan, 1970; Gallagher et al., 1974). Residual strains are also assumed to contribute to the energy balance at the tip of a propagating fracture, a key control in chemically-enhanced subcritical crack growth (Lawn, 1993; Toribio, 1998; Withers, 2007). By accumulating inelastic and plastic deformations subcritical crack growth, in turn, alters the strains state of the material (Atkinson, 1984; Brantut et al., 2014).

2.3.2 Stress corrosion cracking

Chemo-mechanical interactions of water at a stressed material bond, have been found to reduce the brittle fracture strength, in general (Lisabeth & Zhu, 2015; Whalley et al., 1982), increase subcritical fracture propagation velocities (Parks, 1984) and reduce the apparent fracture toughness (Atkinson, 1979a; Atkinson & Meredith, 1981). Stress corrosion cracking combines different micro processes were a stressed bond is chemically altered. As water reacts and dissolves all minerals, to a certain extent (Lawn, 1993; Adolphe Nicolas, 1986; Winkler, 1975), is mobile and phase transition is accompanied by energy uptake as well as release, the chemical kinetics are strong (Grgic & Giraud, 2014), but also divers (Dove, 1995; Peck, 1983; Røyne, Bisschop, et al., 2011). Suggested chemical kinetics range from simple dissolution, as has been reported by (Wiederhorn & Bolz, 1970), to adsorption of hydrogen ion and thus hydrolysis and embrittlement (Michalske & Freiman, 1982), or reduction of surface energies by diffusion (Dunning et al., 1984), hydroxide ion or electrolytes in the fluid, reducing cohesive forces (Parks, 1984). The single chemo-mechanical processes, cannot be ascertained easily and might be coexistent (Atkinson & Meredith, 1987; Bergsaker et al., 2016).

Stress corrosion cracking has been phenomenological described in different formalisms. (Atkinson, 1984) and (Lajtai & Bielus, 1986) adopt the Charles Law to explain the crack velocity of subcritical crack growth as a function of fluid pressure, temperature and stress intensity factor, while (Dunning et al., 1984) assign the subcritical process to the weakening effect of surface energy reduction. A further explanation is based on thermodynamics using an energy balance approach related to the Griffith concept of single crack extension (Darot & Gueguen, 1986; Lawn, 1975). This concept, based on an interatomic energy balance, assumes an activation state or energy level which corresponds to the situation where the bond, at the (atomically sharp) crack tip, is strained up to its limit of rupture. In the presence of a fluid phase, e.g. water, adsorption at the flanks of the cracks take place (Darot & Gueguen, 1986), the adsorptions of the H and O atoms to the crystal structure modifies the bond energies and consequently the energy barrier to rupture (Darot & Gueguen, 1986; Michalske & Freiman, 1982).

The assessment and measurement of stress corrosion cracking stems from material sciences and has been focused on external controls. Tests seek to isolate factors controlling the rates of stress corrosion leading to enhanced subcritical crack growth and consequent failure. To assess the “when” something happens rather than “why”, experiments are performed stress controlled to quantify the relationship of crack velocity and applied stress intensity K_I. Additionally, environmental conditions are varied in the concentration of the fluids or vapour as well as in temperature e.g. (Nara et al., 2011, 2013; Rostom et al., 2013; Røyne, Bisschop, et al., 2011). Usually tests are conducted in laboratory environments at very small scales, single crystal specimen (Røyne, Bisschop, et al., 2011) or small specimen (Ko & Kemeny, 2013), and last for somewhere between a few minutes and several days in double torsion e.g. (Atkinson, 1979a; Darot & Gueguen, 1986; Meredith & Atkinson, 1983) or bending(ref). From the experiments, a phenomenological three stage model has been established to describe the relationship of stress intensity K_I (or mechanical-energy release rate G) and crack velocities subject to environmental conditions (Atkinson, 1979b, 1980; Brantut et al., 2013; Darot & Gueguen, 1986; Ko & Kemeny, 2013). The model is originally developed to describe stress corrosion in glass by (Wiederhorn & Bolz, 1970) and adopted to rocks by e.g. (Atkinson, 1979a, 1984). Systematic tests exhibited in general an extreme sensitivity of velocity to applied load.

If the applied load is at a significant fraction of the short-term critical stress intensity deformation and fracturing rates increase. This is also true for creep tests under constant loads. In the, so called K-v diagram, the fracture intensity (K_I) normalized by the critical fracture toughness (K_{IC}) versus the crack velocity is plotted (**Figure 2.3.7**).

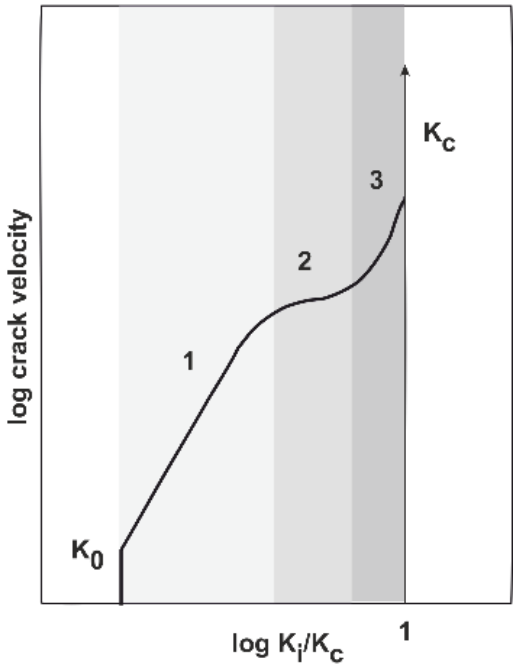

Figure 2.3.7 Schematic crack velocity/normalized stress intensity factor diagramm for stress corrosion cracking (after Ko & Kemeny, 2013)

Three distinct process regimes have been determined within this relationship, governed by different, rate-controlling mechanisms (Atkinson, 1984; Ko & Kemeny, 2013; Lawn, 1993). (i) At stress intensities below what is known as the 'stress corrosion limit' (K_0), no subcritical crack growth is expected (Atkinson, 1984). The velocity of crack growth is attributed to chemical reactions rates at the crack tips following the Charles Law (Atkinson, 1984; Ko & Kemeny, 2013; Lawn, 1993). (ii) Crack growth rates at intensities above this limit (the first process regime) are assumed to be controlled by chemical kinetics at the crack tip (Atkinson, 1984; Ko & Kemeny, 2013; Lawn, 1993). With higher stress intensities, rates of fracture propagation are thought to be controlled largely by the transport of the reactive species to the fracture tip, until (iii) a point at which increasing intensities quickly lead to very high cracking velocities controlled by available mechanical energy (Atkinson, 1984; Brantut et al., 2013; Ko & Kemeny, 2013). The mechanical energy is sufficient to cause and further trigger rupture, characterizing it as a dynamic rupture phase.

In the presence of a chemically active environment, such as water, cracks can grow under low imposed stress conditions $K_I < K_{IC}$ e.g. (Costin, 1983), and while the rate of crack growth can be related to the applied stress intensity factor in glass (Wiederhorn & Bolz, 1970), single quartz crystals (Dove, 1995), and high silica content rocks with (Anderson & Grew, 1977), most rocks do not show the classic three stages velocity curve of crack propagation (Waza et al., 1980). Region two, transport limited velocity, even though observed in some glasses and ceramics, is rarely seen in rocks (Ko & Kemeny, 2013) and there is no indication of a minimum stress intensity threshold for stress corrosion to occur in rock (Costin, 1983). It

seems likely that some degree of stress corrosion will occur whenever tensile stresses are present. Although little data exists, and rates are likely to vary by as much as an order of magnitude, (Costin, 1983) suggests that rates may be less than 10-8 m/s when $K_I < ½ K_{IC}$ irrespective of the chemical environment. The subcritical crack growth or stress corrosion index n varies with moisture, water chemistry and temperature. According to Atkinson & Meredith (1987), the stress corrosion index for rocks ranges from 8 to 169, due to varying conditions but also amongst samples.

Water weakening and plasticity

Besides the chemical effectiveness of water at stressed bond, an overall weakening effect of water in bedrock is observed. The presence of water not only alters the macroscopic deformation mechanism, e.g. change the overall strength of bedrock, effective pore pressure as well as to alter velocities of dynamic elasticity measurements (Grgic & Amitrano, 2009; Turk & Dearman, 1986); but cause crystal plasticity at low temperature and pressure in calcites (Winkler, 1975). Especially the weakening effect of enhanced crystal and grain boundary plasticity has been extensively studied for high pressure and temperature regimes (Griggs, 1967; Kekulawala et al., 1978; Rutter, 1974). About the alteration of the elasticity of rocks and grains as the crystals are soaked in water at ambient temperatures and pressures, it is less known.

Crystal plasticity is even more activated if a fluid is present, which acts as a lubricant; enhancing preferentially intracrystallite movements on cleavage and twin planes (Winkler, 1975). If the material is already embrittled by the presence and adsorption of water, this strain energy cannot be absorbed by plastic deformation ahead of the crack, but the energy is aggregated and leads to failure of the bonds and further to the enhanced brittle fracture propagation. Likewise, a reduction of friction along grain boundaries and crystal interfaces in saturated rocks has been observed by (Baud et al., 2000; A. Nicolas et al., 2016), enabling intergranular slip and glide. Further effects of water on the mechanical behaviour, like the Rehbinder effect, are discussed in the publications (**Chapter 4.1** and **Chapter 4.2**).

2.3.3 Inducement and relaxation of residual elastic strains

Residual elastic strains have been identified as another possible control of subcritical crack growth in geomaterials (Atkinson, 1984, 1987). A relationship which is well-known and investigates in material sciences (Caron et al., 2004; King et al., 2008; Withers, 2015). Both, the inducement and the relaxation of residual elastic strains have been related to inelastic deformation. **The production of a new surface, e.g. by crack growth releases stored elastic energy. The relaxation of previous contraction elastic strains by brittle fracturing or plastic deformation can induce or lock-in extensional elastic strains.**

In general, it is assumed that stored strains in rocks can be relaxed when grains or crystals are freed from the neighbouring constraints (Friedman, 1972). This can be achieved by the opening of microcracks, but also by grain boundary glides and chemically altered grain boundary cohesion (Engelder et al., 1977; Luzin et al., 2014; Silberberg & Hennenberg, 1984). Spatial direction and relative magnitudes of residual strains are controlled by the presence of microcracks created by tectonic stresses, stress relief, and weathering, which in turn influences the mechanical strength of rock (Hoskins & Russell, 1981). Externally applied stresses causing

any local permanent deformation, by distortion of crystal structure, chemical or thermal cementation, could lock-in elastic strains which would overprint pre-existing residual strains (Friedman, 1972; Holzhausen & Johnson, 1979; Withers & Bhadeshia, 2001). The introduction of residual strains is not necessarily spatially uniform due to (i) heterogeneous yielding and stress concentrations at microstructural flaws, (ii) anisotropic thermal expansion coefficients, and (iii) mechanical or thermal stress gradients (Holzhausen & Johnson, 1979; Timoshenko & Goodier, 1970). Likewise, the relaxation of residual strains is spatially variable (Nichols, 1975). Internal damage state relevant for progressive rock failure occurs due to both, the formation of cracks (i.e. strain relief) and the inducement of especially extensional elastic strain.

Explanations of the nature of induced macroscopic residual strains often adduct the mechanical bending of a beam (Holzhausen & Johnson, 1979). We also use a bending configuration in the creep experiments, their set –up is reported in **Chapter 3.2**. It can be assumed that the bending of the beam by a momentum M results in local plastic and elastic yielding (Jaeger et al., 2007; Timoshenko & Goodier, 1970, **Figure 2.3.8**). Upon unloading, only the elastic part of the deformation is recoverable, where it is not obstructed by inelastic, brittle (i.e. microcracking, grain boundary slide), or plastic (i.e. grain boundary glides, dislocation built-up) deformation (Holzhausen & Johnson, 1979; Hudson et al., 1973; Withers, 2007). Following beam theory, it is expected to find different magnitudes of induced residual strains depending on the position along an axial gradient perpendicular to the bending axis and the intermitted stress associated deformation (Holzhausen & Johnson, 1979; Timoshenko & Goodier, 1970, **Figure 2.3.8**). The limits of elastic and plastic deformations and thus the inducement of strains depend on (i) the material elastic range, i.e. Poisson ratio, (ii) environmental condition, i.e. temperature or saturation, as well as (iii) duration, magnitude, frequency (static or dynamic) and mode of loading (Covey-Crump et al., 2006; Logan, 2004; Ramsay, 1967). Macroscale inelastic and plastic deformations are facilitated by subcritical crack growth at the microscale, which can coalescence and form a progressive fracture.

In this example, of macroscopic residual strains, all elastic energy is released upon unloading. That during the mechanical loading also residual strains are locked-in, is in engineering materials described as the Bauschinger effect (Huang & Cui, 2006; Kassner et al., 2009). It is an observable “back-stress“, upon unloading beyond the initial state. The reason for this is that locally, at the microscale elastic strain energy are not balanced due to locking-in, independent of the global macroscopic stress state. Therefore, on the microscale, upon unloading, some of the elastically compressed grains will be able to expand and give up their stored elastic energy and dilate elastically, grains elastically elongated will be able to contract elastically again. However, many of the elastically compressed or elongated particles will be trapped by surrounding matrix and adjacent grain networks and can only release their stored elastic energy if the surrounding grains are rearranged simultaneously. To rearrange the surrounding grains to release the stored elastic strains, dissipative mechanisms, in the form of brittle deformation and plastic strains are needed. Thus the magnitude of this trapped or locked-in elastic energy is governed by the inelastic mechanisms. Progressive damage and fracture can thus be controlled by local residual strain states. The rate and magnitude of the release range from critical sudden burst to subcritical time-dependent mechanisms (Bain, 1931; Nichols & Abel, 1975; Nichols & Savage, 1976). Thermal stresses can also relax and induce residual elastic strains (Luzin et al., 2014).

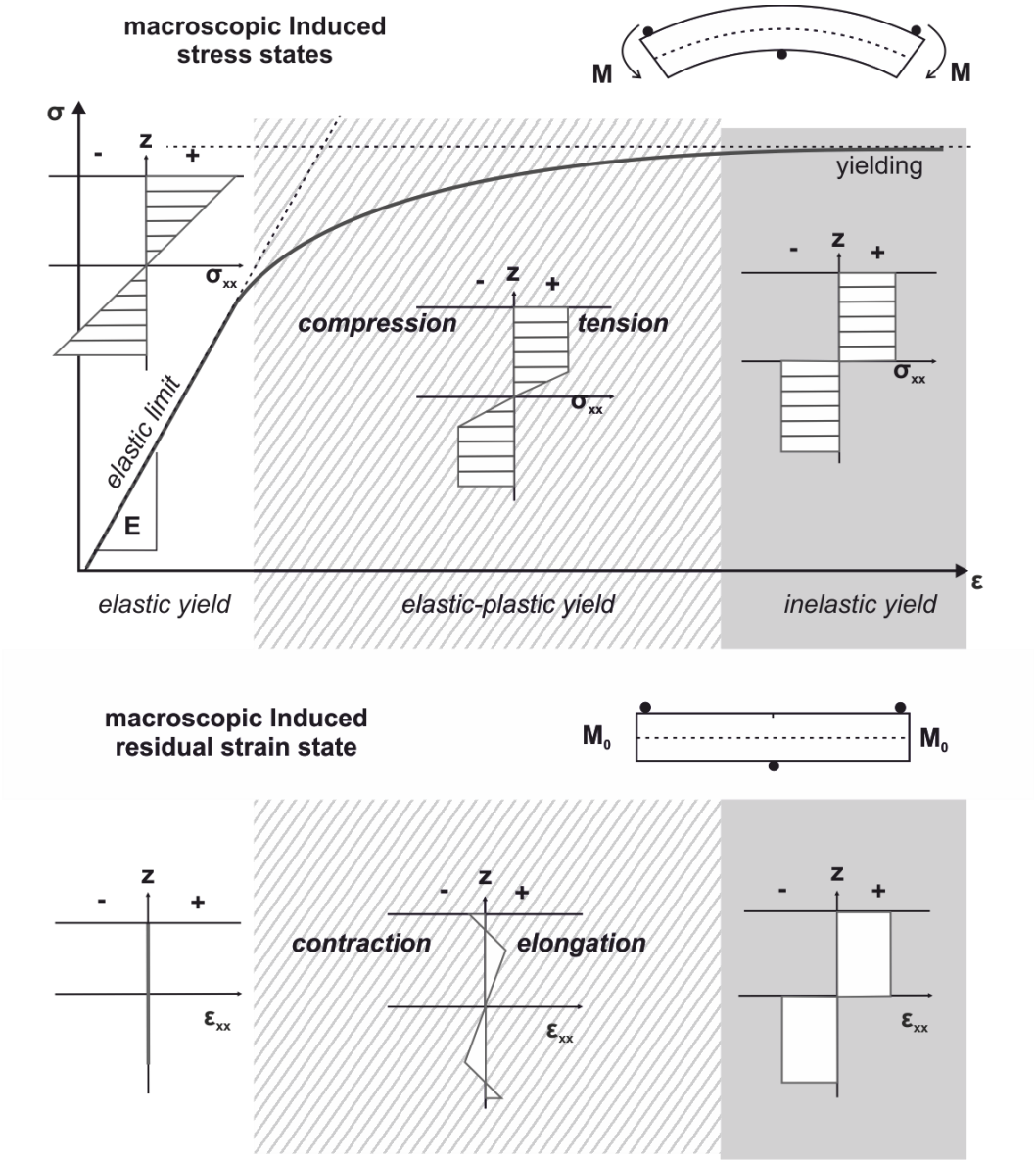

Figure 2.3.8 Schematic illustration of induced macroscopic residual strain in a bent beam (after Timoshenko & Goodier, 1970)

Induced residual elastic strains in engineering materials and resultant behaviour are well studied and used. For example, toughening of glass by tempering, which induces highly compressive strains at the surface or pre-stressed concrete, which cures under compressive forces to counteract tensile stresses, which they are subject to during their lifetime (Withers, 2007; Withers & Bhadeshia, 2001). Enabled and encouraged by measurement technologies from material sciences, such as neutron or X-ray diffraction, residual strains in geomaterials, as well as their effect on the mechanical properties, have gained attention in recent years, especially in the subsurface and fault zones (Chen et al., 2015; Cheung et al., 2017; Hsieh et al., 2015; Kunz et al., 2009). The control of the internal strain state of bedrock on (near) surface processes is to our knowledge not well invested. In the context of progressive rock failure, we suppose that a less contractional internal elastic strain state and the localized accumulation of inelastic strains, ease further degradation and damage by external extensional, thermal or mechanical stresses.

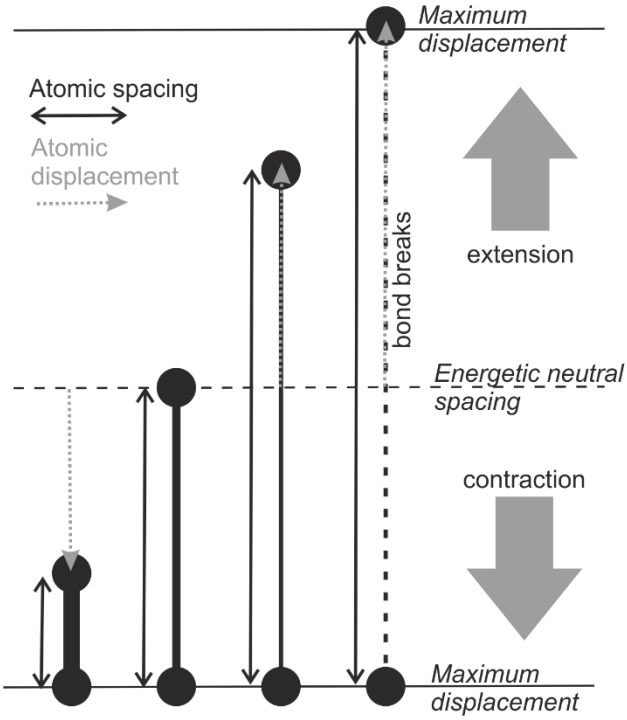

Figure 2.3.9 Schematic of elastic strain rheology at the crystal lattice

Residual strains also affect the rheology of rock (Holzhausen & Johnson, 1979; Voight, 1966). It is reasoned, that the strain magnitude and sign reflect the interatomic spacing, thus the spatial array of atoms in the individual crystal lattices, and their energetic states (Withers & Bhadeshia, 2001). **Figure 2.3.9** shows this schematically. The amount of compressive stress or contraction that atomic bonds can repulse before breaking defines the maximum compressive strength of the crystal and is consequently related to the overall polycrystalline strength. Likewise, the amount of tensile stress a bond can support defines the maximum tensile strength of the material. **Therefore, the elastic strain state of crystal lattice planes (i.e. the energy or spacing of bonds) should define the possible response of rocks to applied external forces, including bulk fracture toughness or strength.**

To exploit the concept of residual elastic strains in rock, both as a proxy for the internal state and control of subcritical crack growth we need to know how to measure them. **Chapter 3** introduces the used material and methods including, neutron diffraction techniques.

3. Material and Methods

The objectives of this thesis, to better understand progressive rock failure, I approached by a series of laboratory experiments. I have focused on 'how rocks break' – in principle. The applied methods are classical and adapted standard rock mechanical tests in combination with techniques from material sciences, namely neutron diffraction to assess the material state and progressive damage states. The laboratory experiments are as analogies suitable, but cannot readily be extrapolated in time and space. A direct application to real cases such as progressive rock slope failure or assessment of structural performance e.g. of infrastructure or sculptures would have been beyond the scope of the thesis project.

As for most of the conditions, responses and aspects of progressive rock failure explored here fundamental knowledge is missing the material used for the experiments to be kept as simple as possible. The demand of a natural, widely homogeneous, isotropic, monomineralic rock, whose rheology had been assessed before was matched by the famous Carrara marble.

Carrara marble is a metamorphic rock. It consists of fine-grained, very homogenous near monomineralic calcite (> 98 % CaCO3). The exemplary properties of Carrara marble favour consistency and repeatability in rheological studies, which has also led to its popular use in arts, architecture and scientific studies (Atkinson, 1979b; Siegesmund et al., 2008). Due to its near-pure calcite phase, distinctive diffraction patterns are formed which enables the straight forward application of diffraction methods. Next to these favourable properties, Carrara marble is also known for its susceptibility towards environmental conditions and stresses. This is evident in previous laboratory studies, natural outcrops, building facades and structures as well as sculptures, like Michelangelo's David statue (Borri & Grazini, 2006; Coli et al., 2010; Rayleigh, 1934; Siegesmund, Ullemeyer, et al., 2000).

As such, Carrara marble offers an excellent model rock to gain clear insights into environmental, external and internal controls of its rheology and enables to explore methodological techniques to quantify the state of the rock and its response to external forcing. All, here reported experiments have been conducted using Carrara marble. Carrara marble is introduced further in **Chapter 3.1**.

The methods employed here measure the properties, response or resulting features of the rock. They are selected to provide insights into the internal state, subcritical crack growth mechanisms and the response to external conditions. Standard, rock mechanical testing of rock is in regard to applied loads. Commonly short-term test to define the intact rock strength, as progressive rock failure is the inverse of long-term strength, the main focus is on long-term or creep experiments. **Chapter 3.2** gives an overview of available mechanical long-term or creep experiments to test for time-dependent behaviour. When planning experiments certain terms and conditions are useful as guidance. These standard tests enable a comparison of data. Experiments within rock mechanical frameworks allow relating observations to existing models. It also provides the framework of what might need to be adapted, altered and modified. As these experiments reported in **Chapter 4.1** have not been run before standard short-term strength and stress intensity assessments of water-saturated Carrara marble samples have been conducted to infer a baseline.

Some of the setups are subjected to environmental condition but more often tests towards environmental conditions, such as freeze-thaw, insolation or saturation are run independently of mechanical loads. A different suite of test setups focusses on combining

environmental and stress enhanced measurements. To follow the reasoning of the adaptation of the standard tests reported in the publications in **Chapter 4.1** and **Chapter 4.2**, these stress corrosion cracking methods summarized in **Chapter 3.3**.

The aforementioned methods and setups are designed to assess the effect of external stresses and conditions on the rock. The observations are also external. The interpretation of the behaviour and properties are based on indirect terms or posthumous analysis of optical analysis like thin sections microscopy. As being reasoned in **Chapter 1** and **2**, our knowledge of the internal state and how it is altered by progressive damage is very limited.

To enhance our knowledge especially on the internal strain state, the introduction and relaxation of strains in the rock (**Chapter 2**) inherited residual elastic strains have been identified as a possible proxy. To measure residual strains several methods are available which are introduced in **Chapter 3.4**. Due to the laboratory scale, we can use material science techniques to assess the structure and state of the rocks. In this thesis, I, therefore, made use of neutron diffraction techniques, which in geosciences is still underemployed. The general methods and the current limited application of neutron diffraction in geosciences are compiled (**Chapter 3.4.1**). Neutron diffraction has not been applied in an integral approach on how the material properties preconditioned due to its formation pose a control on the performance or response of the material to environmental stresses. The measurement procedure and data analysis are explained in **Chapter 3.4.2** using the example of the SALSA Diffractometer utilized in the publication in **Chapter 4.2**.

Further standard methods deployed to characterize rock properties and rheology have been, for example, thin-section microscopy, Scanning Electron Microscopy imagery, and goniometry (Crystallite Preferred Orientation), short-term strain/loading rate controlled strength tests. They are considered standard and auxiliary and not described in detail here.

In summary, the methods and the choice of materials used in this thesis are based in, and are valid for, the following assumptions and simplification:

(i) Limiting the assessments to an endmember lithology, a metamorphic near pure calcite rock, Carrara marble, enables to exclude compositional or structural inhomogeneity and allow neutron diffraction techniques straight forward. This exemplary rock is suitable for repeated mechanical testing as well.

(ii) Tensile mode I fracture stress and extensional strains are the most likely to promote and facilitate progressive damage, at and near Earth's surface. Especially where they can concentrate on the given geometry they promote the initiation and progression of a single macro fracture. Classical single-edge notch three-point bending test provide the predictable location of single fracture development in an extensional stress field.

(iii) Progressive damage conditions can be represented by constant stress experiments. Loading of a fracture in nature would be constant with time and subcritical. Therefore, creep experiments have been deployed. To be able to test several samples at the same time and with a constant load a simple dead weight lever arm system was chosen.

(iv) To compensate for the long-term testing and still limited number of samples that can be tested, experiments were performed as stepped creep tests at several load levels.

(v) Environmental conditions which affect rocks, besides temperature changes, are moisture or saturation changes (see **Chapter 2.2**). The focus here is on endmember air dry and wet (introduction of water) conditions.

(vi) The idea is to mimicking joint or fracture and the extensional stress field at the near-surface. To potentially have a water-filled joint, a requirement for the set up would be an upright notch. For this, a standard rock mechanical test set-up was inverted and samples and monitoring equipment adapted to wet conditions.

(vii) To be able to focus on the controls of stress corrosion in natural environments the reactivity of the fluid was held constant. To limit the dominance of chemical reactions, especially dissolution, water was calcite saturated, similar to what would be expected in natural settings (**Chapter 2.3**).

3.1 Material – Carrara marble

Carrara marble is a fine-grained, near pure calcite, metamorphic rock. Carrara marble was formed during the Apennine orogeny (Cantisani et al., 2009; Leiss & Molli, 2002). Lower to middle Liassic carbonate platform sequences were deformed and metamorphosed under greenschist facies conditions (Oesterling et al., 2007). They are exposed in the Carrara nappe as a tectonic window in the Apennine Alps (Leiss & Molli, 2002). For detail of tectonic history and microstructural evolution of Carrara marble the reader is referred to Molli, 1998; Molli et al., 2018; and Molli & Meccheri, 2012. Due to its bright, pure white tone, compactness and workability Carrara marble has been quarried for more than 2000 years. It has been used for cladding and facades, interior design, infrastructure and was highly appreciated by sculptures. Like many other artists, it is told that Michelangelo came to Carrara to obtain the marble used in his works. Sculpting full-size figures from single blocks, like his David statue (**Figure 3.1.1**) required knowledge of the material and choosing of the right blocks. Getting the Carrara marble used in the experiments in Carrara enabled a visit for me to the quarry, as well. The quarrymen told the story that for example Michelangelo would observe how the block was freed from the confining rock and check whether fractures would emerge during this process. He considered this first phase of choosing the material essential to the creation of his masterpieces. Still today rock blasts have been observed after unloading samples or cutting them free. The in-situ stress state has been investigated through numerical models to anticipate the spalling and unprecedented failure of Carrara marble (Ferrero et al., 2013). But most insights of the rheology in the quarry is unformalized, tacit, and passed on knowledge of the quarrymen. Previous residual strain measurements on Carrara marbles have affirmed the presence in the order of –400μstrains due to their metamorphic history (Scheffzük et al., 2004).

Because Carrara marble has been used for many sculptures and architectural sites, multiple studies have been concerned with the preservation of it. In studying how it can be preserved, progressive deterioration and weathering are assessed by investigating the material properties. Observed features, related to weathering of Carrara marble, have been warping and bending of slabs, dissolution pits and grooves, mineral replacement, as well as decohesion and disintegration of grains. They have been related to the escharotic nature of calcite, especially subject to anthropogenic environmental pollution such as acid rain, its anisotropic thermal expansion coefficients facilitating thermal stress built up and its microstructure of weakly interlocking grains boundaries easing disintegration (Hoke & Turcotte, 2004; Inkpen & Jackson, 2000; Siegesmund, Ullemeyer, et al., 2000; Tschegg et al., 1999; Winkler, 1975).

Figure 3.1.1 Michelangelo's David, wearing nothing but Carrara marble (Borri & Grazini, 2006)

Due to the near monomineralic composition of calcite, chemistry can readily be described by classical carbonic acid reactions (Brantley, 2008). Chemically, the calcite of Carrara marble allows both adsorption and adhesion of fluids by the mixed ionic and covalent bonding (Skinner et al., 1994). Moreover, the mixed bonding in calcite rocks affects the chemical as well as the rheological, plastic and brittle behaviour, as ionic bonds are easy to soluble, low in cohesion, and electrostatically attractive. These ionic bonds tend to favour chemical dissolution (Bergsaker et al., 2016; Rostom et al., 2013) while covalent bonds are strong, susceptible to embrittlement by hydrolysis, and thus generate a brittle behaviour (Dove et al., 1992; Dove, 2003).

For the above-mentioned reasons Carrara marble has also long been used as a model rock in mechanical studies (Atkinson, 1979b; Backers et al., 2003; Covey-Crump et al., 2016; Schubnel et al., 2006). Common short term strength and material properties of Carrara marble are given in **Table 3.1.1** as compiled from literature after Backers (2004).

Table 3.1.1 Material properties of Carrara marble (compiled from literature after Backers (2004))

Uniaxial compressive strength	Tensile strength	Young's modulus	Poisson's ratio	Dry density	Porosity	Fracture toughness
σ_C	σ_T	E	ν	ρ	φ	K_{IC}
[MPa]	[MPa]	[GPa]		[g/cm^3]	[%]	[MPa m$^{1/2}$]
59/101 ± 6	~7	49	0.23	2.7	0.7	2.44 ± 0.07

Carrara marbles have also been tested towards environmental conditions like temperature (Luzin et al., 2014; Rayleigh, 1934) or humidity and water (De Bresser et al., 2005; Winkler, 1996). They have also been used in early studies for the determination of environmentally enhanced subcritical crack growth (Anderson & Grew, 1977; Atkinson & Meredith, 1987; Swanson, 1984). For Carrara marble, recently Nara et al. (2017) determined an average subcritical crack growth or stress corrosion index of n=77 ±4, tested in air at 293 K or ~20°C, and 47% relative humidity (rH) and n=82±10 at 324 K or ~51°C, and 49% rH, and a markedly lower index tested in water of n=33 ±3 at 290 K or ~17 °C and pH 8.2, and n=33 ±7 at 319 K or ~45 °C, and pH 8.0. Crack velocity estimates varied by a magnitude due to higher temperature in the air tested samples, and by nearly a factor of two magnitudes in the water tested samples. The greatest distinctions in the crack velocities are due to the different environments. In air, rates are in the order of $\times 10^{-8}$ to $\times 10^{-7}$, while in water rates are $\times 10^{-5}$ to $\times 10^{-3}$ (Nara et al., 2017). This remarkable increase in crack velocities in water and the mechanisms related to this are discussed further in **Chapter 4.1**.

Figure 3.1.2 Lorano quarry, Carrara, Italy (credits Kerry Leith)

All of the above-mentioned material properties make explorative experiments with Carrara marble feasible but at the same time, challenging. Choosing the right material and the right block was also essential to the creation of the experiments. All experiments reported here have been conducted on a type of Carrara marble known as “bianco C/D”. The samples are wire cut from a single block from the Lorano quarry, Carrara, Italy (44°5’37’’N, 10°7’11’’E, **Figure 3.1.2**). Thin section microscopy indicates a homogeneous distribution of fine-grain sizes between 150 and 250 µm (mean ~200 µm). Grain boundary geometries in all samples are characterized by straight or slightly undulate grain contacts which are poorly interlocked and commonly exhibit 120° triple junctions. This is typical for Carrara marble and the low degree of interlocking can be considered a principal source of mechanical weakness especially if they are oriented in a preferred spatial orientation (Siegesmund, Weiss, et al., 2000). The grain boundaries in the Carrara marble used here though exhibit an overall random orientation of

grain boundaries. Like a typical marble, lamella and twins are also evident, as well as single grain boundary separation or grain boundary microcracks. Carrara marble exhibits a low initial porosity with a dry density between 2.7 and 2.9 g/cm^3.

The Carrara marble used, is near pure calcite ($CaCO_3$) with < ~1% SiO_2 by volume. This corresponds to one or two rounded quartz grains evident in thin sections (~6 cm^2). Other remnants of minor mineralogical changes in the initial sediment, like pyrite, provide some light grey marbling to the otherwise white metamorphic rock. Texture measurements with an X-ray goniometer indicate a near-random crystallographic preferred orientation (CPO, texture) of all axis and crystal planes, thus the marbling does not exhibit foliation, as it has no signature in the CPO measurements. Aside from any inherited damage, not apparent in macroscopic or microscopic investigations, it is expected that the rheological behaviour of the used Carrara marble is macroscopically isotropic. These characteristics facilitated repeatable, comparable mechanical testing, expectable chemical reactivity and relatively unambiguous neutron diffraction patterns.

3.2 Method I – Creep or mechanical long-term experiments

Only little data exists on progressive rock failure. This is related to the fact that most rock physics and material sciences have preferably been interested in the strength of the material, and only more recently on how it deteriorates. Based on the theoretical considerations in Chapter 2 it can be reasoned that the inverse of progressive rock failure is long-term strength. Hence in most rock strength quantifications, the rock samples are tested for the short-term intact rock strength. The short-term strength is usually quantified in various techniques and modes of loading. Commonly, these rock mechanical tests are run strain or stress rate controlled. In these configurations, it can be insured to sample a distinct rheological pattern in response to the applied conditions. Time-independent strength and other material properties (see Tab.3.1.1) can be inferred with these short-term experiments. And the short duration of the experiments makes replications feasibly.

To observe the time-dependent rheology, creep or mechanical long-term experiments are conducted. The difference to short-term experiments, in which critical or maximum stress can be tested for, is the focus on the strain rate or deformation. The absolute or intact short-term strength is often used as a reference of expected maximum values, as the long-term strength has been reported to be a fraction of this (Damjanac & Fairhurst, 2010). In contrast to short term experiments which are run either loading rate or strain rate controlled, creep experiments run at a constant applied load. Besides creep, long-term strength can be terminated by fatigue. For that high frequent, cyclic loading is applied to rock samples. Especially for engineered infrastructures, subject to vibrations, internal flexure and cyclic stresses fatigue failure can be disastrous, as multiple collapses of bridges and dams have shown. On geological time scales, loads can be approximated to be constant and are continually focussed on.

Usually creep tests are run in compressional test set-ups (Brantut et al., 2014; Diederichs, 2003; Heap et al., 2015; Paraskevopoulou et al., 2015). The progressive failure that is observed during compressional creep tests is related to microfractures that form in indirect tension and resulting fractures are in mixed modes of tensile and shear (see Figure 2.3.2, Martin & Chandler, 1994). The observed creep considers the whole sample and rates are given in bulk. In tensional settings creep experiments assess individual fracture propagation. General sample

shapes and loading configuration, as suggested by ISRM are given in Figure 3.2.1. Cut notches are often used to provide sites of stress concentrations to control where fractures initiate. In quantifying the crack opening displacement the evolution of the fracture toughness and concomitantly the increase of the stress intensity is interfered (Ko & Kemeny, 2013; Perras & Diederichs, 2014). If these tests are run as short-term experiments the critical stress intensity can be determined (Backers et al., 2003).

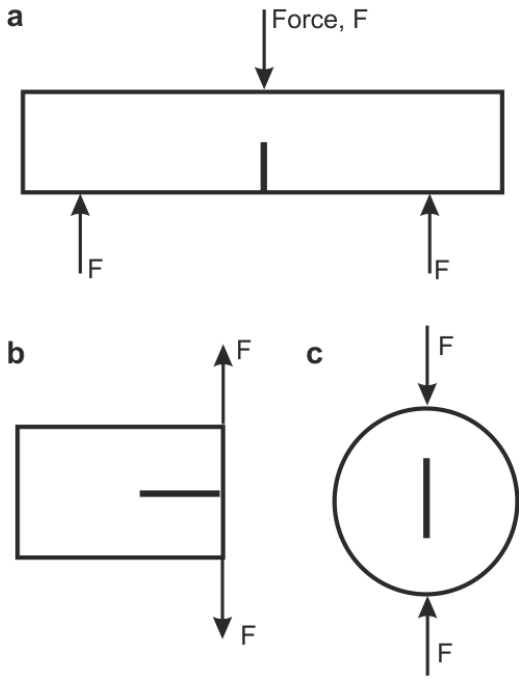

Figure 3.2.1 Schematic sample shapes and loading configuration to assess mode I fracture toughness. **a** notched three-point bending, **b**, torsion, and **c**, notched Brazilian test (after Backers (2004))

To limit the duration of creep test they are commonly run at a high fraction of the short term strength of the rock. Common creep experiments are conducted at a high fraction, of 80-90% of the critical stress intensity K_{IC}, focusing on mechanical analysis of the constant stress-dependent reduction in strength. Bending creep experiment showed that over more than a year the fracture strength in marble decreased by 65-70% due to high constant loads (Garzonio et al., 2000) and 40-60% of decrease by loads of up to 40% of the intact strength (Sorace, 1996). Another way to test the creep rheology at several load levels is to use a stress stepping approach (Aydan et al., 2014; Lockner, 1993). This enables to assess the behaviour of the same sample and its microstructural inhomogeneity at different levels of loads. **Figure 3.2.2** shows schematic stress stepping creep experiment.

Setting up a creep experiment, several presumptions are made about the rheology to be observed. Schematically this is depicted in **Figure 3.2.2**. In the upper panel, the loading is plotted against time. This could be the stress intensity or the uniaxial stress, depending on, in which configuration or mode the samples are tested. In the lower panel the deformational response, thus the strain is plotted versus the time. In the creep experiments, a threshold stress, $\boldsymbol{\sigma_0}$ relating to an instantaneous, thus purely elastic, strain response, $\boldsymbol{\varepsilon_0}$ is assumed. Below this

threshold, no creeping is expected, beyond the sample starts to creep. Practically no data exists on this threshold. The creep rate is related to the loading magnitude. Stepping up the load, like in the schematic **Figure 3.2.2**, would produce an additional creep curve on top of the first one. The creep curve is commonly divided into three stages (**Figure 4.1.1**): (i) Primary creep, which follows the instantaneous strain after loading. In primary creep strain rate increase and then ceases to a near-constant rate. (ii) Secondary creep is characterized by near-constant strain rates. It is therefore also called steady-state creep. This results in a smooth increase of strain with time by the action of plastic and brittle micromechanisms (**Chapter 2.3**). The response of the system is hence delayed. (iii) If a critical level of strain is attained (which is usually unknown) tertiary creep and dynamic rupture commences. This transition is observable in an increase in strain and strain rates, marked by an inflexion point in the creep curve. Creep rates during tertiary creep are driven by the self-reinforcing coalescence of microfractures and macrofracture propagation. Once entered into tertiary creep, failure cannot be prevented due to its highly dynamic nature. Better knowledge of precursors of the dynamic rupture phase would thus be adjuvant to anticipate hazardous rock failures, like in creeping rock slopes or infrastructures. Research, especially on tertiary creep and the prediction of time to failure has been ongoing but still relying on retro-diction (Amitrano & Helmstetter, 2006; Kemeny, 2003; Saito, 1965).

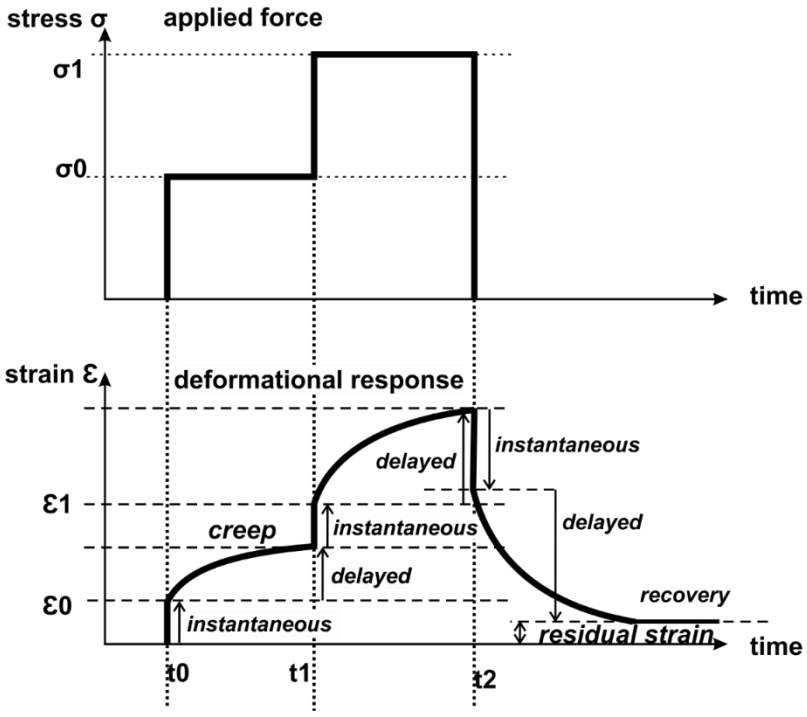

Figure 3.2.2 Schematic stress stepping creep experiment. Upper panel the forcing, lower panel the deformational response. See text for detailed description.

As reported above, we can observe a creeping response of rocks following the application of external force. Creep of rocks can also be observed following unloading. The unloading of rocks can also be divided into an instantaneous and a delayed response (**Figure 3.2.2**). The not recoverable amount of (inelastic) strain, or confusingly also often termed residual strain, can be used as an indicator of the damage accumulated.

Creep rheology has often not only been investigated in regard to mechanical loading but also towards environmental conditions. Largely creep experiments in rock physics, largely tested conditions that mimic solid earth conditions, like high temperature and confining pressures (Brantut et al., 2013; Griggs, 1939; Rutter, 1972, 1974). Realizing that creep or progressive rock failure is likely the cause for deteriorations and natural hazards near or at the Earth surface, experiments are also run under ambient environmental conditions. These experiments demonstrate a decrease in ultimate strength and increased creep rates with increased sample saturation and temperature (Heap et al., 2009; Lockner, 1993). Including environmental conditions in rock mechanical experiments poses several challenges on the objective, feasibility and execution of the experiments. These are introduced in the following chapter.

3.3 Method II - Environmentally conditioned rock mechanical experiments

An exceptional creep experiment under the influence of environmental conditions can be found in Itô (1979). They conducted a dead load bending test on a large granite beam for 30 years and second for three years under constant, high humidity conditions (Itô & Sasajima, 1980). The experiments exhibited maximum strain rates of 10^{-14}/sec (Itô & Sasajima, 1980), which is in accordance with natural strain rates in the earth´s crust of 10^{-13} -10^{-15} /sec (Itô, 1979; Pfiffner & Ramsay, 1982; Zang & Stephansson, 2010). They observed no steady increasing strain but oscillations, e.g. decrease and increase of strain over periods of time (Itô & Sasajima, 1980). An explanation for this 'turn back' behaviour during the creep test they attributed to energy and strain change as cracks forms, but had no measure to prove (Itô & Sasajima, 1980). Even though it is highly respectable to run an experiment for up to 30 or even three years (Itô & Sasajima, 1980), within the scope of most studies and projects this is not feasible. To test for the effect of environmental conditions this is often circumvented by either running the experiments constant strain rate controlled (Atkinson, 1979a; Darot & Gueguen, 1986; Meredith & Atkinson, 1983).

Besides time restrictions, it is also quite challenging to ensure constant loading or environmental conditions for the experiment. To provide constant and homogeneous environmental conditions it is advisable to use small samples. Hence, for most stress corrosion experiments, single crystals or samples of a few centimetres are used, which can be together with the torsion apparatus be fully immersed into a water chamber (Bergsaker et al., 2016; Ko & Kemeny, 2013). A convenient side-effect of the small sample size is that experiments last, only a few minutes to several days in double torsion for example (Atkinson, 1979a; Darot & Gueguen, 1986; Meredith & Atkinson, 1983). Testing at multiple conditions and repetitions thus become feasible. Downsides to the small sample size are the amplification of geometrical and loading heterogeneities, such as grain boundary or sample and crystal geometry (Backers et al., 2004; Grgic & Giraud, 2014). Additional factors such as residual strains or fluid pressure that could provoke further stress concentrations can often not be accounted for in these experiments. Hence a discrepancy between the assumed and applied stress intensity and the effective stress intensity driving the crack velocity occurs (Backers, 2004; Grgic & Giraud, 2014; Withers, 2015). Assessments of the effective stress intensity at a single fracture tip in metals have shown, that relating the applied stress intensity with the response, thus the crack velocity appear foreshortened (Withers, 2015). The benefit of using larger samples is getting a

bulk crack velocity, summing up all heterogeneities like grain boundaries, the downside usually is that only a few samples can be tested.

The experimental setup, time and sample size, of course, restrict the objectives of what can be assessed. The experimental assessment of time-dependent rock deformation has either focused on individual fracture propagation velocity rates with respect to applied stress intensity and environmental conditions (Atkinson, 1984; Ko & Kemeny, 2013; Nara et al., 2013) or, as in creep experiments, bulk strain behaviour at various applied stress levels and environmental conditions (Brantut et al., 2013; Heap et al., 2009; Lockner, 1993). Although changes in fracture propagation velocities are difficult to determine from creep experiments (Atkinson & Meredith, 1987; Ramsay, 1967), these do provide insight into strain rates and processes associated with subcritical crack growth at scales relevant to Earth surface processes and geological timescales. These are though usually loaded in compression, as introduced before.

Environmentally conditioned subcritical crack growth or stress corrosion experiments steaming from material sciences primarily focusses on external factors that control crack velocities and gives less attention to the material properties (King et al., 2008; Lawn, 1993; Wiederhorn & Bolz, 1970). Experiments have been run in various fluids, fluid concentrations and temperatures. It went to such length, that fracture propagation in alcohol was run, which, for geologists and geomorphologists is a somewhat comical testing environment. Overall, these experiments showed that the most efficient environmentally conditioning solution is simply water!

But what do these experiments actually tell us? The assumption is that the reactivity of the material is enhanced by mechanical stress, which in turn leads to crack propagation. Chemically, fracture rate controlled test pose a difficulty as most chemically activated and diffusive processes need an activation time (Orowan, 1944). Especially because common chemical reaction rates are slow (Grgic & Giraud, 2014; Hillner et al., 1992), and even more if the fluids reactive or corrosive potential is low, like in natural environments (Gabet et al., 2006; Küfmann, 2013). Time substitution, by applying constant strain rates, in stress corrosion tests, limit the chemo-mechanical effect to instantaneous surface energy reduction, rather than the often postulated dissolution or hydrolysis kinetics at the strained crack tip, dominated by transport limitation (**Chapter 2.3**). Conceptually, this is problematic for the transfer of results to natural environments in which fractures propagate along grain boundaries over tens, to tens of thousands of years under more or less stable low-stress conditions, where processes can take time, and start to progressively matter over geological times. To observe the chemo-mechanical interactions and feedbacks of stress corrosion cracking, long-term mechanical creep experiments are therefore more appropriate, than short-term experiments.

To be able to assess the influence of the microstructure of the rocks on progressive fracturing few but larger samples were chosen for the in long-term creep experiments (Figure 3.3.1a). To comply with the requirements of mimicking a tensile, possibly water-filled joint from which fracture propagation would be observed, I adapted a classical single-edge notch three-point bending test by turning it upside down. This way the notch faces upwards. To ensure constant load, samples were loaded with dead weights (**Figure 3.3.1b**). The expected stress field during creep and fracture extension at the notch within the beam was numerically modelled in 2D (**Figure 3.3.1c**). It was apparent from this that, even though the samples are loaded stress controlled, and deformation was expected to be time-dependent, one needs to acknowledge that

due to the tensile loading configuration if cracks grew, the stress intensity changed, similar to strain-controlled experiments.

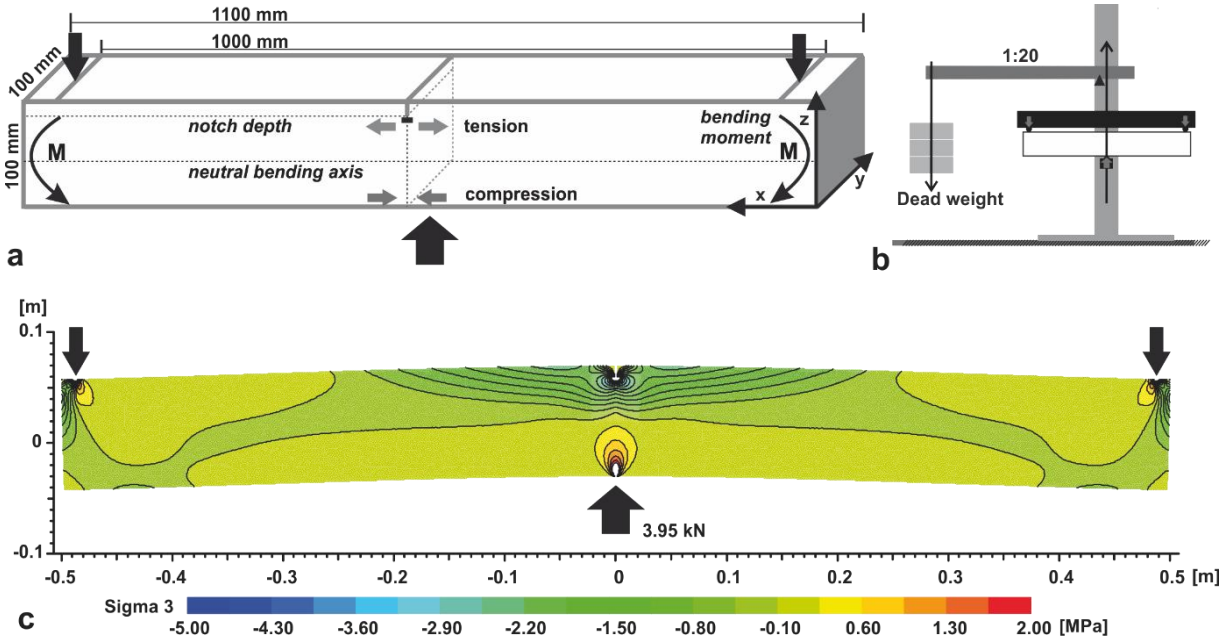

Figure 3.3.1 Inverted single edge notch three-point bending test. **a** Sample dimensions and loading configuration **b** sketch of the testing stand, and **c**, numerical 2D model of the expected stress field within the sample

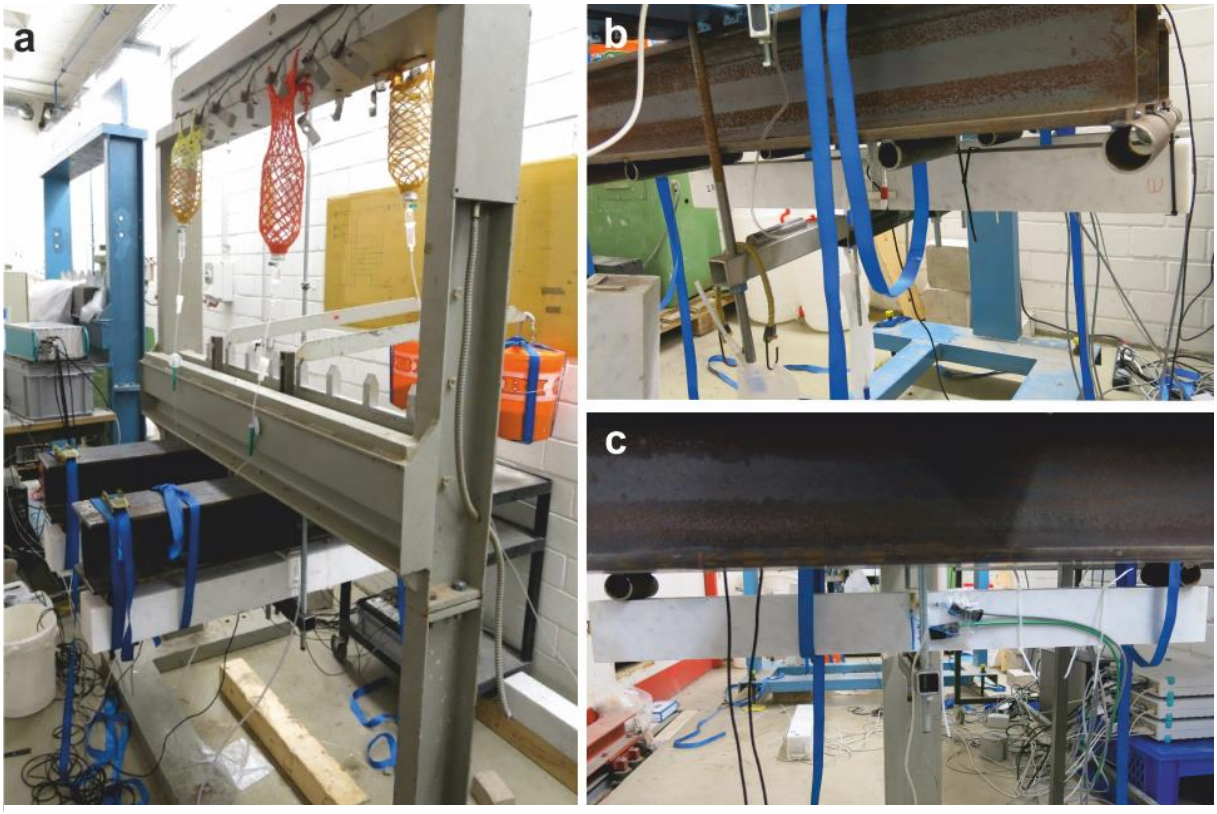

Figure 3.3.2 The actual test stands in the basement of the University of Applied Sciences in Cologne. **a** Load-stand with the water supply and dead weight bucket loading system, **b** and **c** details of loaded samples

Due to the choice of the long-term testing and the large samples size the samples could not be immersed into a fluid as a whole or exposed to thermal changes evenly. Focusing on the single fracture propagation and mimicking an opening joint, water was applied to the notch. Water could diffuse into the sample and was constantly supplied (**Figure 3.3.2**). Acrylic glass covered the top of the notch and sides to prevent evaporation and to keep the notch filled with only supplying water at a low rate to not cause any turbulences in the notch. Details on the set-ups and instrumentation are given in **Chapter 4.1**. Air moisture and temperature were monitored throughout the experiments.

3.4 Method III – Measurement of residual strains

In-situ strains denote those strains, balanced on the large scale. Residual strains remain in a solid material after the original cause of stress, i.e. external stress, temperature gradient or body force, has been removed (Friedman, 1972; Holzhausen & Johnson, 1979). Residual strains in rock develop during exhumation of bedrock changing stress state in the brittle crust (Zang & Stephansson, 2010). Residual strains, in the sense used here, are those strains remaining in the rock matrix after the removal of any far-field stress or traction. In material sciences, it is well known that not all stresses that are applied and transmitted are relieved (e.g. Withers & Bhadeshia, 2001b), in geological material as well (Emery, 1964; Friedman, 1972). This holds not only for inelastic or plastic deformations, where the strain energy is converted in a permanent shape change but also for elastic strain energy, which can be locked in intergranular or intracrystalline in the rock matrix. Most insights into residual strain have been gathered in analogous experiments, for example in photoelastic materials under polarizing light (Friedman, 1972; Gallagher et al., 1974, **Figure 3.4.1**).

We aim to understand how strain concentrates and contributions to progressive fracturing in near-surface bedrocks. In our research, we try to understand how the strain state in rock, as well as their inherited residual strain state, is altered due to applied low load. The recognition of the control of residual strains on fractures and material degradation in glass and metals is well recognized in material sciences, while in geomaterials this is under research and discussion. Most discussions on residual strain or stress ceased in the late 1970s, but recently, especially with advanced techniques, those stored strains in the rock microstructure are again considered (Chen et al., 2015; Kunz et al., 2009; Luzin et al., 2014; Scheffzük et al., 2015).

Initially, so-called “residual stresses” (measured as residual strains) have been examined using strain relief methods including overcoring, microcrack orientation and density maps (Hoskins & Russell, 1981; Zang & Berckhemer, 1989). Destructive and invasive methods measure bulk strains on the surface of rock samples with strain gauges or posthumous in thin sections. Residual strains are assumed to relax and measurable as extensional strains by the creation of new surfaces, thus by microcracking (mode I). This connection to stress relief fracturing is also reflected in the appearance of the terminology of residual stresses in geomorphological conceptual considerations, where residual stresses are linked to rock failure, exfoliation and spalling (Emery, 1964; Kieslinger, 1958; Müller, 1969). Hereby, instantaneous or time-dependent inelastic damage is assumed to relief residual strains greater in the direction magnitudes have been highest. Because these are relative changes, paleostress orientations are usually determined. The quantification of the residual strain may help to constrain the tectonic

history of the rock. Residual strains used to reconstruct paleostress (Friedman, 1972; Holzhausen & Johnson, 1979; Sekine & Hayashi, 2009). The magnitude of residual strain, in situ, is only seldom determined. In strain relaxation methods, such as overcoring it can be problematic to distinguish between residual strains and strains caused by boundary loads – tectonic or topographic forces.

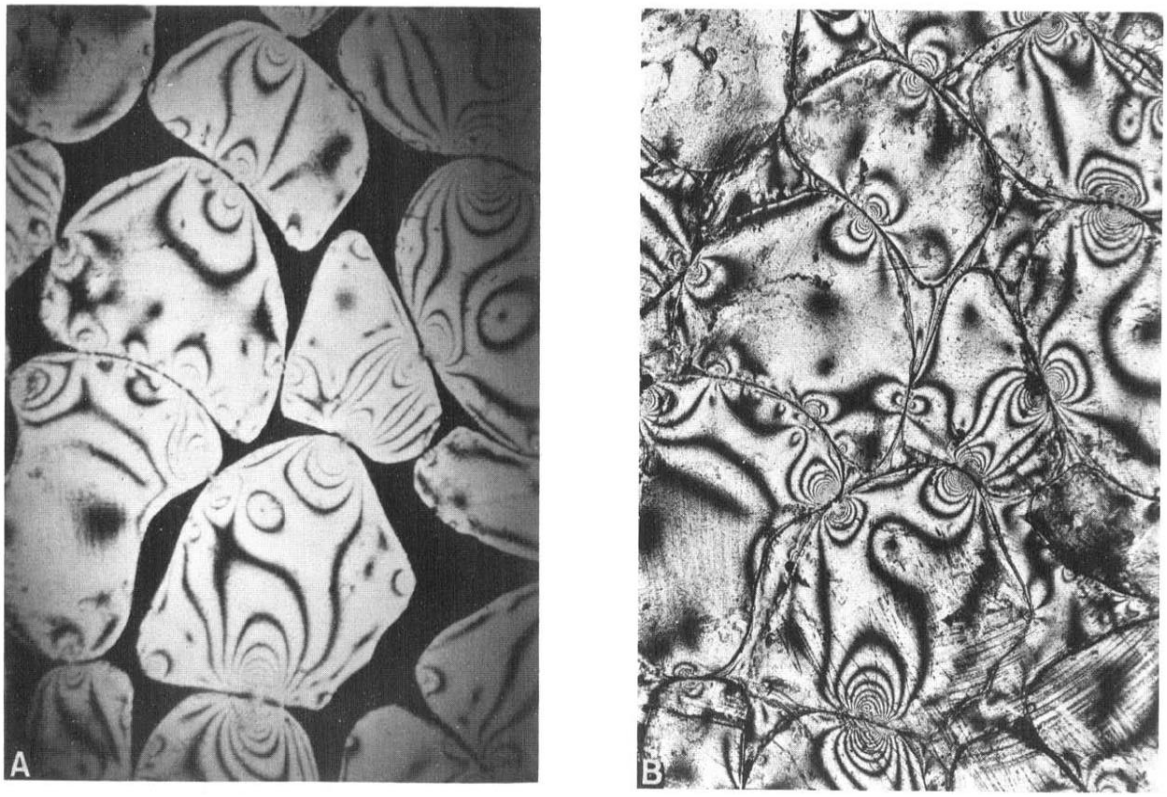

Figure 3.4.1 Photographs of uncemented, vertically loaded, naturally shaped elements of CR-39 (A) and same model cemented with CIBA epoxy and load removed (B). The stored stresses in the "grains" (B) are within about one-half fringe order of those in (A). Isochromatic fringes in the cement (B) indicate some of the load is transferred to the cement upon removing the external load. "Grains" have a maximum diameter of 2.5 cm (after Gallagher 1971), Friedman 1972.

Similar to the determination of the "Kaiser effect" (cf. **Chapter 2.2**), these destructive methods infer the magnitude from the response. Thus there is no direct measure of the internal strain state. The main assumption in testing residual strains by overcoring is, that the rock is near critically strained thus that freeing some confinement will trigger a relaxation which readily creates a new surface. In measuring the whole sample, it is furthermore assumed that the release of the strain energy is homogeneous throughout the material, the response purely brittle and no energy is going into plastic deformation. But what these measurements provide is at least a confirmation that near-surface, not all locked-in strains are relieved or redistributes even over geologic time scales.

Diffraction methods have been applied as well, often using X-ray. Due to the high absorption of X-ray photons strain in thin sections, in very small samples or on surfaces are measured (Chen et al., 2015, 2016; Rybacki et al., 2011). Magnitudes of residual stresses up to 40 MPa have been inferred by methods of strain relief as well as X-ray diffraction techniques in various rocks (Friedman, 1968, 1972). Both X-ray diffraction and strain relief methods are

at least to a degree invasive and limited to surface strains. Using neutrons, which have a higher penetration depth than photons, the non-destructive measurement of sub-gauge volumes in the interior of standard size whole samples (Holden et al., 1995; Schofield et al., 2006; Withers & Bhadeshia, 2001a).

3.4.1 Neutron diffraction of geomaterials

The general principle of neutron diffraction relies on the diffraction properties of crystallites. Thus any material which follows the Bragg condition can be assessed. Neutron diffraction techniques are widely applied and established in material sciences for determination of material properties especially strength and toughness as well as performance due to the presence of residual (micro)strains (Coules et al., 2013; Holden et al., 1995; Pirling et al., 2006; Wu et al., 2008). The application of neutron diffraction is still far from being a standardized method in geomaterials, though its advantages and potentials to assess non-destructively the internal state and properties of geomaterials have been outlined (Frischbutter et al., 2000, 2006). Methodologically we employ material science techniques, neutron diffraction, to determine non-destructive the strain state of the rocks.

Neutron diffraction is the application of neutron scattering to determine the atomic structure of a material. The advantage of neutrons, compared to X-ray diffraction is their penetration depth of up to tens of centimetres (Holden et al., 1995). This allows evaluating the internal structure without surface or edge effects. Neutron diffraction allows assessing elastic strains at the grain-scale on conventionally sized samples (Hall et al., 2011; Schofield et al., 2006). Diffraction measurements make use of the reflective properties of atoms, which follow the Bragg conditions (Bragg, 1924). Atoms arranged in crystal lattice planes have a specific reflection angle (2θ°) and a specific peak position (d_{hkil}) in the according diffraction pattern. Measurement of residual strains relies on elastic deformation within a single- or polycrystalline material that causes changes in the spacing of the lattice planes relative to their strain-free conditions. Due to the residual and induced strains, the reflection properties of the crystallites are altered. Therefore, they can be used as microstrain gauges (Groshong et al., 1984).

The Bragg peak position d_{hkl} is related to the wavelength λ through the angle between the incident and the reflected neutron beams 2θ($d= \lambda/\sin\theta$). Distortions of the lattice planes alter the reflection angle and thus the peak centre position in reference to a strain-free or undistorted lattice (d0hkil) (Withers & Bhadeshia, 2001b). A shift in the peak position is thus a measure of the elastic (micro)strain εhkil, estimated by

$$\varepsilon_{hkil} = \frac{(d_{hkil} - d_{0hkil})}{d_{0hkil}}.$$

Where a positive peak position shift indicates extensional strain, a negative value a relative contraction (**Figure 3.4.2**). These types of (micro)strains are also termed intergranular strains as they have been linked to elastic strains locked in between grains or crystals. Distortions of lattice planes can also alter the dispersion of the reflected neutrons resulting in a change of the peak shape metrics. Assessment of peak shape metrics like the full-width at half maximum (FWHM), which signifies plastic deformation within grains and crystallites.

This means that with neutron diffraction, we are essentially measuring crystal lattice plans and interfere intergranular or intracrystalline elastic strain!

In order to define and distinguish diffraction patterns, neutron diffraction has been applied to a limited set of materials. A necessity is that the material is homogeneous and

isotropic. For geologic material, this means that it is preferred to contain no other memory properties, like a crystallographic preferred orientation (CPO). Hence, single crystals and powders are frequently tested. An example of a calcite standard powder diffraction pattern is given in **Figure 3.4.3** (Jin et al., 2009). Monophase, though polycrystalline structures, like Carrara marble, can be assessed depending on the scale on which isotropy and homogeneity assumptions are valid. Very few neutron diffraction studies exist on polyphase material. Further advances of models, to analyse overlap of diffraction peaks (deconvolution of peaks), and methods to combine the elastic strain analysis with different textures are needed.

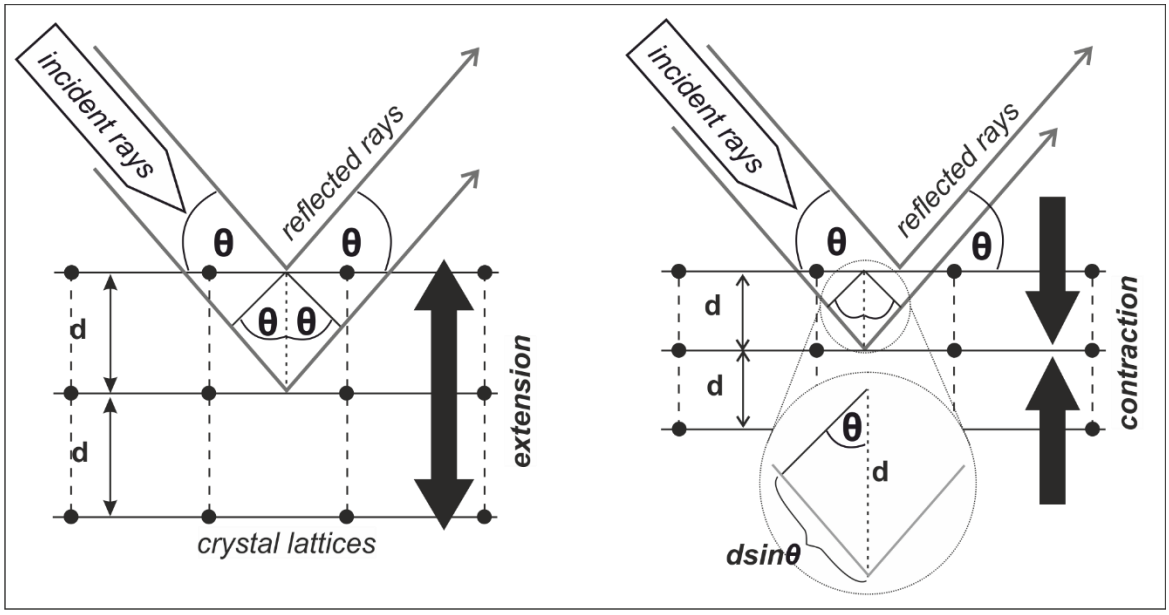

Figure 3.4.2 Bragg's law relating the crystal lattice spacing **d** with the angle of the incident and the reflected rays. On the left crystal lattices are in extension resulting in larger 2Theta, while on the right due to the contraction of the lattice spacing reflected at a smaller 2Theta angle –in comparison.

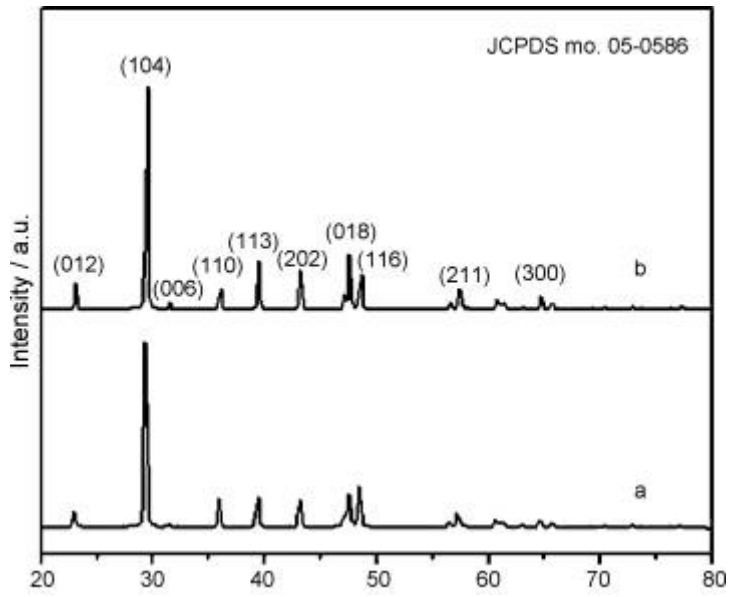

Figure 3.4.3 A standard calcite powder spectrum. Note the distinct peaks without overlap at low angels (from Jin et al., 2009)

Neutron diffraction measurements are possible at specific sites research sites. Instruments, designed to assess single diffraction peaks or small spectra, like the SALSA diffractometer, needs be able to measure low 2Theta angles, for geomaterials (see **Figure 3.4.3** for calcite). Another type of instruments uses so-called time-of-flight methods. Due to the instrument configuration full spectra and spatial orientations can be simultaneously assessed. These type of instruments are especially suitable for thermally or mechanically conditioned in-situ measurements (Frischbutter et al., 2000; Luzin et al., 2014; Scheffzük et al., 2018).

Advancing possibilities of neutron diffraction measurements and techniques, especially providing in-situ testing environments, have increased the application of neutron diffraction in rock physics, for rock mechanical problems and by providing data for numerical models. However, for time-dependent rock deformation experiments, in-situ testing doesn't serve due to time constraints, and testing environments are generally limited to thermal states, as water would absorb neutrons. An alternative is to assess preconditioned materials (Siegesmund et al., 2008).

3.4.2 Residual elastic strain measurements at the diffractometer SALSA

Our neutron diffraction measurements were conducted at the SALSA strain diffractometer at the Institute Laue-Langevin (ILL), Grenoble, France (**Figure 3.4.4**). SALSA is specified to assess the peak positions in 2θ° space, with a precision of ± 3.5× 10^{-5} Å (Pirling et al., 2006). The focus was therefore on the assessment of intergranular strains.

SALSA specializes in metals with a cubic structure, thus only one diffraction peak is commonly measured but allows low angle diffraction as well (Pirling, 2002; Pirling et al., 2006). For geomaterials, at least two diffraction peaks corresponding to the crystal axis should be measured. To measure a chosen diffraction peak, a small spectra range of 2θ was defined and the detector positioned (**Figure 3.4.4**). The simultaneous measurement of spatial orientations is not possible at SALSA, but as our samples have been pretested the spatial orientation of the samples could be manually adjusted. The high resolution of the sampled gauge volumes along the vertical axis of the samples was feasible due to the automated sample stage.

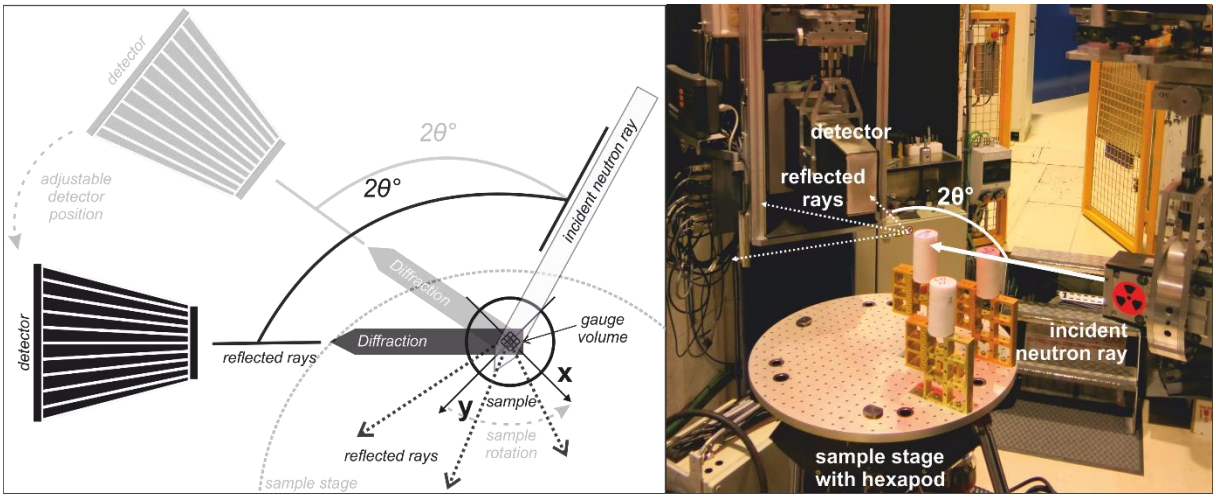

Figure 3.4.4 Schematics of the test stand and testing principle. On the right, the actual testing- stand with samples.

An example of the measured reflections is given in **Figure 3.4.5 a**. The reflections have been assessed in the spectra range of 30-45 2θ [°] of the crystal lattice planes representing hkl (110). In this example, a total of 11 positions each comprising 4000 counts are shown. These scatter plots are converted into intensity distribution plots (**Figure 3.4.5 b**). These plots show already a peak. Peak shape and position are fitted with a Gaussian fit and individual background (volume below the dotted line) is subtracted with the ILL standard analysis LAMP (Richard et al., 2008, **Figure 3.4.5 c**). Other approaches, especially for full spectra, use Rietveld analysis (e.g. Lutterotti et al., 1997; Schäfer, 2002). The resulting d_{hkl} data is then analysed as described above. The 'strain-free' reference is either a theoretically, based on crystallographic properties d_0 or the measured d_{hkl} of a powdered and potentially tempered sample. This can be done for specific crystal planes but also the crystal unit volume. Because these are all relative changes, also assumed initial states – like the not pretested samples, can be used as a reference (Luzin et al., 2014).

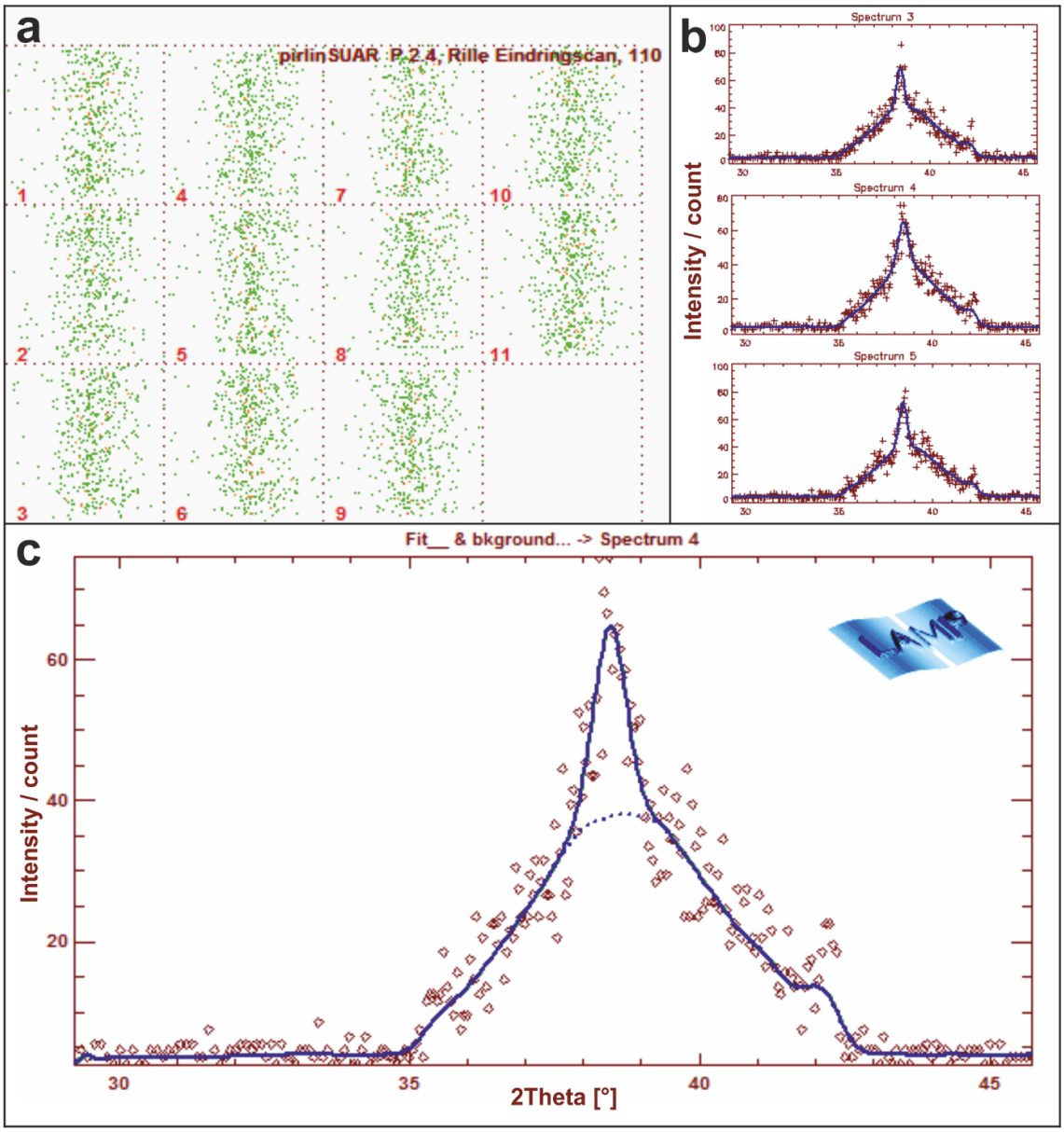

Figure 3.4.5 a Measured reflections of hkl (110), of 11 positions each of 4000 counts are converted into intensity distribution plots **b**. **c** Peak shape and position are fitted with a Gaussian fit and individual background (volume below dotted line) is subtracted with LAMP.

4. Results – Scientific Publications

Theoretical and laboratory experiments have been conducted to explore questions about how rocks break. To address all objectives appropriately, they have been split into studies focussing on external, respectively internal controls of progressive rock failure as well as their combination. Results of these studies are compiled in three publications.

Scientific Publication I

The objectives of the first article (**Chapter 4.1**) were to constrain the dynamics of progressive rock failure and evaluate how this failure is influenced by externally applied stresses and environmental conditions. Progressive rock failure is facilitated by mechanisms of creep. A simple, yet appropriately scaled long-term creep test was designed and implemented under controlled laboratory conditions. An inverted single edge notch bending test was applied to a 1-m long benchmark-type Carrara marble sample. This arrangement successfully emulates an open joint on a steep rock wall, with the facility to introduce water to the notch. This enabled us to identify both chemo-mechanical and mechanical effects of water on the progressive failure of this rock type. The mechanisms are coupled with mechanical loading conditions, expressed in the creep rate and the extent of subcritical crack growth. We were also able to observe the response -ductile or brittle-to the introduction of water to the imposed notch, is conditioned by the stress state (Rehbinder effect). In additional experiments, we could show that the same chemo-mechanical and mechanical effects by the introduction and presence of water, like enhanced subcritical crack growth or the Rehbinder effect apply to quartzite rocks (Voigtländer et al., 2017b). The study on Carrara marble has been published as:

Voigtländer, A., Leith, K., & Krautblatter, M. (2018). *Subcritical crack growth and progressive failure in Carrara marble under wet and dry conditions*. In the Journal of Geophysical Research: Solid Earth, 123, 3780–3798. https://doi.org/10.1029/2017JB014956.

The article is based on long-term experiments which have been designed by Anne Voigtländer and Dr Kerry Leith. The realization and monitoring of the experiments, as well as data analysis, were principally lead by Anne Voigtländer. All authors discussed and analysed the results. Anne Voigtländer wrote the manuscript. All authors revised the manuscript. Overall, 70 % was contributed by Anne Voigtländer, 20% by Dr Kerry Leith and 10% by Prof. Dr Michael Krautblatter.

Scientific Publication II

The objective of the second study was to infer how the internal, inherited strain state of rock contributes to the overall stress state. Residual elastic strains constrained by neutron diffraction techniques are used as a proxy for the internal stress state as no direct or non-destructive measures presently exist. The second published article (**Chapter 4.2**) of this thesis, builds upon and uses pretested Carrara marble samples from the experiments conducted for the first article. We collected neutron diffraction data of an intact sample and three mechanically and chemo-mechanically pretested Carrara marble samples. We assumed that the initial residual strain state is similar in all samples as they had all been cut from the same block (**Chapter 3.1**). With these neutron diffraction data, we intended to i) define the initial residual strain state of Carrara marble, ii) assess the inducement of strain due to the mechanical pretesting, and iii) infer the role of the internal (i.e. initial residual strain) and external (i.e. subcritical mechanical

loading and dry and wet testing conditions) factors on the induced damage extent. By comparing the relative effect of external and internal factors, our study provides novel insights into the role of residual strains and the internal state on progressive rock failure. The results and discussion are published in:

Voigtländer, A., Leith, K., Walter, J. M., & Krautblatter, M. (2020). *Constraining internal states in progressive rock failure of Carrara marble by measuring residual strains with neutron diffraction.* In Journal of Geophysical Research: Solid Earth, 125, e2020JB019917. https://doi.org/10.1029/2020JB019917

Anne Voigtländer and Dr. Kerry Leith designed the study. All authors contributed to the successful grant application for the use of the SALSA Diffractometer, run by Dr Thilo Pirling at the Institute Laue-Langevin (ILL) in Grenoble, France. Anne Voigtländer, Dr Kerry Leith and Dr Jens M. Walter conducted the neutron diffraction measurements. Anne Voigtländer compiled and analysed the data and results. All authors discussed the results and Anne Voigtländer wrote the manuscript. All authors revised the manuscript. In summary, 70 % was contributed by Anne Voigtländer, 15% by Dr Kerry Leith, 5% by Dr Jens M. Walter and 10% by Prof. Dr Michael Krautblatter.

Scientific Publication III

The neutron diffraction measurements demonstrated that the overall contractional elastic strains are 'locked-in' the Carrara marble, which can be attributed to rock sample's geologic history and thus resemble a rock stress memory. More specifically, residual elastic strains constitute a structural inherency of rocks. Other pre-existing structural conditions, like faults, foliations and polyphase materials are also likely to control progressive rock failure, yet their discussion remains beyond the scope of this study. In a theoretical geomorphology context, all of these inherited conditions have been also termed tectonic predesign (Hantke & Scheidegger, 1999), but are unfortunately often overlooked in studies of time-less rock slope instabilities (Stead & Wolter, 2015). In recent years' great attention has been paid to understanding the mechanisms of rock breaking at or the Earth's surface (e.g. Eppes & Keanini, 2017; Jerolmack & Daniels, 2019). These research efforts do not account for inherited geological structures into account. Concepts, empirical models and data of subcritical crack growth exist in rock physics and material science research, yet do not necessarily account for the environmental conditions and stress fields which come from a geomorphological perspective. Combining and administering rock physics and material sciences concepts of subcritical crack growth with tectonic predesign surprisingly reveal simple and applicable theories for geomorphological processes and landscape evolution. These further research possibilities, strategies and objectives are deduced in the third publication (**Chapter 4.3**).

In geomorphology, we employ a figurative, formative and illustrative language, therefore in the publication in **Chapter 4.3**, playful and thought-provoking graphics are used to introduce and combine subcritical crack growth and tectonic predesign to geomorphologists. In drawing from the different disciplines it offers new perspectives and is useful to basic and applied geoscience communities. The resulting paper comprises the experimental and theoretical studies of this thesis and is published in the ESEX Commentary series as:

Voigtländer, A., & Krautblatter, M. (2019). *Breaking rocks made easy. Blending stress control concepts to advance geomorphology.* In the journal Earth Surface Processes and Landforms, 44(1), 381–388. https://doi.org/10.1002/esp.4506

The article originates from a poster presentation at the EGU 2017 (Voigtländer & Krautblatter, 2017). The idea, theory and design of the poster was by Anne Voigtländer. Reasons for implementing a comic-strip like style presentation are given in a blog entry for the EGU Geomorphology division (available here:

https://blogs.egu.eu/divisions/gm/2017/12/10/theoretical-geomorphology-selling-a-seemingly-boring-topic/).

The poster presentation received a lot of attention and stimulated discussions during the conference and in subsequent correspondence. Due to its success, poster presentation has been transformed into a commentary. Anne Voigtländer wrote the manuscript. All authors discussed the conversion of the illustrated scientific ideas into written words and revised the manuscript. Anne Voigtländer contributed >70% and Prof. Dr Michael Krautblatter ~20% to the article.

In order to publish this work in peer reviewed and internationally acclaimed journals, articles in **Chapter 4.1** and **4.2** needed to be written in US American English while **Chapter 4.3** and the rest of the thesis are written in British English.

4.1 Scientific Publication I

Subcritical crack growth and progressive failure in Carrara marble under wet and dry conditions.

Anne Voigtländer, Kerry Leith and Michael Krautblatter (2018)

Journal of Geophysical Research: Solid Earth, 123, 3780–3798.
https://doi.org/10.1029/2017JB014956

Subcritical crack growth and progressive failure in Carrara marble under wet and dry conditions

***Anne Voigtländer**, Kerry Leith and Michael Krautblatter*

Abstract

Our concept of progressive rock slope failures is on the one hand embedded in aggregated subcritical crack growth mechanisms, and on the other sensitive to environmental conditions, especially water. To anticipate failure dynamics in rock slopes, it is a key requirement to reveal the influence of water on subcritical crack growth mechanisms and material properties. We present experimental data on the time-dependent deformation of an exemplary rock, Carrara marble. We employed inverted single-edge notch bending (iSENB) creep tests on large Carrara marble samples to mimic an open joint system with controlled water supply. Constant stress was applied in two steps approaching 22 - 85 % of a previously determined critical baseline stress. Introducing calcite-saturated water to subcritical stressed samples caused an immediate increase in strain by up to an order of magnitude. Time-dependent accumulation of inelastic damage at the notch tip occurred in wet and dry samples at all load levels. Subcritical crack growth and the evolution of localized intergranular fractures are enhanced if water is present, and readily approach tertiary creep when loaded above 80 %. The immediate strain response is attributed to the reduction of surface energy and diffusion of the water into the rock. The resultant more compliant and weaker rheology can even turn the subcritical stress into a critical state. Over time, subcritical and chemically enhanced mechanisms progressively alter especially grain boundaries, which become the key controls of progressive failure in Carrara marble.

Key Points:

- The introduction of water increases the magnitude and rate of strain in subcritically stressed marble.
- Brittle and plastic deformations are enhanced in wet samples in comparison to dry samples.
- Subcritical crack growth mechanisms preferentially exploit microstructural predispositions, especially grain boundaries.

4.1.1 Introduction

Progressive rock slope instabilities are evident throughout mountainous landscapes. Understanding the manner in which slow-moving rock masses accelerate and translate into catastrophic failures is a key aspect of hazard prediction (Loew et al., 2016; Petley et al., 2005). A profound and quantifiable knowledge of the precursory phase of time-dependent deformation leading up to dynamic rupture is, however, still lacking (Ventura et al., 2010). Progressive deformations cannot readily be captured in short-term peak strength tests, as rock strength dynamically decreases with time, and increases in susceptibility to environmental conditions (Brantut et al., 2013; Crozier, 1989; Viles, 2013). Limit state assumptions, even though relying on a conceptually defined long-term strength (N. A. Chandler, 2013; Damjanac & Fairhurst, 2010; Jaeger et al., 2007) don't necessarily reveal the mechanisms to define that limit.

Creep tests are an important means of obtaining data required to assess the long-term rheological behavior of rocks. These are often undertaken under constant load conditions (e.g. Brantut et al., 2012, 2014a). Creep is characterized by a non-uniform stress-strain behavior, ranging from a precursory phase of time-dependent deformation to dynamic rupture (Ramsay, 1967)(**Figure 4.1.1a**). In general, creep tests reveal (i) a lower limit for plastic and brittle yielding (compared to short-term tests), (ii) time-dependent strength reduction in dependency of the applied stress magnitude, and (iii) effects of environmental factors, such as temperature or water saturation, on the rheological behavior (Griggs, 1939; Lockner, 1993; Sorace, 1996). As creep tests are time-consuming, they are often conducted at near critical stress levels of 80 – 90 % of the peak strength (Brantut et al., 2013; Kranz, 1979). To extend observations to lower stress levels a stress stepping approach has been introduced (e.g. Heap et al., 2015). Macroscopic creep behavior has been described by several mechanical models (e.g. Paraskevopoulou et al., 2015). In these models, brittle creep is theorized to result from time-dependent microfracturing at the tip of pre-existing discontinuities (Brantut et al., 2012)(**Figure 4.1.1b**). Applied stresses concentrate at microstructural flaws and interfaces, and when they locally and temporarily exceed the elastic limit they induce brittle cracking and plastic deformation (**Figure 4.1.1b**). This allows the redistribution of these stresses which may drive further plastic and/or brittle deformation and crack coalescence (Nicolas, 1986; Withers, 2015)(**Figure 4.1.1b**). These intermittent stress-dependent dynamics lead to a local competition between subcritical and critical propagation. On the microscale, this results in a range of cracking velocities and crack front locations, while the macroscopic deformation averaged over greater space and time intervals may remain steady (Lengliné, 2011a,b). Monitoring the relaxation of strains during, and after unloading of the samples can provide additional constraints on the degree of inelastic (i.e. brittle and plastic) deformation (**Figure 4.1.1a**).

Subcritical crack growth mechanisms promote the accumulation of inelastic strain until an internal threshold is met and becomes evident as macroscopic creep deformation. Therefore, the nature of these mechanisms plays a significant role in the time-dependent failure of the rock. Subcritical crack growth is influenced by (i) external factors such as applied stress and pressure state, temperature, chemical activity and kinetics, and (ii) internal rock properties (microstructure, lithology, residual strain)(e.g. Atkinson & Meredith, 1987). Both internal and external factors directly influence the energy barrier to rupture or deform the material bonds by subcritical crack growth mechanisms, like stress corrosion, diffusion, or (micro)plasticity (Atkinson, 1984).

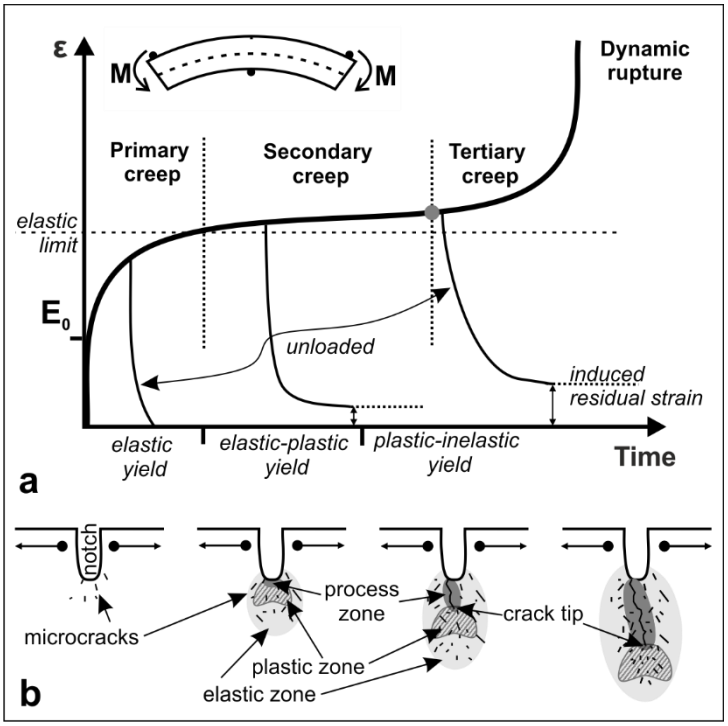

Figure 4.1.1 a Schematic creep phases of an iSENB beam test. **b** Progressive microcracking and a primary fracture, plastic and inelastic process zone development under tensile load perpendicular to a starter notch.

To better constrain environmental and (micro-)mechanical controls of long-term rock strength, we conduct creep experiments on a well-researched exemplary rock, Carrara marble. The homogeneous, dense metamorphic rock consisting of nearly pure calcite provides favorable conditions with regard to test consistency and repeatability, making it popular in material science studies e.g. to study material damage by thermal forcing (Luzin et al., 2014; Rayleigh, 1934). Carrara marble, like other calcite rocks, exhibit brittle and semi-brittle deformation even at low temperature and pressure regimes and can display plastic behavior at ambient temperatures (Fredrich et al., 1989; Schubnel et al., 2006). The presence of water tends to reduce the fracture toughness, and increase rates of enhanced subcritical crack growth (Atkinson, 1979; Nara et al., 2017). The reversible chemical kinetics of calcite rocks, leading to dissolution and precipitation, with the same chemical but not necessarily mechanical properties, are generally well established (Bögli, 1978; Colombani, 2016). The equilibrium between reactants and products depends on temperature, pressure, and the chemical composition and concentration of the liquid as well as the stress state of the calcite (Arvidson et al., 2003; Croizé et al., 2010; Schott et al., 1989). Despite this relatively good characterization, however, long-term strength degradation and the combined effect of water and mechanical stresses is still not fully understood (Risnes et al., 2005; Rutter, 1972).

The main mechanism postulated for subcritical crack growth is stress corrosion (Anderson & Grew, 1977; Atkinson, 1984; Brantut et al., 2014a). Stress corrosion and the effects of the diffusion of water in the rock matrix significantly contribute to subcritical crack growth mechanisms in calcite rocks. Stress corrosion features pressure or temperature activated dissolution kinetics at the stressed bonds at the crack tip or hydrolysis and associated

embrittlement (Michalske & Freiman, 1982; Stipp, 1999). Both mechanisms are also depending on the diffusion and exchange of water in the rock. The diffusion of water has also chemo-mechanical effects, as the adsorption of H^+ and O^{2-} ions to crystal interfaces through hydration of exchangeable cations or osmotic attraction (i) wedges interfaces apart, which has a macroscopic expression as hygroscopic expansion or dilatancy, and (ii) reduces surface energies (Darot & Gueguen, 1986; Stipp, 1999). The reduction in surface energy even lowers the barrier for ductile and brittle deformation, if the material bonds are already stressed, known as the "Rehbinder effect" (Bergsaker et al., 2016; Dunning & Huf, 1983; Lawn, 1993; Rostom et al., 2013). Water also reduces intergranular compressive stresses and associated grain boundary friction, by diffusing into the rock and adsorbing onto mineral interfaces and leaving the rock to appear more compliant if stressed (Baud et al., 2000; Nicolas et al., 2016; Winkler, 1975). Upon drying, diffusion associated deformations are assumed to vanish, unless the wetting caused the rupture of bonds, the formation of secondary minerals or precipitates, or the release of residual strain energy (Harper et al., 1979; Rehbinder & Shchukin, 1972; Swanson, 1984). Single chemo-mechanical mechanisms are not be ascertained easily and are coexistent (Atkinson & Meredith, 1987; Bergsaker et al., 2016).

Formalisms to calculate rates of stress corrosion cracking are typically based either on free energy criterions, incorporating thermodynamic theory and adopting a modified Griffith concept (Bergsaker et al., 2016; Wan et al., 1990), or empirical stress intensity – crack velocity relations as described by i.e. the Charles' law, (Atkinson, 1984; Charles, 1958; Wiederhorn & Bolz, 1970). These provide evidence of three phenomenological regimes that (i) at very slow rates of crack growth or creep, external factors like applied stress magnitude or chemical activity dominate; (ii) the system is less sensitive to the stress magnitude but limited in the velocities by transport of reactive species to and from the crack tips; (iii) if stress intensities are near critical, either by additional load or an extension of a primary fracture, the crack growth kinetics are unaffected by the environment. The evolution from primary, through secondary, and into tertiary creep can lead to a spatially discernable expression of the associated processes in resulting fracture surface morphologies of creep tests (**Figure 1**). Especially the chemical processes in the primary and secondary regime might also impose a time-dependency on the creep behavior (Lawn, 1975; Lengliné et al., 2011a; Orowan, 1944).

To better understand progressive damage in natural rock slopes, we designed a long-term test under well-controlled laboratory conditions using 1m long benchmark-type Carrara marble specimen. We designed a simple Mode I creep setup of an inverted single-edge notch bending test, mimicking an open joint on a steep rock wall, with the possibility to introduce water to the notch. We focus on (i) progressive strain accumulation due to the presence of water and applied stress levels, (ii) magnitude and rates of water weakening effects and subcritical crack growth mechanisms, and (iii) their control on the long-term behavior of Carrara marble.

4.1.2 Materials and Methods

4.1.2.1 Material characterization

Carrara marble was formed during the Apennine orogeny (Cantisani et al., 2009; Leiss & Molli, 2002). Lower to middle Liassic carbonate platform sequences were deformed and metamorphosed under greenschist facies conditions (Oesterling et al., 2007) and exposed in the Carrara nappe as a tectonic window (Leiss & Molli, 2002). We use a type of Carrara marble

known as “bianco C/D” (**Figure 4.1.2a**). Our samples are wire cut from a single block from the Lorano quarry, Carrara, Italy (44°5’37’’N, 10°7’11’’E). Thin sections of our Carrara marble indicate a homogeneous distribution of fine grain sizes between 150 and 250 µm (mean ~200 µm), and an overall random orientation of grain boundaries (**Figure 4.1.2b, c**). Grain boundary geometries are characterized by straight or slightly undulating grain contacts, 120° triple junctions are common, and interlocking is rare (**Figure 4.1.2b, c**). Together, these properties support suggestions that the grain boundary geometry is likely the principal source of mechanical weakness in Carrara marble (Siegesmund et al., 2000). Further microstructural inherited flaws like marble lamella, twins, and single grain boundary microcracks are evident in thin sections from our samples (**Figure 4.1.2b, c**). One to two rounded quartz grains are located in each thin section representing less than 1% SiO_2 by volume, with no obvious influence on the microstructure. Remnants of minor mineralogical phases in the initial sediment, like pyrite, provide some light grey marbling to the otherwise white metamorphic rock (**Figure 4.1.2a**). Texture measurements with an X-ray goniometer indicate a near random crystallographic preferred orientation (CPO, texture) of axis and crystal planes (**Figure 4.1.S1**). The initial porosity of our Carrara marble is low with a dry density between 2.7 and 2.9 g/cm^3. Aside from any inherited damage, not apparent in macroscopic, or microscopic investigations, we, therefore, expect the rheological behavior of our marble to be macroscopically isotropic.

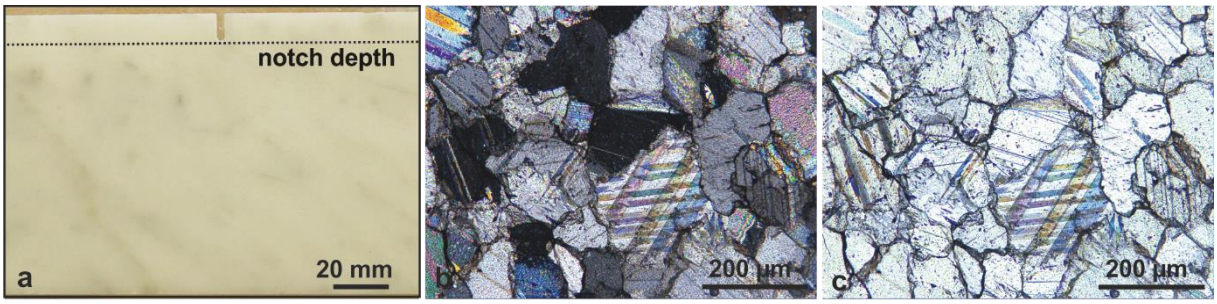

Figure 4.1.2 a Carrara marble sample example with saw cut notch. Petrographic thin section of Carrara marble in polarized **b**, and parallel light **c**, showing weakly interlocking grain boundaries and multicolored twin lamellas, displaying inter- and intragranular discontinuities and flaws.

4.1.2.2 Inverted three-point bending creep tests

We employ an inverted configuration of a standard single-edge notch three-point bending tests (iSENB). The simple testing configuration allows us to (i) keep the applied stress magnitude constant for long testing periods (month/years) and (ii) to use sample dimensions relevant to the evaluation of macroscopic fracture propagation within bedrock (**Figure 4.1.3**). The inversion of the configuration allows for the introduction and preservation of water within the notch (**Figure 4.1.3b**). Loads are generated by a dead weight and a lever system pulling upwards along a line load at the bottom of the samples (**Figure 4.1.3a**). Our Carrara marble samples are 1100 mm long, with a span length between the bearings of 1000 mm, a cross-section of 100 x 100 mm and a 10 mm deep notch in the outer bending radius (**Figure 4.1.3a**). To maintain a stable environment (thermal and hygrometric conditions), creep tests are undertaken in a basement laboratory.

Following classical beam theory, our iSENB samples under a given load are stressed in tension in the upper half, with a decreasing magnitude towards the neutral axis and increasing in compression in the lower half towards the load line (**Figure 4.1.3a**)(Holzhausen & Johnson, 1979; Jaeger et al., 2007; Timoshenko & Goodier, 1970). With the edge notch, we create Mode I tensile stress concentrations at its tip. Since an interaction of the oppositional stress fields can lead to dynamic rupture (Fakhimi & Tarokh, 2013; Le et al., 2014), we evaluate the induced stresses in the loaded sample with a simple finite element method (FEM) model using RS2 v9 from Rocscience (**4.1.S2, Table 4.1.S2.1**). Our beams are sized such that the cracks below the notch can propagate, while a separation of the stress fields is maintained.

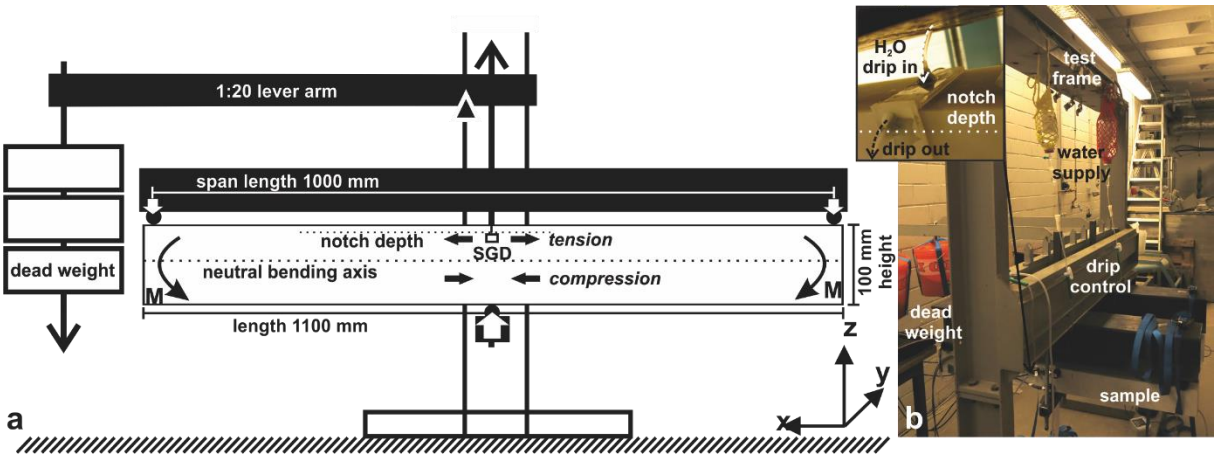

Figure 4.1.3 a Geometry of the three-point bending Carrara marble samples, the location of the saw-cut notch with the strain gauge (SGD) position below, as well as the loading configuration with line loading positions (white arrows), the bending moment M, and an indication of induced stresses. **b** Three-point bending test frame with the water supply and control system. Inset with the detail of water supply at the notch in the wet samples.

4.1.2.2.1 Determination of baseline short-term strength

In order to establish a baseline fracture toughness of our Carrara marble samples for our long-term creep tests, we undertook two standard SENB tests on 100 x 100 x 550 mm sized samples following ASTM recommendations (ASTM, 2003, 2012). Samples had a 500 mm span between support points, half of that of the long-term beams but with the same cross-section. A 10 mm deep and 3 mm wide notch was cut across the center of the samples. The standard procedure also requires a known moisture condition of the samples. This is commonly attained by drying the samples. This can lead to uncontrolled microcracking in Carrara marble, as the thermal expansion coefficient is anisotropic (Logan, 2004; Luzin et al., 2014). Instead, we attain consistent conditions by immersing the samples in water for five days. It is presumed that this water-saturation of the samples results in a lower short-term strength than (air-)dried tested samples would yield. The attained baseline fracture toughness represents thus a lower limit. Samples were taken from the water bath and mounted with the notch facing downwards in a servo-controlled mechanical testing apparatus (Zwick Troll). They were loaded from above at a rate of 0.1 mm/min. The samples failed at a mean load of F ~9.27 kN (9.30 kN and 9.25 kN). The ultimate flexural strength was calculated using Equation (1):

$$\boldsymbol{\sigma = \frac{3Fl}{2w(h-a)^2}}. \quad (1)$$

where F is the applied force, l is the span length, w and h are the sample width and height, and a is the initial depth of the notch. This equates to an ultimate flexural strength σ of ~8.6 MPa. The equivalent failure load for our 1000 mm span length samples is estimated, following Equation (1), to be 4.65 kN.

Subcritical crack growth studies use critical Mode I stress intensity (K_{IC}) or fracture toughness and fractions of thereof as a reference unit. To compare our baseline results with published K_{IC} values, we can estimate the stress intensity at the notch tip as a function of the sample geometry, applied load, and material properties (Lawn, 1993). There are several possible calculation approaches of stress intensity (Backers, 2004). We assume plane strain conditions and adopt Equation (2) after Broek (1982, p.181, eq. 7.3):

$$\boldsymbol{K_{IC}} = \frac{\boldsymbol{F}}{\boldsymbol{w\sqrt{h}}}\left[\frac{3\frac{\boldsymbol{l}}{\boldsymbol{h}}\sqrt{\frac{\boldsymbol{a}}{\boldsymbol{h}}}}{2\left(\boldsymbol{1}+2\frac{\boldsymbol{a}}{\boldsymbol{h}}\right)\left(\boldsymbol{1}-\frac{\boldsymbol{a}}{\boldsymbol{h}}\right)^{\frac{\boldsymbol{3}}{\boldsymbol{2}}}}\left[\boldsymbol{1.99}-\frac{\boldsymbol{a}}{\boldsymbol{h}}\left(\boldsymbol{1}-\frac{\boldsymbol{a}}{\boldsymbol{h}}\right)\left[\boldsymbol{2.15}-\boldsymbol{3.93}\frac{\boldsymbol{a}}{\boldsymbol{h}}+\boldsymbol{2.7}\left(\frac{\boldsymbol{a}}{\boldsymbol{h}}\right)^{\boldsymbol{2}}\right]\right]\right] \qquad (2)$$

The critical stress intensity K_{IC} of our water-saturated Carrara marble is estimated to be ~1.3 MPa $m^{½}$. This is about half of $K_{IC} \approx 2.4$ MPa $m^{½}$ determined in a three-point bending test of dry Carrara marble samples (Backers, 2004). Estimates of K_{IC} derived by the double torsion method reach a $K_{IC} \approx 1.31$ MPa $m^{½}$ in small air-dry Carrara marble samples at ~50°C and 50 % relative humidity (RH)(Nara et al., 2017) but only a $K_{IC} \approx 0.644$ MPa $m^{½}$, thus half of our estimates, in samples immersed in water (Atkinson, 1979). In general, our results agree with the suggested range of fracture toughness of calcite rocks (Atkinson, 1984), which is used to determine an applicable subcritical load range in the creep tests.

4.1.2.2.2 Sample preparation

All samples were cut from a single block of Carrara marble and similarly oriented to their original position during preparation. An edge notch of ~10 mm depth and ~3 mm width was cut in the center of each beam with a diamond saw (**Figure 4.1.2a**). Notched samples were then pre-loaded to ~ 66 % of the estimated wet fracture toughness in order to nucleate a sharp crack tip. A pre-load of about 2/3 of the short-term strength was chosen, based on literature values allocating loads of 40 - 60 % of the principal stress to the crack initiation phase followed by stable crack growth (i.e. Hoek & Martin, 2014). Samples were immersed in water for five days beforehand to ensure consistent conditions. Saturated samples were mounted with the notch facing downwards and loaded from above at a rate of 0.1 mm/min to 3 kN over a 1 m span in the same testing frame used for the determination of the short-term strength. Pre-loaded samples were then air-dried for 24 hours before the notch region of the prospective wet samples were sealed with acrylic glass (fixed using a standard non-acid silicon, **Figure 4.1.3b**). The acrylic plate above the notch had a small drilled hole to allow water inflow (**Figure 4.1.3b**), while a ~3 mm diameter hole was drilled above the notch tip level on one side to create an outflow (**Figure 4.1.3b**). To ensure a constant and slow drip rate, we use standard medical drips (Exapod, **Figure 4.1.3b**), while simple urine bags were used to capture the outflowing water. The usage of this standard equipment ensured a budgeted but reliable and practicable long-term water supply. Wet samples are supplied with $CaCO_3$-saturated water to create a wet, though non-aggressive or corrosive environment within the notch. Herefore, deionized water was mixed with powdered marble. The solution was filtered for particles and reached a pH of ~7.5 - 8, and a $CaCO_3$ content of ~50 mg/L.

Strain was monitored using electrical resistance strain gauges (SGD, 6 mm, 350 Ω, precision 10^{-5}, full Wheatstone bridges) glued 2 mm below the notch tip of a total of eight samples using X60 glue (HBM, **Figure 4.1.3a**). Strain gauges were covered with an acid-free strain gauge silicon sealant (SG250, HBM) to prevent electrical noise due to possible air moisture fluctuations. On sample M1-M5 strain gauges were mounted on one side, on sample M6-M8 on both sides below the notch. Data was captured using a standard resistance acquisition system (Spider-8, HBM) with a sampling rate of 1Hz. Measurements were zeroed and started while the samples were still in a neutral stress position. Ambient temperature and humidity were monitored with a data logger (Onset HOBO) with sensors positioned within a 3 m radius of the testing frames.

4.1.2.2.3 Testing protocols

We tested eight samples (M1-M8) employing a stress stepping protocol to reveal the various effects of (i) loading level, path, and duration, (ii) wet and dry conditions. Stress steps were defined as percentages of the estimated wet baseline stress intensity K_{IC} (1.3 MPa $m^{½}$), ranging from 22 % to 85 % (see Section 4.1.2.2.1, **Table 4.1.1**). Two batches of tests were run, with results from the first five creep tests, involving samples M1-M5, feeding into the design of the testing protocol for the second three samples, M6-M8.

In our first test run, water was introduced to samples M1-M4 four days after mounting and loading the samples to the first load stage. Sample M5 was pre-loaded wet, then air-dried for five days before being mounted and manually loaded. M5 was kept dry throughout the testing period. Tests were interrupted prior to failure, which allowed us to assess the progressive damage. Therefore, samples were manually unloaded. They were carefully placed with the notch oriented vertically on a planar horizontal surface, in order to allow the samples to relax and air-dry under a neutral stress state.

Table 4.1.1 Samples dimensions and loading scheme of the long-term test.

Sample		***Geometry [mm]***			***Load [% of K_{IC}/~kN] and environmental condition***				***Note***
		(span) length	*width/ height*	*notch depth*	*1st loading*	*condition*	*2nd loading*	*condition*	
	M1	(1000) 1100	100/ 104	9	22/ 0.99	dry → wet	55/ 2.47	wet	error
	M2	(1000) 1100	100/ 102	8	55/ 2.47	dry → wet	77 (80)/ 3.46 (3.6)	wet	*
	M3	(1000) 1100	100/ 101	8	22/ 0.99	dry → wet	85/ 3.82	wet	
	M4	(1000) 1100	100/ 102	9	55/ 2.47	dry → wet	85/ 3.82	wet	*
	M5	(1000) 1100	100/ 102	9	55/ 2.47	dry	77/ 3.46	wet	
	M6	(1000) 1100	100/ 104	14	55/ 2.47	dry → wet	85/ 3.82	wet	error, **
	M7	(1000) 1100	100/ 104	14	55/ 2.47	dry	85/ 3.82	dry → wet	**
	M8	(1000) 1100	100/ 105	15	55/ 2.47	dry	85/ 3.82	dry	

**denotes tertiary creep, **denotes failed samples*

In the second round of testing, we aimed to constrain the effect of the introduction of water on near-critically loaded samples (85 % K_{IC}). Contrary to the first round of testing, samples were allowed to continue through tertiary creep and fail. This allowed us to assess their time-to-failure as well as the post-failure fracture surfaces. We tested three samples (M6-M8) with the same loading path (→55% → 85 % K_{IC}) but varied the timing of the introduction of water (**Table 4.1.1)**. All samples were air-drying for four days and then mounted in the testing frame and loaded to 55 % K_{IC}. Water was introduced to M6 after two days, and to M7 two weeks after the load had been increased in a second step to 85 % K_{IC}. M8 was kept dry throughout the test. If samples of one of the testing rounds did not approach tertiary creep or fail within a year, tests were terminated and samples unloaded.

4.1.2.3 Microstructural analysis

To characterize the microstructural response and brittle damage induced during the creep test we extracted longitudinally oriented thin sections from below the notch of samples M2, M4, and M5. These were immersed in a two-component epoxy resin, which was dyed with a fluorescent pigment (EpoDye), before being double polished, glued to carrier glasses, bisected and double-polished to a thickness of ~30 ± 5 µm. The fluorescent dye causes voids and cracks to glow neon-green when observed with black light. Digital image mosaics were taken at 5x and 20x magnification with a Leica DMLM microscope, captured by an Olympus DP 25 camera and automatically stitched with the Image Composition Editor (ICE) to provide the full view of thin sections. Scanning electron microscopy (SEM) images were obtained from fracture surfaces of second-round failed samples M6 and M7 using a Zeiss Gemini SEM 300. This SEM accepts air-dried samples and does not necessarily require surface preparation with evaporated gold or graphite, which may cause thermal cracking.

4.1.3 Results

Here we present the results of our wet and dry stepped iSENB creep tests on eight Carrara marble samples. We report observations concerning (i) the introduction of water, (ii) the load response, (iii) progression to failure, (iv) damage accumulation, and (v) the expression of subcritical crack growth on the microscale. We denote extensional strains as positive and contractional strains as negative.

4.1.3.1 Response to the introduction of water

When water was introduced to the notch of samples M1-M4 on day four of the first testing round, strains increased with rates decaying over the subsequent 24 hours (**Figure 4.1.4**). The mean strain accumulated by the samples over this period is ~90 µm/m, approximately equal to that induced by the initial loading of M2 and M4 to 55 % K_{IC} (**Figure 4.1.4**). Water was introduced to sample M7 on day 29 at a load of 85 % K_{IC} (**Figure 4.1.5a**). The introduction of water caused an immediate increase in strain, and the sample failed within less than 10 hours (**Figure 4.1.5a, b**). Upon the introduction of water, the strain rates increased gradually for about 30 minutes reaching a maximum of 0.4 $x10^{-9}$ s^{-1}, before slowing down, delimiting the primary creep phase (**Figure 4.1.5b**). The secondary creep phase lasted for about 6.5 hours with rates ranging between ~0.5 – 1.16 $x10^{-10}$ s^{-1}. The maximum strain recorded by the strain gauges was ~ 500µm/m (**Figure 4.1.5b**).

4.1.3.2 Long-term strain variations

Long-term strain magnitudes were relatively stable for both the dry tested sample M8 and the wet samples M1 and M3. M8 maintained a stable strain level of ~60 – 65 µm/m at 85% K_{IC} for 13 months until it was unloaded. Fluctuations in the strain level were modest and ranged within ± 5 µm/m over several days. Fluctuation in strain levels on wet sample M1 and M3 were in the range of ± 10 µm/m. M3 demonstrated a mean of ~550 µm/m at 85 % K_{IC} over 12 months at the time the test was terminated and the sample unloaded. M1 gradually decreased from a strain level of ~140 µm/m to a strain of ~90 µm/m at 55 % K_{IC} over two months, when the strain gauge became erroneous and sample was unloaded.

All first round samples displayed a gradual progression of extensional (M3 and M4) or contractional strain (M1, M2, and M5), with minor deviations associated with strong fluctuations in relative humidity (e.g. Day 12 and 19, **Figure 4.1.4**). Responses are more pronounced in the wet samples at lower loads (M1, M3, 22 % K_{IC}) and in dry sample M5 (**Figure 4.1.4**). During the second round (i.e. **Figure 4.1.5a**) and continued testing of M1 and M3, relative humidity only showed minor and gradual fluctuations and no associated strain changes were observed.

Further changes in the strain level have been associated with discontinuous water supply or disturbance of sample M1 by the unloading of adjacent sample M5, where a drop from ~ 180 µm/m to ~140 µm/m was observed (**Figure 4.1.4**). A decrease in strain on sample M3 between days 29 – 35 corresponds to a period in which the water flow was reduced due to a blockage in the dripping device. With a return to normal flow on Day 35 strain returned to the level of Day 29 within a day (**Figure 4.1.4**).

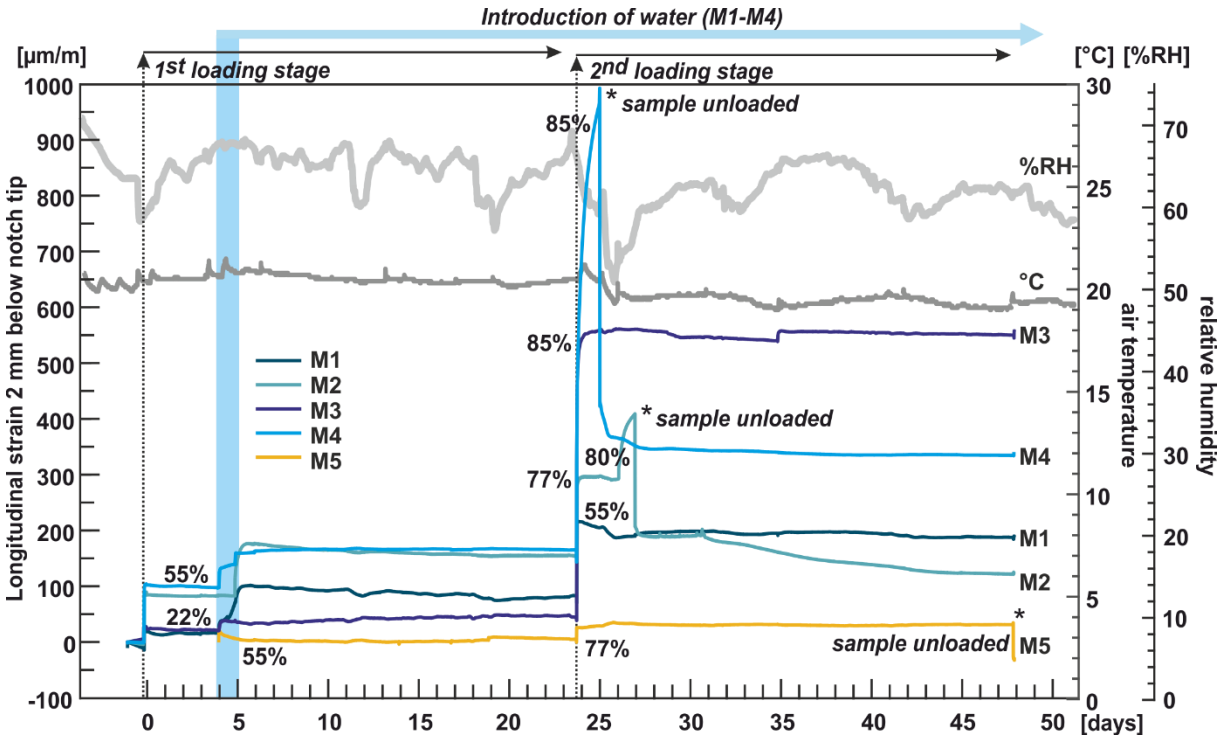

Figure 4.1.4 Temporal strain variations measured below notch tips on our Carrara marble samples M1-M5. Loading was applied at day 0 and day 24. Additional increments of strain in M1-M4 are associated with the onset of water dripping or restart. Relative air humidity [% RH] and air temperature [°C] are also plotted.

4.1.3.3 Response to loading

We observe distinct differences in the strain response to increased loading associated with wet and dry conditions in the Carrara marble samples (**Figure 4.1.4**). The initial loading of all samples was in dry conditions and the response instantaneous. Even though samples M2, M4, and M5 in the first-round of tests were all initially loaded to 55 % K_{IC}, M5 showed a strain of ~ 20 µm/m, about 1/5 of the two prospective wet samples (**Figure 4.1.4**). This is possibly related to the longer drying period of M5 of five days after pre-cracking vs. ~48 hours for M1-M4. This was avoided in the second round by air-drying all samples for five days before mounting and loading them in the test frame. Thus, when samples M6, M7, and M8 were initially loaded to 55 % K_{IC}, they yielded a strain of about 20 µm/m to 25 µm/m, the same as in sample M5 of the first round. The load on the dry sample M5 was increased from 55 % to 77 % K_{IC} and the strain instantaneously increased to ~30 µm/m, stabilizing at ~35 µm/m within

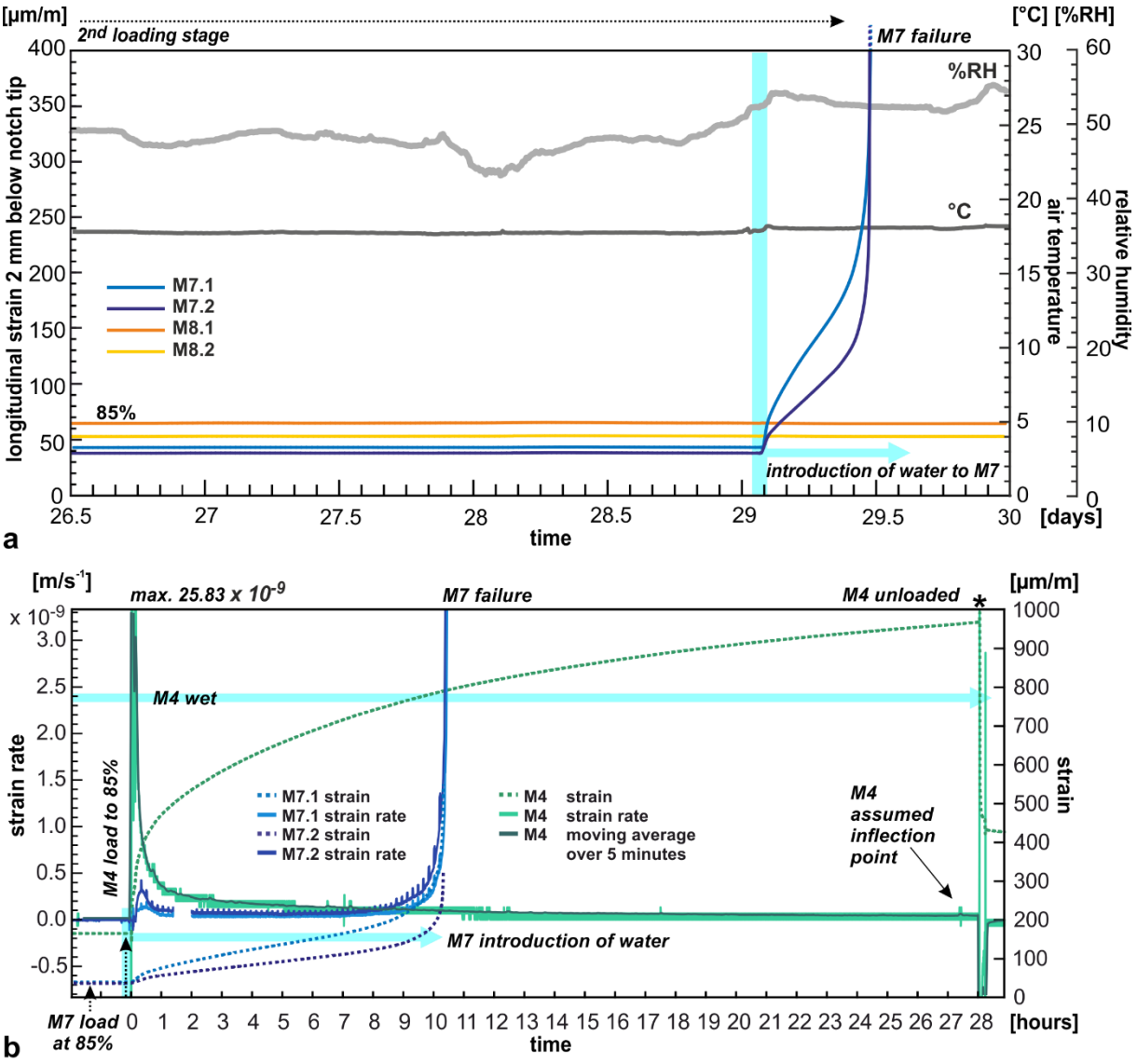

Figure 4.1.5 a Measured strain from day 26 to day 30 of the second long-term test of M7 and M8, both loaded to 85 % K_{IC} in dry condition, with two strain gauges each. Strains rapidly increase for M7 in direct response to the introduction of water (vertical thick blue line). **b** Strain and strain rate of sample M7 (two strain gauges) and M4 (one strain gauge) over the hours prior to failure, and unloading, respectively.

hours. When the load was increased to 85 % on the samples 13 days into the experiment, M7 and M8 were still in dry condition and strain response was instantaneous. Strain magnitudes levelled within an hour to ~40 µm/m and ~60 µm/m, respectively, which they maintained in the following weeks (**Figure 4.1.5a**).

Additional loading of wet samples M2-M4 on Day 24 caused the samples to exceed the pre-loading level of 66 % K_{IC}. Along with M1 which was loaded to 55 % K_{IC}, these samples showed an instantaneous response, with strains progressing for at least the next 30 hours (**Figure 4.1.4)**. The effect of the load increase on sample M2 (55 % → 77 % K_{IC}) settled at ~300 µm/m after a few hours and load was raised in a third step to 80 %. Sustained creep was observed following final loading of samples M2, M4, and M6. About 30 hours after the increase in load to 85 % K_{IC} on sample M4, and a third increase to 80 % K_{IC} on sample M2, both samples appeared to be entering tertiary creep. These samples were then manually unloaded to prevent failure. However, subsequent analysis of the strain rate indicated a minor fluctuation, rather than a true inflection of the strain curve (**Figure 4.1.5b**). The strain rate of ~$0.33 – 1.33 \times 10^{-10}$ s^{-1} observed in M4 is, however, similar to that in the secondary creep phase of M7, but lasted for at least 28 hours (**Figure 4.1.5b**). In the second round of testing samples, M6-M8 were allowed fail. Sample M6 was observed to fail on Day 17, 94 hours after the increase in load to 85 % K_{IC}. Unfortunately, strain data was not recovered.

In general, higher loads produced greater total strains, however, the absolute strain levels varied with loading path. For example, sample M1, which was initially loaded to 22 % K_{IC} exhibited a strain increase that is 0.25 times greater when loaded to 55 % K_{IC} than samples M2 and M4, wet at 55 % K_{IC} in the first load stage. This effect is perhaps more apparent when comparing samples M4 and M3 following the second loading. Whereas M4 continuously increased in strain and was unloaded when strain approached ~950 µm/m and dynamic rupture was expected. M3, which had been loaded to 22 % in the first stage, stabilized after 30 hours at a total strain of ~550 µm/m.

4.1.3.4 Induced residual strain in unloaded samples

Following unloading of samples and relaxation on a horizontal surface, residual strains were observed in all samples. Samples M2 and M4 were unloaded and disconnected from the dripping device to prevent dynamic rupture and to observe the microstructural changes. For the latter, dry sample M5 was also unloaded on Day 47 (**Figure 4.1.4**). Further samples were unloaded due to the termination of the tests (M3 and M8) or erroneous strain gauges (M1). Samples M2 and M4 demonstrated an immediate partial elastic relaxation and then a gradual reduction in strain in the days following the unloading and drying (**Figure 4.1.4,** M2 and M4). At the termination of the strain measurement on these samples on Day 48, they retained approximately 30 % of their maximum strain. Unloading of the dry sample M5, after 39 days of testing, caused an immediate reduction in strain below the notch to ~-30 µm/m (**Figure 4.1.4**, M5). Upon the termination of the tests and unloading after 12 months, wet sample M3 retained extensional strains of ~300 µm/m following five days of relaxation and air-drying on a horizontal surface. When unloaded after more than 14 months, the dry sample M8 immediately reduced in strain but retained extensional strain of ~30 µm/m, even after four days of relaxation on a planar horizontal surface. The magnitude of residual strain of unloaded wet samples exceeded those of the dry tested samples by an order of magnitude.

4.1.3.5 Microstructural damage and chemo-mechanical signature

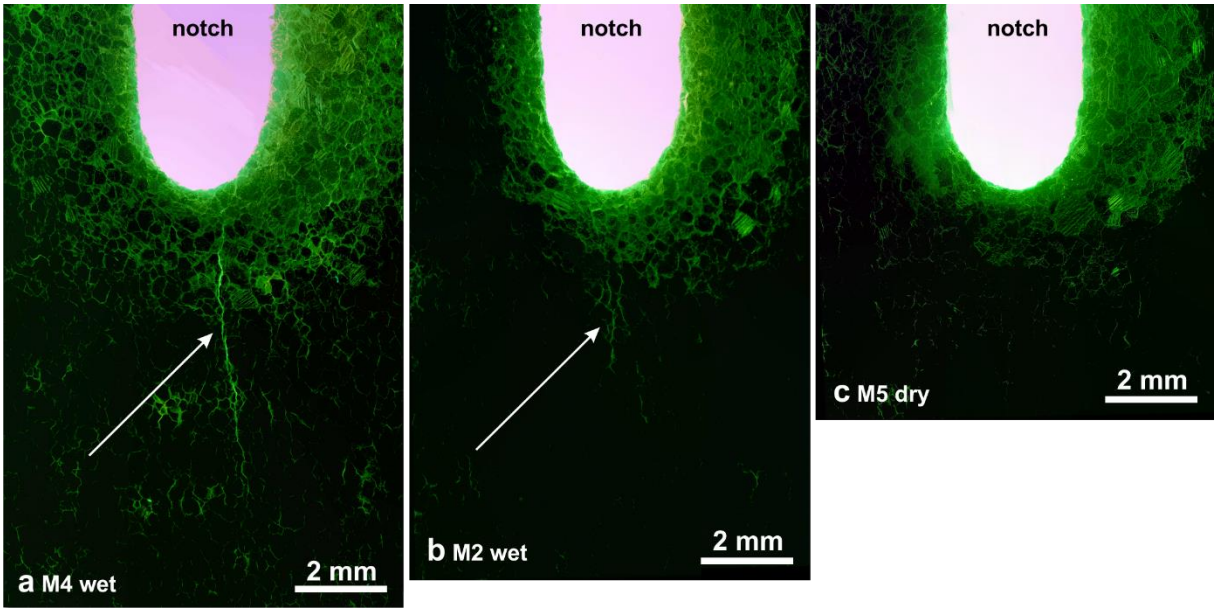

Figure 4.1.65 Fluorescent thin sections of the notch area in the x-direction of the wet samples **a**, M4 and **b**, M2, exhibiting a fracture path along grain boundaries (arrows), while in **c**, the dry sample M5 no progressive single fracture is visible. The lack of damage prevented our stitching algorithm from arranging images in the lower portion of slides derived from M2 and M5 resulting in variations in image sections.

Thin sections of the notch tip region and SEM images of post-failure fracture surfaces indicate subcritical crack growth occurs preferentially along grain boundaries. We observe brittle damage and discontinuities in a diffuse damage zone extending up to 0.3 mm from the saw cut-notch in specimens M2, M4, and M5 (**Figure 4.1.6**). In the two wet tested samples, microcracks radiate and disperse further outwards than the in the dry sample (**Figure 4.1.6a, b**), while one or two distinct fractures are evident, extending away from the notch tip (~4 mm in M2 and ~7 mm in M4, see **Figure 4.1.6a, b**). Following Equation (2), the extension of these fractures may have increased stress intensities from ~0.85 to ~ 1.04 MPa $m^{½}$ in M2, and from ~0.99 to ~1.33 MPa $m^{½}$ in M4. A narrow process zone of cracking along grain boundaries adjacent to the main fracture paths in M2 and M4 is depicted. A detailed view of the fracture path of M4 is provided in the Supporting Information (**Figure 4.1.S3**). Localized fracturing is entirely absent in the dry sample M5 (**Figure 4.1.6c**).

SEM images of the upper centimeters in M6 and immediately below the notch in M7, show faceted and rock-candy-like fracture morphology, with many triple points. These suggest subcritical crack growth occurred primarily along grain boundaries (**Figure 4.1.7**). Single microcracks perpendicular and parallel to the main fracture surface are evident in M6, marking the extent of the processes zone (**Figure 4.1.7b**). Intracrystalline cracks can be seen to exploit inherent flaws and crystal structures, such as lamella and cleavage planes (**Figure 4.1.7b, c**). Besides brittle cracking, disperse chemical alteration features are observed close to the notch in the SEM images. We observe indicators for dissolution of calcite as pitted surfaces and smoothed edges (**Figure 4.1.7c, d**) and precipitates as plastered fracture morphology (**Figure 4.1.7b**). Smooth and flat cleavage planes seem less affected by dissolution features (**Figure 4.1.7f,** arrows). Chemical alteration features are more evident on fracture surfaces of sample

M6 than M7, the latter of which had only been in contact with water for ~10 hours (vs. 12 days for M6). Dynamic high-speed ruptures in the form of cleavage steps and feather markings cut across the crystals a few millimeters below the notch tip in M7 (**Figure 4.1.7e**), suggesting an acceleration of the fracturing as the crack tip propagated away from the notch.

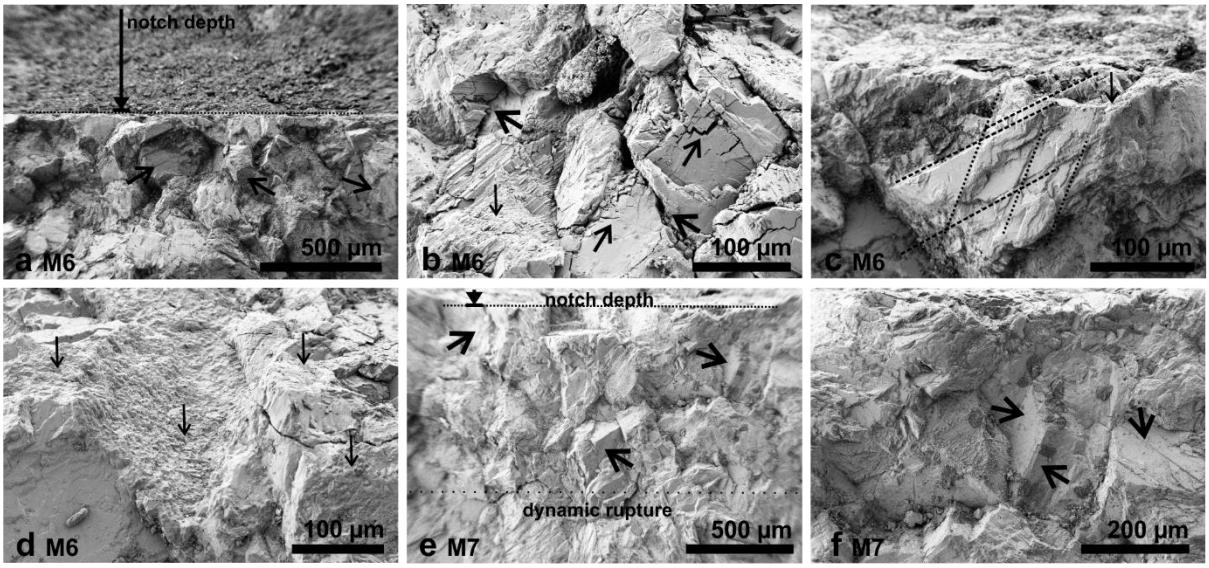

Figure 4.1.7 a-d SEM images of the fracture planes from M6, which failed wet at 85% K_{IC} after 21 days and **e-f** M7, which failed at 85% K_{IC} within one day from the introduction of water. Fractures appear to exploit pre-existing structure during propagation, as they are evident along grain boundaries (thick inclined arrows, **b**, **e**, **f**), lamellae (dotted lines, **c**), or cleavage planes (thin inclined arrows, **b**). Dissolution and precipitation features appear as rough, pitted and patchy surfaces (**b**, **c**, **d**, thin vertical arrows).

4.1.4 Discussion

Our laboratory experiments are a novel attempt to observe and constrain long-term mechanisms of progressive damage under controlled conditions, similar to those in natural rocks. Here, we discuss the subcritical crack growth mechanisms in the framework of observed processes in natural settings.

4.1.4.1 Effect of the introduction of water

The introduction of water to the notch induced an immediate increase in strain in all samples, with a continued gradual response for several hours depending on the loading level (M1-M4, **Figure 4.1.4**). Sample M7 proceeded to failure without an increase in load (**Figure 4.1.5**). We hypothesize that the instantaneous additional strain with the onset of water dripping results from the diffusion and associated hydro-mechanical responses. These responses can be both passive, e.g. expressed by a more compliant behavior, and active, e.g. by hygroscopic expansion. Upon wetting, samples loaded with moderate levels of 22 % and 55 % K_{IC} (M1-M4, first round) show a different response than sample M7, loaded to a near critical level (85% K_{IC}). The rheology of moderately stressed samples is more compliant if wetted (Rehbinder & Shchukin, 1972). Hereby surface energy is reduced along the diffusion front in the subcritically stressed wetted region around the notch (Bergsaker et al., 2016; Darot & Gueguen, 1986). In porous calcite rocks the diffusion of water relates to an overall decrease in cohesion of grain

boundaries and interfaces (Risnes et al., 2005; Røyne, Bisschop, et al., 2011); a common behavior also observed in steels and single crystals (Malkin, 2012; Maugis, 1985; Rehbinder & Shchukin, 1972; Traskin, 2009). Strain rates gradually decrease and the strain levels stabilize 12 to 30 hours after the onset of water dripping (**Figure 4.1.4**). The time-span corresponds with prior observations that most of the water absorption and diffusion occurs in 24 hours (Ozcelik & Ozguven, 2014). The uptake of water in marble is very limited owing to the high initial density and drying marbles respond over a similar time-span and manner in rates (Bellopede et al., 2016; Karaca, 2010). Reducing strain rate approaching maximum saturation are consistent with hygroscopic expansion experiments on several rock types, including marbles (Hockman & Kessler, 1950; Ruedrich et al., 2011; Weiss et al., 2004). Associated deformations are observed to be, at least partially, reversible (Koch & Siegesmund, 2004; Swanson, 1984). This partially reversible effect became accidentally evident in the first round of our tests, where a gradual reduction of strain level of sample M3 is associated with an interruption of water inflow on Day 29 (**Figure 4.1.4**). Over a six days period, the notch of M3 at 85 % K_{IC} was not supplied with water and could dry. Over that period, we observe a recoverable contraction of ~35 µm/m and its rapid recovery to the former strain level, once the anomaly was corrected (**Figure 4.1.4**). The magnitude of additional strain due to the presence of water is similar to the hygroscopic expansion of 0.001 - 0.0025 % (≈ 10 – 25 µm/m) observed in marble in an unstressed state (Koch & Siegesmund, 2004; Ozcelik & Ozguven, 2014; Winkler, 1996). The general gradual strain level change due to humidity fluctuations, as observed during the first loading stage of the first testing round, have also been observed in previous creep experiments (Bérest et al., 2005; Itô, 1979; Itô & Kumagai, 1994). In our cases, we cannot completely rule out electrical or mechanical measurement errors associated with the strain gauges or the adhesive bonding of them to the rock. However, the effect of each fluctuation seems to be rather an increase, then decrease of the long-term trend (either extension or contraction) for each sample, suggesting the effects were more likely associated with deformation of the samples.

The introduction of water to the near critically stressed sample M7 lead to a seemingly spontaneous brittle rupture (**Figure 4.1.5**). This contrasts the formerly described effect of a plastification at subcritical stress level as well as the behavior of samples M4 and M6, with the same loading path, though wetted at the first loading step. Water was introduced to sample M7 weeks after the second increase in load to 85% K_{IC} and at stable strain levels of ~40µm/m. Once wet, M7 progressed through all stages of creep and failed within 10 hours. This is about 1/3 of the time required for sample M4 to approach tertiary creep (**Figure 4.1.5b**). Though strain rates in the secondary creep phase of sample M4 and M7 were in the same order of magnitude of approximately 10^{-10} s^{-1}, the creep mechanisms seemed to be different. The overall strain magnitude of strain in M7 when wetted approached about 1/3 of that observed in M4, indicating a brittle and stiff rheological behavior. According to Rehbinder & Shchukin, (1972), it could be argued that the introduction of water caused a sudden drop in surface energy of the grain and crystal interfaces, whose bonds had already been critically strained, resulting in their rupture. A strong positive dependency of a decrease in surface energy by the presence of water and applied stress magnitudes has been observed in calcite single crystals resulting in accelerated crack growth (Bergsaker et al., 2016; Rostom et al., 2013). In our test set-up, the assumed damage zone of ductile and plastic deformation suddenly increases and localize fractures upon the introduction of water, which in turn self-enhances stress concentrations and crack growth until a critical stress and dynamic rupture. This is also evident in the limited vertical extent of a process zone dominated by subcritical crack growth following grain boundaries and an

extensive zone of prevailing transgranular fractures indicative of dynamic, high-speed fractures (**Figure 4.1.7e**). The response of our samples and thus of an open joint system to the introduction of water thus seems to be highly dependent on its strain/stress state.

4.1.4.2 Long-term strain behavior in wet and dry conditions

The alteration of the rheological behavior of the wet samples became obvious upon the second increase in loading in the first round of testing. Dry sample M5 exhibited a rapid, short-lived rate increase and linear strain response to the increase in applied stress, while wet samples (M1-M4) continue to increase in strain for an extended period of hours to days (**Figure 4.1.4**). This effect is evident throughout the range of our tested loads. In terms of the magnitude of strain developed below the notch tip, we observe approximately 8 times greater strains on wet samples (M2 and M4, ~160 µm/m) than our dry samples (M5, M7, M8, ~22 µm/m) when loaded to 55 % K_{IC}. At loads of 85 % K_{IC}, we observe ~10 times greater strains in wet sample M3 (~550 µm/m than in the dry sample M8 (~60 µm/m). An increase in deformability or compliance of rocks in the presence of a fluid or high humidity has also been observed in uniaxial compressive tests by (Bérest et al., 2005; Grgic & Giraud, 2014), as well as in torsion tests (Chen et al., 2017). A similar change in the mechanical behavior of water saturated creep test samples was found by Lockner (1993). The observed high strain magnitudes, without necessary rupture, during the tests, can be attributed to a reduced elastic modulus in wet samples (e.g. Wong et al., 2016).

The microscopic mechanisms to explain the macroscopic more compliant behavior can be derived from diffusion associated reduction in friction and water enhanced (micro)plasticity. The barrier to deformation, both in terms of temperature and stress, has been shown to reduce when Carrara marble is wet (Rutter, 1972). While Rutter (1972, 1974) deduced a reduction in cohesion but not in friction by interstitial water in a Carrara marble, more recent experiments on the rheological behavior of wet carbonate rock indicate a decrease in the frictional strength in triaxial tests (Nicolas et al., 2016). Reducing frictional and cohesive strength by the presence of water in the microstructure would ease intergranular slides and glides. Another Carrara marble specific cause for the eased deformations can be attributed to the near straight geometry of the grain boundaries (**Figure 4.1.1b, c**), which provide minor mechanical resistance to friction. In this context, have the strongest permanent macroscopic deformations (bowing) been observed in calcareous metamorphic building stones with granoblastic microstructure and straight grain boundaries, like our Carrara marble (Bellopede et al., 2016). Next-to the intergranular deformations, microplasticity is known to be enhanced in the presence of water (Atkinson, 1984; Winkler, 1975). Microplasticity absorbs strain energy by building up intracrystalline strain which stiffens and embrittles the crystals and leads to stress concentrations at interfaces (Chen et al., 2011; Lee & Kirby, 1984; Newman, 2002), thus as a preparatory control on further rheological behavior. These water enhanced plastic deformations might explain why we observe a 25% higher strain magnitude in sample M1 initially loaded to 22 % K_{IC}, when raised to 55% than sample M2 and M4, initially loaded to that extent (**Figure 4.1.4**).

4.1.4.3 Damage due to chemo-mechanical effects

Chemo-mechanical effects may also drive an increase in strain through, e.g. stress corrosion cracking. In contrast to other stress corrosion studies on calcite and Carrara marble using deionized water or various pH or ion concentrations (Nara et al., 2017; Rostom et al., 2013), we used carbonated water near the saturation limit. This was important as we aimed to

focus on the interaction of water with subcritically stressed bonds at the crack tip, rather than solely focusing on dissolution kinetics.

Our thin section and SEM analyses revealed evidence of water enhanced subcritical crack growth (**Figure 4.1.6a, b**) and chemical alterations (**Figure 4.1.6a, b, 4.1.7a-d**). Dissolution features in the form of grooves, pitted surfaces, smoothed edges, and terraces formed along cleavage planes in the upper millimeters below the notch of sample M6 and M7 (**Figure 4.1.7**). In the same region, we observe patchy evidence of precipitates on grain surfaces and in vesicles. Chemical alteration features in our samples appear similar to features attributed to intergranular precipitation and dissolution following stress corrosion tests observed by X-ray tomography in a polycrystalline material (King et al., 2008b). The spatial distribution and proximity of precipitates and dissolution features are indicative of a chemical kinetic system close to equilibrium (Dohmen et al., 2013; Rostom et al., 2013). The system is susceptible to minor changes in boundary conditions over the course of the experiment, such temperature, and humidity fluctuations or partial pressure variations. In our test setup especially applied stresses, damage accumulation, and stress intensity increase due to i.e. crack propagation could alter the partial pressure of the solute within the rock matrix. At sites of raised pressure, the reactivity level increases locally and enables dissolution even in transport-limited regimes in tight cracks and pore spaces (Schott et al., 1989). Locally increased chemical potential gradients have been associated with stressed grain contacts, high dislocation density or an increase in the number of active surface sites (Keszthelyi et al., 2016; Laanait et al., 2015; Schott et al., 1989). Precipitation or sintering, on the other hand, may be associated with localized decreases in mechanical stress, lower partial pressure and thus an oversaturation of the fluid (Dove et al., 2005; Schott et al., 1989). Even though the chemical properties of the calcite crystals and the precipitates are the same, their mechanical properties, especially their elasticity is altered. This elastic mismatch of the more porous and stiff precipitate vs. the mineral grains can generate layer parallel stresses in excess of the composite strength, which are eventually released by fracturing (Geisler et al., 2015; Kranz, 1983; Ruiz-Agudo et al., 2016). Overall, chemo-mechanical alterations can generate microstructural inhomogeneity over time (Swanson, 1984).

4.1.4.4 Subcritical cracks grow along grain boundaries

Almost all fracturing evident within 20 mm of the crack tip in our post-failure sample M6 occur along grain boundaries (**Figure 4.1.7a-d**), as the majority of the surface appears to be composed of unfractured grains, generating a stepped and cleaved morphology. In the thin sections of sample M2 and M4, ~95 % of fracture propagation occurred along grain-grain contacts, with a minor component along cleavage planes (**Figure 4.1.6a, b**). These observations are consistent with results from wet subcritical loading experiments on dolomite (Barnhoorn et al., 2010), dolerite, gabbro, granite (Atkinson & Rawlings, 1981; Meredith & Atkinson, 1983), sandstone and Carrara marble (Atkinson, 1979), and quartz (Dove, 1995). While the weakly interlocking grain boundaries evident in our samples likely provide little mechanical resistance to movement, this may also be due to the suggestion that grain boundaries both provide the most available surface area for adsorption of water, and have lower bond strengths relative to the crystals themselves (Croizé et al., 2010; Putnis, 2014). Aside from grain boundaries, some samples also exhibit fracturing along cleavage planes (**Figure 4.1.7 a-d**), reflecting the low bond density and surface energies along these features, especially if water is present (Santhanam & Gupta, 1968; Stipp et al., 1994). We take this to be further evidence for a progressive, rather than dynamic propagation of fractures immediately below the notch.

In our thin sections, we noted a narrow process zone of microcracking of ~100 µm surrounding the localized fractures in the wet samples (**Figure 4.1.6a, b, 4.1.S3**). Our observation is similar to those in creep experiments on silicate rocks, where microcracks along the primary fractures are marginal (Labuz et al., 1987; Zang et al., 2000). This is also consistent with results from experiments of stress corrosion cracking in stainless steel, where a localized fracture progressed along interconnected grain boundaries while neighboring ones remained largely unaffected (King et al., 2008b). These observations scrutinize our employed conceptual model in Figure 1b, with a process zone of a microcrack population, and associated mechanical models (i.e. Brantut et al., 2012), if the fracturing is water enhanced.

4.1.4.5 Residual strains and damage accumulation

Evidence for inelastic strain accumulation is apparent from the unloading of samples. M2 and M4, which were unloaded as we assumed they were approaching tertiary creep, retained around one-third of the maximum extensional strain after unloading and drying up. This indicates that permanent strains were induced during the testing period of 27 and 25 days. The retention of this extensional strain is comparable to the theoretical behavior described in **Figure 4.1.1a**. Supportive of inelastic deformations is a diffuse zone of microcracks and localized fractures in the thin sections (**Figure 4.1.6a, b**). As a reference to sample M2 and M4, dry sample M5 was unloaded after 39 days. We observed a relative contraction of ~-30 µm/m below the notch tip, with respect to the initial relaxed state. We interpret this to be an indication that plastic and brittle deformation on this sample was limited to the region immediately below the crack tip, and the compression of the measured volume on unloading is caused by principally elastic deformation in the remainder of the sample. This is supported by our thin section analysis, which indicates the region of microcracking in M5 extends only a few millimeters below the notch tip (**Figure 4.1.6c**). This damage zone, observed in all three samples could also relate to the sample preparation and pre-cracking procedure (**Figure 4.1.6**). The pronounced difference in residual strain in wet and dry sample implies a strong control of the environmental condition on subcritical crack growth and progressive failure.

The magnitude of residual strain in sample M3 after a year of testing is similar to that of M2 and M4 of ~300 µm/m. Even though M3 was wet and loaded to 85% K_{IC} it did not approach tertiary creep. A reason for the diverging behavior might be the loading path (**Table 4.1.1**). While a minor increase in the loading of sample M1 (22 % → 55 % K_{IC}) resulted in a strain softening behavior, M3 experienced a major increase from 22 % to 85 % resulting in a strain hardening behavior (**Figure 4.1.4**). Strain hardening in calcite rocks has been reported by several authors (Brantut et al., 2014b; Vajdova et al., 2012) which results in a seemingly stable creep of the sample over long periods of time.

Maximum strains in our dry samples M5 (~35 µm/m at 77 % K_{IC}) and M8 (~65 µm/m at 85 % K_{IC}) were an order of magnitude lower than their similarly loaded wet counterparts. Both were initially loaded to 55 % K_{IC}, generating strains of between 20 µm/m and 25 µm/m. When unloaded M8 retained an extensional strain of ~ 30 µm/m, thus nearly half of its maximum strain level, while M5 exhibited contractional strains of that magnitude. The main difference in these samples was the testing period, in which M8 exceeded that of M5 by more than a year. Although it is not possible to determine whether the difference in behavior between M5 and M8 is a result of the duration of the test or also affected by slightly higher load. A similar time-dependent behavior in static and cyclic bending tests on Carrara marble beams, which remained in an extensional strain state, when unloaded, was attributed to accumulated

inelastic deformation (Cardani & Meda, 2004). Even though the long-term strain level of M8 seemed to be constant, and no damage accumulation expected, the retained strain upon unloading suggested subcritical deformations. Zoomed in, the strain measurement of M8 show minor fluctuations and variation of increasing and decreasing rates. These small stick- and slip-motions, analogous to the stick-slip motion of earthquakes and failure events, might be indicative for the accumulation of damage at geologic low strain rates (van der Baan et al., 2016; Ferdowsi et al., 2013; Maugis, 1985).

4.1.4.6 Broader implications

In this series of experiments, we take steps to transfer insights derived from classical subcritical crack growth experiments in laboratory environments to scales and conditions relevant to fracture propagation in real near-surface bedrock settings. We want to highlight three aspects: (i) the short-term and long-term effect of water on progressive failure, (ii) microscale controls, and (iii) subcritical damage traits.

The associated effects of water infiltration into rock slope instabilities may be somewhat more complicated than the traditionally assumed increase in pore pressure, and associated decrease in effective stresses on a sliding plane (Handwerger et al., 2016; Petley et al., 2005; Yerro et al., 2016). We find that water can immediately induce both an active and passive response of the rock through processes such as hygroscopic expansion and plastification (**Figure 4.1.4, 4.1.5**). These effects are likely to be dominant over those associated with a reduction in effective stress where near-surface tensile fractures determine modes of instability. The response of the near critically stressed sample M7, by dynamically rupturing within 10 hours of the introduction of water, demands a better knowledge of the in-situ stress or strain state. That the effect of external factors on progressive rock slope failures varies depending on the material stress state has been reported for several field settings (Arosio et al., 2009; Mainsant, Larose, Brönnimann, et al., 2012; Obermann et al., 2014).

Results from our long-term static loading experiments provide insights into the interaction of chemical processes with mechanical stresses that are not possible to capture in small-scale rate-dependant experiments. We observed fracturing predominantly tracing grain boundaries, a process that can both increase permeability and local tensile stresses by making way for dissolution and sintering on the created surfaces (**Figure 4.1.6, 4.1.7**). A similar granular disintegration has been reported for natural marble decay by other authors (Eppes & Griffing, 2010; Shushakova et al., 2013; Siegesmund, Ruedrich, et al., 2008). Comparing naturally and artificially aged marbles, Bellopede et al. (2016) observed an overall similar strength decay but no increase in the effective porosity in the artificially aged samples. This underscores the importance of chemical processes along interfaces (Putnis, 2014; Ruiz-Agudo et al., 2016). However, popular models of stress corrosion rates focus on dissolution kinetics based theories (i.e. Eppes & Keanini, 2017). The main issue is that dissolution rates of carbonate rocks in laboratory studies exceeds those in natural environments by 1-3 orders of magnitudes (Casey et al., 1993; Velbel, 1993; White & Brantley, 2003). Applying these dissolution rates to stress corrosion cracking (i.e. Atkinson, 1984; Eppes & Keanini, 2017) likely overestimates the chemical effects. Enhanced subcritical crack growth in our experiments appears only partially driven by dissolution (**Figure 4.1.7**).

During the long-term experiments, it seemed that nothing really happened unless a boundary condition was changed or an internal threshold was met. In our test set-up, we had several factors that had a self-enhancive trait, like chemo-mechanical processes or the stress

concentration. Internal thresholds in the experiment might have been the maximum subcritical fracture length/stress intensity (M4 and M6, **Figure 4.1.6b**) or strain state (M7). A threshold of damage accumulation as a control of rock slope failures has been suggested already in 1968 by Bjerrum & Jørstad, but the multiple pathways and dependencies (i.e. lithology, environmental conditions, preconditioning) render quantification and predictions challenging (Brantut et al., 2014a; Kranz & Scholz, 1977). Even though we choose the exemplary, simple and homogeneous Carrara marble memory effects (i.e. formation related residual strains) might have a strong effect on the subcritical crack growth and progressive failure (Kranz & Scholz, 1977; Krautblatter & Moore, 2014; Logan, 2004).

4.1.5 Conclusions

We have presented new experimental data on the time-dependent deformation of Carrara marble with a focus on the varying microstructural and mechanical properties due to the presence of water. Besides the diverse chemo-mechanical mechanisms and their feedbacks enhancing brittle subcritical cracking, plastic deformation, water weakening effects, and elasticity changes can be observed in long-term tests on Carrara marble beams. Induced subcritical stresses, in combination with water at the notch clearly alter the macroscopic as well as microscopic behavior. We identified five main observations from our tests:

- Extensional strains beneath the notch tip increase immediately with the introduction of water. This 'water-weakening' is likely due to physical changes on intergranular bonds by either active, e.g. hygroscopic expansion or passive mechanisms e.g. plastification.
- Strain magnitudes as well as residual strains, indicating inelastic damage accumulation, in wet samples are up to an order of magnitude higher than in the dry loaded counterpart.
- Subcritical damage occurred in Carrara marble at load levels above 22% K_{IC} in both, wet and dry samples. Tertiary creep and failure is commonly observed in wet samples loaded above 80% $K_{IC,}$ or similarly loaded dry samples which have water introduced.
- Inelastic damage accumulation is path-/time-dependent and the response of rock to an addition of load or water is reminiscent of the loading and environmental history.
- Prominent microstructural features, such as the grain boundaries geometry in Carrara marble, exert a key influence on subcritical crack growth behavior. Chemo-mechanical mechanisms progressively alter the local material toughness and elasticity preferentially along grain boundaries.

Here we demonstrate that the progressive development of bedrock fractures in response to environmental conditions and applied external loading provides a primary control on the long-term strength of bedrock. These results apply to a broad range of fields, including geomorphology, geotechnical engineering, and architecture. We encourage further work to gain insight into the physics of processes in the region of crack tips, with particular consideration to stress and environmental memory effects.

Acknowledgments and Data

Carrara marble was gratefully provided by Marmi Carrara s.l.r., Carrara, Italy. The experiments improved by discussions with Florian Amann and Anja Røyne. Long-term testing was possible at the TH Cologne, Baustofflabor and SEM images were taken at the Research Museum König, Bonn. AV was supported with a BMBF Scholarship by the Rosa-Luxemburg-Foundation. The manuscript improved greatly by the comments from the associated editor, two anonymous reviewers, and Xiaofeng Chen.

The supporting information file contains further information on crystallographic preferred orientations of our Carrara marble (**4.1.S1**), preliminary numerical model (**4.1.S2**) as well as a detailed image of the fracture path of sample M4 (**4.1.S3**). Data for this paper is available following doi 10.14459/2014md1442265.

4.2 Scientific Publication II

Constraining internal states in progressive rock failure of Carrara marble by measuring residual strains with neutron diffraction.

Anne Voigtländer, Kerry Leith, Jens M. Walter and Michael Krautblatter (2020)

Journal of Geophysical Research: Solid Earth, 125, e2020JB019917.
https://doi.org/10.1029/2020jb019917

Constraining internal states in progressive rock failure of Carrara marble by measuring residual strains with neutron diffraction

***Anne Voigtländer**, Kerry Leith, Jens M. Walter and Michael Krautblatter*

Abstract

Knowledge of the internal state of rock is key to anticipate its rheological response and susceptibility to external factors. Time-dependent failure in rock is controlled by internal state changes, like damage accumulation or strength degradation. But assessing internal states and changes thereof, non-destructively and independent of external forcing is not straight forward. Residual strains, measured with neutron diffraction techniques are used as a proxy for the internal state in material sciences. We investigated its potential for progressive rock failure by measuring residual strain states of an untested and three mechanically and chemo-mechanically pretested Carrara marble samples. We collected neutron diffraction data for three crystal lattice planes $\{10\bar{1}4\}$, $\{0006\}$, and $\{1\bar{1}20\}$. Measurements showed an initial overall contractional spatially homogeneous residual unit cell volume strain state of about -400µstrain, though magnitudes were strongly partitioned among measured crystal lattice planes. However, they are equal within the spatial orientations of the intact sample. For the pretested samples, the induction and relaxation of strains varied spatially with the pretesting stress field and environmental conditions. The vertical extent of superposition of the initial residual strain state was greatest in wet samples, the magnitude of induced extensional strain highest in the dry sample. This indicates chemo-mechanically enhanced subcritical crack growth with concomitant residual strain relaxation as well as the mitigation of extensional strain built up by the presence of water during pretesting. Our experiments show, that residual strain has a significant potential to provide insights into past and actual internal states to anticipate progressive rock failure.

Key Points:

- Neutron diffraction techniques allow non-destructive assessment of internal strain states of rocks
- Inherited residual strain state of Carrara marble is overall contractional
- Residual strain is indicative of the strength and possible damage state of rocks

4.2.1 Introduction

The failure of rocks impacts the face of the earth by driving landscape evolution, limiting infrastructure performance and causing natural hazards. While in brittle rock, failure proceeds in a progressive manner, where microscopic, subcritical damage extends over time and eventually leads to critical deformation and macroscopic failure, the capability to anticipate their evolution is still restricted. This is partially due to methodological limitations to gain direct and non-destructive insight into material states, and few experimental studies on the accommodation of subcritical deformation and damage at the grain-scale. Conventionally, rheological characterization of rocks relies on destructive tests that measure the divergence from an initial state (Brantut et al., 2012, 2014b; Diederichs, 2003b; Eberhardt et al., 1999). These experiments are generally restricted to measure whole-rock-sample properties, like strength and deformation, and are not designed to determine a pre-existing initial state independent of external forcing (Covey-Crump & Schofield, 2009; Schofield et al., 2003, 2006). In material sciences, focusing on long-term strength, toughness and performance of engineered materials, thus material properties in resistance to progressive failure, methods and mechanistic concepts have been established to assess the internal state of the materials and changes thereof (Ritchie, 2011; Withers, 2015). Residual elastic strains, measured with diffraction techniques are used as a proxy for the internal state in material sciences. With the concept of residual elastic strains, in short, residual strains, internal states and rheology of engineered materials can be described (Withers & Bhadeshia, 2001a, 2001b). Here, we apply the concept of residual strain to natural rocks and measure those with neutron diffraction to better understand their internal state and progressive failure.

Rocks are subject to stresses throughout their geologic lifespan. As they exhume, both, imposed confinement and ambient temperatures reduce and introduce differential stresses (Zang & Stephansson, 2010). During exhumation and the accompanied unloading, not all of the induced elastic strain energy is released. Strains that remain in a rock in the absence of boundary loads are referred to as "residual" (Voight, 1966b). Residual strains equilibrate globally but can vary locally at the grain-scale (Friedman, 1972). Residual stresses or strains in rocks may result from thermal or mechanical induced purely elastic processes, inelastic yielding or a combination of both (Holzhausen & Johnson, 1979). Permanent deformation locks-in elastic strains within the rock, similar to tempered glass. Elastic distortions could also be locked in by internal self-constraint of neighboring crystallites and their crystallographic geometry (Meredith et al., 2001). Emery (1964, p. 244) stated, therefore, that '[…] any rock, because it is a rock, must have in it more or less conserved elastic strain energy and that its present condition is a transient one and represents the sum of all that has happened to the rock'. Since then, studies have reported residual strain in rocks indicating grain-scale strain magnitudes in the order of $\times 10^{-3}$μstrain (Friedman, 1972; Siegesmund, Mosch, et al., 2008). In geological materials, unlike for engineered materials, stress conditions and magnitudes of external forces which were necessary to produce the observed residual strains are unknown. The residual strain state has, therefore, itself been widely used to infer the stress magnitude and spatial direction of former geological stress fields (Engelder & Sbar, 1977; Sekine & Hayashi, 2009; Zang & Berckhemer, 1989).

Residual strains also affect the rheology of rock (Holzhausen & Johnson, 1979; Voight, 1966b). It is currently reasoned that the strain magnitude and sign reflect the interatomic spacing, spatial array of atoms in the individual crystal lattices, and their energetic states

(Withers & Bhadeshia, 2001b). The amount of compressive stress that atomic bonds can repulse before breaking, defines the maximum compressive strength of the crystal and is consequently related to the polycrystalline strength. Likewise, the amount of tensile stress a bond can support defines the maximum tensile strength of the material. The strain state of crystal lattice planes strongly defines the possible response of rocks to applied external forces, including bulk fracture toughness or strength. Next to the influence of residual stresses and strains on rock deformation, externally applied forces can relax pre-existing as well as induce new strains.

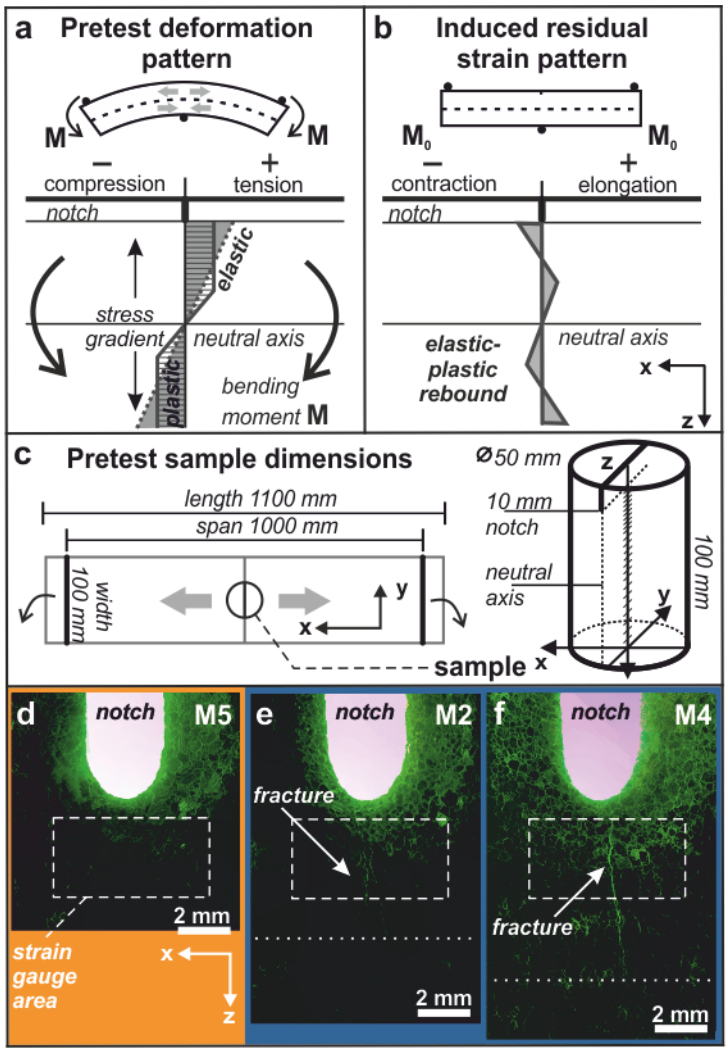

Figure 4.2.6 a Schematic pretest deformation pattern, **b** resulting induced global residual strain state without brittle fracturing. **c** Pretest and measured sample dimensions, direction and measurement point distribution along the vertical axis. Fluorescent dyed thin section image of the notch area of **d** sample M5, pretested with dry condition at the notch, **e** and **f** sample M2 and M4, pretested with wet condition at the notch. The extent of localized fractures is indicated by a dotted line. The dashed area highlights the position of strain gauge measurements during the pretest.

In general, it is assumed that stored strains can be relaxed when grains or crystals are freed from the neighboring constraints (Friedman, 1972). This can be achieved by the opening of microcracks, but also by grain boundary glides and chemically altered grain boundary cohesion (Engelder et al., 1977; Luzin et al., 2014; Silberberg & Hennenberg, 1984). Spatial

direction and relative magnitudes of residual strains are controlled by the presence of microcracks created by tectonic stresses, stress relief, and weathering, which in turn influences the mechanical strength of rock (Hoskins & Russell, 1981). Externally applied stresses causing any local permanent deformation, by distortion of crystal structure, chemical cementation or thermal recrystallization, could lock-in elastic strains which would overprint pre-existing residual strains (Friedman, 1972; Holzhausen & Johnson, 1979; Withers & Bhadeshia, 2001b). The introduction of residual strains is not necessarily spatially uniform (**Figure 4.2.1a, b**) due to (i) heterogeneous yielding and stress concentrations at microstructural flaws, (ii) anisotropic thermal expansion coefficients, and (iii) mechanical or thermal stress gradients (Holzhausen & Johnson, 1979; Timoshenko & Goodier, 1970). Likewise, the relaxation of residual strains is spatially variable (Nichols, 1975). Internal damage state relevant for progressive rock failure occurs due to both, the formation of cracks (i.e. strain relief) and the inducement of especially extensional elastic strain.

In engineered materials not only the effect of mechanical stresses on residual strain is investigated but also environmental conditions. Physical and chemical weathering cause alteration of material properties, including stiffness, and can enhance subcritical crack growth (Atkinson & Meredith, 1987; Nara et al., 2017; Peck, 1983). Residual strain response and deformation mechanisms to thermally induced stresses have been determined in geologic materials (Luzin et al., 2014; Meredith et al., 2001; Siegesmund, Mosch, et al., 2008). However, the effect of moisture or chemically-enhanced mechanisms, have only been reported for metals and engineered materials. Here, residual strains pose a first-order control on chemically enhanced subcritical crack growth, referred to as stress corrosion (King et al., 2008a; Toribio, 1998). The effect of residual strains on stress corrosion cracking in rocks has been postulated but has not been investigated (Atkinson & Meredith, 1987).

Initially, so-called "residual stresses" (measured as residual strains) have been examined using strain relief methods including overcoring, microcrack orientation and density maps (Hoskins & Russell, 1981; Zang & Berckhemer, 1989). Likewise, in conceptual approaches, residual stresses have been linked to rock failure, exfoliation and spalling (Emery, 1964; Kieslinger, 1958; Müller, 1969). Hereby, instantaneous or time-dependent inelastic subcritical damage is assumed to decrease strain magnitudes. These destructive and invasive methods measure bulk strains on the surface of rock samples. As the relaxation of the residual strains is assumed to be achieved by the creation of new surfaces, these microcracks can then be evaluated in thin sections. In contrast to this, neutron diffraction techniques enable the non-destructive measurement of residual strain in the interior of solid polycrystalline rock materials (Holden et al., 1995; Schofield et al., 2006; Withers & Bhadeshia, 2001a). Deviations in lattice parameters can be quantified and subsequently elastic strain, microstructural properties and damage can be derived. Neutron diffraction allows assessing elastic strains at the grain-scale on conventionally sized samples (S. A. Hall et al., 2011; Schofield et al., 2006). These methods enable us to explore phenomena such subcritical crack growth and creep, where deformation-induced microstructural and strain change are expected to be small and to assess the spatial variability of strain change within the rock sample.

Advancing possibilities and especially in-situ testing have increased the application of neutron diffraction in rock physics, for rock mechanical problems and by providing data for numerical models. However, for time-dependent rock deformation experiments, in-situ testing is not applicable due to time constraints at research reactors, and testing environments are

generally limited to thermal experiments, as water absorbs neutrons. To assess time-dependent rock deformation and wet conditions with regards to internal strain states we simplified the problem: We i) focused on a well-studied Carrara marble, a homogeneous, and monomineralic metamorphic rock, and ii) used mechanically or chemo-mechanically pretested samples to evaluate different altered states. Neutron diffraction data was collected of an intact sample and three mechanically and chemo-mechanically pretested samples, assuming, that the initial residual strain state is similar in all samples, enabling their comparison. With these data we i) defined the initial residual strain state of Carrara marble, ii) assessed the inducement of strains due to the mechanical pretesting, and iii) inferred the role of the internal (i.e. initial residual strain) and external (i.e. subcritical mechanical loading and dry and wet testing conditions) factors on the induced damage extent. By comparing the relative effect of external and internal factors, our study provides novel insights into the role of residual strains on progressive rock failure.

4.2.2 Material characterization and methods

Here we report on the essential characteristics of the material and the pretesting with regard to the applied neutron diffraction techniques. The main characteristics of the used Carrara marble (section 4.2.2.1), and the sample preparation, pretest set-up and observations (section 4.2.2.2) are given. Details on both were reported and discussed by Voigtländer et al. (2018). In section 2.3 we introduce the applied neutron diffraction technique and describe the measurement procedure applied in this study (section 4.2.2.4).

4.2.2.1 Carrara marble

The Carrara marble used, consisted of monomineralic calcite (> 98 % $CaCO_3$) with a mean grain size of ~200 μm and a dry density of ~ 2.7-2.8 g/cm^3. The polycrystalline metamorphic rock samples display a near-random crystallographic preferred orientation and are therefore regarded as texturally nearly isotropic (Voigtländer et al., 2018, **Figure 4.2.S1**).

Distinctive diffraction patterns are formed due to the trigonal crystal structure of calcite (unit cell dimensions and axis: $a = b \neq c$, $\alpha = \beta = 120°$, $\gamma = 90°$, $a \approx 4.9887$ Å, $c \approx 17.0623$ Å (Rao et al., 1968)). These characteristics facilitated repeatable mechanical testing and relatively unambiguous neutron diffraction patterns. Previous neutron diffraction measurements on Carrara marbles have affirmed the presence of residual strains within in the order of –400μstrains due to their metamorphic history (Scheffzük et al., 2007).

4.2.2.2 Sample preparation to induce residual strain and damage states

To obtain mechanically and chemo-mechanically altered states of Carrara marble we pretested samples under dry and wet conditions previously described in Voigtländer et al. (2018). These pretests consisted of inverted single edge notch three-point (iSENB) bending creep tests on Carrara marble beams (**Figure 4.2.1a**). All samples were cut from the same block. Samples dimension were 1100 mm x 100 mm x 100mm with a 10 mm notch in the center (**Figure 4.2.1c**). The principal longitudinal stress direction was in the x-direction of the sample. Due to the loading configuration, the induced stress state was graded along the vertical axis (z-direction) as the stress shifts from tension in the upper half to compressive stresses in the lower half of the beam (**Figure 4.2.1a**). Macroscopic surface deformation in the axial direction was monitored with strain gauges at the notch tips during the pretesting (**Figure 4.2.1d**, **e**, **f**,

Voigtländer et al., 2018). Carrara marble samples, M2, M4 and M5 used for this study, were mechanically loaded in two stages, with dead weights loads calculated for the initial sample geometry and percentage wet fracture toughness (K_{IC}, ~1.3 MPa/$m^{1/2}$, Voigtländer et al., 2018). First, the three samples (M2, M4, and M5) were loaded to ~55% K_{IC}. In a second step, loads were raised to ~77% K_{IC} in M5 and M2 (subsequently increased to ~80% K_{IC}) and to ~85% K_{IC} in M4. Throughout the testing period, calcite-saturated water was added to the notch of sample M2 and M4, while M5 remained dry, at ambient temperature and humidity.

Because these samples were to be used in this study on the internal states they were only allowed to creep but not to fail. We had no criterion when that would happen. Experiments showed that, as soon as tertiary creep was reached, failure of the samples could not be prevented. This was (i) due to our simple dead weight loading system, and (ii) the speed of dynamic fracturing. To prevent this, we unloaded the samples when the strain rates at the notch tip increased by an order of magnitude and we assumed that tertiary creep was being approached. This was the case for samples M2 and M4, with wet condition at the notch loaded to ≥80% K_{IC} after 27, respectively 25 days in the pretest. Dry samples in the same testing configuration did not approach tertiary creep during testing periods even at loads of ~85% K_{IC} unless water was introduced to the notch. Possible chemo-mechanical effect leading to these behaviors are discussed in Voigtländer et al. (2018) and references within. M5, the dry pretested case was unloaded at the termination of the testing period after 48 days. **Figure 4.2.1d**, **e** and **f** are fluorescent dyed thin section images of the notch areas of samples M5, M2 and M4, highlighting the microstructurally visible damage induced during the pretest. Thin sections of samples tested with water present at the notch (**Figure 4.2.1e** and **f**) revealed single localized fractures along grain boundaries. No induced fracture was observed in the thin section of sample M5 (**Figure 4.2.1d**).

Cylindrical subsamples (ø = 50 mm, h = 100 mm) were cored vertically through the center of samples M5, M2 and M4 for the neutron diffraction measurements (**Figure 4.2.1c**). For the study reported here the 'wet' pretested samples M2 and M4 represent coupled chemo-mechanical altered states, the 'dry' M5, a mechanically superimposed residual strain state. The loading path and duration of the three samples varied. These time- and stress-dependent effects cannot be resolved with the applied method. With the neutron diffraction, we determine the vertical extent of the damage zone and the associated grain-scale deformations. Next to the pretested samples a reference sample, M0 was cored from an untested Carrara marble beam, to assess the initial, inherited residual strain state.

4.2.2.3 Neutron diffraction

Neutron diffraction is the application of elastic neutron scattering to determine the atomic structure of a material. The advantage of neutrons, compared to X-ray diffraction is their penetration depth of up to tens of centimeters (Holden et al., 1995). This allows evaluating the internal structures of polycrystalline materials without surface or edge effects. Diffraction measurements utilize the reflective properties of atoms ordered in crystal lattice planes, following Bragg conditions (Bragg, 1924). These structures show specific reflection angles (2θ°) and specific peak positions (d_{hkil}) in the according diffraction patterns (**Figure 4.2.2a**). Measurements of residual strains rely on the elastic deformation within polycrystalline materials, which cause changes in the spacing of the lattice planes (d-spacing) relative to their strain-free conditions. These distortions of the lattice planes alter the reflection angle and with it the peak position in reference to a strain-free or undistorted lattice (d_{0hkil}) (Noyan & Cohen,

1987; Withers & Bhadeshia, 2001b). A shift in the peak position is thus a measure of the elastic microstrain ε_{hkil}, estimated by

$$\varepsilon_{hkil} = \frac{(d_{hkil} - d_{0hkil})}{d_{0hkil}}$$

[1].

Where a positive peak position deviation indicates extensional strain, a negative value a relative contraction (**Figure 4.2.2b)**. These types of microstrains are also termed intergranular strains as they have been linked to elastic strains locked in between grains or crystals (Withers & Bhadeshia, 2001a). Distortions of lattice planes can also alter the dispersion of the reflected neutrons resulting in changes of the peak positions and shape metrics (Ungár, 1998). Our neutron diffraction measurements were conducted at the SALSA strain diffractometer at the Institute Laue-Langevin (ILL), Grenoble, France (**Figure 4.2.2c**) which is specified to measure the peak positions in 2θ° space, with a precision of approximately ± 3.5×10^{-5} Å (Pirling et al., 2006). Assessment of peak shape metrics like the full-width at half maximum (FWHM), which signifies plastic deformation within grains and crystallites, are therefore viewed as subsidiary

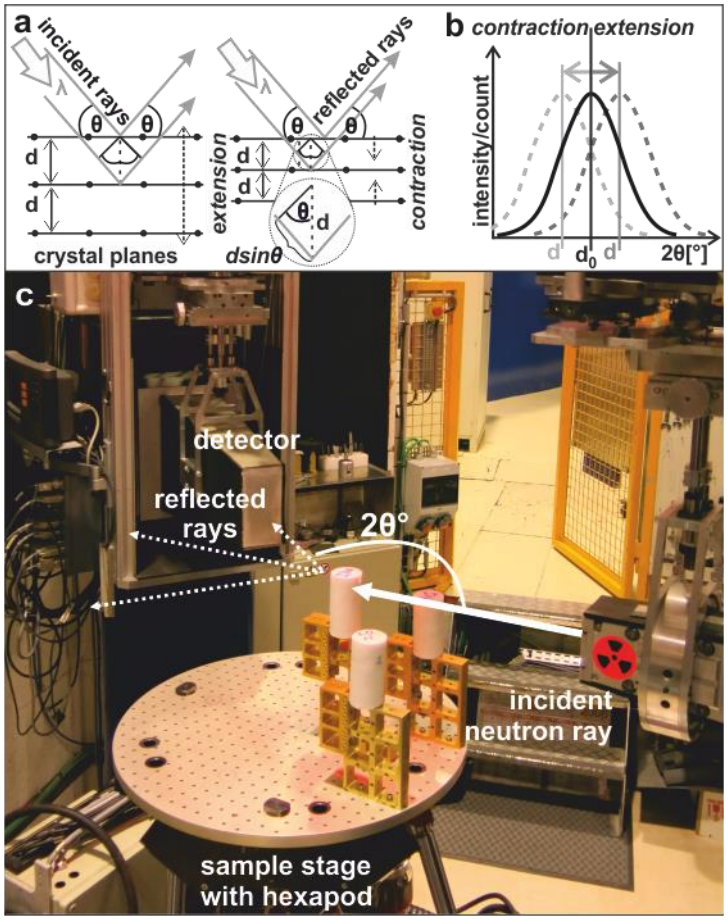

Figure 4.2.2 a Angle dependence of incident and reflected rays due to crystal lattice d-spacing, and **b** schematics to evaluate intergranular elastic strains by peak position shift **c** SALSA diffractometer and experimental set-up.
and are reported in **Supplement Information 4.2.1**.

4.2.2.4 Measurement protocol and strain estimation

SALSA measures small sections of diffraction pattern spectrum covering mainly single reflection peaks. For this study, neutron diffraction data was collected of diffraction peaks corresponding to crystallographic planes $\{1\bar{1}20\}$, orthogonal to the a-axis, and {0006}, orthogonal to the c-axis. By measuring these two orientations we can describe the unit cell of the calcite crystal. Additionally, $\{10\bar{1}4\}$, a prism face, was measured alongside with $\{1\bar{1}20\}$ due to the close position of the diffraction peaks in the recorded spectra. At SALSA, the thermal neutrons flux is continuous with an intensity of $\sim 5\times10^{7}$ ns^{-1} cm^{-2}. We measured with a wavelength of λ= 1.64 Å. Neutron wavelengths are selected by a double-focusing monochromator and SALSA is equipped with radial focusing collimators for a precise gauge volume, in our stud of 40 mm^3 (2 x 2 x 10 mm).

The geometry of the experimental setup, shown in **Figure 4.2.2c**, is chosen with the detector positioned in regard to the direction of the sample to measure with the scattering vector parallel to the pretesting loading direction x (hereafter referred to as axial strain, ε_x), or perpendicular, in y (hereafter referred to as tangential strain, ε_y, **Figure 4.2.1c**). Samples are then manually adjusted and placed horizontally to collect data along the z-axis from the notch or in the case of the reference sample M0 from its upper surface to the bottom of (hereafter referred to as vertical strain, ε_z). At each measurement point, strain was measured in the three spatial orthogonal directions (**Figure 4.2.1c**). Sampling progressed in 0.5 mm steps of gauge volume from the surface or notch for the first 5 mm below before the interval was increased to 10 - 20 mm for the rest of the samples M2, M4, and M5. Steps were again reduced to 0.5 mm for the 5 mm from the bottom of the sample in M0. Results provided at least 25 measurement points per sample, direction, and crystal lattice planes. Each measurement point comprises 4000 scatter counts.

Diffraction data were fitted using a single Gaussian peak fit in LAMP (Large Array Manipulation Program), the standard diffraction fitting software provided by the ILL (Richard et al., 1996). An individual background fit clearing standard instrumental errors has been applied to all diffraction spectra. In addition to the acquisition of the peak position of the three crystal planes, we estimated the unit cell volume regular calcite crystal structure, based on $\{1\bar{1}20\}$ and {0006} measurements. Strain-free reference states (d_{0hkil}) are theoretically derived based on calcite single crystal unit cell dimensions (Rao et al., 1968). To isolate the effects of the mechanical and chemo-mechanical pretesting (see section 2.2), these calculations were compared to the untested sample M0. Serving as a reference state, the mean peak position along the measured section of M0 was used exempt the five measurement points near the surface top and bottom, as they might show edge effects.

4.2.3 Results

4.2.3.1 Residual strain state of Carrara marble

Neutron diffraction data of the pristine sample M0 showed an overall contractional residual strain state throughout the vertical measured section and sample spatial orientations (x, y, and z, **Figure 4.2.3, 4.2.S2**). The sum of the unit cell volumetric lattice strain in the three spatial directions was non-zero (**Figure 4.2.3, 4.2.S3**). The magnitudes of residual strains varied by measured crystal planes, ranging from an average of -435 (±455) µstrain in $\{10\bar{1}4\}$, to -890 (±500) µstrain in {0006}, to -2015 (±697) µstrain in $\{1\bar{1}20\}$ in all sampled spatial orientations

(**Figure 4.2.3**). The unit cell volumetric strain related to an average volumetric contractional state of about -370 (±160) µstrain (**Figure 4.2.3**). We use this initial strain state as the background against which the changes in the pretested samples, described below, are interpreted.

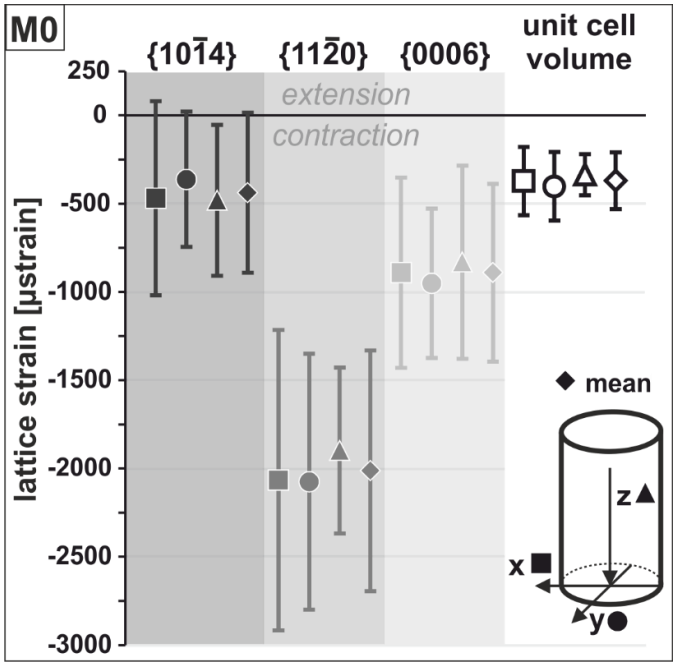

Figure 4.2.3 Average residual lattice strains of sample M0 in the three spatial direction and their mean in crystal planes {10$\bar{1}$4}, {1$\bar{1}$20}, {0006}, and the unit cell volume. The overall strain state is contractional. Magnitudes vary by crystal planes and less by spatial orientation.

4.2.3.2 Strain state pretested Carrara marble

Here we present the principal observations of the residual strain state measured in the pretested samples working downwards from the notch tips to the base of the samples (**Figure 4.2.1c**). The overall residual strain states of the preceded tested samples M2, M4, and M5 were contractional (**Figure 4.2.4-6**). Extensional, intergranular axial strains, in reference to the mean strain state of untested sample M0, were observed in all samples in the measurement points 10 - 20 mm (in z) below the notch. Beyond these points, the strain states were contractional and approached the reference mean strain of M0 towards the neutral axis. Measurements below the neutral axis of the samples exhibited a less contractional strain state than the reference strain state. The crystallographic planes {0006} and {10$\bar{1}$4} showed a greater absolute deviation from the reference sample M0 (up to 4000µstrain and 2000µstrain, respectively), while crystal planes of {1$\bar{1}$20}, kept a compressive strain of about -2000µstrain in all samples and all spatial directions (**Figure 4.2.4-6**). A general difference between the dry (M5, **Figure 4.2.4**) and the wet pretested (M2 and M4) samples was observed in the vertical extent and magnitude of the induced strain pattern (**Figure 4.2.5**, **4.2.6**).

4.2.3.2.1 Strain state in the 'dry' mechanically pretested case

The overall residual strain state of the mechanically dry pretested sample M5 was contractional for all three crystal planes and in the unit cell volumetric strain (**Figure 4.2.4**). However, the strain state within the first 5 mm below the notch (in z) of the sample was extensional, markedly in the axial-direction (**Figure 4.2.4a**). The magnitude of these induced

extensional intergranular axial strains just below the notch-tip range from ~500 to 1800µstrain in $\{10\bar{1}4\}$ (**Figure 4.2.4a**), ~1000 to 3500µstrain in {0006} (**Figure 4.2.4b**), and ~200 to 400µstrain in unit cell volumetric strain (**Figure 4.2.4d**). In opposition to the extensional axial strain state, tangential strains were contractional, in the range of about -250 to -500µstrain in $\{10\bar{1}4\}$, -2500 to -3500µstrain in {0006}, and -500 to -600µstrain in the unit cell volume below the notch.

4.2.3.2.2 Strain state in the 'wet' chemo-mechanically pretested cases

In the wet pretested samples, a change in the assessed crystal lattice planes and the unit cell volume in reference to M0 was detected up to 30 mm below the surface along the vertical measured section (in z, **Figure 4.2.5, 4.2.6**). The unit cell volumetric strains were in an overall contractional state between -1000 and -50µstrain in all spatial directions, while the individually measured crystal planes exhibited local extensional strain primarily in the x-direction (**Figure 4.2.5, 4.2.6**).

In the axial direction of sample M2 an absolute extensional strain state was observed within the first 2 mm below the notch in crystal lattice planes {0006} (**Figure 4.2.5b**). In crystal planes $\{1\bar{1}20\}$, the strain deviated from the reference sample M0 of up to 1000µstrain (**Figure 5c**). In the unit cell volume, the axial strain corresponds with the reference strain state up to ~12 mm below the sample surface (**Figure 4.2.5d**). Below these first millimeters, up to 25 - 30 mm of the vertical section, the strain state in the axial direction showed a strong contractional strain state in all measured crystal lattice planes. These strong contractional axial strains were contrasted by less contractional strains (in reference to M0) in the y- and z-direction.

Sample M4 showed extensional axial strain at the notch tip of ~900µstrain, as well as at 17 mm of ~1400µstrain in lattice planes $\{10\bar{1}4\}$ (**Figure 4.2.6a**). In between these extensional strains, a steady increase and a subsequent decrease in contraction was observed which terminates at ~16 mm. Extensional strain states at 15 - 20 mm (in z) were also observed in diffraction peaks of crystal planes {0006} of ~500 to 1800µstrain (**Figure 4.2.6b**) and less contractional strain in the unit cell volume (**Figure 4.2.6d**). The superimposed change in reference to the state of M0, vertically exceeds the visible fracture tip (**Figure 4.2.1f**) by about 1.5 mm, below this, the strain state in all spatial directions is contractional.

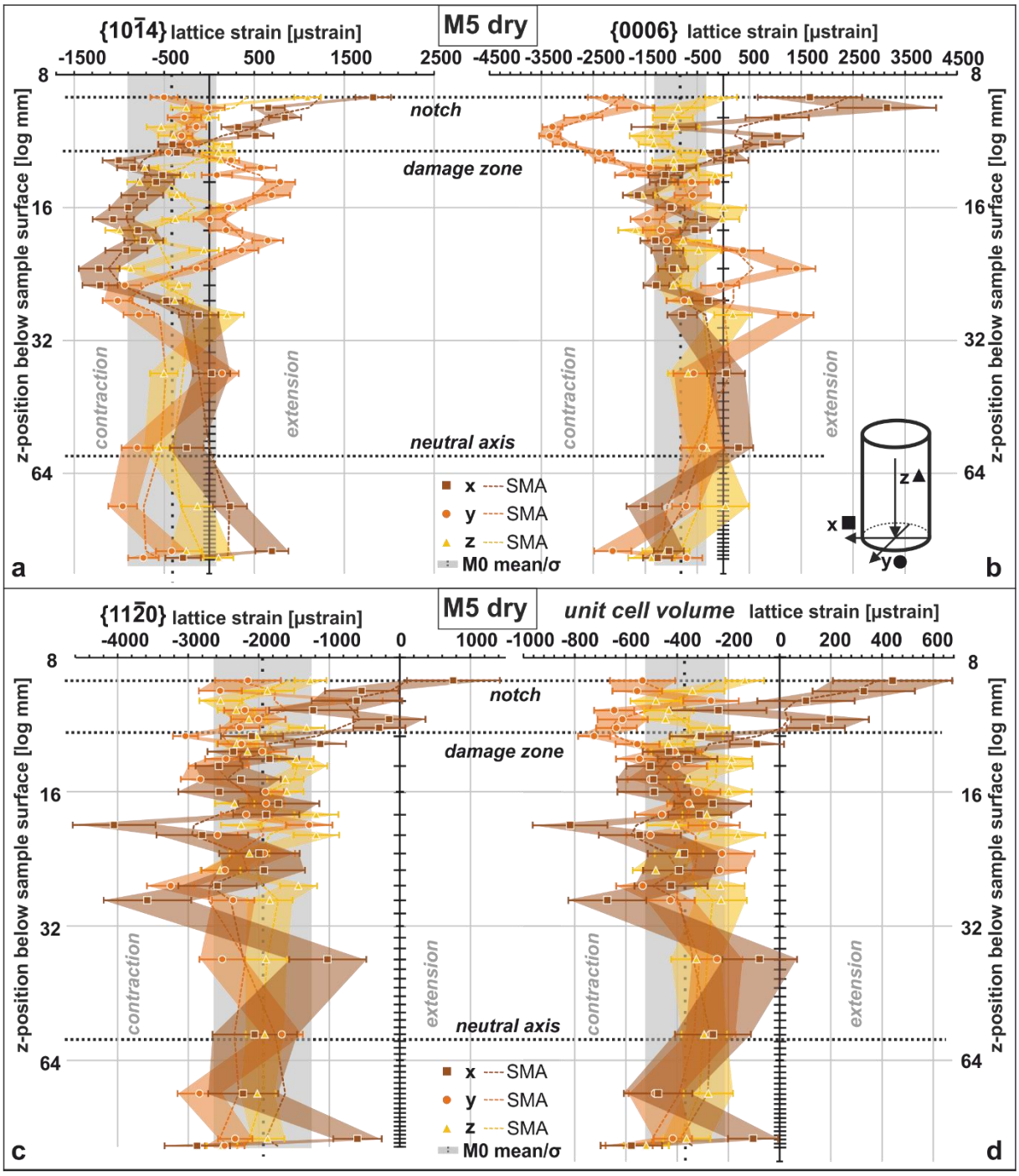

Figure 4.2.4 Residual lattice strain of single crystal plane and unit cell volume of sample M5 along the vertical measured section. **a** Crystallographic planes {10$\bar{1}$4}, **b** {0006}, **c** {11$\bar{2}$0}, and **d** the unit cell volume. The spatial direction are indicated by color and symbol. Strains are given with their error bounds and a three-point running average in dashed lines (SMA). Vertical black dashed line represents the mean, the grey bound the standard deviation of reference M0. Vertical extent (in z) of the notch is inferred from a thin section image (**Figure 4.2.1d**, Voigtländer et al., 2018). The extent of the damage zone is discussed in the text.

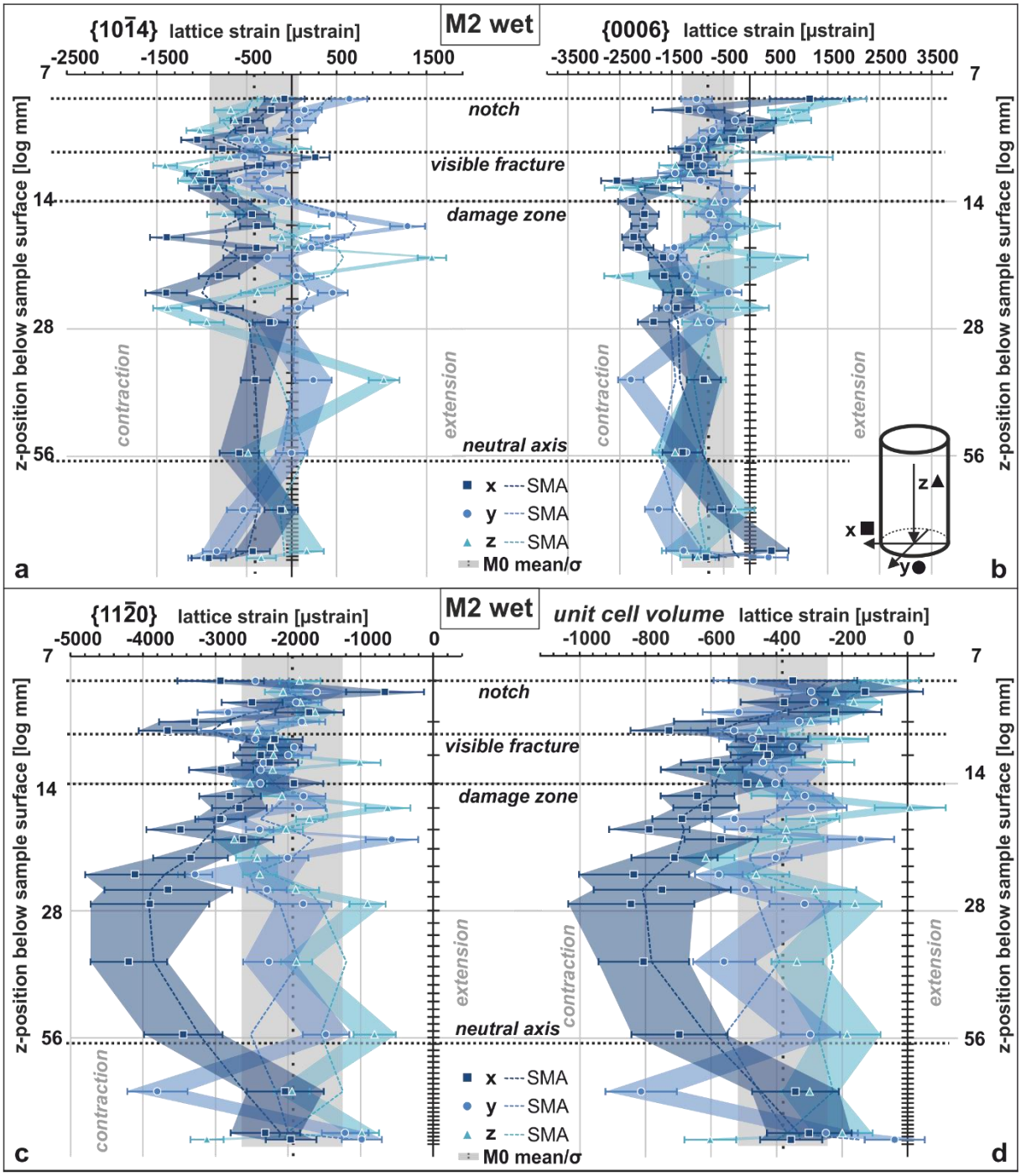

Figure 4.2.5 Residual lattice strain of single crystal plane and unit cell volume of sample M2 along the vertical measured section. **a** Crystallographic planes{10$\bar{1}$4}, **b** {0006}, **c** {1$\bar{1}$20}, and **d** the unit cell volume. The spatial direction are indicated by color and symbol. Strains are given with their error bounds and a three-point running average in dashed lines (SMA). Vertical black dashed line represents the mean, grey bound the standard deviation of the reference M0. Vertical extent (in z) of the notch and visible fracture are inferred from a thin section image (**Figure 4.2.1e**, Voigtländer et al., 2018). The extent of the damage zone is discussed in the text.

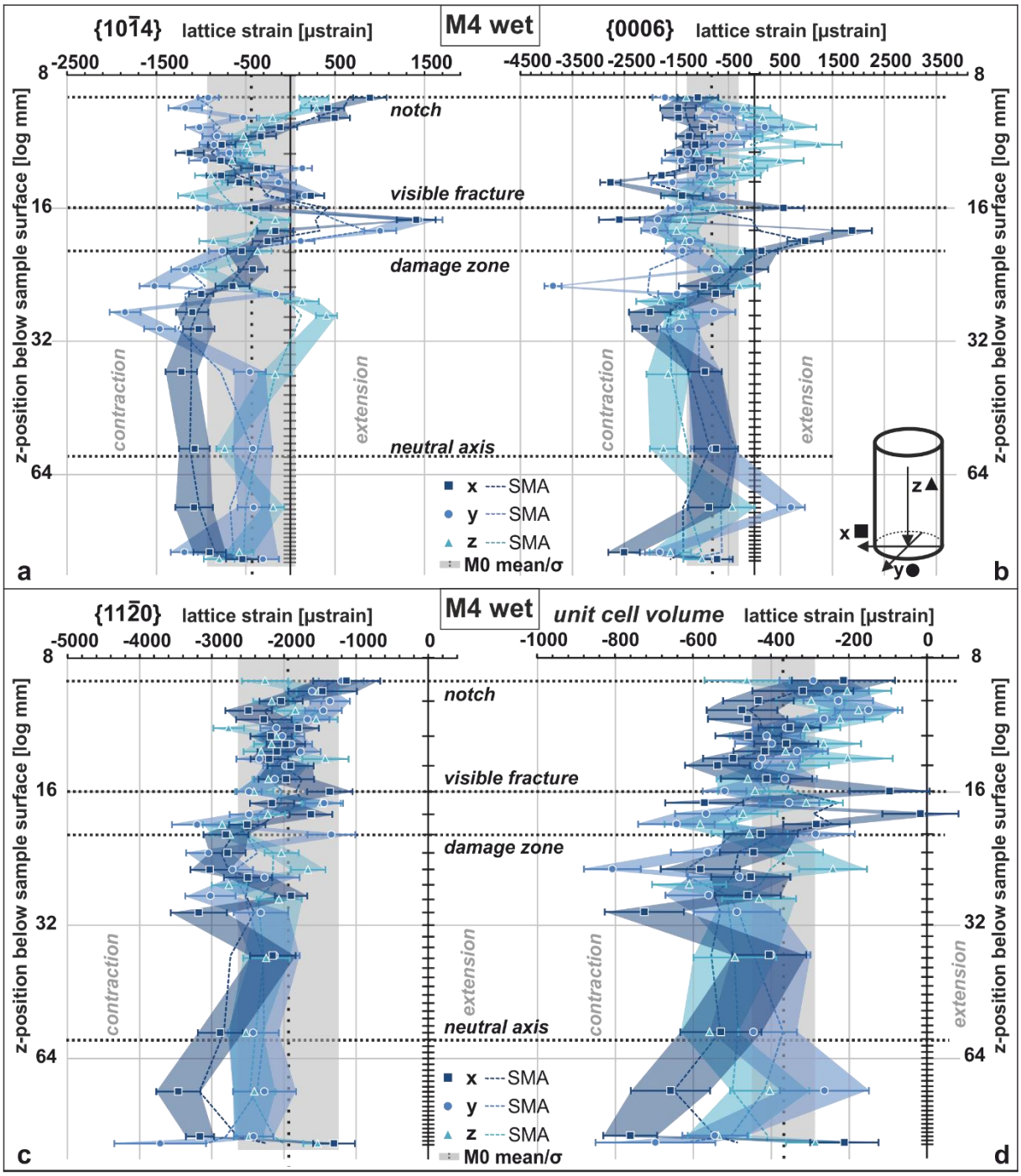

Figure 4.2.6 Residual lattice strain of single crystal plane and unit cell volume of sample M4 along the vertical measured section. **a** Crystallographic planes {10$\bar{1}$4}, **b** {0006}, **c** {11$\bar{2}$0}, and **d** the unit cell volume. The spatial direction are indicated by color and symbol. Strains are given with their error bounds and a three-point running average in dashed lines (SMA). Vertical black dashed line represents the mean, grey bound the standard deviation of the reference M0. Vertical extent (in z) of the notch and visible fracture are inferred from a thin section image (**Figure 4.2.1f**, Voigtländer et al., 2018). The extent of the damage zone is discussed in the text.

4.2.4 Discussion

We measured the residual strain of Carrara marble samples by neutron diffraction to better understand their influence on the rheology and how they are altered by time-dependent and environmentally enhanced deformation. Neutron diffraction techniques essentially measure the lattice planes of the crystallites. Due to the nearly randomized crystallographic preferred orientations (CPO) of our Carrara marble (**Figure 4.2.S1**) no distinct influence of texture on the diffraction pattern was expected. The peak position of the three measured lattice planes, $\{10\bar{1}4\}$, $\{0006\}$ and $\{1\bar{2}10\}$ in reference to strain-free positions represent/indicates the bulk intergranular strain state of the assessed gauge volume. In our experiment, it was ~2 × 2 × 10 mm (~40 mm^3), equivalent to ~20 grains. The measured magnitude and sign represent the sum of all residual strains of the individual crystallographic planes within that gauge volume. The strain state is discussed concerning this representative elementary volume (REV) of rock.

First, we discuss the initial residual strain state of Carrara marble with the observations of the untested reference sample M0. Second, we compare the residual strain of pretested samples, M2, M4 and M5 with the initial residual strain state of M0, to infer the role of the internal and external factors on progressive rock failure. We focus on how subcritical crack growth during the pretest have caused inducement and relaxation of initial residual strain state and speculate how the initial residual state might have influenced the progression and extent of damage during the pretest.

4.2.4.1 Initial residual strain state

The general expectation of the internal strain state of the untested sample M0 would be that, as there was no traction on the surface, the sample would be macroscopically in elastic equilibrium. Neutron diffraction data of the intact reference sample M0 showed, that the Carrara marble maintained contractional strains in the order of $\times 10^{-4}$ in the unit cell volumetric and $\times 10^{-3}$ in single crystal lattice orientations at the location and scale of the representative elementary volume (**Figure 4.2.3, 4.2.S2**). The sum of the unit cell strains in the three spatial directions was contractional by about -1000µstrain (**Figure 4.2.S3**). If the sum is not equilibrated at this scale, it implies that the material has undergone deformation along and in-between grains (Pintschovius, 1992). Analogous experiments have shown that extensional and contractional strains are both present, in close proximity to each other on the local grain-boundary scale (Friedman, 1972; Gallagher et al., 1974; Holzhausen & Johnson, 1979). The bulk contractional residual strain state of our sample thus indicates that contractional strains dominate within the crystal structures measured in the diffraction gauge volumes along the vertical sample section. For our Carrara marble, we assume that the material deformed as a continuum with locking-in residual strains homogenously throughout the material while it was deformed and exhumed in the crust. Here, the sum of the measured gauge volumes is the representative elementary volume discussed in the following. In this context, we observed for our intact sample spatially isotropic unit cell volume strain magnitudes of -400 (± 190) µstrain in x-, -370 (± 190) µstrain in y-, and -340 (±115) µstrain in the z-direction (**Figure 4.2.3**). We discuss the generality of these states and their implications for the interpretation of stress memory and first order, highly idealized material properties in a stress-based framework. In detail, this assumption is not valid as a polycrystalline material like Carrara marble will have deformed and build up strain in a non-continuous fashion across grain boundaries and crystals. However, this distinction is not resolved in our neutron diffraction measurements.

In geological studies, most residual strain data of rocks is considered as strain memory and interpreted regarding the potential paleo-stress field (Engelder & Sbar, 1977; Sekine & Hayashi, 2009; Zang & Berckhemer, 1989). A scenario of how the residual strains are locked-in the Carrara marble would either be by the external tectonic forcing or internally organized by material properties during the formation of the Apuan Alps. For Carrara marble, it has been reported that the rocks were buried to a depth of 20 to 40 km when reaching metamorphic peak conditions (D1), followed by successive rapid exhumation up to a depth of 10 – 15 km (D2) (Balestrieri et al., 2011; Carmignani & Kligfield, 1990). Our samples showed a relative homogeneous microstructure and a near-random crystallographic preferred orientation (CPO) (Voigtländer et al., 2018). These microstructures are the result of static recrystallization during these deformation phases (Molli et al., 2018; Molli & Heilbronner, 1999). Deviatoric stresses, which might have been arising from decompression and cooling during exhumation would have balanced each other when rock reached the surface (Zang & Stephansson, 2010). However, our data show, that residual strains still exist in the intact Carrara marble sample, M0. This would indicate that the residuals strains were induced, highly simplified speaking, under hydrostatic condition. The potential to develop residual strains under hydrostatic conditions has been described by Savage (1978) for granites. Due to varying thermal expansion coefficients in the two considered materials by him, residual strains form due to the cooling rock bodies. Resulting shear stress at the interfaces of the two material would lock-in elastic strains without volume or shape changes, similar to variational principles of Hashin and Shtrikman (Avseth et al., 2010; Hashin & Shtrikman, 1962; Watt & Peselnick, 1980). In a monomineralic material as the Carrara marble, this can be explained by considering the specific thermal properties of calcite. Calcite crystals show highly anisotropic thermal expansion coefficients, with expansion parallel to the crystallographic c-axis and contraction parallel to the crystallographic a-axis (e.g. Rao et al., 1968). In our Carrara marble, where we have randomly distributed orientations of the crystal axis, the highly anisotropic cooling response of the crystallographic axis of the calcite minerals would result in elastic mismatch and deviatory strains especially along grain boundaries with different crystallite orientations and thermal expansion coefficient. The calcite rock volume, would thus internally tense up during the general cooling. This thermally driven locking mechanism of strains, analogous to the tempering of glass, would probably affect the rheological properties of the rock and especially its strength (Bruner, 1984; Hoskins & Russell, 1981; Nichols & Abel, 1975).

In material science, the residual strain state is often interpreted concerning its effect on rheology and material strength (Toribio, 1998; Withers, 2007). Applying this broadly to rock, the inherited measured general contractional strain state of our Carrara marble can be described as a degree of rock strength. Rock strength is typically indicated in a stress-based framework. A first-order estimate, following Hooke's law, assuming a Young's modulus of 49 GPa (Alber & Hauptfleisch, 1999), and taking our measured mean unit cell volumetric strain of -370µstrain of sample M0, equates to residual stresses of -18.1 MPa. To exploit residual strain measurements in a stress-based framework, elastic constants would need to be measured in the same material as well. In addition, if the estimated general residual stress state is compressive, like in our Carrara marble sample M0, this would exert indirect tensile stresses at the same time. The magnitude of the indirect tensile stress would be the contractional residual stress times the Poisson's ratio. Assuming a Poisson's ratio of about 0.19 - 0.29 (Alber & Hauptfleisch, 1999) the general residual stress state of our Carrara marble would indirectly stress the bulk material, in a first approximation, by about 3.4 – 5.2 MPa. Independent Brazilian indirect tensile strength

tests of the same Carrara marble yield a bulk strength of about 5 MPa (Voigtländer et al., 2017a). Accordingly, we interpret that the rock is near critically pre-stressed. Additionally, induced contractional strains in the order of -400µstrain though, could facilitate indirect tensile microcracks. The relaxation of residual strains is readily accomplished by microcracking, mainly along grain boundaries. The contractive pre-stressed or pre-strained microstructure thus would define the fracture toughness and long-term fundamental strength of the rock. Residual strains would, at least partially, define the magnitude of external loading or stress intensity required to initiate or progress fracturing in intact rock. This is discussed in regard to the pretested samples in the following section 4.2.4.2.

Despite the uniform residual strain pattern in all spatial orientations along the measured section, we observed a distinct variation in the magnitudes of residual strains among the three measured crystal lattice planes, from an average of -435µstrain in $\{10\bar{1}4\}$, to -890µstrain in $\{0006\}$, to -2015µstrain in $\{1\bar{1}20\}$ (**Figure 4.2.2**). The variation of the magnitude of residual strain in the measured crystal lattice planes can be attributed to the crystal structure of calcite, which forms the Carrara marble. In crystallographic deformation experiments, the basal plane *c*, thus on $\{0006\}<1\bar{1}20>$, and especially the prism face *<r>*, on $\{10\bar{1}4\}<20\bar{2}1>$, have been determined as common slip planes in calcite crystals (Barber et al., 2007; De Bresser & Spiers, 1997). While slip along $\{10\bar{1}4\}<20\bar{2}1>$ is even active at room temperature and low critical resolved shear stress (De Bresser & Spiers, 1997), c-slip has only been found at high temperatures (Barber et al., 2007; Borg & Handin, 1967). Active slip on these planes would counteract the induction and locking-in of strain. Therefore, it can be argued that either during the formation of the Carrara marble less strain energy could be locked-in on crystal planes $\{0006\}$ and $\{10\bar{1}4\}$ or, that time-dependent relaxation since the Apennine orogeny took place preferentially on those planes. In crystal planes $\{1\bar{1}20\}$, on the contrary, higher magnitudes of residual strains can build up because they don't slip, but are in the c-slip direction and thus elastic strains can preferentially be locked-in along those. The initial lower magnitude of compressive residual strains makes those crystal planes more susceptible to external forces and conditions, and evoke a rheological anisotropy.

4.2.4.2 Superposition of residual strain state by mechanical and chemo-mechanical pretests

During the inverted single edge-notch bending creep pretest samples M2, M4, and M5 exhibited various degrees of macroscopic strain at the notch tip and exhibited a remnant strain upon unloading (Voigtländer et al., 2018). Thin sections of notch area showed single localized fractures initiated at the notch in the sample, M2 and M4 tested with water present at the notch during the pretest (**Figure 4.2.1e, f**). The effect of this induced damage, its extent and the possible mechanisms involved on the residual strain state we assess by comparing the measured residual strain states against the intact initial residual strain state of sample M0. Knowing the initial residual strain state of our Carrara marble (**Figure 4.2.3**) we can then speculate how this might have influenced the progression and extent of damage during the pretest. By this, we ultimately, want to infer the relative role, and control, of internal and external factors on progressive rock failure. Slight initial variations samples may have implications on the degree of inferred induced and relaxed residual strains in the pretested samples.

The overall pattern of alteration of the residual strain state by pretesting the samples corresponded to the loading configuration (**Figure 4.2.1a, b**), as expected. In all three samples, spatially heterogeneous superposition of the initial residual strain state was visible along the

vertical axis. The rebound pattern follows the graded externally applied stress, the principal stress directions and stress concentrations due to the inverted single edge notch three-point bending configuration (**Figure 4.2.1a, b**). We define the vertical extent of the superposition of residual strains as the 'damage zone' (**Figure 4.2.4, 4.2.5, 4.2.6**). The vertical extent of the induced strain pattern differs remarkably by to the environmental conditions during pretesting. The strongest superposition of the initial residual strain state is observed along $\{10\bar{1}4\}$ lattice planes, the least along $\{1\bar{1}\bar{2}0\}$. The magnitude of induction of residual strains corresponds to the variation in the initial magnitude of each measured crystal lattice planes in the reference M0. Even though the residual strain state is altered by the external factors, the overall residual strain states of pretested samples are still in contraction (**Figure 4.2.4, 4.2.5, 4.2.6**).

Spatially variable changes in residual strains of the pretested samples exhibited two levels of internal self-constraint, as individual crystallites are unable to expand or contract as they would like in response to any external loading because of the concomitant expansion and contraction of their neighboring crystallites. One level is due to the bonded polycrystalline bulk structure of the sample, and another due to the interdependency of the calcite crystal axis. The first level we discuss with the focus on crystal lattice planes $\{10\bar{1}4\}$, along which we observed the strongest superposition in the samples spatial orientations. Comparing all three measured spatial orientations, extensional strains in x-direction near the notch or fracture tip are countered by contractional strains in the y- and z-direction (**Figure 4.2.4a, 4.2.5a, 4.2.6a**). Because our neutron diffraction measurements were conducted on unloaded samples, the relationship does not follow the Poisson's ratio as would be expected during loading conditions. Due to the unloading, elastic strains could rebound at the termination of the pretest where they were not obstructed by any permanent damage around them in the vertical section. Due to tensile stress concentration near the notches, induced and relaxed strains showed the strongest deviation in comparison to reference sample M0 in the major principal deviatoric stresses in the axial direction of the pretest configuration. This may explain the local extensional strain enhancement near the notch tip in M5, as well as the stronger contractional strain below until the neutral axis (**Figure 4.2.4a**). The stronger contraction, compared to the mean reference state, would be the effect of the induced extensional strains in the section above, which instead of rebounding the elastic strain back to the initial state created a strain shadow or deficit below the permanent deformation. Holzhausen & Johnson (1979) showed this pattern and response conceptually in analogous experiments of bent beams. In the three-dimensional case, the rebound or relaxation of the strain pattern might be less pronounced as a reduction in one spatial direction can be balanced by an increase in one or another.

The second level of accommodation of the strain change is observed within the crystals structure, as single-axis are not able to rebound freely. This type of internal self-constraint within the crystal axis as has been described regarding thermal stressing (Meredith et al., 2001). An internal self-constraint is obvious in comparison of the crystallographic planes $\{0006\}$ and $\{1\bar{1}\bar{2}0\}$ and the corresponding changes in the unit cell volume. Because unit cell volume has been calculated from the $\{0006\}$ and $\{1\bar{1}\bar{2}0\}$ measurements, corresponding changes of the *a*- and *c*- axis are subsumed within. Within the damage zone of sample M2 and M4, the unit cell volumetric strain in all spatial directions is close to the initial reference mean strain state of M0 (**Figure 4.2.5d, 4.2.6d**). Inducement or relaxation of strain along one axis was likely balanced by the other. Below the damage zone, the unit cell volume strain diverges more, especially in the axial strain. Within this section, the dominant crystal lattice plane for the strain state is $\{1\bar{1}\bar{2}0\}$. Along these lattice planes, strains could have been build up during the pretesting, as

glides and slides, which might relax strain, are countered by the initially high contractional residual strain magnitudes (**Figure 4.2.3**), resulting in a local strain enhancement.

The spatial variable introduction and relaxation of residual strains during the pretesting produced a spatial anisotropy within the initially spatially isotropic residual strain state in Carrara marble (**Figure 4.2.3-6**). It has been observed that spatial persistence of residual strains would be aligned with preferred orientations of fractures in rocks (Friedman & Logan, 1970; Weinberger et al., 2010; Zang & Berckhemer, 1989). If the residual strain is spatially inhomogeneous, it is expected that the local strain may lead to a change in direction of fracture propagation that is not necessarily aligned with the global stress direction (Friedman & Logan, 1970; S. Y. Lee et al., 2011). It has been shown for engineering materials, that the propagation of a single fracture is influenced by the residual strain state at its tip (Withers, 2015). If the residual strain state at the fracture or notch tip is contractive, it poses a counterforce against applied tensile stresses and thus retards further fracture propagation. Contrary, in an extensional residually strained state, fracture propagation is likely to be enhanced (Withers, 2015). If we take into consideration the initial overall compressive residual strains within the representative element volume and the sum of them found in the Carrara marble (**Figure 4.2.3**), they should have counteracted the induced extensional strain during the pretesting. The unloaded state we have measured though shows extensional strain in the dry, and less contractional strains in the wet pretested samples. Re-loading this "new" pre-existing strain state would face less resistance to critical deformation and macroscopic failure, thus the progressive damage sate. Implying, that these strain or stress components are additive, then rocks can potentially fail under significantly lower external loads than expected. It has been shown that hygroscopic or thermally triggered expansion adds to pre-existing extensional strains by mechanical loading (Collins & Stock, 2016b; Voigtländer et al., 2018).

The environmental conditions during the pretest seem to have largely affected the mechanisms and pattern of relaxation and induction of strains, and thus the progressive damage state. While the vertical extent of superposition of the initial strain state is greatest in wet samples M2 and M4 (**Figure 4.2.5, 4.2.6**), the magnitude of induced extensional strain is highest in the dry sample (**Figure 4.2.4**). Mechanistic explanations for the introduction and relaxation of residual strains in rocks are still preliminary (Scheffzük et al., 2004; Varnes & Lee, 1972). The inducement of extensional strains and relaxation of contractional residual strains are probably complementary and conditioning processes. Similar to the rate and magnitude of subcritical damage mechanisms, knowledge on the induction or release of residual strain energy over time is still limited (K. Chen et al., 2015; Engelder, 1993; Nichols, 1975). In the following, we discuss possible mechanisms regarding the influence of the 'dry' and 'wet' pretest conditions that i) build up strain or ii) lead to relaxation, in both cases contributing to the progressive damage.

4.2.4.2.1 Superposition by subcritical mechanical stress in 'dry' condition

In the 'dry' pretested sample M5 the strain state is particularly altered at the notch and in the axial direction where tensile stress had been greatest and the geometry fostered stress concentration. The stress was not critical to initiate a macroscopic fracture, as only some grain boundary decohesion around the notch was evident in thin section analysis (**Figure 4.2.1d**, Voigtländer et al., 2018). From the microstructural analysis, we would assume that the sample was still intact and has the same fracture toughness as the untested sample. From the residual strain measurements though, we see differences in comparison to the reference sample M0. The

residual strain magnitude is reduced and even in extension in the first 5 millimeters below the notch, in all three measured crystal planes and an expansion of the unit cell volume in the x-direction (**Figure 4.2.4**). The measured gauge volumes in these millimeters below the notch we call the damage zone. We attribute these strain states to damage mechanisms which were incomplete in the creation of new surfaces. Even though inelastic intergranular deformations in calcite, like grain boundary sliding, can be activated at room temperature (Passchier & Trouw, 2005), it seems that the subcritical loading has not fully facilitated the necessary critical stress. Thus, they caused no or little relaxation and instead locked-in extensional strains (in x-direction) by local, probably only partial but permanent plastic deformation like glides, tilts, twists of grain boundaries (Platt & De Bresser, 2017). Even small induced deformations would lead to residual strain build-up due to the dense, brittle and self-constraining microstructure of the Carrara marble. It has also been shown by Darling et al. (2004), that, even though deformations at the grain boundaries make up only a few percent of the material volume, they can dominate the average lattice strain of the REV.

The residual strain state along the vertical measured section in the dry sample M5 mimics the expected stress gradient and orientation dependency found in beam theory of material sciences (Holzhausen & Johnson, 1979; Timoshenko & Goodier, 1970). Below the damage zone, there is little to no superposition. At the bottom of the samples, where stress magnitudes were also high but due to the loading configuration in compression, the strain state is close to the mean reference state. This can be expected, as rocks and material bonds are generally stronger in compression than in tension (Damjanac & Fairhurst, 2010). Dry mechanisms to lock-in strain or to relax are controlled by the applied stress magnitude and mode. (Brantut et al., 2014b) showed that failure of rock, though in compression, occurs at the same amount of inelastic strain, independent of the loading rate. The induced residual strain, although disparate from the use of inelastic strain as a proxy in the aforementioned study, indicates that the amount of strain (energy) was not met to initiate a fracture and possibly fail, independent of the longer pretesting period of sample M5 (section 2.2). To initiate and progress a fracture in a simple Griffith crack scenario either the applied stress would need to be risen or the conditions altered. The introduction of water can readily change the potential surface energy and shift the Griffith curve from a non-propagating to a propagating crack (Lawn, 1993; Sadananda et al., 2017). This could be observed in dry Carrara marble samples loaded in the same testing configuration which would not fracture and fail at loads ≥ 80% of the fracture toughness, unless water was introduced (Voigtländer et al., 2018). This behavior has also been reported for other geomaterial and engineered materials (Malkin, 2012; Rehbinder & Shchukin, 1972).

4.2.4.2.2 Superposition by subcritical mechanical stress in 'wet' conditions

The 'wet' pretested samples document the combined influence of subcritical loading conditions and reactive fluid on the residual strain state. In reference to the dry sample M5, the vertical extent of the damage zones is greater in the wet samples M2 and M4 (**Figure 4.2.5, 4.2.6**). Within these sections the residual strains are extensional only in the measured crystallographic planes but not for the unit cell volumetric strain. Residual strains in the x-direction are superimposed to a less contractional state in reference to M0. In microstructural thin section analysis of the notch area localized developing fractures were visible in both samples. The visible fracture tips were at a depth of ~12 mm in M2 and ~16 mm in M4 (**Figure 4.2.1e, f**). The fractures are localized and follow grain boundaries (Voigtländer et al., 2018).

Regarding the mechanisms altering the residual strain state, the creation of traction free surfaces by a progressed fracture is assumed to be a key control (Friedman & Logan, 1970; Nichols & Abel, 1975). However, in our samples, the effect of the local relaxation of residual strains seems to be weaker on the bulk measurement, than the introduction of strains, where a small fraction of grain boundaries affect the gauge volume (Darling et al., 2004). The general assumption that microcracks and fractures relax internal elastic strains by creating traction-free surfaces may only be confirmed i) at the very local level, and ii) for cracks near free-surfaces where they can result in volumetric extension. As the initiation or progression of a fracture entails the redistribution of the stresses that caused the process in the first place. However, the localized fracture is within bulk material where crystallographic planes are still in contraction. In the interior of the sample, the concomitant grains around the narrow fracture path dominate the residual strain state of the measured gauge volume. In the vicinity of the fracture tips, we observe more extensional strain states, similar to the notch area in the dry sample, indicating the introduction of elastic strains, without the creation of new surfaces. Another, not yet further investigated feedback could arise from fracture energetic perspective because residual strain stores energy it will likely affect the dynamics of brittle fracturing by providing additional fracture energy if released (Davies et al., 2012; Hill, 1963). As brittle intergranular damage can release stored strain energy, its dissipation contributes to further brittle fracture progression or the induction of strains ahead of the fracture (Lawn, 1993; Withers, 2015).

The combined effect of the mechanical loading and the wet conditions in samples M2 and M4 likely lead to the initiation of the fractures observed in the thin sections. During the pretesting, material bonds were mechanically strained in extension, which likely lowered the activation energy for chemical reactions, resulting in the rupture of the bonds and the progression of the fracture at loads ≥ 80% of the fracture toughness. This is in agreement with Griffith flaw extension theories (Lawn, 1993; Sadananda et al., 2017). Though the slightly higher deadweight loading in comparison to the dry pretested sample (80-85% compared to 77% K_{IC}) cannot be completely be ruled out of having had an effect, chemo-mechanically enhanced subcritical crack growth in our pretesting configuration would have caused a positive feedback on the stress intensity, at the same loads. Chemical and mechanical reasons for enhanced damage and strain changes in rocks in wet environments have traditionally been discussed separately. Stimulated by material sciences research, the interactive nature and positive feedback of chemical and mechanical mechanisms have recently raised increasing interest. Stress corrosion cracking has been introduced to geosciences and is assumed to be an important control in rock mechanics and earth surface processes (Atkinson & Meredith, 1987; Brantut et al., 2013; Eppes & Keanini, 2017). Stress corrosion cracking is an umbrella term for mechanisms which involve lowering of the activation energy for chemical processes, by thermal or mechanical strain energy. In the case of calcareous Carrara marble, the chemical process would be dissolution. In rock mechanics application, the enhancement of this chemical process is generally considered to be due to externally applied stress. The effect of residual strains have been mentioned but not included in numerical models or interpretations of stress corrosion tests (Atkinson & Meredith, 1987; Potyondy, 2007). In material sciences, residual strains have been recognized to be integral parts of these chemically-enhanced progressive fracture mechanisms, especially if the strain state is extensional (Toribio, 1998; Withers, 2007). General enhancement of dissolution kinetics due to strain or stress concentration has been experimentally demonstrated in calcite crystals (Schott et al., 1989). Based on the initial contractional residual strain state we would expect that they delayed stress corrosion

mechanisms in our 'wet' pretested samples M2 and M4 until induced extensional strains outpaced the residual strains and lowered the reactivity limit. Residual intergranular strains, their magnitude and sign as well as their variation in the measured crystallographic planes, could mechanistically explain observed general effects of stresses on chemical kinetics and the anisotropy of crystal reactivity, in dissolution and weathering (Pollet-Villard et al., 2016; Wheeler, 2018).

Besides chemical effects, there seems to be a mechanical effect of water on the superposition of residual strains. The wetting of weakly interlocking grain boundaries can lower the resistance to friction, by lubrication and wedging (Baud et al., 2000; A. Nicolas et al., 2016). While dry slides would be built up strains by friction and wear, wet, lubricated, smooth interfaces can glide along each other without the inducement of new strains (Homola et al., 1989; Violay et al., 2014). This can explain the remaining overall, and average contractional unit cell volumetric strain state of the wet samples (**Figure 4.2.5d, 4.2.6d**), although sample M2 and M4 exhibited greater vertical damage extent than dry sample M5. Likewise, the lower overall extensional residual strains observed in wet samples may derive from more efficient relaxation after the pretests, as grain boundaries slides could be reversed. While we observed chemo-mechanical enhancement of subcritical crack growth, the presence of water also mitigates strain built up or the locking-in of extensional strains. This effect has not been described before but may play an important role especially in progressive rock failures in the upper crust, where water is ubiquitously present.

4.2.5 Conclusions

We addressed the impact of residual strains on progressive rock failure, a subject of considerable field, experimental and numerical studies. The importance of internal controls on progressive rock failure has been stressed in hazardous rock slope failures, but concepts and proxies to assess them, have not yet been clear (Bjerrum & Jørstad, 1968; Krautblatter & Moore, 2014). Progressive rock failure studies in the context of building materials such as Carrara marble façade panels have highlighted material properties and the internal state (Koch & Siegesmund, 2004; Siegesmund, Ruedrich, et al., 2008). They showed how the extent of progressive damage is controlled by environmental conditions. It could be shown that the bowing potential of these panels can be linked to material properties including residual strains (Scheffzük et al., 2004). Our study differs from previous work on progressive rock failure in that it considers internal controls and the change thereof in a systematic and conceptual framework. We assessed the internal state with the proxy of residual strain states, measured with neutron diffraction techniques. The results from our study provide first insights into the residual strain state of Carrara marble and the superposition by mechanical and chemo-mechanical alteration in relation to what is commonly referred to as the stress memory.

We further documented the relationship between the initial state and the response of the rock to external loading. Results also show how dry or wet pretesting conditions affect the damage mechanism and the resulting transient residual strain state. Our experiment demonstrates that subcritical mechanical and chemo-mechanical external loading can relax stored contractional residual strains, and induce extensional strains in Carrara marble samples. We, therefore, hypothesize, that the initial residual strain state defines the general efficiency of external drivers to progressively weaken the rock. Our results show that the overall residual strain state of our Carrara marble is contractional, and thus provides an initial counterforce

towards extensional stresses. The homogeneous and isotropic initial state of the rock is readily superimposed and a spatial anisotropy in the strains introduced. Varying magnitudes of residual strain along the measured crystal lattice planes also indicate a microstructural anisotropy, which is likely exploited by external conditions and loading.

We could show how, in principle, internal states can be investigated. For the study of progressive rock failure, this implies that both time-dependency as well as internal state dependency need to be considered, and at best be quantified. Quantification of the residual strain states of rocks thus helps to explore a wide range of challenges and characterize mechanical and rheological properties of rocks. Residual strain states could also be used to define the initial material strength, independent of an applied stress and extensional strains could be used to describe internal damage states. Neutron diffraction methods, therefore, contribute to better characterize the internal state of rocks and anticipate progressive rock failures.

Acknowledgments and Data

Diffraction measurements were made possible by a granted proposal (1-02-149) at the Institute Laue-Langevin (ILL), Grenoble, France. Beamline scientist Thilo Pirling supported us throughout and contributed to successful measurements. The marble samples were gratefully provided by Marmi Carrara s.l.r., Carrara, Italy. Anne Voigtländer was supported with a BMBF Scholarship by the Rosa-Luxemburg-Foundation. The manuscript improved by discussions with Rebecca Kühn, Frank R. Schilling and Jens M. Turowski.

Supplementary Information 1 can be obtained from the journals homepage and contains additional figures 4.2.S1, 4.2.S2 and 4.2.S3.

Data can be accessed via http://doi.ill.fr/10.5291/ILL-DATA.1-02-149.

4.3 Scientific Publication III

Breaking rocks made easy. Blending stress control concepts to advance geomorphology.

Anne Voigtländer and Micahel Krautblatter (2019)

Earth Surface Processes and Landforms, 44(1), 381–388. https://doi.org/10.1002/esp.4506

Breaking rocks made easy.
Blending stress control concepts to advance geomorphology

Anne Voigtländer *and Michael Krautblatter*

Abstract

All landscapes are subject to stress fields, conditioned by their formation and ongoing tectonic and geomorphic changes. With this ESEX Commentary we wish to stimulate a debate on this invisible but persistent stress control on landforms, processes and materials in geomorphology. We address the legacy of active and passive stress fields, which translates into the concept of 'tectonic predesign', in conjunction with a perspective of geomorphic processes being driven by subcritical stresses. These concepts complement each other as 'subcritical processes' are controlled by tectonic predesign and in turn modulate the stress fields. This offers new theoretical and practical perspectives on how landscapes evolve, processes form materials and how rocks break easily.

Introduction

Underlying concepts, theories and assumptions predefine our understanding of the evolution of landscapes and the processes forming them. Explicitly and implicitly geomorphological imaginaries form. They evolve by a repeated probing of the interplay between reason and desire, social and symbolic order, and the real and its expressions in visual, statistical, or other representational modes of imaging. Imaginaries can facilitate scientific developments, an apparent sense of objectivity and certitude in our research and teaching. A simple and widely used framework to explain landscapes, landforms and changes thereof, from short-term to long-term evolution, has been employing the triangle relationship of form, material and processes (MFP triangle) (Church, 2010; Phillips, 2017). Materials generally constitute resisting forces while processes drive the change in form. Thus any process and change in form occur if the extractable disturbing forces exceed the mobilized resisting forces. Or as Gilbert (1877:93-94) stated: *"[a]ll indurated rocks and most earths are bound together by a force of cohesion which must be overcome before they can be divided and removed"*. This may imply relative simple relationships, the primacy of erosional processes and the search for critical states. We could also reconsider whether this imaginary of landscape evolution still matches the conceptual framework or if our assumption of critical states in processes yield the observed outcome? To a greater extent, Yatsu (1992) in his highly debated reconsideration of geomorphology argued that by hiding behind descriptions and suggestive models, geomorphologists neglect physical laws and impede transferability, reproducibility and knowledge of geomorphic processes and forms. While this could be dismissed as a provocative exaggeration, some limitations of the aforementioned framework and its imaginaries in geomorphology have surfaced, especially in quantitative geomorphology and system predictions.

First of all, the relationships of form, material and processes are probably not linear, are essentially feedback relations, and depend on initial conditions, memory effects, and internal thresholds (Krautblatter & Moore, 2014; Phillips, 2003; Smith et al., 1999). This is not new, but most rate and process laws cannot adequately reproduce these system linkages, and non-linear systems challenge quantification strategies and model designs (Viles, 2005). Second, each component of the triangular relationship is treated individually or in relation to one other, which can have some intriguing results. For example, for studies solely focussing on the physics of a process the integration of simple rock properties can become an outstanding challenge or it appears as a seemingly surprising fact that there is a topographic control of bedrock fractures and erosion (DiBiase et al., 2018; Moon et al., 2017; Roy et al., 2016). Third, although each study of the component of the MFP triangle might have a clear foundation in physics they are limited to the specific domain (by parameters or concepts) they do not offer a common framework on how these components are interconnected.

In this ESEX Commentary, we wish to stimulate a debate in geomorphology by suggesting a conceptual perspective on the processes, materials and forms we study. We won't reinvent the wheel but rather point out the complementary nature of two existing concepts, namely subcritical processes and tectonic predesign, which have been dwelling separately in the geoscience community for decades. Their common conceptual ground is the stress control perspective. Stress control in the sense that dynamic stresses are the driver of processes, static stresses state the form and internal stress or strength characterizes materials. By combining these concepts, we think this provides a new perspective which can strengthen our

understanding of how landscapes evolve. The ideas in this commentary have been presented in a comic style poster at the General Assembly of the European Geoscience Union 2017 (**4.3 Supplement Material**), which sparked many fruitful discussions in an otherwise stern and sober discourse of theoretical geomorphology. We tried to adopt this style to illustrate our proposed conceptual blend. In the following, we want to briefly introduce both concepts and show where they overlap and interdepend, and then sketch the suggested benefits of their combination.

Of geomorphic processes and subcritical mechanisms

By geomorphic processes, we ascribe the bulk change in form or volume, subtractive or accumulative in space and time grouped to e.g. fluvial, glacial, or hillslope domains. These changes or processes are themselves driven by tectonics and gravity, providing uplift (renewal of material) and potential gradients, and solar radiation, enabling atmospheric circulations. If these processes are pictured independent of the resisting forces (material), as the sole driving force of change, this can transmit extreme imaginaries of processes such as buzz-sawing glaciers, or rivers, aggressively incising their bed (**Figure 4.3.1a**). Hence if we would actually place the magnitude of the processes in relation to the bulk material strength, the extractable driving forces reach typically about 1-10% of the resisting forces, and are therefore subcritical (Brain et al., 2014; Hantke & Scheidegger, 1999; N. R. Iverson et al., 2003; Preisig et al., 2016; Wolman & Miller, 1960). Nevertheless, the prevailing erosional origin of valleys by fluvial or glacial shear forces is a widely accepted theory (Scheidegger, 2004). To deem processes to the oppositional view of glaciers simply cleaning up or rivers juggling sediment (**Figure 4.3.1b**), neither enhances our understanding of where and at what rate geomorphic work is done or stresses are effective. Notably in slope (in)stabilities, the apt adjective “effective” has been posted by Terzaghi to denote those forces (stress, cohesion, pressure) which in interaction with e.g. material strength, deformation, shape and environmental conditions (especially water pressure), are actually available (Terzaghi, 1943, 1962; Whalley, 1974). Still this does not solve the apparent discrepancy between the magnitudes of the driving and resisting forces.

Because erosion and fractures are ubiquitous there have to be some mechanisms acting at subcritical stress levels, which over time and aggregated, exhibit behaviour we call process. In this sense, processes can be conceptualized as functional integrals of specific mechanisms (Derbyshire et al., 1979; Whalley, 1987). These subcritical mechanisms are considered to be stress controlled in two ways. On the one hand, by the internal stress state of the material, due to preconditioning and stress concentrations. On the other hand, by interact of the former with the subcritical external driving forces. Next to the stress controls, geometric and scale properties pose a control on subcritical processes, especially subcritical crack growth. Concepts of subcritical crack growth thus widely rely on the so called Griffith criterion which postulates that the effectiveness to progressively fracture a material depends on the geometry and length of an initial flaw or crack subject to the subcritical stress or energy (Griffith, 1921; Lawn, 1993).

The concept of subcritical processes has, in a more specific notion known as subcritical crack growth, been adopted from material sciences and introduced in geosciences in the 1970s by Atkinson (1987). In studies concerned with the rheological behaviour, it is an increasingly advanced and reviewed concept (Brantut et al., 2013; Ko & Kemeny, 2013; Nara et al., 2010). Similarly, Bjerrum and Jørstad (1968) also suggested in the late 1960s to conceptualize and investigate rock slope failures as an input of energy at subcritical levels in concert with the

material (pre)conditions. In geomorphology, this conceptual idea or subcritical crack growth was not further pursued except in some weathering studies (i.e. Whalley et al., 1982). Recently this has been invoked to explain weathering under subcritical thermo-mechanical stresses and chemically enhanced stress-corrosion (Aldred et al., 2016; Eppes & Keanini, 2017) and is adducted in a few examples to explain progressive rock slope failures (Faillettaz et al., 2010; Voigtländer et al., 2018).

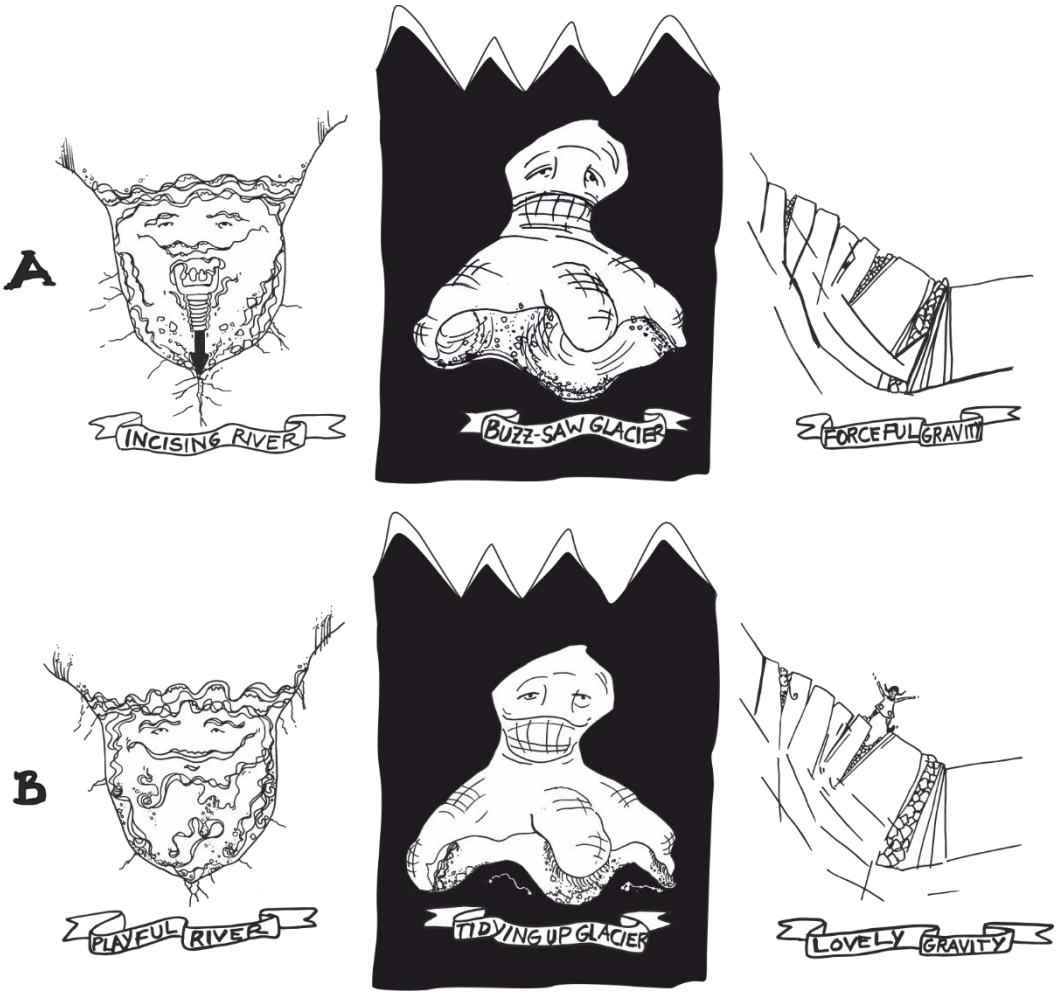

Figure 4.3.1 a (upper triplet): Persistent geomorphological imaginaries of the primacy of erosional processes, where rivers forcefully incise and glacier buzz-sawing their bed or gravity pushes rocks apart. Its exaggerated antipode in **b** (lower triplet), where rivers simply juggling sediments, glaciers clean up valleys and gravity provides a lovely place to be.

In a conceptual view of subcritical processes, the geomorphic processes simply provide forces of a certain magnitude and direction. The forces exerted on an interface, thus stress, facilitates (subcritical) mechanisms like abrasions and plucking, wear, corrosion, cracking, pressure solution and friction, flaking and fatigue, armouring, sorting and packing of materials (i.e. Beer et al., 2017; Egholm et al., 2012; Eppes and Keanini, 2017; Jia et al., 2015; Krabbendam and Glasser, 2011). These mechanisms are physical/mechanical and, or chemical and, or biogenic by nature. Subcritical mechanisms operate on the microscale (Atkinson, 1987; Lawn, 1993), where they manifest in observed macroscopic behaviour, thus processes (i.e Brantut et al., 2012; Gratier et al., 2012; Masteller and Finnegan, 2017; Pelletier and Jerolmack,

2014). However, knowledge of this upscaling behaviour is still limited because the investigated mechanisms are usually isolated from possible emergent geomorphic processes, considering only single fractures or local abrasion. Nonetheless, one of the great debates of the early 20th century (and ongoing), on the primacy of fluvial over glacial erosion or vice versa (Heim, 1885; Leith et al., 2018; Penck, 1905), could thus be turned into the quantifiable question of the efficiency of each agent to abrade, pluck and crack the rocks, and thus finally be settled.

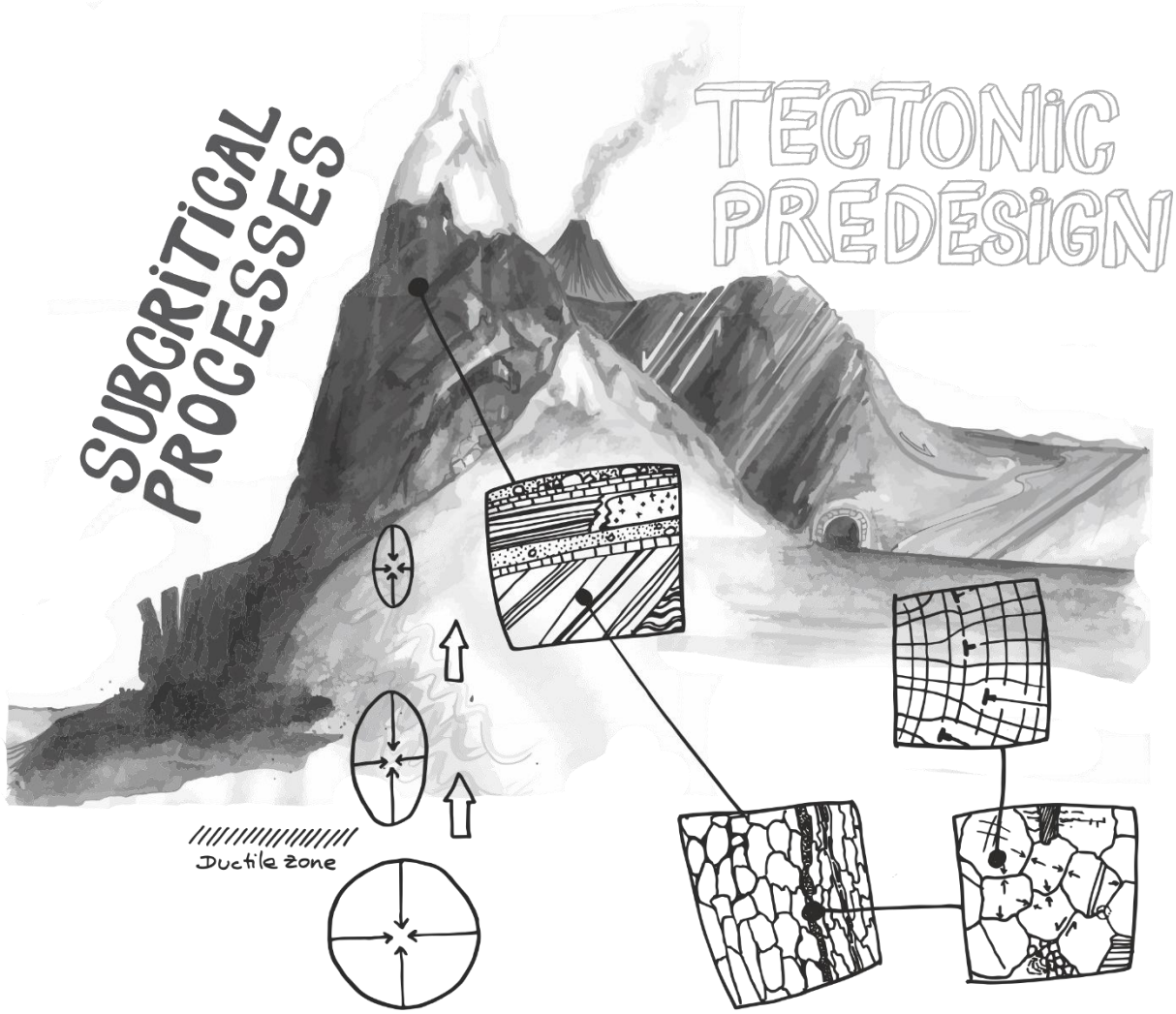

Figure 4.3.2 Subcritical processes and tectonic predesign both root in the same stress control perspective. Tectonic predesign provides a concept of the active and passive stress fields, which can provide the circumstances for subcritical stress levels to be sufficient for subcritical processes to fracture, erode and transport the material, which in turn influences the stress fields. The combination and their stress control also offer a conceptual bridging of spatial and temporal scales.

Besides the driving forces, the state of the material controls how much stress is needed for each mechanism, their rates, and the overall effect and path. More precisely, due to the fact that the mechanisms work on interfaces on the microscale, the internal structure and stress state of the material poses an important control. This aspect is not well integrated into the studies of subcritical processes in geomaterials so far. A possibility to integrate the stress state into the

concept of subcritical mechanisms is to link it with another established concept which provides this, such as ‘tectonic predesign’ (**Figure 4.3.2**).

Of tectonically predesigned and stress controlled materials

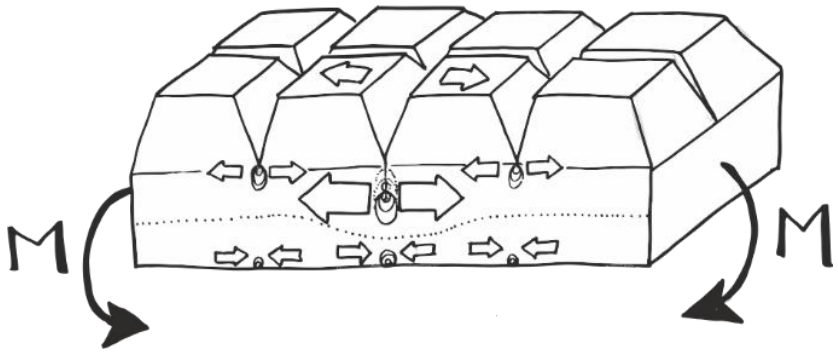

Figure 4.3.3 Stress concentration analogue: a chocolate bar. Due to bending force M, tensile stresses concentrate at the notch tips and eases the breaking apart. Luckily the chocolate or landscape is only locally affected and the remainder stays intact.

All rocks on earth are subject to varying stress fields throughout their geologic lifespan and are structurally (pre)conditioned by them (Emery, 1964; Engelder, 1993; Zang & Stephansson, 2010). We could define active first order stress fields exerted by gravity, second order by (neo-)tectonics and third order by topography and so on. Passive stress fields would result from structural conditioning during formation of rocks, sediment bodies and landscapes. They are evident as deformational features from the microscale to fault systems spanning hundreds of kilometres, and render the material residually stressed (Emery, 1964; Engelder, 1993; Kieslinger, 1958). Together the active and passive stress fields are dubbed ‘tectonic predesign’ (Hantke & Scheidegger, 1999). The legacy of these stress fields have been seen in the contingency of landforms, erosional features and seismic activity following their pattern (Engelder, 1993; Fjeldskaar et al., 2000; Scheidegger & Ai, 1986). Gerber and Scheidegger (1969) suggested that along sites where stresses concentrate are fracturing, weathering and erosion fostered, especially in extensional regimes. This very local effect of stress concentration can readily be imaged by breaking a bar of chocolate, where you exploit the grooves to focus stresses (**Figure 4.3.3**). Then subcritical stress is sufficient to initiate and propagate a localized fracture through the chocolate or bedrock (Atkinson, 1987; Sturgul, 1967; Sturgul & Scheidegger, 1967). This principle appears to be valid on all spatial scales (Gudmundsson, 1999; Lawn, 1993; Molnar, 2004). It can also be argued that the stress state provides a strengthening of the material, hampering weathering and erosion (Bruthans et al., 2014; Mattheck & Burkhardt, 1990; Müller, 1969). This can be imagined by two bears sitting on three chairs (**Figure 4.3.4**). The external force (F) provided by a big bear, little bear or no bear influence the internal differential stress state of the chairs (or landscape). The applied force can cause internal deformation and damage but also, by providing confinement, hinder the chair to be moved, i.e. eroded. Thus local stress or no stress can govern geomorphic processes which in turn reinforce topography and stress fields (Bruthans et al., 2014; Gerber & Scheidegger, 1969; Miller & Dunne, 1996). The character of the relationship between the subcritical processes and

the internal stress state also affects the sensitivity and performance of the system, as it may result in a stabilization or a metastable state in which the slightest external disturbance is sufficient to start fracture, erosion or transport (Brunsden & Thornes, 1979; Haefeli, 1965).

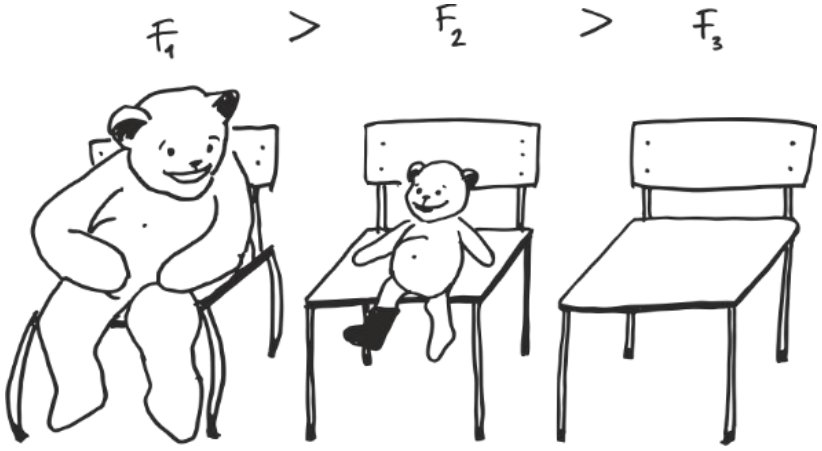

Figure 4.3.4 External (bear) forces (F) can alter the internal stress state of the form (chair). The internal stress state (forms or chairs are quite stable, strong and in static equilibrium by themselves) responds to these external forces with deformation or damage, but also poses a feedback control on the magnitude of force needed to move the chair, i.e. erode the form.

The active stress field component of tectonic predesign is widely integrated into geomorphological investigations, especially triggered by the rapid technological evolution of numerical landscape modelling (Church, 2010). These models imply that the stress fields provide the circumstances and locations in which geomorphic processes (fluvial, glacial, gravitational, seismic etc.) take place in the landscape (i.e. Fjeldskaar et al., 2000; Miller and Dunne, 1996; Molnar, 2004; Savage and Swolfs, 1986). Yet, numerical studies assessing the control of topographic stresses and topographic history on bedrock fracture density (Moon et al., 2017; St.Clair et al., 2015) and glacial valley evolution (Leith et al., 2014b) (**Figure 4.3.5**) often draw their explanation and validation from contingency and similarity of geophysical and geological observations in selected landscapes and valleys.

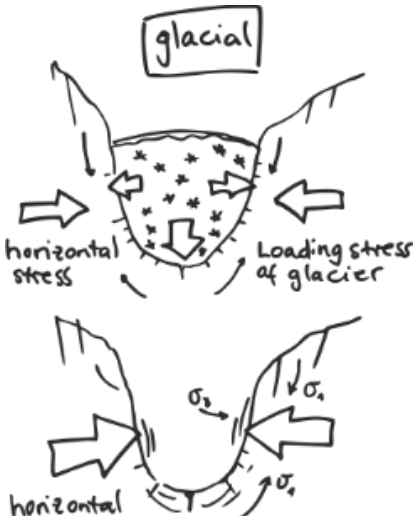

Figure 4.3.5 Stress fields with and without a valley glacier, where differential topographic stresses evolve which exceed the microfracture threshold (after Leith et al., 2014).

The passive stress fields component in the modelled responses of rock on the other hand, which introduces a history, (pre)conditioning or a so-called 'memory effects' of the material properties and rheological behaviour has remained (mechanically) simplistic in geomorphology, as it includes only bulk processes and properties (Hart, 1986; Yatsu, 1992). Lithological and erodability parameters are often given in qualitative ranking orders, for example from "weak" to "strong" (Giachetta et al., 2014; Prasicek et al., 2015; Shobe et al., 2017). In this regard, assumes and reports the study by Roy et al. (2016) a higher erodability with reinforcement of strain localization within a shear zone as the river incises (**Figure 4.3.6**). We would argue that in the absence of clear definition of the mechanisms and stress/strain conditions, the model result is self-fulfilling. These models enable us to include stress fields, but they lack a description of the functional relationship between the assumed processes, mechanisms and material properties. This 'rock control' (Yatsu, 1966), is not consequently adopted in the concept of tectonic predesign which is inherently static. To integrate dynamic geomorphic processes and their interrelation with the evolving stress fields, we suggest combining tectonic predesign with the concept of subcritical processes (**Figure 4.3.2**).

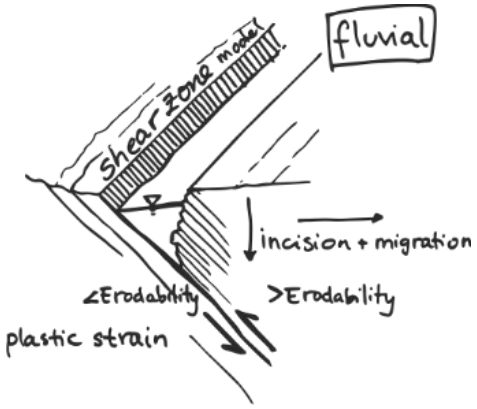

Figure 4.3.6 Rivers incise where erodability is lower which reinforces the plastic strain in a shear zone (after Roy et al., 2016).

Stronger together?

Both concepts, subcritical processes and tectonic predesign, touch on fundamental assumptions of driving (processes) and resisting (material) forces promoting, landforms and landscapes (form) without mobilizing greatest or critical forces (some extreme events are okay). Each concept has itself proven to provide testable explanations and prediction about geomorphic processes, materials and forms. Both root in the notion of stress fields and complement each other. So let's combine them: Subcritical processes provide the dynamics and mechanisms of the processes that exploit and use the tectonic predesigned locations which in turn reinforce and further ease the geomorphic processes. Additionally, the combination of these two concepts allows to integrate different spatial and temporal scales or at least broach the topic of the effect of the mechanisms at the microscale on the macro response. By defining landscape evolution in terms of a stress-controlled framework the surface processes can also be harmonized with other subsurface or atmospheric processes (Kleidon, 2010; Koons et al., 2012). Observational and theoretical inconsistencies arising from the aforementioned separation of process-form-materials can be obviated. To substantiate these theoretical amalgamations, we will outline possible research approaches and questions in the following.

Stressed landscapes

We could include stress fields in our research (which is easier said, then done). For that, we would need to quantify the stress, force or energy input typically for a geomorphic process, similar to Wolman and Miller (1960). Even though we are dealing with coupled systems of a multitude of surface processes they all should have common grounds in (thermo-)mechanics, energy dissipation and storage (Kleidon, 2010), so we could try to use these to define their units. Given that we can define what we need to quantify, we can look for, adapt and try out methods from other fields and disciplines to measure those. Subsequent we would need to investigate the response of geomaterials to those stress magnitudes, frequencies and orientations to determine what stress or energy levels have an impact and when. There is still a paucity on quantification and delimitation of the mechanisms of subcritical processes (Bergsaker et al., 2016; Sadler & Jerolmack, 2015; Ventura et al., 2010). Also, we would need to test their feedback relations to other controlling parameters, such as confinement, environmental condition, structural precondition, lithology, rate and magnitude of stresses (i.e Atkinson, 1987; Jaeger et al., 2007; Ramsay, 1967). To detect how subcritical processes govern the evolution of the resisting forces, we would need to actually look at the rocks, sediments and soils, from microstructures to plate tectonics. We would need to characterize and parametrize materials on different scales, to get to know our objectives, which is sometimes not sufficiently done in present-day modelling, provenance and dating studies.

Relationships and structures

The combination of the concepts highlights the feedback relationships of the geomorphic MFP triangle. Their nature, as well as spatial and temporal scaling relations, offer new possibilities to conceptualize and formalize appropriate geomorphic laws. They might exhibit an internal threshold or gradual emergent behaviour, or are dominated by external extreme events. Here we could fall back on other existing concepts such as ‘geomorphic thresholds’ (Schumm, 1979), or ‘landscape sensitivity’ (Brunsden & Thornes, 1979). This non-linearity of the processes is matched by the standard situation of anisotropy in the material.

Linearity and isotropy may be useful assumptions for first-order relations or may oversimplify and disguise the nature of relationships we are investigating. The structural preconditioning, sorting and deposition of the materials are evident on various scales, defining bedding, layering or lithological discontinuities, remaining as fabric, texture and compositions, and presenting microcracks, fractures, joints, faults and folds. Their abundance, orientation and spatial distribution aggregate to define the heterogeneity of the mechanical and hydraulic properties, strength and erodability (Clarke & Burbank, 2011; Dühnforth et al., 2010). This internal structure is expressed in preferential orientation of ridges and valleys (Castelltort et al., 2012; Eyles et al., 1997; Hodgkinson et al., 2006; Scheidegger & Ai, 1986) or in differential weathering (Holzhausen, 1989; Røyne et al., 2008; Whalley et al., 1982). Structural (strength) anisotropy is an important control in geomorphology as it determines the spatial orientation in which erosion or cracking is eased, while hampered in another (M. R. Chandler et al., 2016; Kieslinger, 1958). These mechanical and morphological anisotropies effect however not only the strength and deformation behaviour but also the stress distribution within the material (Müller, 1963, 1964). This aspect also becomes evident when reconsidering a movie scene where a car speeds through a safety glass window of a bank (**Figure 4.3.7**).

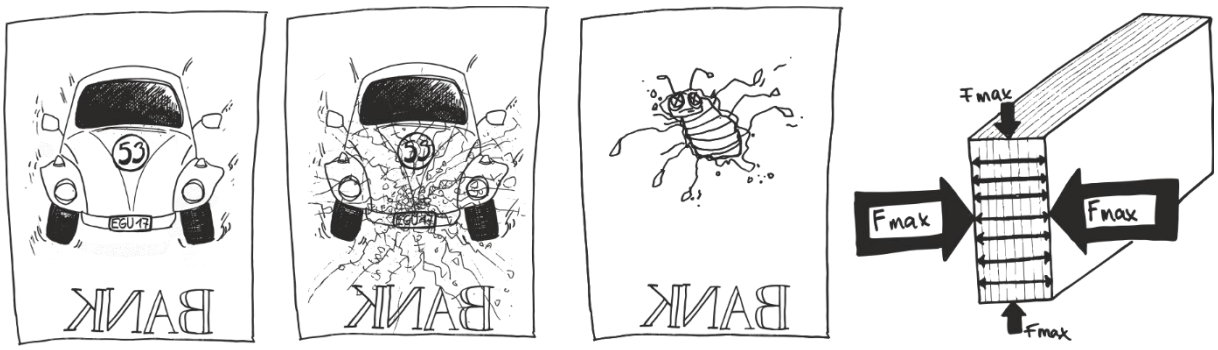

Figure 4.3.7 Anisotropy and heterogeneities are ubiquitous material properties in geomaterials. They highly matter if referenced to applied stresses. To picture this, imagine a random movie scene where a car (mass, m = 1500 kg) speeds up (speed, v = 150 km/h) and bursts through a safety glass window of a bank (compressive strength ~ 900 MPa and flexural strength ~ 90 MPa). Speeding towards the window the car has an impulse (P = m*v), over an impact time of t ~ 0.5 s, and thus exerts a force (F = P/t) over an impact area (~1000 x 10 mm = 10000 mm^2), thus a stress of 12.5 MPa on the glass. Compared to the strength of safety glass, the beetle car would look like a smashed bug on the windscreen. Parallel to the window, a scratch or nudge would be sufficient to shatter the glass.

Geomorphological modes

Turning to the effect of applied forces on the material, and back to stress field and form, the spatial direction and location, in reference to structural properties, represent key factors on the efficiency of the subcritical mechanisms. Therefore, we should assess where stresses can concentrate, strains build up and damage accumulates. We need to determine in which manner (fracture mechanical mode) the materials and structures are stressed, torn, crushed, and wedged, statically or dynamically and which subcritical stress magnitudes matter (**Figure 4.3.8**). These where and how questions play a decisive role in the rate and extent that subcritical processes can facilitate progressive fracture, weathering and erosion. In addition, we must integrate the dependence of material rheology and properties on environmental conditions (thermal, hydro, hydraulic, chemical etc.) in the critical zone.

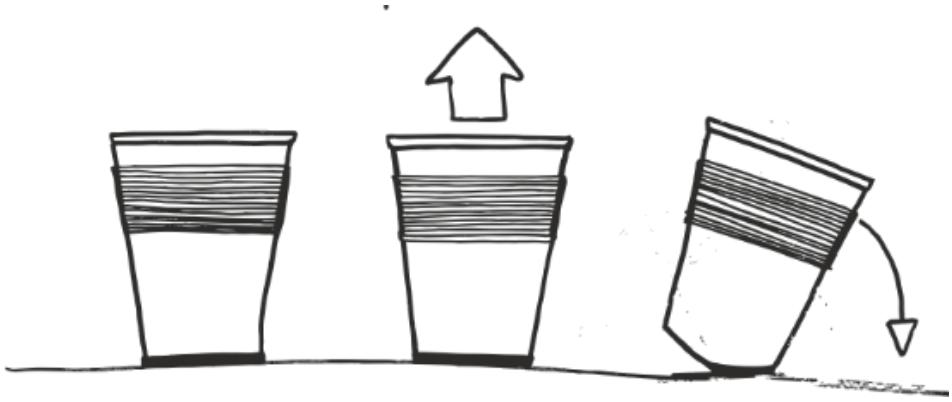

Figure 4.3.8 The efficiency of a force also depends on the mode and direction it is applied in, e.g. plucking, flaking or cracking. This mechanical control is readily imaged if your cup is glued to a table (by mistake). If you simply tried to pull it off, a major or critical force is needed. If you tear it off step by step, subcritical stress levels are sufficient and can even be reduced as the detached area or crack lengthens, to remove it.

We hope we have planted the seed that theoretical geomorphology can be tangible and can provide a useful framework to build and organize research. If underlying theoretical concepts and assumptions are made more explicit in research and publications this can strengthen the discourse of geomorphology and its imaginaries. In combining subcritical processes and tectonic predesign we see a great opportunity to better explain, why and where we see a geomorphic divers' landscape. The merger of these two concepts provides a framework for further research that accounts for the driving forces of the processes, resisting and enabling material states and forms, to better understand the trajectories of the forms we study, and to break rocks easily.

Acknowledgements

We would like to thank the editors of ESPL for venturing with us, not only in the way of illustration but also in providing a space to come forward with this comment. Comments by an anonymous reviewer and Brian Whalley triggered further discussion and greatly enhanced the manuscript.

5. Discussion

The three studies in this thesis all address the outstanding questions of how rocks break. Each scientific publication focused on different aspects and methods to assess progressive rock failure. A deeper understanding of controlling factors on progressive fracturing is beneficial to anticipate rock slope failures, as well as in more general terms the disintegration of rocks for landscape evolution, infrastructure performance or preservation of artworks.

In **Chapter 4.1**, I investigated the coupled effect of constant subcritical stress magnitudes and environmental conditions on progressive rock failure in long-term creep experiments. A key observation was that the introduction of water has a chemical as well as a mechanical effect on how and at what rate fractures propagate.

In **Chapter 4.2**, I related the geological inherited property of residual elastic strains and changes thereof by external forces to the internal state. Residual elastic strains were measured by neutron diffraction on subsamples of the long-term creep experiments, reported in **Chapter 4.1**. These measurements indicated that the 'memory state' of the Carrara marble was in an overall contractional strain state and that this inheritance has likely affected the rheology of the samples during the pretesting. Remnants of inelastic damage and induced extensional elastic strains are found along the measured vertical section of all pretested samples. The variable extent of the superposition in the dry and wet-tested samples are attributed to differing subcritical mechanisms.

Since both studies (**Chapter 4.1** and **Chapter 4.2**) involved laboratory experiments, several assumptions and simplifications about rocks and progressive failure have been made, which it poses a challenge when scaling the results to geologic and geomorphological systems. The assumptions are based on established and accepted conceptual views. Only by testing these concepts in real-world scenarios can they be considered appropriate. I applied these relationships and outcomes of the experimental studies to geomorphological scenarios. In **Chapter 4.3**, I provided a graphical-conceptual scheme to the question: 'How do rocks break?', and recommended further research directions to anticipate progressive rock failure and related geomorphological processes. Because **Chapter 4.3** is a commentary, going beyond reviewing existing concepts it is both a starting point and the end product of the theory behind the experiments. Although these three studies each emphasized different aspects of the outstanding research question and are comprehensive by themselves, synergies arise when viewed in concert. In the following, five of these aspects are discussed in the realm of the published studies.

In **Chapter 5.1**, I highlight the importance of time in the conducted experiments. One of the prerequisites of the experiments has been that we can separate and control constituents of the system under investigation. This also roots in the assumption that the system evolves with time. In the experimental studies, time has been treated as an independent variable. This supposed time-dependency is discussed regarding the choice and meaning of long-term experiments and the temporal scale of the mechanisms and processes involved in progressive rock failure.

In **Chapter 5.2**, I discuss system states. As a response of a system (i.e. rock) to an external factor is only detected when compared to an initial system state. As a consequence, we need to quantify or at least define the system states. In addition, the system state itself controls

– at least partially – the response. Here I emphasize how knowing the internal system states and their properties can change how we interpret the responses.

In **Chapter 5.3**, I discuss a particular response of rock: wet rheology. The differing response of rock to the introduction of water depending on the stress state is seldom reported, partly because of the conceptual and experimental separation of factors considered in wetting-drying and standard rock mechanical tests. The separation of concepts, for example into chemical and physical weathering, or distinguishing between chemical and physical strain energy, created apparent entities, which then require new concepts to bring them back together. One of these re-coupled chemo-mechanical mechanisms is stress corrosion cracking.

Coupled chemo-mechanical mechanisms are discussed in **Chapter 5.4**. As all experiments have been run on a near pure calcite rock, Carrara marble, I review the widely accepted, silicates based chemo-mechanical models regarding their applicability to carbonate rocks.

In **Chapter 5.5**, I return to the aspect of time. There, I consider the broader implication of time within the experiments – on a temporally short scale (days-month-year) –, and the previous chapters on geological time. This synopsis follows the timeline at which rocks form, reach the earth surface and progress towards failure.

5.1 Time-dependency

Progressive rock failure is often synonymously termed time-dependent (e.g. Jaeger, 1971; Kemeny, 2005; Paraskevopoulou, et al., 2015; Swanson, 1984). And it essentially is the deformation of rock over time. The reasoning for time-dependency arises from the need to answer the question when rocks will fail. Knowing the time-to-failure is crucial for potentially hazardous rock slope failures and would have been useful to know at the beginning of the creep experiments reported in **Chapter 4.1**. But does progressive rock failure really depend on time? If there is a time-dependency, what relationship do we expect? What are the time-scales over which we observe creeping deformation? If, in contrast, rock failure progresses over time, but is not time-dependent, what does observed creep depend upon?

Creep or the deformation of rock over time is commonly divided into two to three phases. An instantaneous elastic strain response to loading marks the first phase, followed by deceleration and so-called steady-state second phase. These creep behaviours are termed primary and secondary, or in combination transient creep (Cruden, 1970). This is similar to what was observed in the creep experiments on the dry samples reported in **Chapter 4.1**. Tertiary or accelerated creep commences when a critical amount of inelastic volumetric strain or critical crack length is reached (Brantut et al., 2014b). This phase is characterized by dynamic rupture. In attempting to time dynamic rock slope failure for the mitigation against natural hazards, this phase is of special interest (Amitrano & Helmstetter, 2006; Intrieri et al., 2019).

In the experimental studies of this thesis, and other creep experiments that are published, creep did not accelerate within the set time of the experiments, month to years (Sorace, 1996) and in a special laboratory case for thirty years (Itô, 1979). The timescales of progressive rock failure are of geologic or geomorphic scales. Over geological time scales, it seems that time-dependency is phrased rather in a metaphoric fashion, like a time-line along which damage evolves. This is discussed further in **Chapter 5.5**.

To be able to observe the acceleration of creep and determine the time-to-failure, experiments are usually conducted with a load that corresponds to a high percentage of the intact strength or fracture toughness of the rock samples. Creep could just as well be termed stress-dependent. Many empirical laboratory studies have therefore focussed on determining tertiary creep rates for several rocks and loading conditions (Brantut et al., 2013; Cruden, 1974; Kranz & Scholz, 1977). Empirical creep models have suggested linear, exponential as well as power-law relationships with time during tertiary creep (Jaeger et al., 2007). The phase of accelerated creep can be very short – in the experiments in **Chapter 4.1** it lasted minutes. In order to anticipate rock failure, especially rock slope failures, we need a better understanding of the precursory phases that lead to the initiation of tertiary creep. However, laboratory studies of transient creep are rare, due to their duration. In addition, in the reported experiments, strain rates in dry samples even though loaded to high fractions of the fracture toughness (>80% K_{IC}), did not accelerate unless water was introduced. This environmental condition-dependency has also been observed in progressive rock slope failures (Abellán et al., 2017; Collins & Stock, 2016a; Gischig et al., 2011a).

In the experiments reported in **Chapter 4.1**, changes in the boundary conditions – increased loading or the introduction of water – push the material towards a metastable or unstable state (cf. **Figure 2.1.3**) and accelerate the creep rates, eventually causing dynamic rupture. This shows a dependency on stress and environment in addition to a time-dependency (**Figure 5.1.1**). Overall, the system response, modulated by the feedbacks between the variable, determines the rate at which it progresses towards failure.

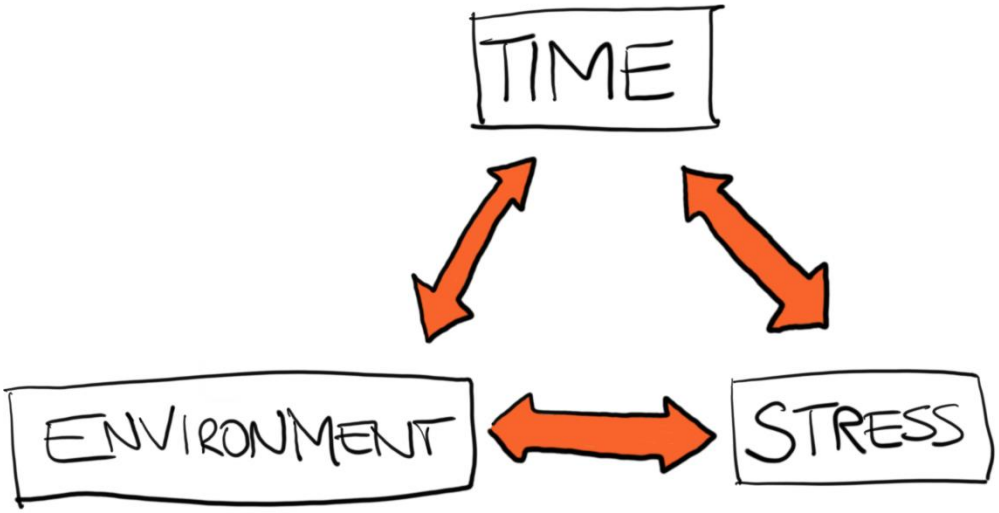

Figure 5.1.1 Three constituent variable: time-dependency, stress-dependency, environment-dependency

Following Brantut et al. (2014), it can be argued, that progressive rock failure might be better constrained and predicted by an internal damage state dependency. They compare the amount of internal volumetric strain in rate- and time-dependent experiments and find that the amount of inelastic strain coincided at the onset of dynamic rupture, regardless of the duration of the experiment. This is similar to the question raised by Voight (1966:56) "How does elastic deformation energy behave in space and time and the conditions that are responsible for this?" A first insight into how elastic and inelastic strain states look like, at least spatial and under controlled environmental conditions was assessed by the proxy of residual elastic strains in

Chapter 4.2. Instead of using the inelastic strain accumulated during testing, residual elastic strain states were observed with neutron diffraction techniques. Here the internal damage state also did not reveal a time-dependency, as the extent of superposition in the dry pretested sample was considerably smaller than in the wet pretested sample, even though it was loaded for a longer period of time. To address questions about the rate of change of the internal state, and thus how stored strain energy behaves through time and under which environmental conditions, more measurements are necessary. In conclusion, both internal inelastic damage accumulation and induced extensional elastic strains, define the susceptibility of rock to failure.

Testing rocks in long-term, time-dependent experiments still has benefits, especially in combination with a chemically active environment. The dissolution of calcite, for example, proceeds at a certain rate. To infer if and how the subcritical loading might affect the dissolution rate as part of stress corrosion, it needs to be referenced to a constant, here time. Testing in a time-dependent framework would enable the assessment of the dependency of progressive rock failure to environmentally enhanced subcritical crack growth.

The challenge with classifying rock failure as time-dependent might be that it suggests it is a seemingly continuous process over time. Instead, the timescale of progressive rock failure is defined by the rate at which micromechanisms cause internal inelastic and elastic strain to accumulate. If we adopt the notion that the amount of internal strain or damage matters, the question is when began its failure? At what point in time is rock considered to have failed?

5.2 System states

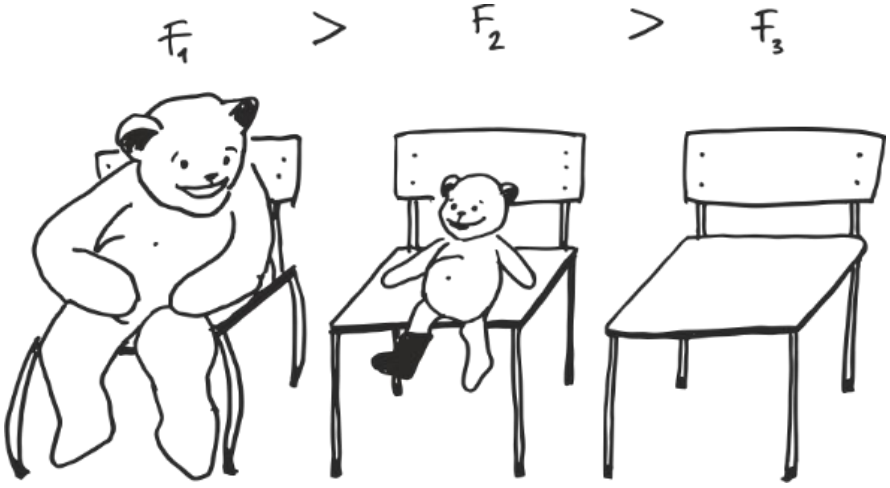

Figure 5.2.1 Two bears and three chairs. The applied force (F) on the chairs is greatest for the big bear and smallest for no bear. (Same figure as **Figure 4.3.4**)

In the previous chapter, the temporal dimension of a system has been introduced as a reference state. Other system states can be related to the external conditions and forces as well as the internal state of the material. To illustrate the different system states and how they are related to each other we can refer to the analogy of two bears and three chairs from **Chapter 4.3** (**Figure 5.2.1/4.3.4**). Initially, all three chairs would have been identical – in their material properties and manufacturing. Their shape and structure can be described, measured and weighed. Once, figuratively speaking, the big bear sits on one of the chairs, strong deformation is observed. Because of the large amount of deformation from the initial shape of the chair, it

is interpreted that the load was near-critical or close to the strength of the chair. If instead of the big bear the small bear sits on a chair, only minor deformation, if any at all, is observed. The response of the chair to the small bear can therefore not easily be interpreted, as the initial state is similar to the loaded one. Scientifically speaking, this means that if a greater external force is applied to a rock, the difference we see is only in reference to a previous state. The deformation in the elastic regime is generally assumed to be proportional to the applied force. In rock mechanics, this results in a stress-strain diagram (see also **Figure 5.3.1**). From this visible deformation state, the material properties, like the strength are deduced. If the load is well below the instantaneous strength, deformation can be observed over a longer period and material parameters inferred. For this purpose, creep experiments are typically run.

Most creep experiments have been performed at loads of >50% of the intact strength (Heap et al., 2008; Lajtai, 1991; Sorace, 1996). The reported experiments in **Chapter 4.1** used starting loads of 22-55% of the wet fracture toughness. Loads in the lower percentile range are still highly understudied, which means that the system response to low loads is not known. This is partly due to the duration and measurement resolutions of previous experiments. At lower loads, creep experiments are expected to last longer, occupying load testing racks, which means that fewer samples can be tested. The challenges posed by the measurement resolution are two-fold; firstly, the monitoring system has to be reliable, independent of other influences and constantly running. In reality, this can be a challenge even in laboratory settings, as one can face electrical power outage, incautious colleagues or corroding (presumably) stainless steel sensors. The second issue relates to the wavelength of the deformations and measurement techniques. This has been partially addressed by introducing neutron diffraction techniques in **Chapter 4.2**, which can also be applied in-situ. Seismic monitoring is a promising, though indirect and bulk method that can potentially reveal the internal state of rock structures and hillslope materials (Azzola et al., 2018; Dietze et al., 2017; Snieder & Larose, 2013). Through noise correlation or active sources, wave velocity changes can be assigned to system states. One big assumption that has to be made is still the initial or reference state.

In summary, we can only observe the deviation from a reference point or what is often called an initial state. In most experimental settings, conditions at the start of the experiment, equal the initial state and the start of observable change (Brantut et al., 2014b; Heap et al., 2008; Sorace, 1996). In the experiments reported in **Chapter 4.1**, the observed creep rates are compared to the start of the experiment, when samples were first dry and loaded. Another reference point in these experiments was at the time of water introduction; a controlled change in environmental conditions. Defining reference states becomes necessary, though sometimes seems arbitrary when considering field sites. Monitored progressive rock slope failures in Preonzo, Switzerland (Gschwind et al., 2019; Loew et al., 2016) or of the Veslemannen, Norway (Abellán et al., 2017; Rouyet et al., 2017) have reported increased slope deformation with the onset of precipitation. The increase, due to the change in the environmental conditions is referenced to former and presumed dry states. The particularity of wet rheology is discussed in **Chapter 5.3**.

To return to **Figure 5.2.1**., the empty chair does not show any deformation. Gravity alone acts on the chair, and as long as the mass and structure can withstand this, no deformation will occur. What remains unknown is whether this chair was loaded before the beginning of this analogy. If the big bear had sat on this chair before, it may have accumulated damage and could potentially fail even if the small bear would sit on it. This may sound unrealistic but such

unanticipated and unexpected failures have been observed in many infrastructures, e.g. bridges. For most experiments, we assume that the initial state is intact and any change starts with the beginning of changing the conditions or with the loading the sample. The fact that the response that we observe is conditioned by the internal state and its memory is often ignored. The internal relationship of applied force, stress/strain thus cannot be deduced from the external observables, as it is also conditioned by its history. Preconditioning of landscapes is a frequently revisited theme as we can see this across many scales in geology for examples related to tectonics (Scheidegger, 1984, 1998; Scheidegger & Ai, 1986) or gravitational mass movements (Bjerrum & Jørstad, 1968; Crozier, 1989; Krautblatter & Moore, 2014). All of these studies ascribe the importance of rock stress memory on rock failures. The role of these memory effects on the predictability of stability or instability is avoided as the accessibility of the internal and inherited state is restricted.

Whether in laboratory experiments or for monitored slopes or infrastructures, the state and response of the rocks are usually only observed when external forces are near critical, or already in tertiary creep. In this thesis, I wanted to go beyond these limitations. While in the experimental setup in **Chapter 4.1** the initial internal state, once again was assumed to be strain-free thus the origin equaled zero, the initial internal state was inferred from neutron diffraction measurements in **Chapter 4.2**. Strain state deviations due to the pretesting are then referenced to the non-zero initial residual strain state of the untested sample. But do residual strain measurements really depict the internal state? And what would be its initial state? In the following, I discuss the internal state and the lasting issue of an initial state using the example of residual elastic strains in rocks.

Broadly speaking, the initial state we pick as a reference point, limits what we can deduct from the response system. In **Chapter 4.2**, I applied neutron diffraction techniques to assess the residual strain state of an intact Carrara marble sample and three pretested samples indicative to the internal strain state of the rock. The neutron diffraction results suggest that the rock is residually elastically strained. This contractional strain state is interpreted as inherited. This ‘memory’ affects how the rock would then respond to superposition by the subcritical loading and wet conditions. The significance of prior or initial-deformation on the rheology has also been shown for high-temperature torsion experiments on a Carrara marble (Bruijn et al., 2011). Yet little is known about this path dependency. In natural settings with less exemplary and intact rock as the Carrara marble samples, an important feature that determines the internal state are structural preconditions. Pre-existing joint sets, shear planes, faults, folds and foliations have been omitted in the reported studies but are likely to have significant control on how strains are stored, relaxed and stresses transmitted.

Residual strain measurements, from over-coring or diffraction methods, have, in the context of structural geology been used to infer paleo stress fields (Engelder, 1993; Kunz et al., 2009; Zang & Stephansson, 2010). The use of residual strain magnitudes and spatial orientations to reconstruct the formation and deformation history of the rocks is challenging and only works with the assumption that the stress field is being locked-in the rock; the microstructure and texture remain unchanged. The superposition of residual strains in both magnitude and spatial orientation is possible in Carrara marble, as in Chapter 4.2. The internal reorientation of the residual strains upon fracturing evokes local stress intensity, inducement and relaxation of residual strains, influenced by environmental conditions (Withers, 2015). Due to the simple monomineralic and the homogeneous nature of the Carrara marble and the

measurement resolution, we assumed isotropic elasticity and stress response. If a polyphase rock is assumed, like studies on granite (Nichols, 1980; Nichols & Savage, 1976), inducement and relaxation of residual strains and an accompanied reorganization of stresses would likely lead to a differential response within the constituent minerals. In-situ neutron diffraction experiments demonstrate that the mineral composition of the rock strongly influences the rheology and the strain state (Covey-Crump et al., 2006, 2013). Which stress fields are measured in the rock depends on the assumptions made of the behaviour of elastic deformation energy through time and space and which conditions induce or release them in the microstructure of rocks and beyond (Voight, 1966a). Using residual strains in rocks to determine both the paleo stress field and to infer its internal state, seems to confuse the cause and the response.

In material sciences, the stresses that produce a certain state are controlled and monitored and the internal strain state is used as an indicator of the structural performance, especially the fracture toughness of the material. This is where residual strain measurements in rocks can be very beneficial, as it provides an independent measure or reference point to an initial state, which is solely internally determined. The response of the system or rock to external factors such as stress, even subcritical stress could be investigated by establishing a reference point. The conclusion that rocks can be residually stressed or strained, even though they are simply lying around, is important when considering the effects of weathering and the establishment of stress corrosion rates. Regarding the toughness, is it actually the locked in strain energy that makes rocks tough? Like tempered glass?

A cohesive conceptual framework of residual strain/stress development, persistence, relaxation and/or superposition in rocks does not exist. Attempts to describe the development and relaxation are preliminary, highly simplified and are specific to a rock type and fabric (Holzhausen & Johnson, 1979; Kunz et al., 2009; Meredith et al., 2001). Residual strains and their role in progressive fracturing and stress corrosion cracking in material sciences have for most studies only investigated tensile mode fractures (Potyondy, 2007; Withers, 2007, 2015). Mode 2/3 shear stresses and fractures are not and only slightly considered and are also present in rock structures and slopes and are probably the mode in which fractures will coalesce and dynamically rupture (Backers, 2004; Diederichs, 2003b; Ko & Kemeny, 2011). Insights into how these stored elastic energy plays a role in dynamic fracturing, fragmentation and comminution, as mentioned by Davies et al. (2019, 2020) is still not finally explored. Residual strain magnitudes and their role and mechanisms in rock mechanics are largely unknown. Additional studies to quantify residual strain magnitudes and orientations of polyphase rocks and textures are in much need. Open questions remain about by which magnitudes and transmission of stress, and which conditions and by which mechanisms elastic strains are locked-in and relaxed. For a better understanding of the effect of residual strains on rheology, in situ experiments of both the rate of inducement and relaxation of residual strains are necessary. Generally, more experiments are needed to gather data, discern the effects and behaviour of elastic deformation energy, or residual strains in rocks.

5.3 Wet rheology

In Earth surface sciences we are generally concerned with rocks and their response to environmental conditions, especially the presence of water, and mechanical loading by geomorphic processes. But little is known about how the response of the rock (fracturing,

disintegration, erosion) changes due to wet conditions and stress states. I will now emphasize the wet rheology observed in the long-term inverted three-point bending test.

In the subcritical load range, the rheology of solid materials has been shown to be susceptible to environmental conditions (Wiederhorn & Bolz, 1970). Further, it has been shown in material sciences that the strain or stress state of the system (both, externally applied loads as well as the internal, residual strain state) influences the response to environmental condition. While the chemo-mechanical effect of stress corrosion is getting more and more rediscovered in geosciences (Brantut et al., 2013; Eppes & Keanini, 2017; Nara et al., 2011), the mechanical effect of the introduction of water, for example, to rock slopes only considers effective pore pressure changes (i.e. Agliardi, et al., 2020; Upton, et al., 2018). In the experiments reported in **Chapter 4.1**, two distinct behaviours have been observed upon the introduction of water which can easily be transferred to real-world examples. First, we observed the strain of the samples increased roughly threefold when water was introduced to the notch compared to the dry sample at the same subcritical load of ~22 to 55% of the wet fracture toughness. Second, we observed sudden brittle failure upon the introduction of water to the notch of dry samples at near-critical load (> 85%). These distinct behaviours can easily be re-enacted with this thesis if printed on paper. If water is spilt onto the thesis while laid in your hands, it will become deformable. If the pages are under a tensional grip and water is spilt on them, they will instantaneously rip. These distinct, stress-dependent responses to the introduction of water have already been observed by material scientists Rehbinder & Shchukin (1972), but often disregarded in rock physics. (Why this is, I cannot retrace as before). The so-called Rehbinder effect explains the distinct behaviour by strain state change in the surface energy first by loading and then by the wetting of the surfaces. Depending on the stress level, the state of the system is already unstable and will fracture in brittle fashion as soon as water reduces the surface energy. Alternatively, the system is metastable and shows a transient deformation. The interconnectedness of the stress state and environment has implications for the wet rheology of natural slopes, but also in which way and by which material properties we can quantify it in laboratories and the field.

The transient deformation of wetted rock is usually assigned to hydrological expansion, which has also been observed in dense rocks, like Carrara marble (Labuz & Berger, 1990; Ruedrich et al., 2011; Weiss et al., 2004). Yet in the combination with subcritical loading, wetting, as could also be argued, affects and alters material properties. The base of all of these considerations is that the deformability of the material is affected by hydrogen bonding. In the long term, it can lead to hydrogen embrittlement, which is known and feared particularly in metals (Gamboa & Atrens, 2005; Toribio et al., 2007). For a sustained time, it is also reported that wet rocks behave in more ductile fashion due to a reduction in friction (A. Nicolas et al., 2016; Rutter, 1974). The reduced friction in wet rheology can have a strong effect on strength especially if this is applied to earthquake ruptures (Violay et al., 2013, 2014). A broader implication of wet rheology would be that the elastic moduli change. First indications for this come from petrology and fault zone related studies but should be extended to testing environments at or near Earth surface (Risnes et al., 2005; Røyne et al., 2015; Zhang et al., 2017). In rock mechanics, elastic moduli are often determined over a range of high temperatures and pressures, which is less relevant for the assessment of progressive rock failure at the near-surface of the Earth. Studies which showed that freezing temperature affect the strength and deformability of rocks did not necessarily report the change in elastic moduli (Krautblatter et al., 2013; Mellor, 1973; Voigtländer et al., 2014).

Very little data is available for wet rocks rheology, rock strength, and fracture toughness. If the data acquired in the experiments in **Chapter 4.1** is plotted as a stress-strain diagram, the divergent rheology of the dry and wet tested samples is clear and differs by a magnitude during the loading stages (**Figure 5.3.1**). The majority of rocks are tested in dry conditions, due to the associated standards in engineering sciences where this method being rooted. Natural rocks samples are dried in an oven at 70 ±5 °C until a constant mass is measured before testing rock strength and elastic moduli (DIN EN 12372). This ensures that the tests are comparable and reproducible. However, if these estimates are used for rock slope stability assessments, thus for rocks which are in environments which prevent sufficient drying, they should be treated with caution. For some rock types, such as the Carrara marble, the suggested procedure to attain a baseline condition by heating can cause damage to the samples. Heating a Carrara marble sample to 70°C will likely induce thermal strains, as calcite crystals have highly anisotropic thermal expansion coefficient (Rao et al., 1968). Thermal cracking in natural examples at similar temperatures as the suggested 70°C is an efficient weathering mechanism (Aldred et al., 2016; Eppes et al., 2016; Eppes & Griffing, 2010). For rock strength and property measurement within the scope of geomorphology, I would recommend testing rocks saturated with water. All samples irrespective of rock type could also be immersed in water and saturated until a constant mass is measured before testing. This was done for the samples used to determine the wet fracture toughness in **Chapter 4.1** and a study on sandstones (Krautblatter et al., 2018).

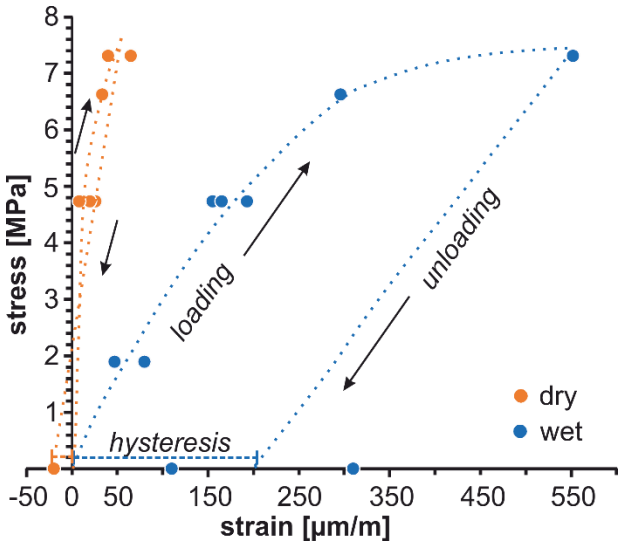

Figure 5.3.1 stress strain replotted data of long-term three-point bending tests in dry and wet conditions

For sandstones, it has been shown that water saturation in tensile fracture testing can result in a more ductile or brittle response depending on the microstructure and properties (Alfes, 1993). Very little is understood about the saturation thresholds of the rock which will affect the rheology. For rock slope instabilities triggered by precipitation, the internal saturation state and the addition of water is key. Saturation effects have been explored for soil landslides, but not for rock slope failures. (R. M. Iverson, 1985, 1986b, 1986a, 2015; Reid & Iverson, 1992).

The second distinct observation was that sudden brittle failure occurred without previous strain increase when water was introduced to dry samples at near-critical load (> 85%). This response could readily be explained by taking into account the Griffith criterion and it

changes in critical surface energy in the presence of water (Lawn, 1993; Sadananda et al., 2017). The response of a slope to a precipitation event, for example, may not be principally affected by the volume of water, but more the stress state. Few studies have focused on the so-called Rehbinder effect; the assumption that the timing of wetting relates to the strain state change in the surface energy. Depending on the stress state of the slope the effect could be dramatic or delayed. For rock slopes, the response (magnitude and timing) to a rain event might be related rather to long-standing and/or previous processes and responses. The adjustment of the response to external factors due to the systems stress/strain state is crucial, especially in the anticipation of rainfall, snowmelt or thermal triggering of rockfall or landslide events (Collins & Stock, 2016a; Gischig et al., 2011b; Loew et al., 2016). Moreover, this is important for infrastructure and sculptures, where cracks dry and re-wet by rain or snow-melt and are therefore vulnerable to this mechanical effect. Wetting and drying of rock slopes in susceptibility studies have so far only been related to hydraulic pressure and effective stress change. How wetting and drying of rocks affect rock failure mechanisms and rheology has not been investigated.

Temperature changes, evoking deviatoric stresses due to anisotropic thermal expansion or insolation, play an important part in progressive rock failure and weathering of rocks (Collins et al., 2018; Eppes et al., 2016; K. Hall & Thorn, 2014). Temperatures are also likely to affect the rheology of the rock. In which manner a rock response changes at high temperatures, has been indicated by a recent study: “To creep or to snap? How does induced heat govern the brittleness of matter?” (Vincent-Dospital et al., 2020). It is promising to see more environmental conditions are including mechanical aspects of progressive rock failure.

5.4 Coupled chemo-mechanical mechanisms in carbonate rocks

The mechanical effects of the interaction of the stress state and the environmental conditions have been discussed in the previous chapter. Most of these mechanisms like the Rehbinder effect originate from material sciences. This is also true for chemo-mechanical mechanisms, where most models of stress corrosion cracking on ferrous and siliceous materials (Lawn, 1993; Wiederhorn & Bolz, 1970). Coupled chemo-mechanical mechanisms were investigated on a carbonate rock for this thesis, the particularity of probable rate laws for carbonate rocks are discussed in the following section.

The effects of the stress or strain state of rocks on chemical activity are only recently being re-considered within work from the rock mechanics and weathering communities (Brantut et al., 2013; Eppes & Keanini, 2017). This is surprising because a famous article by Gerber & Scheidegger (1969) on “stress-induced weathering” which mention residual stresses, has been frequently cited in geological, geomorphological and engineering papers and textbooks. The chemical aspect would in this context constitute another facet of the material properties. In rock mechanics, this is often overlooked even though physicochemical conditions prevailing on Earth’s surface.

Studies generally pick either the chemical or the mechanical component, reflecting the expertise and scope taught in each discipline. The delineation in the first place might be the problem. Making a distinction between chemical and mechanical processes might even impede synergies, e.g. existing coherences between activation energy and strain energy. Stress corrosion cracking demonstrates this nicely and is likely to be one mechanism of many where chemical and mechanical processes enhance, suppress and/or facilitate each other. Currently

accepted models of stress corrosion have focused on mode I stress intensity and dissolution reactions and rely on transport-controlled kinetics (Atkinson, 1987; Eppes & Keanini, 2017; Ko & Kemeny, 2013; Lawn, 1993).

Coupled dissolution-precipitation processes

This assumption may be too simplistic and cause problems when trying to reconcile dissolution model rates with experimental or field data. From the chemistry perspective, this might be indicated by new insights into the geochemical analysis of dissolution-precipitation processes at mineral-solution interfaces (Putnis, 2014; Ruiz-Agudo et al., 2016; Ruiz-Agudo & Putnis, 2012). Additionally, strain or stress concentrations are found within and at the edges of single crystals, at crystal defects, dislocations. Stress concentrations, and thus a possible enhancement of dissolution rates are not only found at fracture tips (i.e. Schott, et al., 1989). Thus, multiple reaction sites are found which in the bulk alter the dissolution rates, possibly causing a positive or negative feedback loop (i.e. Ilgen, et al., 2018). Studies on the mineral-solution interfaces found not only dissolution but physical alteration due to hydration and hydrolysis as well as precipitates. The difference in the elasticity of the precipitate and mineral grains (Dohmen et al., 2013; Ruiz-Agudo et al., 2016) can generate layer parallel stresses in excess of the composite strength, as a result of an elastic mismatch at the interface to the original material (Kranz, 1983). Further studies, of an integrated chemo-mechanical framework with recent models and use of novel techniques, are still pending. In situ stress or strain, generation is known in material sciences and with the advancements of high-resolution techniques, this might be examined further.

If we accept that stress corrosion cracking is driven by dissolving stressed material bonds (Atkinson, 1984; Eppes & Keanini, 2017; Wiederhorn & Bolz, 1970), the question is still on the rate at which it proceeds. Since the reaction timescale is determined by the reaction rate, stress corrosion rates are ultimately controlled by how fast a mineral bond dissolves and how long the fluid stays in contact with the interface. In chemical weathering studies, the reaction rates and transport phenomena are related and formalized in the non-dimensional Damköhler number (Damköhler, 1936; Maher & Navarre-Sitchler, 2019). Applying this approach to stress corrosion cracking studies can facilitate the accounting of rate variations in the transport–limited regime, as it specifically comprises fluid transport or residence time. The exact formula for the Damköhler number varies according to the rate law equation and material involved of course (Maher & Chamberlain, 2014; Yu & Hunt, 2017). The Damköhler number for a single fracture has been observed to vary (Durham et al., 2001), yet without accounting for any stress/strain enhancement. It would also need to be adapted to include the stress/strain enhancement of the reaction rates like the stress corrosion rate factor, **n** or such.

Stress corrosion cracking rates in carbonates

Common calculations of stress corrosion cracking rates are derivatives of the Charles law or the Paris law and are based in dissolution rates and stress intensity (Eppes & Keanini, 2017; Lawn, 1993). The motivation to investigate rock-like materials was driven by an early interest in silicate or glass decay (Fowler, 1880). Wiederhorn & Bolz (1970) specifically looked at the environmentally enhanced crack growth in glass. More recently, in connection to the storage of nuclear waste, borosilicate's and their long-term chemistry at the interface has been investigated, though most without factoring stress or strain (Geisler et al., 2015, 2019; Lenting et al., 2018). Subsequent chemical kinetic descriptions, reaction laws and reaction pathways, have been established for glass and silicates (Michalske & Freiman, 1982; Wiederhorn & Bolz,

1970). As most studies come from material sciences, data of measurements and calculation stress corrosion rates are on glasses or metals.

Stress corrosion rates for carbonate rocks have been investigated and found that there might be several reasons that they differ in comparison with the silicate reactions. The main divergence is grounded in the different reaction kinetics of carbonates. This includes (i) a more or less inverse relationship of activation and temperature, (ii) reversible reactions of dissolution and precipitation, and (iii) stronger reactivity and mechanisms at the solution-material interface.

These issues imply for example that the commonly used Charles law, where activation is increased with temperature, would need to be adapted in the thermal activation term. As carbonates are easier to dissolve relative to silicates, this could lead to an overestimation of stress corrosion rates in carbonates. In geochemistry communities' studies on carbonates, involved kinetics, mechanisms, and reaction rates cause variability of bulk weathering and dissolutions rates in, for example, pure calcite by up to 2.5 magnitudes (Fischer & Lüttge, 2017) and are 1-3 orders of magnitude higher than in natural environments (Casey et al., 1993; Velbel, 1993; White & Brantley, 2003). This explains the reasoning that dissolution rates of carbonates can better be described by spectra (Lüttge et al., 2013). Using the mean dissolution and weathering rates in calculation of stress corrosion cracking probably overestimates the chemical effects.

High-resolution techniques, like atomic force microscopy, interfaces and structural aspects that influence local dissolution reveal additional controls on the variability of reaction rates (Bibi et al., 2018; Levenson & Emmanuel, 2013; Renard et al., 2019; Ruiz-Agudo & Putnis, 2012). As argued by Schott et al. (1989), strained calcite minerals exhibit higher reactivity than an unstrained single crystal. Structural aspects of usually investigated single crystals include flaws and defects, edges and dislocations (Clark et al., 2015; Laanait et al., 2015; Stipp et al., 1994). Depending on the carbonate type and the crystal structure and crystal lattice planes themselves, there are differences in reactivity (Jordan & Rammensee, 1998; Lardge et al., 2010; Liang & Baer, 1997). If this is applied to rocks with additional sites of stress, concentrations emerge and dissolution rates are not independent of the strain state. Though in carbonates, because of its reversible reaction, as soon as the strain energy is used to dissolve, the fluid can be oversaturated. Generally, the system is metastable likely both to dissolute as well as to precipitate (Ilgen et al., 2018).

Coupled dissolution-precipitation chemo-mechanical processes

Evidence, that more chemical mechanisms, than dissolution, have been active during the long-term experiments might be seen in the cathodoluminescence microscopy image of a thin section of sample M4 (**Figure 5.3.1**). Cathodoluminescence has often been applied to infer (paleo) hydro-chemistry and structural properties of carbonates (Götze, 2012; Machel, 1985; Toffolo et al., 2019). Trying this with the samples conditioned in **Chapter 4.1**, the image (**Figure 5.3.1 B**), could be interpreted that lately recrystallized and precipitated calcite illuminate brighter than older grain regions e.g. dark core (circle), due to lower electrical excitement. Light red grain boundaries following the fracture could be attributed to environmental enhanced dissolution, fracture propagation, followed by precipitation. A similar pattern has been observed in mode I microfracturing and fluid flow in damage zones (Anders et al., 2013). Around the notch tip area, where stress concentrations were not expected, local hydro-chemical alteration due to the diffusion of the calcite saturated water and precipitation

are likely. Our thin sections being dyed with fluorescent resin, though, did not qualify for further investigation.

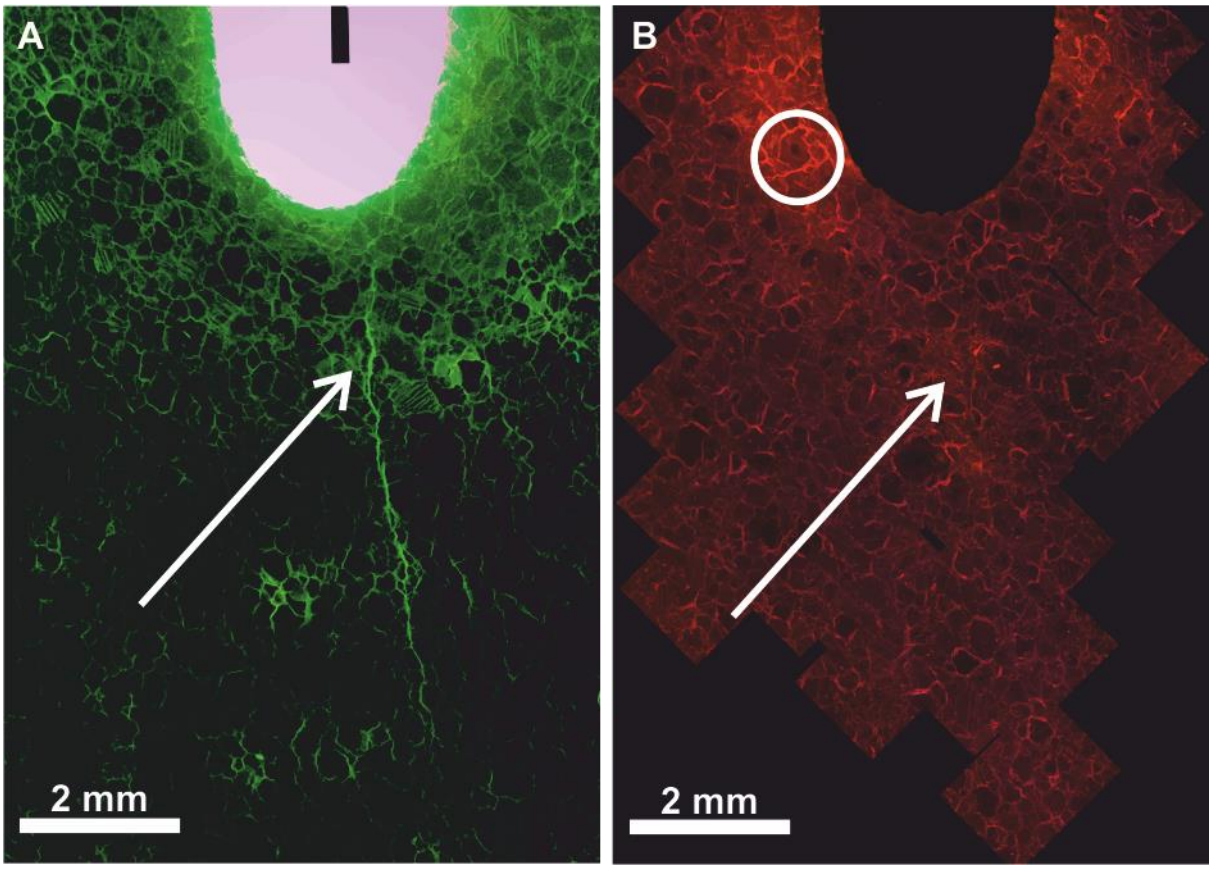

Figure 5.4.1 Carrara marble sample M4 (A) shows a fracture along grain boundaries (arrow) and decohesion around notch tip area in a fluorescent thin section of the notch tip area due to the long-term testing. Cathodoluminescence microscopy image of the same thin section (B), exhibits newly altered calcite in light red colours in the notch tip area as well as along fractured grain boundaries (arrow).

A factor that needs to be considered when trying to understand stress corrosion in carbonates and natural settings, is that dissolution-precipitation reactions cannot simply be separated as independent sequential processes (Pedrosa et al., 2017). Both dissolution and precipitation depend on the fluid composition at the reaction interface. The fluid composition and its reactivity are furthermore affected by temperature and pressure. In my studies, both conditions have been ambient and regarded as constant. The effect of the thermal regime on the reactivity pathways of dissolution in calcite have been investigated elsewhere (Pedrosa et al., 2017; Sjöberg & Rickard, 1984), and found to affect stress corrosion rates (Atkinson, 1984; Das & Scholz, 1981; Nara et al., 2017). This is still in need of investigation. Fluid pressure changes during the experiments and an effect on precipitation-dissolution are expected. In SEM images, discussed in **Chapter 4.1**, we observed dissolution and precipitation features in close proximity. The rationale of this is that in a saturated medium, like the calcite-saturated water we used for the experiments, the reactivity likely depends largely on pressure. Pressurizing the fluid along grain boundaries and in voids, as it diffused into the rock would have been readily accomplished by the subcritical stressed rock matrix as well as, what we learned from the residual elastic strain measurements, discussed in **Chapter 4.2**, the stored strain energy in the

rock. The pressurization of the saturated water leads to a higher reactivity and thus enhanced dissolution. Together with the reduced activation energy needed, by the physically extensionally strained atomic mineral bonds (Schott et al., 1989), by the applied loads, stress corrosion cracking could progress. As cracks propagate, stress redistribute and depressurize the fluids at the mineral interfaces. This can lead to supersaturation of the fluid and consequently precipitation of calcite. Calcite precipitates can build up pressure by crystal growth and enhance stress concentration by wedging the fracture or crack walls apart (Gratier et al., 2012; Røyne, Meakin, et al., 2011). In-situ experiments are necessary to fully understand these reaction patterns. Both chemically as well as rock mechanically focused research would benefit from observation and description of the interactions and controls of these coupled mechanisms. If applied to natural rock slopes the combination of dissolution and precipitation facilitating progressive fracturing is likely and should be investigated together.

In this coupled interaction of dissolution–precipitation not only the material, as highlighted above, but also the solute needs to be accounted for. This is similar to the driving and resisting force concept of slope stability discussed in **Chapter 2**. The chemical reactions are highly dependent on the fluid composition and it has been shown that the fluid composition, due to different solutions and pH, is a control on subcritical crack growth (Bergsaker et al., 2016; Rostom et al., 2013; Røyne, Bisschop, et al., 2011). They especially evoke changes in surface energy. In terms of stress corrosion, surface potentials in carbonates might be an important factor, while mechanisms like hydrolysis and hydration are active possibly more important in silicates (Stipp, 1999; Stipp et al., 1994; Stipp & Hochella, 1991).

Contrary to the environments taken into account in the aforementioned studies and material sciences, in natural settings we do not expect these strong variations in pH or sudden changes in fluid concentration. For example, it has been shown that the carbonate waters from rocks, and fractures around the Zugspitze, in the Northern Calcareous Alps is that the waters are nearly or fully carbonate saturated (Küfmann, 2013). When we observe an enhanced reactivity in these settings, it could be reasoned that it is enabled by mechanical straining of bonds. A better understanding of stress corrosion rates of carbonates could be also important regarding the carbon cycle and silicate weathering (Brantley et al., 2011; Goudie & Viles, 2012; Maher & Chamberlain, 2014). This is particularly the case for the critical zone where weathering is facilitated in wet conditions and under subcritical stress magnitudes (Moon et al., 2017; Slim et al., 2015).

5.5 Geomorphological and geological time scale of progressive rock failure

In the context of geomorphology, rocks spend a long time failing. In our experiments, we can only see snapshots of how rock failures might progress through time. From these, one could reason that its passage follows an overall creep curve (**Figure 5.5.1**). As soon as the rock is formed and uplifted, progressive failure begins. Elastic and inelastic rebound accompany the rock as it is exhumed. Relaxing the internal state reduces the contractional elastic strains. External processes and conditions induce extensional strains and promote coupled chemo-mechanical subcritical mechanisms. Evolving to a more extensionally strained internal state the susceptibility to environmental conditions increases. Morphology creates stress concentrations, and localizes and facilitates tensile fracturing. **Figure 5.5.1** depicts this evolution with some detailed real-world but small scale examples. At which point the rock has actually failed is in the eye of the beholder or the context.

At which state along this creep curve we are and which aspects of this evolution needs consideration varies highly by the spatial scale of interest, for example, a rock slope, infrastructure or landscape evolution. It is important to consider that the rocks and associated fractures extend across geologic time.

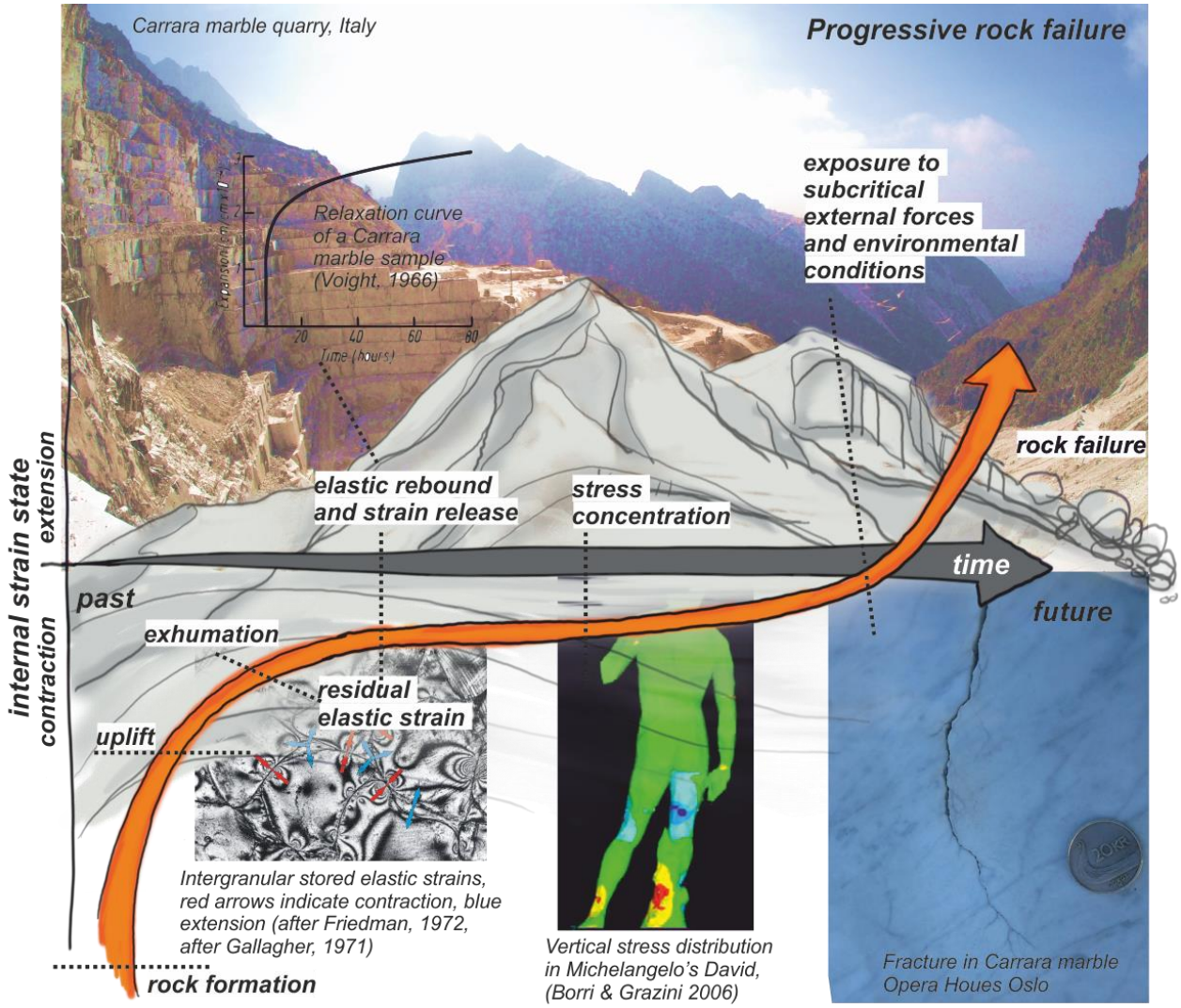

Figure 5.5.1 Progressive rock failure evolution concept. See text for details.

The temporal, as well as the spatial scale of the experiments, provides a relative estimation of the rate and operation of progressive rock failure outside of the controlled laboratory. The relative time we can deduct from the experiments is difficult to extrapolate to the absolute timescale. To pinpoint any change, we need reference points, which we seldom have. If we upscale the laboratory rate in space and/or time, we might overestimate, or even underestimate progressive failure, because we are unable to constrain the conditions and net forces acting upon rocks. What we can derive from the experiments and directly apply to the assessment real-world examples is that rocks break long before we see critical deformation and failure.

Time is inherent in rocks. Even if we pick a perfect rock sample and call it "intact", test it for its short term or peak strength, predicting how it would behave, at which rate it will deteriorate and at which stress intensity it will fail, will be limited by the time over which

subcritical crack growth rates are negligible. The duration of this timespan is still not known. Controls of this progressive rock failure have been investigated in this thesis which would need to be taken into consideration. Concerning progressive rock slope failure, this long term or temporal aspect indicates that it cannot be readily modelled and anticipated with limit equilibrium approaches unless the internal or damage states and forces acting on it are known and progressively updated. Limit equilibrium approaches are inherently time-independent. This might be appropriate for applications in engineering and infrastructure of geomaterials. For rock slope stability in a geomorphological context and landscape evolution, a better understanding of the parametrization and models of creep rates, acceleration phases and memory effect could be a focus for the future.

Chapter 4.3 highlighted the importance of material and that rock properties and rheology need to be incorporated more frequently in geomorphological analysis. Emphasising the material is also a way of reiterating past processes, stresses and forms. Another aspect which has only been mentioned briefly is the resulting form or geomorphology of progressive rock failure. In the previous paper, this aspect was partially and indirectly picked up by the setup and sample geometry which led to stress concentrations. 'Form' is not only a result, or a threshold (slope), but an active part where, for example, topographic stresses feedback into the stress state – possibly at subcritical magnitudes.

6. Conclusion

The principal objective of this dissertation was to illustrate the controls of progressive rock failure in a geomorphological context. I demonstrated the benefits of increased synergy between the fields of geomorphology and geology on the one side and rock physics, physical chemistry and material sciences on the other. These fields are complementary in assessing progressive rock failure, though there are very few examples in the literature of truly integrated investigations (Collins et al., 2019; Collins & Stock, 2016b; Leith et al., 2014a, 2014b). I suggest that this is a result of an apparent disconnect between the disciplines; one primarily deals with landforms and processes, while the other is focused on stresses and materials. The neglect of materials and quantitative assessments of stresses exerted by geomorphic processes as well as preconditioned and inherited within rocks in many geomorphological studies has hampered investigations of how rocks break. The ignorance of dynamics, ambient condition and geological time scales in rock physics and material sciences has hindered the transfer of methods and concepts. I reissued an existing, although in Geosciences poorly utilized concept of residual elastic strain and its measurement by neutron diffraction, to assess the internal and inherited state of rock, the so-called rock stress memory. I addressed the coupled chemical and mechanical effects of Earth surface environmental conditions on the progressive failure of rocks. I combined the subcritical fracture mechanics and geomorphological processes within a coherent framework. The strength of this investigation was the range of complementary observations. Specifically, I suggest that we need to research both internal and external states of rocks to truly understand their progressive failure.

The outcomes of this thesis provide a common ground for all disciplines to investigate progressive rock failure. By combining knowledge from these disciplines, one expects practitioners to gain greater insight into how potential future geohazards, infrastructure, or artwork loss by progressive rock failure can be anticipated. The new framework also leaves many open opportunities for future experimental research. I conclude by giving some suggestions for future work along with interrelated aspects of progressive rock failure. These aspects are subdivided into seven themes – Methods – Theory – Rocks – Limits – Failure – Strength – Stress. These themes have been (re)emerging throughout the process of compiling this thesis and might also set the next stepping stones for future research.

On methods

I suggest the use of all methods available when appropriate and to not be afraid to borrow and adapt approaches from other disciplines while still being aware of their limitations and simplifications.

One of the outstanding challenges in studies of progressive rock failure was: How can the inside of rocks be observed without destroying it? Implications of the experiments and the neutron diffraction measurements are that there are some indirect ways. Non-invasive or non-destructive techniques, like neutron or X-ray diffraction or tomography, have been developed, especially in material sciences. Their application is often limited to small laboratory samples, and because of time restrictions at research facilities provide spalling sources and accelerator duration of experiments are limited. For measuring residual elastic strains in rock, some facilities offer testing environments that enable mechanical and thermally stressed in-situ experiments. With time-of-flight neutron diffraction it is also possible to assess polyphase rock

types, which could extend our understanding of how not only microstructure but also compositional properties affect the rheology (Covey-Crump et al., 2003, 2013).

Insights from laboratory-based methods can also be used to develop, test and calibrate complementary geophysical methods, like seismic velocities. Geophysical methods have been widely utilized to infer changes in internal properties of e.g. hillslopes, glaciers, moraines and bedrock, but are so far unable to determine the actual stress state and thus predict their dynamics (Guillemot et al., 2020; Mainsant, Larose, Brnnimann, et al., 2012; Obermann et al., 2014).

Potential methods, for understanding why rocks break, are not necessarily limited to the physical or engineering sciences. For the theory experiment, for example, I developed a technique I would like to call "drawing/sketching as inquiry" – broadly related to the scientific method of writing as inquiry. In this social sciences method, writing is seen as a way of knowing or knowledge production (Richardson & Adams St. Pierre, 2018). It seems that drawing and sketching is also a way of knowing and has –especially in the theoretical and conceptual rethinking of: how do rocks break? What inherits a rock? What controls progressive rock failure? And how does it relate to geomorphology? – been articulated before words were found to describe possible answers. Even though some of these scientific drawings now illustrate this thesis, they also have an analytical character and are not simply illustrations. Or as Humboldt wrote, figures should "speak to the senses without fatiguing the mind" (Public domain/Wikimedia Commons), which fits like a pointed remark to progressive rock failure.

On theory

Enabled by collaborating in interdisciplinary communities' new concepts could emerge. My fascination with the principles of geomorphology has had an impact on how this thesis has evolved. It can be challenging to bring these various concepts and perspectives together, especially when dealing with the temporal scales of progressive failures which are addressed differently in geology, engineering geology and material sciences. Divisions between the disciplines are evident when a geologist explains to a material scientist that as a geologist one does not know or can tweak the production, respectively the formation of rocks. Other examples such as stress corrosion and residual strains appear naturally coupled in material science theories but are not often linked in rock mechanics.

Surprisingly though, there are many similarities and overlaps of theories that exist between the disciplines when investigating progressive fracturing. The most coherent concept is based on 'energy'. They range from energy-based concepts of landscape sensitivity (Brunsden & Thornes, 1979), to the build-up of elastic strain energy by crystal growth (Røyne, Meakin, et al., 2011) and subcritical mechanism base on the Griffith criterion and macroscopic expansion (Lawn, 1993; Røyne, Bisschop, et al., 2011; Sadananda et al., 2017). It might be promising to streamline the physical, chemical and mechanical fracture laws in terms of energetics.

On rocks

The fundamental concept to investigate geomorphology – from my perspective – resides in the triangular relationship of Form – Process – Material (see **Chapter 4.3** and **Supplement 3**). Geomorphological research on progressive rock failure and slope instabilities seem to

neglect “material”, unlike rock mechanics which seems to be focused on it, while forgetting about the “form”. Rocks are part of the process and the form, the form also affects the stress state of the rock and which processes are possible. Processes alter the material and change the form, which affects the stress state of the rock, which also likely controls the efficiency of the processes acting upon the form. I suggest to include rock properties in geomorphological studies beyond phenomenological references such as weaker and stronger lithology, to be able to account for these interactions. Before interpreting process efficiency, geomorphic work or associated rates, ways of quantification of exerted, transmitted, dampened and enhanced stresses within geomorphological processes need to be established.

Rocks are usually not intact. There are fractures in rock at all scales. Structural inheritances, from residual elastic strains in crystal lattices, the shape and orientations of grain boundaries and fault and shear zones define where and how rocks break. The role of structural inheritance in the rocks is entirely not clear; though the scale of them seems to matter (Samsu et al., 2020). Dependent on the scale, some inherited features pose a stronger control on the rheology of rocks than others. These still need to be determined. For many rock mechanical studies and for the sake of comparison and feasibility, experiments are run on exemplary and intact rock samples. Further studies on the influence of structural inherited features on fracture mechanisms and extent promise to be beneficial for engineering geology drilling into rocks for exploitation, geothermal power or infrastructure but also in understanding the comminution of bedrock in geomorphology (M. R. Chandler et al., 2016; Forbes Inskip et al., 2018; Scott & Wohl, 2018; Sklar et al., 2017).

On limits

The choice of material, testing mode and neutron diffraction techniques within the laboratory studies, limit the direct application of results to real rock slopes. Carrara marble is an exemplary rock for laboratory experiments and sculptures, but its properties are very proprietary and its spatial distribution limited. It would be advantageous to be able to relate the neutron diffraction measurements of residual elastic strains to the in-situ stresses in the field. The long-term laboratory creep test was set up to test fractures in mode I. This testing mode enabled single fracture to establish at the expense of microcracks. These controlled loading conditions are not necessarily found in natural rock slopes. In addition, in natural rock settings as well as in the laboratory, the mode of loading is not necessarily the same mode of fracture (Backers, 2004). All subcritical mechanisms discussed in this thesis apply to opening fracture modes. Shear or mixed-mode fractures due to stress concentrations and transmissions have likely been present as well. However, our knowledge of subcritical crack growth in all fracture modes is still very limited.

Another limit to a mutual concept of slope failures is related to the mode of fracturing. Long-term slope stability concepts like the ‘Limits to relief’ (Schmidt & Montgomery, 1995) or time-less limit equilibrium analysis assume shear failure. Due to gravitational compressive loading, shear stresses arise at an assumed interface or plane. If they exceed the critical shear strength they form a fracture. Suppose that stresses acting in rock slopes are subcritical, they would more easily form tensile fractures. Including tensile failure in rock slope stability analysis could help to anticipate especially rock falls.

On failure

A question I tried to answer in this thesis was: How do rocks break? In regard to progressive rock failure, the question rather turned into: What is failure? For the anticipation of rock slope failures, many studies have shown that it is essential to understand the deformation prior to the failure (Collins et al., 2019; Collins & Stock, 2016b; Loew et al., 2016; Ventura et al., 2010). Deformation can be very small, so methods to detect these minor changes need to be improved. The velocity of deformation for subcritical monitoring needs to be reliable for a long time. The surficial and visible deformation referred to here is assumed to be caused by volumetric inelastic damage. This damage parameter could also be expressed by other internal variables like the residual elastic strain, as shown in this thesis. Extensional elastic strain states are commonly assumed as a damage indicator in material sciences (Withers, 2007).

Deformation before failure would thus include any elastic or inelastic work being done. Or as Lyell (1832:173) in his Principles of Geology wrote: "The real point on which the whole controversy turns is the relative amount of work done by mechanical force in given quantities of time, past and present." An evolution law relating the rate of elastic and inelastic properties to the stress and strain history would be great to have to predict progressive rock failure.

On strength

Progressive rock failure is inherently linked to rock strength. But what is strength? Strength of the material is usually measured as dependent on applied stress. An independent description of this variable is difficult as it has been shown that the stress state affects the response of the rock, such that an apparent higher strength of rocks is reached in triaxial tests (e.g. Diederichs, 2003). This effect is probably related to the suppression of opening fractures. It was shown that the residual strain or stress state if in compression, can have implications for the rock strength as well.

It is reasoned that the inducement and relaxation of elastic strains depend on the magnitude of thermal and mechanical stresses (Holzhausen & Johnson, 1979). The rate of change in these conditions determines how much of these elastic strains are stored. This is because the rate of mechanical or thermal unloading can also evoke inelastic damage. In relaxation creep tests, as well as in studies on quarrying – both essentially testing rock response to unloading – it has been observed that rock stress partially rebounds and forms microcracks (Cruden, 1971; Nichols, 1975, 1980; Paraskevopoulou et al., 2015). In granites, these rebound features are known to form rift planes (Engelder, 1993). All of this allows the conclusion that the rate of change of conditions poses a control on the rock strength.

Applying this to a geological and geomorphological context, I propose that uplift and exhumation rates, rates of exposure and unloading by e.g. erosion, seismic activity or quarrying, control not only fracture density but also resistance to progressively fracture. This, in turn, effects the extent and rates of progressive damage, weathering and erosion. These types of rate effects are largely unstudied.

On stress

In this thesis, I could also show that internals strains can be superimposed by low magnitude stresses and environmental conditions. The effect of subcritical external forcing and

conditions on the strain state is important in regards to drastic changes in those due to climatic change and exploitation of solid Earth resources, like glacial retreat or steep open mines. Effects on progressive fracture and related phenomena due to glacial loading and unloading as well as naturally created and man-made topographic stress fields are brought increasingly into the research focus of geomorphologists (Gerber & Scheidegger, 1969; Leith et al., 2014b; Moon et al., 2017; St.Clair et al., 2015). Subcritical stresses and environmental conditions should also be seen in terms of strengthening of rocks is often overlooked (Bruthans et al., 2014).

Whether stress effects cause a weakening or strengthening of rock partly depends on the applied stress magnitude. From the theoretical consideration of this thesis, it can also be concluded that the direction in which these forces are applied determined whether it weakens or strengthens the material. Mechanically stressing rocks in tension even at subcritical stress magnitudes always weakens, while in compression low-stress magnitudes could lead to an initial strengthening (Darwin, 1883; Gudehus & Touplikiotis, 2017; Řihošek et al., 2016). The interaction of environmental conditions like water and temperature can also have a strengthening, by providing cohesion and pressure, or weakening effect by reduced friction. What these optimal levels are, is still open to future research.

All of the aforementioned conclusions are the result of this long-term project. A personal conclusion is that an optimal stress level for geomorphologists exists as well: some stress is good, too much will fatigue and lead to failure.

References

Abellán, A., Kristensen, L., Jaboyedoff, M., & Blikra, L. (2017). Real-time forecasting of slope kinematics in response to precipitation. Application to Veslemannen (SW Norway). In *ISRM Progressive Rock Failure Conference* (p. 4). Ascona, Switzerland: International Society for Rock Mechanics and Rock Engineering.

Agliardi, F., Scuderi, M. M., Fusi, N., & Collettini, C. (2020). Slow-to-fast transition of giant creeping rockslides modulated by undrained loading in basal shear zones. *Nature Communications*, *11*(1), 1–11. https://doi.org/10.1038/s41467-020-15093-3

Alber, M., & Hauptfleisch, U. (1999). Generation and visualization of microfractures in Carrara marble for estimating fracture toughness, fracture shear and fracture normal stiffness. *International Journal of Rock Mechanics and Mining Sciences*, *36*(8), 1065–1071. https://doi.org/10.1016/S1365-1609(99)00069-6

Aldred, J., Eppes, M.-C., Aquino, K., Deal, R., Garbini, J., Swami, S., et al. (2016). The influence of solar-induced thermal stresses on the mechanical weathering of rocks in humid mid-latitudes. *Earth Surface Processes and Landforms*, *41*(5), 603–614. https://doi.org/10.1002/esp.3849

Alfes, C. (1993). *Bruchmechanisches Werkstoffverhalten von Sandstein unter Zugbeanspruchung* (Aachener B). Aachen: Verlag der Augustinus Buchhandlung.

Amitrano, D., & Helmstetter, A. (2006). Brittle creep, damage, and time to failure in rocks. *Journal of Geophysical Research: Solid Earth*, *111*(11), 1–17. https://doi.org/10.1029/2005JB004252

Anders, M. H., Schneider, J. R., Scholz, C. H., & Losh, S. (2013). Mode I microfracturing and fluid flow in damage zones: The key to distinguishing faults from slides. *Journal of Structural Geology*, *48*, 113–125. https://doi.org/10.1016/j.jsg.2012.11.010

Anderson, O. L., & Grew, P. C. (1977). Stress corrosion theory of crack propagation with applications to geophysics. *Reviews of Geophysics and Space Physics*. https://doi.org/10.1029/RG015i001p00077

Arosio, D., Longoni, L., Papini, M., Scaioni, M., Zanzi, L., & Alba, M. (2009). Towards rockfall forecasting through observing deformations and listening to microseismic emissions. *Natural Hazards and Earth System Sciences*, *9*(4), 1119–1131. https://doi.org/10.5194/nhess-9-1119-2009

Arvidson, R. S., Ertan, I. E., Amonette, J. E., & Luttge, A. (2003). Variation in calcite dissolution rates: A fundamental problem? *Geochimica et Cosmochimica Acta*, *67*(9), 1623–1634. https://doi.org/10.1016/S0016-7037(02)01177-8

ASTM. Standard test method for measurement of fracture toughness, E 1820-0 § (2003). https://doi.org/10.1520/E1820-09.2

ASTM. Standard test method for flexural strength of concrete (using simple beam with center-point loading) (2012). https://doi.org/10.1520/C0293

Atkinson, B. K. (1979). Fracture toughness of Tennessee sandstone and Carrara marble using the double torsion testing method. *International Journal of Rock Mechanics and Mining Sciences & Geomechanics Abstracts*, *16*, 49–53.

Atkinson, B. K. (1984). Subcritical crack growth in geological materials. *Journal of Geophysical Research*, *89*(B6), 4077–4114. https://doi.org/10.1029/JB089iB06p04077

Atkinson, B. K. (1987). *Fracture mechanics of rock*. (B. K. Atkinson, Ed.). London, Orlando,

San Diego: Academic Press.

Atkinson, B. K., & Meredith, P. G. (1987). The theory of subcritical crack growth with applications to minerals and rocks. In B. K. Atkinson (Ed.), *Fracture mechanics of rock* (pp. 111–166). London: Academic Press.

Atkinson, B. K., & Rawlings, R. D. (1981). Acoustic emission during stress corrosion cracking in rocks. In D. Simpson & P. G. Richards (Eds.), *Earthquake Prediction: An International Review* (Maurice Ew, pp. 605–616). Washington, D.C.: AGU. https://doi.org/10.1029/ME004p0605

Avseth, P., Mukerji, T., Mavko, G., & Dvorkin, J. (2010). Rock-physics diagnostics of depositional texture, diagenetic alterations, and reservoir heterogeneity in high-porosity siliciclastic sediments and rocks — A review of selected models and suggested work flows. *Geophysics*, *75*(5), 75A31. https://doi.org/10.1190/1.3483770

Azzola, J., Schmittbuhl, J., Zigone, D., Magnenet, V., & Masson, F. (2018). Direct Modeling of the Mechanical Strain Influence on Coda Wave Interferometry. *Journal of Geophysical Research: Solid Earth*, *123*(4), 3160–3177. https://doi.org/10.1002/2017JB015162

van der Baan, M., Eaton, D. W., & Preisig, G. (2016). Stick-split mechanism for anthropogenic fluid-induced tensile rock failure. *Geology*, *44*(7), 503–506. https://doi.org/10.1130/G37826.1

Backers, T. (2004). *Fracture toughness determination and micromechanics of rock under mode I and mode II loading*. PhD Thesis, Universität Potsdam.

Balestrieri, M. L., Pandeli, E., Bigazzi, G., Carosi, R., & Montomoli, C. (2011). Age and temperature constraints on metamorphism and exhumation of the syn-orogenic metamorphic complexes of Northern Apennines, Italy. *Tectonophysics*, *509*(3–4), 254–271. https://doi.org/10.1016/j.tecto.2011.06.015

Barber, D. J., Wenk, H. R., Gomez-Barreiro, J., Rybacki, E., & Dresen, G. (2007). Basal slip and texture development in calcite: New results from torsion experiments. *Physics and Chemistry of Minerals*, *34*(2), 73–84. https://doi.org/10.1007/s00269-006-0129-3

Barnhoorn, A., Cox, S. F., Robinson, D. J., & Senden, T. (2010). Stress- and fluid-driven failure during fracture array growth: implications for coupled deformation and fluid flow in the crust. *Geology*, *38*(9), 779–782. https://doi.org/10.1130/G31010.1

Baud, P., Zhu, W., & Wong, T. F. (2000). Failure mode and weakening effect of water on sandstone. *Journal of Geophysical Research*, *105*(B7), 16,371-389. https://doi.org/10.1029/2000JB900087

Beer, A. R., Turowski, J. M., & Kirchner, J. W. (2017). Spatial patterns of erosion in a bedrock gorge. *Journal of Geophysical Research: Earth Surface*, *122*(1), 191–214. https://doi.org/10.1002/2016JF003850

Bellopede, R., Castelletto, E., & Marini, P. (2016). Ten years of natural ageing of calcareous stones. *Engineering Geology*, *211*, 19–26. https://doi.org/10.1016/j.enggeo.2016.06.015

Bérest, P., Blum, P. A., Charpentier, J. P., Gharbi, H., & Valès, F. (2005). Very slow creep tests on rock samples. *International Journal of Rock Mechanics and Mining Sciences*, *42*, 569–576. https://doi.org/10.1016/j.ijrmms.2005.02.003

Bergsaker, A. S., Røyne, A., Ougier-Simonin, A., Aubry, J., & Renard, F. (2016). The effect of fluid composition, salinity, and acidity on subcritical crack growth in calcite crystals. *Journal of Geophysical Research: Solid Earth*, *121*, 1631–1651.

https://doi.org/10.1002/2015JB012723

Bibi, I., Arvidson, R. S., Fischer, C., & Lüttge, A. (2018). Temporal Evolution of Calcite Surface Dissolution Kinetics. *Minerals*, *8*(6), 256. https://doi.org/10.3390/min8060256

Bjerrum, L., & Jørstad, F. A. (1968). Stability of rock slopes in Norway. *Norwegian Geotechnical Institut*, *79*, 1–11.

Bögli, A. (1978). *Karsthydrographie und physische Speläologie*. Berlin, Heidelberg, New York: Springer.

Borg, I., & Handin, J. (1967). Torsion of calcite single crystals. *Journal of Geophysical Research*, *72*(2), 641–669. https://doi.org/10.1029/jz072i002p00641

Bragg, W. L. (1924). The refractive indices of Calcite and Aragonite. *Proceedings of the Royal Society of London*, *105*(732), 370–386.

Brain, M. J., Rosser, N. J., Norman, E. C., & Petley, D. N. (2014). Are microseismic ground displacements a significant geomorphic agent? *Geomorphology*, *207*, 161–173. https://doi.org/10.1016/j.geomorph.2013.11.002

Brantley, S. L., Megonigal, J. P., Scatena, F. N., Balogh-Brunstad, Z., Barnes, R. T., Bruns, M. A., et al. (2011). Twelve testable hypotheses on the geobiology of weathering. *Geobiology*, *9*(2), 140–165. https://doi.org/10.1111/j.1472-4669.2010.00264.x

Brantut, N., Baud, P., Heap, M. J., & Meredith, P. G. (2012). Micromechanics of brittle creep in rocks. *Journal of Geophysical Research: Solid Earth*, *117*, B08412. https://doi.org/10.1029/2012JB009299

Brantut, N., Heap, M. J., Meredith, P. G., & Baud, P. (2013). Time-dependent cracking and brittle creep in crustal rocks: A review. *Journal of Structural Geology*, *52*, 17–43. https://doi.org/10.1016/j.jsg.2013.03.007

Brantut, N., Heap, M. J., Baud, P., & Meredith, P. G. (2014a). Mechanisms of time-dependent deformation in porous limestone. *Journal of Geophysical Research*, *119*, 5444–5463. https://doi.org/10.1002/2014JB011186

Brantut, N., Heap, M. J., Baud, P., & Meredith, P. G. (2014b). Rate- and strain-dependent brittle deformation of rocks. *Journal of Geophysical Research: Solid Earth*, *119*, 1818–1836. https://doi.org/10.1002/2013JB010448

De Bresser, J. H. P., & Spiers, C. J. (1997). Strength characteristics of the r, f, and c slip systems in calcite. *Tectonophysics*, *272*(1), 1–23. https://doi.org/10.1016/S0040-1951(96)00273-9

Broek, D. (1982). *Elementary engineering fracture mechanics* (3rd ed.). The Hague, Boston, London: Martinus Nijhoff Publishers.

Bruijn, R. H. C., Kunze, K., Mainprice, D., & Burlini, L. (2011). Mechanical and microstructural development of Carrara marble with pre-existing strain variation. *Tectonophysics*, *503*(1–2), 75–91. https://doi.org/10.1016/j.tecto.2010.09.029

Bruner, W. M. (1984). Crack growth during unroofing of crustal rocks: Effects on thermoelastic behavior and near-surface stresses. *Journal of Geophysical Research*, *89*(B6), 4167–4184. Retrieved from file://localhost/Users/jescartin/WORK/Referencias/pdfs/Bruner1984.pdf

Brunsden, D., & Thornes, J. B. (1979). Landscape sensitivity and change. *Transactions of the Institute of British Geographers*, *4*(4), 463–484. https://doi.org/10.2307/622210

Bruthans, J., Soukup, J., Vaculikova, J., Filippi, M., Schweigstillová, J., Mayo, A. L., et al.

(2014). Sandstone landforms shaped by negative feedback between stress and erosion. *Nature Geoscience, 7*, 597–601. https://doi.org/10.1038/NGEO2209

Byerlee, J. D. (1978). Friction of rocks. *Pageoph, 116*(4–5), 615–626. https://doi.org/10.1007/BF00876528

Cantisani, E., Pecchioni, E., Fratini, F., Garzonio, C. A., Malesani, P., & Molli, G. (2009). Thermal stress in the Apuan marbles: relationship between microstructure and petrophysical characteristics. *International Journal of Rock Mechanics and Mining Sciences*, *46*, 128–137. https://doi.org/10.1016/j.ijrmms.2008.06.005

Cardani, G., & Meda, A. (2004). Marble behaviour under monotonic and cyclic loading in tension. *Construction and Building Materials*, *18*(6), 419–424. https://doi.org/10.1016/j.conbuildmat.2004.03.012

Carmignani, L., & Kligfield, R. (1990). Crustal extension in the northern Apennines: the transition from compression to extension in the Alpi Apuane core complex. *Tectonics*, *9*(6), 1275–1303.

Casey, W. H., Banfield, J. F., Westrich, H. R., & McLaughlin, L. (1993). What do dissolution experiments tell us about natural weathering? *Chemical Geology*, *105*, 1–15. https://doi.org/10.1016/0009-2541(93)90115-Y

Castelltort, S., Goren, L., Willett, S. D., Champagnac, J. D., Herman, F., & Braun, J. (2012). River drainage patterns in the New Zealand Alps primarily controlled by plate tectonic strain. *Nature Geoscience*, *5*(10), 744–748. https://doi.org/10.1038/ngeo1582

Chandler, M. R., Meredith, P. G., Brantut, N., & Crawford, B. R. (2016). Fracture toughness anisotropy in shale. *Journal of Geophysical Research: Solid Earth*, *121*, 1706–1729. https://doi.org/10.1002/2015JB012756.

Chandler, N. A. (2013). Quantifying long-term strength and rock damage properties from plots of shear strain versus volume strain. *International Journal of Rock Mechanics and Mining Sciences*, *59*, 105–110. https://doi.org/10.1016/j.ijrmms.2012.12.006

Charles, R. J. (1958). Static fatigue of glass. *Journal of Applied Physics*, *29*(11), 1549–1553.

Chen, K., Kunz, M., Tamura, N., & Wenk, H. R. (2011). Deformation twinning and residual stress in calcite studied with synchrotron polychromatic X-ray microdiffraction. *Physics and Chemistry of Minerals*, *38*, 491–500. https://doi.org/10.1007/s00269-011-0422-7

Chen, K., Kunz, M., Tamura, N., & Wenk, H. R. (2015). Residual stress preserved in quartz from the San Andreas Fault Observatory at Depth. *Geology*, *43*(3), 219–222. https://doi.org/10.1130/G36443.1

Chen, X., Eichhubl, P., & Olson, J. E. (2017). Effect of water on critical and subcritical fracture properties of Woodford shale. *Journal of Geophysical Research: Solid Earth*, *122*(4), 2736–2750. https://doi.org/10.1002/2016JB013708

Church, M. (2010). The trajectory of geomorphology. *Progress in Physical Geography*, *34*(3), 265–286. https://doi.org/10.1177/0309133310363992

Clark, J. N., Ihli, J., Schenk, A. S., Kim, Y.-Y., Kulak, A. N., Campbell, J. M., et al. (2015). Three-dimensional imaging of dislocation propagation during crystal growth and dissolution. *Nature Materials*, *14*(8), 780–784. https://doi.org/10.1038/nmat4320

Clarke, B. A., & Burbank, D. W. (2011). Quantifying bedrock-fracture patterns within the shallow subsurface: Implications for rock mass strength, bedrock landslides, and erodibility. *Journal of Geophysical Research*, *116*, F04009. https://doi.org/10.1029/2011JF001987

Collins, B. D., & Stock, G. M. (2016a). Rockfall triggering by cyclic thermal stressing of exfoliation fractures. *Nature Geoscience*, *9*, 395–401. https://doi.org/10.1038/ngeo2686

Collins, B. D., & Stock, G. M. (2016b). Rockfall triggering by thermal stressing of exfoliation fractures. *Nature Geoscience*, *9*, 395–401. https://doi.org/10.1038/NGEO2686

Collins, B. D., Stock, G. M., Eppes, M. C., Lewis, S. W., Corbett, S. C., & Smith, J. B. (2018). Thermal influences on spontaneous rock dome exfoliation. *Nature Communications*, *9*(1), 1–12. https://doi.org/10.1038/s41467-017-02728-1

Collins, B. D., Stock, G. M., & Eppes, M. C. (2019). Relaxation Response of Critically Stressed Macroscale Surficial Rock Sheets. *Rock Mechanics and Rock Engineering*, *52*(12), 5013–5023. https://doi.org/10.1007/s00603-019-01832-6

Colombani, J. (2016). The alkaline dissolution rate of calcite. *Journal of Physical Chemistry Letters*, *7*(13), 2376–2380. https://doi.org/10.1021/acs.jpclett.6b01055

Covey-Crump, S. J., & Schofield, P. F. (2009). Neutron Diffraction and the Mechanical Behavior of Geological Materials. In L. Liang, R. Rinaldi, & H. Schober (Eds.), *Neutron applications in Earth, Energy and Environmental Sciences* (pp. 257–282). Boston, MA: Springer. https://doi.org/10.1007/978-0-387-09416-8_9

Covey-Crump, S. J., Schofield, P. F., Stretton, I. C., Knight, K. S., & Ben Ismail, W. (2003). Using neutron diffraction to investigate the elastic properties of anisotropic rocks: Results from an olivine plus orthopyroxene mylonite. *Journal of Geophysical Research: Solid Earth*, *108*(B2), 15. https://doi.org/2092 Artn 2092

Covey-Crump, S. J., Schofield, P. F., & Daymond, M. R. (2006). Using neutrons to investigate changes in strain partitioning between the phases during plastic yielding of calcite+halite composites. *Physica B: Condensed Matter*, *385–386*, 946–948. https://doi.org/10.1016/j.physb.2006.05.279

Covey-Crump, S. J., Schofield, P. F., Stretton, I. C., Daymond, M. R., Knight, K. S., & Tant, J. (2013). Monitoring in situ stress/strain behaviour during plastic yielding in polymineralic rocks using neutron diffraction. *Journal of Structural Geology*, *47*, 36–51. https://doi.org/10.1016/j.jsg.2012.10.003

Croizé, D., Renard, F., Bjørlykke, K., & Dysthe, D. K. (2010). Experimental calcite dissolution under stress: Evolution of grain contact microstructure during pressure solution creep. *Journal of Geophysical Research*, *115*(9), B09207. https://doi.org/10.1029/2010JB000869

Crozier, M. J. (1989). *Landslides: Causes, consequences and environment*. Routledge.

Cruden, D. M. (1970). A theory of brittle creep in rock under uniaxial compression. *Journal of Geophysical Research*, *75*(17), 3431–3442. https://doi.org/10.1029/JB075i017p03431

Cruden, D. M. (1971). The recovery of Pennant sandstone from uniaxial compressive load. *Canadian Journal of Earth Sciences*, *8*(5), 518–522. https://doi.org/10.1139/e71-054

Cruden, D. M. (1974). The static fatigue of brittle rock under uniaxial compression. *International Journal of Rock Mechanics and Mining Sciences And*, *11*(2), 67–73. https://doi.org/10.1016/0148-9062(74)92650-3

Damjanac, B., & Fairhurst, C. (2010). Evidence for a long-term strength threshold in crystalline rock. *Rock Mechanics and Rock Engineering*, *43*, 513–531. https://doi.org/10.1007/s00603-010-0090-9

Damköhler, G. (1936). Einflüsse der Strömung, Diffusion und des Wärmeüberganges auf die Leistung von Reaktionsöfen: I. Allgemeine Gesichtspunkte für die Übertragung eines

chemischen Prozesses aus dem Kleinen ins Große. *Zeitschrift Für Elektrochemie Und Angewandte Physikalische Chemie*, *42*, 846–862. https://doi.org/10.1002/bbpc.19360421203

Darling, T. W., TenCate, J. A., Brown, D. W., Clausen, B., & Vogel, S. C. (2004). Neutron diffraction study of the contribution of grain contacts to nonlinear stress-strain behavior. *Geophysical Research Letters*, *31*(16), 31–34. https://doi.org/10.1029/2004GL020463

Darot, M., & Gueguen, Y. (1986). Slow crack growth in minerals and rocks: theory and experiments. *Pure and Applied Geophysics*, *124*(4/5), 677–692. https://doi.org/10.1007/bf00879604

Darwin, G. H. (1883). On the horizontal thrust of mass of sand. *Minutes of the Proceedings of the Institution of Civil Engineers*, *71*(1883), 350–378. https://doi.org/10.1680/imotp.1883.21802

Das, S., & Scholz, C. H. (1981). Theory of time-dependent rupture in the Earth. *Journal of Geophysical Research: Solid Earth*, *86*(B7), 6039–6051. https://doi.org/10.1029/JB086iB07p06039

Davies, T. R. H., McSaveney, M. J., & Boulton, C. J. (2012). Elastic strain energy release from fragmenting grains: Effects on fault rupture. *Journal of Structural Geology*, *38*, 265–277. https://doi.org/10.1016/j.jsg.2011.11.004

Davies, T. R. H., McSaveney, M. J., & Reznichenko, N. V. (2019). What happens to fracture energy in brittle fracture? Revisiting the Griffith assumption. *Solid Earth*, *10*(4), 1385–1395. https://doi.org/10.5194/se-10-1385-2019

Davies, T. R. H., Reznichenko, N. V., & McSaveney, M. J. (2020). Energy budget for a rock avalanche: fate of fracture-surface energy. *Landslides*, *17*(1), 3–13. https://doi.org/10.1007/s10346-019-01224-5

Derbyshire, E., Gregory, K. J., & Hails, J. R. (1979). *Geomorphological processes*. Dawson, Boulder: Folkestone.

DiBiase, R. A., Rossi, M. W., & Neely, A. B. (2018). Fracture density and grain size controls on the relief structure of bedrock landscapes. *Geology*, *46*(5), 399–402. https://doi.org/10.1130/G40006.1

Diederichs, M. S. (2003a). Manuel Rocha Medal Recipient Rock Fracture and Collapse Under Low Confinement Conditions. *Rock Mechanics and Rock Engineering*, *36*(5), 339–381. https://doi.org/10.1007/s00603-003-0015-y

Diederichs, M. S. (2003b). Rock fracture and collapse under low confinement conditions. *Rock Mechanics and Rock Engineering*, *36*(5), 339–381. https://doi.org/10.1007/s00603-003-0015-y

Dietze, M., Turowski, J. M., Cook, K. L., & Hovius, N. (2017). Spatiotemporal patterns, triggers and anatomies of seismically detected rockfalls. *Earth Surface Dynamics*, *5*(4), 757–779. https://doi.org/10.5194/esurf-5-757-2017

Dohmen, L., Lenting, C., Fonseca, R. O. C., Nagel, T., Heuser, A., Geisler, T., & Denkler, R. (2013). Pattern formation in silicate glass corrosion zones. *International Journal of Applied Glass Science*, *4*(4), 357–370. https://doi.org/10.1111/ijag.12046

Dove, P. M. (1995). Geochemical controls on the kinetics of quartz fracture at subcritical tensile stresses. *Journal of Geophysical Research*, *100*(B11), 22349–22359. https://doi.org/10.1029/95JB02155

Dove, P. M., Han, N., & De Yoreo, J. J. (2005). Mechanisms of classical crystal growth

theory explain quartz and silicate dissolution behavior. *Proceedings of the National Academy of Sciences of the United States of America*, *102*(43), 15357–15362. https://doi.org/10.1073/pnas.0507777102

Dühnforth, M., Anderson, R. S., Ward, D., & Stock, G. M. (2010). Bedrock fracture control of glacial erosion processes and rates. *Geology*, *38*(5), 423–426. https://doi.org/10.1130/G30576.1

Dunning, J. D., & Huf, W. L. (1983). The effects of aqueous chemical environments on crack and hydraulic fracture propagation and morphologies. *Journal of Geophysical Research: Solid Earth*, *88*(B8), 6491–6499. https://doi.org/10.1029/JB088iB08p06491

Durham, W. B., Bourcier, W. L., & Burton, E. A. (2001). Direct observation of reactive flow in a single fracture. *Water Resources Research*, *37*(1), 1–12. https://doi.org/10.1029/2000WR900228

Eberhardt, E., Stead, D., & Stimpson, B. (1999). Quantifying progressive pre-peak brittle fracture damage in rock during uniaxial compression. *International Journal of Rock Mechanics and Mining Sciences*, *36*, 361–380. https://doi.org/10.1016/S0148-9062(99)00019-4

Egholm, D. L., Pedersen, V. K., Knudsen, M. F., & Larsen, N. K. (2012). Coupling the flow of ice, water, and sediment in a glacial landscape evolution model. *Geomorphology*, *141–142*, 47–66. https://doi.org/10.1016/j.geomorph.2011.12.019

Emery, C. L. (1964). Strain energy in rocks. In W. R. Judd (Ed.), *State of Stress in Earth's Crust* (pp. 234–279). New York: Elsevier.

Engelder, T. (1993). *Stress regimes in the lithosphere*. Princeton: Princeton University Press.

Engelder, T., & Sbar, M. L. (1977). The relationship between in situ strain relaxation and outcrop fractures in the Potsdam Sandstone, Alexandria Bay, New York. *Pure and Applied Geophysics*, *115*(1–2), 41–55. https://doi.org/10.1007/BF01637096

Engelder, T., Sbar, M. L., & Kranz, R. L. (1977). A mechanism for strain relaxation of Barre Granite: opening of microfractures. *Pure and Applied Geophysics*, *115*.

Eppes, M.-C., & Griffing, D. (2010). Granular disintegration of marble in nature: A thermal-mechanical origin for a grus and corestone landscape. *Geomorphology*, *117*(1–2), 170–180. https://doi.org/10.1016/j.geomorph.2009.11.028

Eppes, M.-C., & Keanini, R. (2017). Mechanical weathering and rock erosion by climate-dependent subcritical cracking. *Reviews of Geophysics*, *55*, 470–508. https://doi.org/10.1002/2017RG000557

Eppes, M.-C., Magi, B., Hallet, B., Delmelle, E., Mackenzie-Helnwein, P., Warren, K., & Swami, S. (2016). Deciphering the role of solar-induced thermal stresses in rock weathering. *Geological Society of America Bulletin*. https://doi.org/10.1130/B31422.1

Eyles, N., Arnaud, E., Scheidegger, A. E., & Eyles, C. H. (1997). Bedrock jointing and geomorphology in southwestern Ontario, Canada: an example of tectonic predesign. *Geomorphology*, *19*(1), 17–34. https://doi.org/10.1016/S0169-555X(96)00050-5

Faillettaz, J., Sornette, D., & Funk, M. (2010). Gravity-driven instabilities: Interplay between state and velocity-dependent frictional sliding and stress corrosion damage cracking. *Journal of Geophysical Research*, *115*(3), B03409. https://doi.org/10.1029/2009JB006512

Fakhimi, A., & Tarokh, A. (2013). Process zone and size effect in fracture testing of rock. *International Journal of Rock Mechanics and Mining Sciences*, *60*, 95–102.

https://doi.org/10.1016/j.ijrmms.2012.12.044

Ferdowsi, B., Griffa, M., Guyer, R. A., Johnson, P. A., Marone, C., & Carmeliet, J. (2013). Microslips as precursors of large slip events in the stick-slip dynamics of sheared granular layers: A discrete element model analysis. *Geophysical Research Letters*, *40*(16), 4194–4198. https://doi.org/10.1002/grl.50813

Fischer, C., & Lüttge, A. (2017). Beyond the conventional understanding of water–rock reactivity. *Earth and Planetary Science Letters*, *457*, 100–105. https://doi.org/10.1016/j.epsl.2016.10.019

Fjeldskaar, W., Lindholm, C. D., Dehls, J. F., & Fjeldskaar, I. (2000). Postglacial uplift, neotectonics and seismicity in Fennoscandia. *Quaternary Science Reviews*, *19*(14–15), 1413–1422. https://doi.org/10.1016/S0277-3791(00)00070-6

Forbes Inskip, N. D., Meredith, P. G., Chandler, M. R., & Gudmundsson, A. (2018). Fracture properties of Nash Point shale as a function of orientation to bedding. *Journal of Geophysical Research: Solid Earth*, 1–17. https://doi.org/10.1029/2018JB015943

Fowler, J. (1880). III.— On the process of decay in glass, and, incidentally, on the composition and texture of glass at different periods, and the history of its manufacture. *Archaeologia*, *46*, 65–162. https://doi.org/10.1017/s0261340900006068

Fredrich, J. T., Evans, B., & Wong, T. F. (1989). Micromechanics of the brittle to plastic transition in Carrara marble. *Journal of Geophysical Research*, *94*(B4), 4129–4145.

Friedman, M. (1972). Residual elastic strain in rocks. *Tectonophysics*, *15*(4), 297–330. https://doi.org/10.1016/0040-1951(72)90093-5

Friedman, M., & Logan, J. M. (1970). Influence of residual elastic strain on the orientation of experimental fractures in three quartzose sandstones. *Journal of Geophysical Research*, *75*(2), 387–405. https://doi.org/10.1029/JB075i002p00387

Gallagher, J. J., Friedman, M., Handin, J. W., & Sowers, G. M. (1974). Experimental studies relating to microfracture in sandstone. *Tectonophysics*, *21*(3), 203–247. https://doi.org/10.1016/0040-1951(74)90053-5

Gamboa, E., & Atrens, A. (2005). Material influence on the stress corrosion cracking of rock bolts. *Engineering Failure Analysis*, *12*(2), 201–235. https://doi.org/10.1016/j.engfailanal.2004.07.002

Geisler, T., Nagel, T., Kilburn, M. R., Janssen, A., Icenhower, J. P., Fonseca, R. O. C., et al. (2015). The mechanism of borosilicate glass corrosion revisited. *Geochimica et Cosmochimica Acta*, *158*, 112–129. https://doi.org/10.1016/j.gca.2015.02.039

Geisler, T., Dohmen, L., Lenting, C., & Fritzsche, M. B. K. (2019). Real-time in situ observations of reaction and transport phenomena during silicate glass corrosion by fluid-cell Raman spectroscopy. *Nature Materials*, *18*(4), 342–348. https://doi.org/10.1038/s41563-019-0293-8

Gerber, E., & Scheidegger, A. E. (1969). Stress-induced weathering of rock masses. *Eclogae Geologicae Helvetiae*, *62*(2), 401–415.

Giachetta, E., Refice, A., Capolongo, D., Gasparini, N. M., & Pazzaglia, F. J. (2014). Orogen-scale drainage network evolution and response to erodibility changes: Insights from numerical experiments. *Earth Surface Processes and Landforms*, *39*(9), 1259–1268. https://doi.org/10.1002/esp.3579

Gilbert, G. K. (1877). *Report on the Geology of the Henry Mountains*. Washington, D.C.

Gischig, V. S., Moore, J. R., Evans, K. F., Amann, F., & Loew, S. (2011a). Thermomechanical forcing of deep rock slope deformation: 1. Conceptual study of a simplified slope. *Journal of Geophysical Research: Earth Surface*, *116*(4), 1–18. https://doi.org/10.1029/2011JF002006

Gischig, V. S., Moore, J. R., Evans, K. F., Amann, F., & Loew, S. (2011b). Thermomechanical forcing of deep rock slope deformation: 2. the Randa rock slope instability. *Journal of Geophysical Research: Earth Surface*, *116*(4), 1–17. https://doi.org/10.1029/2011JF002007

Götze, J. (2012). Application of cathodoluminescence microscopy and spectroscopy in geosciences. *Microscopy and Microanalysis*, *18*(6), 1270–1284. https://doi.org/10.1017/S1431927612001122

Goudie, A. S., & Viles, H. A. (2012). Weathering and the global carbon cycle: Geomorphological perspectives. *Earth-Science Reviews*, *113*(1–2), 59–71. https://doi.org/10.1016/j.earscirev.2012.03.005

Gratier, J.-P., Frery, E., Deschamps, P., Røyne, A., Renard, F., Dysthe, D. K., et al. (2012). How travertine veins grow from top to bottom and lift the rocks above them: The effect of crystallization force. *Geology*, *40*(11), 1015–1018. https://doi.org/10.1130/G33286.1

Gregory, K. J., & Lewin, J. (2015). Making concepts more explicit for geomorphology. *Progress in Physical Geography*, *39*(6), 711–727. https://doi.org/10.1177/0309133315571208

Grgic, D., & Giraud, A. (2014). The influence of different fluids on the static fatigue of a porous rock: Poro-mechanical coupling versus chemical effects. *Mechanics of Materials*, *71*, 34–51. https://doi.org/10.1016/j.mechmat.2013.06.011

Griffith, A. A. (1921). The phenomena of rupture and flow in solids. *Philosophical Transactions of the Royal Society of London. Series A, Containing Papers of a Mathematical or Physical Character*, *221*, 163–198.

Griggs, D. T. (1939). Creep of Rocks. *The Journal of Geology*, *47*(3), 225–251.

Gschwind, S., Loew, S., & Wolter, A. (2019). Multi-stage structural and kinematic analysis of a retrogressive rock slope instability complex (Preonzo, Switzerland). *Engineering Geology*, *252*, 27–42. https://doi.org/https://doi.org/10.1016/j.enggeo.2019.02.018

Gudehus, G., & Touplikiotis, A. (2017). On the stability of geotechnical systems and its fractal progressive loss. *Acta Geotechnica*, 1–12. https://doi.org/10.1007/s11440-017-0549-x

Gudmundsson, A. (1999). Postglacial crustal doming, stresses and fracture formation with application to Norway. *Tectonophysics*, *307*(3–4), 407–419. https://doi.org/10.1016/S0040-1951(99)00107-9

Guillemot, A., Helmstetter, A., Larose, É., Baillet, L., Garambois, S., Mayoraz, R., & Delaloye, R. (2020). Seismic monitoring in the Gugla rock glacier (Switzerland): ambient noise correlation, microseismicity and modelling. *Geophysical Journal International*, *221*, 1719–1735. https://doi.org/10.1093/gji/ggaa097

Haefeli, R. (1965). Creep and progressive failure in snow, soil, rock, and ice. In *Sixth Intern. Conf. Soil Mechanics and Found. Eng. Proc.* (Vol. 3, pp. 134–148). Montreal.

Hall, K., & Thorn, C. E. (2014). Thermal fatigue and thermal shock in bedrock: An attempt to unravel the geomorphic processes and products. *Geomorphology*, *206*, 1–13. https://doi.org/10.1016/j.geomorph.2013.09.022

Hall, S. A., Wright, J., Pirling, T., Andò, E., Hughes, D. J., & Viggiani, G. (2011). Can intergranular force transmission be identified in sand? *Granular Matter*, *13*(3), 251–254. https://doi.org/10.1007/s10035-011-0251-x

Handwerger, A. L., Rempel, A. W., Skarbek, R. M., Roering, J. J., & Hilley, G. E. (2016). Rate-weakening friction characterizes both slow sliding and catastrophic failure of landslides. *Proceedings of the National Academy of Sciences*, *113*(37), 10281–10286. https://doi.org/10.1073/pnas.1607009113

Hantke, R., & Scheidegger, A. E. (1999). Tectonic predesign in geomorphology. In S. Hergarten & H. J. Neugebauer (Eds.), *Process Modelling and Landform Evolution* (pp. 253–266). Springer.

Harper, T. R., Appel, G., Pendleton, M. W., Szymanski, J. S., & Taylor, R. K. (1979). Swelling strain development in sedimentary rock in Northern New York. *International Journal of Rock Mechanics and Mining Sciences & Geomechanics Abstracts*, *16*, 271–292. https://doi.org/10.1016/0148-9062(79)90239-0

Hart, M. G. (1986). *Geomorphology, pure and applied*. London: Allen & Unwin Ltd.

Hashin, Z., & Shtrikman, S. (1962). A variational approach to the theory of the elastic behaviour of polycrystals. *Journal of the Mechanics and Physics of Solids*, *10*, 343–352. https://doi.org/10.1016/0022-5096(62)90005-4

Heap, M. J., Baud, P., Meredith, P. G., Vinciguerra, S., Bell, A. F., & Main, I. G. (2008). Time-dependent brittle deformation in Etna basalt. *Eos*, *89*(53), Fall Meet. Suppl., Abstract V23G-2206.

Heap, M. J., Brantut, N., Baud, P., & Meredith, P. G. (2015). Time-dependent compaction band formation in sandstone. *Journal of Geophysical Research: Solid Earth*, *120*, 4808–4830. https://doi.org/10.1002/2015JB012022.

Heim, A. (1885). *Handbuch der Gletscherkunde*. Stuttgart: Engelhorn.

Hill, R. (1963). Elastic properties of reinforced solids: Some theoretical principles. *Journal of the Mechanics and Physics of Solids*, *11*(5), 357–372. https://doi.org/10.1016/0022-5096(63)90036-X

Hockman, A., & Kessler, D. W. (1950). Thermal and moisture expansion studies of some domestic granites. *Journal of Research of the National Bureau of Standards*, *44*, 395–410.

Hodgkinson, J. H., McLoughlin, S., & Cox, M. (2006). The influence of geological fabric and scale on drainage pattern analysis in a catchment of metamorphic terrain: Laceys Creek, southeast Queensland, Australia. *Geomorphology*, *81*(3–4), 394–407. https://doi.org/10.1016/j.geomorph.2006.04.019

Hoek, E., & Martin, C. D. (2014). Fracture initiation and propagation in intact rock – A review. *Journal of Rock Mechanics and Geotechnical Engineering*, *6*(4), 287–300. https://doi.org/http://dx.doi.org/10.1016/j.jrmge.2014.06.001

Holden, T. M., Root, J. H., Holt, R. A., & Hayashi, M. (1995). Neutron-diffraction measurements of stress. *Physica B: Condensed Matter*, *213–214*(C), 793–796. https://doi.org/10.1016/0921-4526(95)00282-E

Holzhausen, G. R. (1989). Origin of sheet structure, 1. Morphology and boundary conditions. *Engineering Geology*, *27*, 225–278.

Holzhausen, G. R., & Johnson, A. M. (1979). The concept of residual stress in rock. *Tectonophysics*, *58*, 237–267.

Homola, A. M., Israelachvili, J. N., Gee, M. L., & McGuiggan, P. M. (1989). Measurements of and relation between the adhesion and friction of two surfraces separated by molecularly thin liquid films. *Journal of Tribology*, *111*, 675–682.

Hoskins, E. R., & Russell, J. E. (1981). The origin of the measured residual strains in crystalline rocks. In N. L. Carter, M. Friedman, J. M. Logan, & D.W. Stearns (Eds.), *Mechanical Behavior of Crustal Rocks: The Handin Volume, 24* (Geophysica, pp. 187–198). Washington, D.C.: American Geophysical Union. https://doi.org/10.1029/GM024p0187

Ilgen, A. G., Mook, W. M., Tigges, A. B., Choens, R. C., Artyushkova, K., & Jungjohann, K. L. (2018). Chemical controls on the propagation rate of fracture in calcite. *Scientific Reports*, *8*(1), 1–13. https://doi.org/10.1038/s41598-018-34355-1

Intrieri, E., Carlà, T., & Gigli, G. (2019). Forecasting the time of failure of landslides at slope-scale: A literature review. *Earth-Science Reviews*, *193*(March), 333–349. https://doi.org/10.1016/j.earscirev.2019.03.019

Itô, H. (1979). Rheology of the crust based on long-term creep tests of rock. *Tectonics*, *52*, 629–641.

Itô, H., & Kumagai, N. (1994). A creep experiment on a large granite beam started in 1980. *International Journal of Rock Mechanics and Mining Sciences & Geomechanics Abstracts*, *31*(4), 359–367. https://doi.org/10.1016/0148-9062(94)90903-2

Iverson, N. R., Cohen, D., Hooyer, T. S., Fischer, U. H., Jackson, M., Moore, P. L., et al. (2003). Effects of basal debris on glacier flow. *Science*, *301*(5629), 81–4. https://doi.org/10.1126/science.1083086

Iverson, R. M. (1985). A constitutive equation for mass-movement behavior. *The Journal of Geology*, *93*(2), 143–160.

Iverson, R. M. (1986a). Unsteady, Nonuniform Landslide Motion: 1. Theoretical Dynamics and the Steady Datum State. *The Journal of Geology*, *94*(1), 1–15.

Iverson, R. M. (1986b). Unsteady, Nonuniform Landslide motion: 2. Linearized Theory and the Kinematics of Transient response. *The Journal of Geology*, *94*(3), 349–364.

Iverson, R. M. (2015). Scaling and design of landslide and debris-flow experiments. *Geomorphology*, *244*, 9–20. https://doi.org/10.1016/j.geomorph.2015.02.033

Jaeger, J. C. (1971). Friction of Rocks and Stability of Rock Slopes. *Géotechnique*. https://doi.org/10.1680/geot.1971.21.2.97

Jaeger, J. C., Cook, N. G. W., & Zimmerman, R. W. (2007). *Fundamentals of Rock mechanics* (4th ed.). Blackwell Publishing Ltd.

Jerolmack, D. J., & Daniels, K. E. (2019). Viewing Earth's surface as a soft-matter landscape. *Nature Reviews Physics*, *1*(12), 716–730. https://doi.org/10.1038/s42254-019-0111-x

Jia, H., Xiang, W., & Krautblatter, M. (2015). Quantifying rock fatigue and decreasing compressive and tensile strength after repeated freeze-thaw cycles. *Permafrost and Periglacial Processes*, *26*, 368–377. https://doi.org/10.1002/ppp.1857

Jordan, G., & Rammensee, W. (1998). Dissolution rates of calcite (1014) obtained by scanning force microscopy: Microtopography-based dissolution kinetics on surfaces with anisotropic step velocities. *Geochimica et Cosmochimica Acta*, *62*(6), 941–947.

Karaca, Z. (2010). Water absorption and dehydration of natural stones versus time. *Construction and Building Materials*, *24*(5), 786–790.

https://doi.org/10.1016/j.conbuildmat.2009.10.029

Kemeny, J. (2005). Time-dependent drift degradation due to the progressive failure of rock bridges along discontinuities. *International Journal of Rock Mechanics and Mining Sciences*, *42*(1), 35–46. https://doi.org/10.1016/j.ijrmms.2004.07.001

Keszthelyi, D., Dysthe, D. K., & Jamtveit, B. (2016). First principles model of carbonate compaction creep. *Journal of Geophysical Research: Solid Earth*, *121*, 3348–3365. https://doi.org/10.1002/2015JB012481

Kieslinger, A. (1958). Restspannung und Entspannung im Gestein. *Geologie Und Bauwesen*, *24*(2), 95–112.

King, A., Johnson, G., Engelberg, D., Ludwig, W., & Marrow, J. (2008a). Observations of intergranular stress corrosion cracking in a grain-mapped polycrystal. *Science*, *321*, 382–385. https://doi.org/10.1126/science.1156211

King, A., Johnson, G., Engelberg, D., Ludwig, W., & Marrow, J. (2008b). Supplement-Observations of intergranular stress corrosion cracking in a grain-mapped polycrystal. *Science*, *321*, 382–385. https://doi.org/10.1126/science.1156211

Kleidon, A. (2010). Life, hierarchy, and the thermodynamic machinery of planet Earth. *Physics of Life Reviews*, *7*(4), 424–460. https://doi.org/10.1016/j.plrev.2010.10.002

Ko, T. Y., & Kemeny, J. (2011). Subcritical crack growth in rocks under shear loading. *Journal of Geophysical Research: Solid Earth*, *116*, B01407. https://doi.org/10.1029/2010JB000846

Ko, T. Y., & Kemeny, J. (2013). Determination of the subcritical crack growth parameters in rocks using the constant stress-rate test. *International Journal of Rock Mechanics and Mining Sciences*, *59*, 166–178. https://doi.org/10.1016/j.ijrmms.2012.11.006

Koch, A., & Siegesmund, S. (2004). The combined effect of moisture and temperature on the anomalous expansion behaviour of marble. *Environmental Geology*, *46*(3–4), 350–363. https://doi.org/10.1007/s00254-004-1037-9

Koons, P. O., Upton, P., & Barker, A. D. (2012). The influence of mechanical properties on the link between tectonic and topographic evolution. *Geomorphology*, *137*(1), 168–180. https://doi.org/10.1016/j.geomorph.2010.11.012

Krabbendam, M., & Glasser, N. F. (2011). Glacial erosion and bedrock properties in NW Scotland: Abrasion and plucking, hardness and joint spacing. *Geomorphology*, *130*(3–4), 374–383. https://doi.org/10.1016/j.geomorph.2011.04.022

Kranz, R. L. (1979). Crack growth and development during creep of Barre granite. *International Journal of Rock Mechanics and Mining Sciences & Geomechanics Abstracts*, *16*(1), 23–35. https://doi.org/10.1016/0148-9062(79)90772-1

Kranz, R. L. (1983). Microcracks in rocks: a review. *Tectonophysics*, *100*, 449–480. https://doi.org/10.1016/0040-1951(83)90198-1

Kranz, R. L., & Scholz, C. H. (1977). Critical dilatant volume of rock at the onset of tertiary creep. *Journal of Geophysical Research*, *82*(30), 4893–4898.

Krautblatter, M., & Moore, J. R. (2014). Rock slope instability and erosion: toward improved process understanding. *Earth Surface Processes and Landforms*, *39*(9), 1273–1278. https://doi.org/10.1002/esp.3578

Krautblatter, M., Funk, D., & Günzel, F. K. (2013). Why permafrost rocks become unstable: A rock-ice-mechanical model in time and space. *Earth Surface Processes and*

Landforms, *38*(8), 876–887. https://doi.org/10.1002/esp.3374

Krautblatter, M., Voigtländer, A., & Weraneck, K. (2018). *StoneMon Echtzeitmonitoring von Rissbildung in Naturstein durch umweltbedingte Spannungszustände* (No. DBU AZ 32483). München.

Küfmann, C. (2013). Solution dynamics at the rock/snow interface during ablation period in subnival karst of the Wetterstein mountains (Northern Calcareous Alps, Germany). *Zeitschrift Für Geomorphologie*. https://doi.org/10.1127/0372-8854/2013/0121

Kunz, M., Chen, K., Tamura, N., & Wenk, H. R. (2009). Evidence for residual elastic strain in deformed natural quartz. *American Mineralogist*, *94*(7), 1059–1062. https://doi.org/10.2138/am.2009.3216

Laanait, N., Callagon, E. B. R., Zhang, Z., Sturchio, N. C., Lee, S. S., & Fenter, P. (2015). X-ray-driven reaction front dynamics at calcite-water interfaces. *Science*, *349*(6254), 1330–1334. https://doi.org/10.1126/science.aab3272

Labuz, J. F., & Berger, D. J. (1990). Moistureffects and the mechanical response of granite beams. In *Rock Mechanics Contributions and Challenges: Proceedings 31st US Symposium, Golden, 18–20 June 1990* (pp. 605–611). American Rock Mechanics Association.

Labuz, J. F., Shah, S. P., & Dowding, C. H. H. (1987). The fracture process zone in granite: evidence and effect. *International Journal of Rock Mechanics and Mining Sciences & Geomechanics Abstracts*, *24*(4), 235–246. https://doi.org/10.1016/0148-9062(87)90178-1

Lajtai, E. Z. (1991). Time-dependent behaviour of the rock mass. *Geotechnical and Geological Engineering*, *9*(2), 109–124. https://doi.org/10.1007/BF00881253

Lardge, J. S., Duffy, D. M., Gillan, M. J., & Watkins, M. (2010). Ab initio simulations of the interaction between water and defects on the calcite (101?? 4) surface. *Journal of Physical Chemistry C*, *114*(6), 2664–2668. https://doi.org/10.1021/jp909593p

Lawn, B. R. (1975). An atomistic model of kinetic crack growth in brittle solids. *Journal of Materials Science*, *10*, 469–480.

Lawn, B. R. (1993). *Fracture of brittle solids* (2nd ed.). Cambridge: Cambridge University Press.

Le, J.-L., Manning, J., & Labuz, J. F. (2014). Scaling of fatigue crack growth in rock. *International Journal of Rock Mechanics and Mining Sciences*, *72*, 71–79. https://doi.org/10.1016/j.ijrmms.2014.08.015

Lee, R. W., & Kirby, S. H. (1984). Experimental deformation of Topaz crystals: possible embrittlement by intracrystalline water. *Journal of Geophysical Research*, *89*(B6), 4161–4166.

Lee, S. Y., Choo, H., Liaw, P. K., An, K., Hubbard, C. R., Choo, H., & Rogge, R. B. (2011). A study on fatigue crack growth behavior subjected to a single tensile overload: Part II. Transfer of stress concentration and its role in overload-induced transient crack growth. *Acta Materialia*, *59*(2), 485–494. https://doi.org/10.1016/j.actamat.2010.09.049

Leiss, B., & Molli, G. (2002). "High-temperature" texture in naturally deformed Carrara marble from the Alpi Apuane, Italy. *Journal of Structural Geology*, *25*, 649–658.

Leith, K., Moore, J. R., Amann, F., & Loew, S. (2014a). In situ stress control on microcrack generation and macroscopic extensional fracture in exhuming bedrock. *Journal of Geophysical Research*, *119*(1), 594–615. https://doi.org/10.1002/2012JB009801

Leith, K., Moore, J. R., Amann, F., & Loew, S. (2014b). Subglacial extensional fracture development and implications for alpine valley evolution. *Journal of Geophysical Research: Earth Surface*, *119*, 62–81. https://doi.org/10.1002/2012JF002691

Leith, K., Fox, M., & Moore, J. R. (2018). Signatures of Late Pleistocene fluvial incision in an Alpine landscape. *Earth and Planetary Science Letters*, *483*, 13–28. https://doi.org/10.1016/j.epsl.2017.11.050

Lengliné, O., Toussaint, R., Schmittbuhl, J., Elkhoury, J. E., Ampuero, J.-P., Tallakstad, K. T., et al. (2011). Average crack-front velocity during subcritical fracture propagation in a heterogeneous medium. *Physical Review E - Statistical, Nonlinear, and Soft Matter Physics*, *84*(3), 1–13. https://doi.org/10.1103/PhysRevE.84.036104

Lengliné, O., Schmittbuhl, J., Elkhoury, J. E., Ampuero, J.-P., Toussaint, R., & Mly, K. J. (2011). Downscaling of fracture energy during brittle creep experiments. *Journal of Geophysical Research: Solid Earth*, *116*(8), 1–14. https://doi.org/10.1029/2010JB008059

Lenting, C., Plümper, O., Kilburn, M., Guagliardo, P., Klinkenberg, M., & Geisler, T. (2018). Towards a unifying mechanistic model for silicate glass corrosion. *Npj Materials Degradation*, *2*(1). https://doi.org/10.1038/s41529-018-0048-z

Levenson, Y., & Emmanuel, S. (2013). Pore-scale heterogeneous reaction rates on a dissolving limestone surface. *Geochimica et Cosmochimica Acta*, *119*, 188–197. https://doi.org/10.1016/j.gca.2013.05.024

Liang, Y., & Baer, D. R. (1997). Anisotropic dissolution at the CaCO3(1014) - water interface. *Surface Science*, *373*, 275–287. https://doi.org/10.1016/S0039-6028(96)01155-7

Lockner, D. A. (1993). Room temperature creep in saturated granite. *Journal of Geophysical Research*, *98*(B1), 475–487. https://doi.org/10.1029/92JB01828

Loew, S., Gschwind, S., Keller-Signer, A., & Valenti, G. (2016). Monitoring and early warning of the 2012 Preonzo catastrophic rockslope failure. *Landslides*, *17*, 12289. https://doi.org/10.1007/s10346-016-0701-y

Logan, J. M. (2004). Laboratory and case studies of thermal cycling and stored strain on the stability of selected marbles. *Environmental Geology*, *46*(3–4), 456–467. https://doi.org/10.1007/s00254-004-1047-7

Lüttge, A., Arvidson, R. S., & Fischer, C. (2013). Fundamental controls of dissolution rate spectra: comparisons of model and experimental results. *Procedia Earth and Planetary Science*, *7*, 537–540. https://doi.org/10.1016/j.proeps.2013.03.115

Luzin, V., Dmitry, N., & Siegesmund, S. (2014). Temperature induced internal stress in Carrara marble. *Materials Science Forum*, *777*, 148–154.

Lyell, C. (1832). *Principles of Geology. Being an attempt to explain the former changes of the earth's surface, by reference to causes now in operation.* (Volume I). London: John Murray, Albemarle-Street.

Machel, H.-G. (1985). Cathodoluminescence in calcite and dolomite and its chemical interpretation. *Geoscience Canada*, *12*(4), 139–147.

Maher, K., & Chamberlain, C. P. (2014). Hydrologic regulation of chemical weathering and the geologic carbon cycle. *Science*, *343*(6178), 1502–4. https://doi.org/10.1126/science.1250770

Maher, K., & Navarre-Sitchler, A. (2019). Reactive Transport Processes that Drive Chemical

Weathering: From Making Space for Water to Dismantling Continents. *Reviews in Mineralogy and Geochemistry*, *85*(1), 349–380. https://doi.org/10.2138/rmg.2018.85.12

Mainsant, G., Larose, E., Brönnimann, C., Jongmans, D., Michoud, C., & Jaboyedoff, M. (2012). Ambient seismic noise monitoring of a clay landslide: Toward failure prediction. *Journal of Geophysical Research*, *117*(1), 1–12. https://doi.org/10.1029/2011JF002159

Mainsant, G., Larose, E., Brnnimann, C., Jongmans, D., Michoud, C., & Jaboyedoff, M. (2012). Ambient seismic noise monitoring of a clay landslide: Toward failure prediction. *Journal of Geophysical Research: Earth Surface*, *117*(1), 1–12. https://doi.org/10.1029/2011JF002159

Malkin, A. I. I. (2012). Regularities and mechanisms of the Rehbinder's effect. *Colloid Journal*, *74*(2), 239–256. https://doi.org/10.1134/S1061933X12020068

Masteller, C. C., & Finnegan, N. J. (2017). Interplay between grain protrusion and sediment entrainment in an experimental flume. *Journal of Geophysical Research: Earth Surface*, *122*(1), 274–289. https://doi.org/10.1002/2016JF003943

Mattheck, C., & Burkhardt, S. (1990). A new method of structural shape optimization based on biological growth. *International Journal of Fatigue*, *12*(3), 185–190. https://doi.org/http://dx.doi.org/10.1016/0142-1123(90)90094-U

Maugis, D. (1985). Review Subcritical crack growth, surface energy, fracture toughness, stick-slip and embrittlement. *Journal of Materials Science*, *20*(9), 3041–3073. https://doi.org/10.1007/BF00545170

McGarr, A., & Gay, N. C. (1978). State of stress in the Earth's crust. *Annual Review of Earth and Planetary Sciences*, *6*, 405–436.

Mellor, M. (1973). Mechanical properties of rocks at low temperatures. In *2nd International Conference on Permafrost, Yakutsk* (pp. 334–344). Potsdam: International Permafrost Association.

Meredith, P. G., & Atkinson, B. K. (1983). Stress corrosion and acoustic emission during tensile crack propagation in Whin Sill dolerite and other basic rocks. *Geophysical Journal of the Royal Astronomical Society*, *75*, 1–21. https://doi.org/10.1111/j.1365-246X.1983.tb01911.x

Meredith, P. G., Knight, K. S., Boon, S. A., & Wood, I. G. (2001). The microscopic origin of thermal cracking in rocks: An investigation by simultaneous time-of-flight neutron diffraction and acoustic emission monitoring. *Geophysical Research Letters*, *28*(10), 2105–2108. https://doi.org/10.1029/2000GL012470

Michalske, T. A., & Freiman, S. W. (1982). A molecular interpretation of stress corrosion in silica. *Nature*, *295*(5849), 511–512. https://doi.org/10.1038/295511a0

Miller, D. J., & Dunne, T. (1996). Topographic perturbations of regional stresses and consequent bedrock fracturing. *Journal of Geophysical Research*, *101*(B11), 25523. https://doi.org/10.1029/96JB02531

Molli, G., & Heilbronner, R. (1999). Microstructures associated with static and dynamic recrystallization of Carrara marble (Alpi Apuane, NW Tuscany, Italy). *Geologie En Mijnbouw*, *78*, 119–126.

Molli, G., Vitale Brovarone, A., Beyssac, O., & Cinquini, I. (2018). RSCM thermometry in the Alpi Apuane (NW Tuscany, Italy): New constraints for the metamorphic and tectonic history of the inner northern Apennines. *Journal of Structural Geology*, *113*, 200–216. https://doi.org/10.1016/j.jsg.2018.05.020

Molnar, P. (2004). Interactions among topographically induced elastic stress, static fatigue, and valley incision. *Journal of Geophysical Research: Earth Surface*, *109*(F2), n/a-n/a. https://doi.org/10.1029/2003JF000097

Moon, S., Perron, J. T., Martel, S. J., Holbrook, W. S., & St.Clair, J. (2017). A model of three-dimensional topographic stresses with implications for bedrock fractures, surface processes, and landscape evolution. *Journal of Geophysical Research: Earth Surface*, *122*(4), 823–846. https://doi.org/10.1002/2016JF004155

Müller, L. (1963). Application of rock mechanics in the design of rock slopes. In William R Judd (Ed.), *State of Stress in Earth's Crust* (pp. 575–605). Santa Monica, California: Elsevier.

Müller, L. (1964). The stability of rock bank slopes and the effect of rock water on same. *International Journal of Rock Mechanics and Mining Sciences*, *1*(d), 475–504.

Müller, L. (1969). Geomechanische Auswirkungen yon Abtragungsvorgängen. *Geologische Rundschau*, *59*(1), 163–178.

Nara, Y., Yoneda, T., & Kaneko, K. (2010). Influence of temperature and water on subcritical crack growth in sandstone. *Engineering Geology*, *179*, 41–49. https://doi.org/10.1016/j.enggeo.2014.06.018

Nara, Y., Morimoto, K., Yoneda, T., Hiroyoshi, N., & Kaneko, K. (2011). Effects of humidity and temperature on subcritical crack growth in sandstone. *International Journal of Solids and Structures*, *48*(7–8), 1130–1140. https://doi.org/10.1016/j.ijsolstr.2010.12.019

Nara, Y., Kashiwaya, K., Nishida, Y., & Ii, T. (2017). Influence of surrounding environment on subcritical crack growth in marble. *Tectonophysics*, *706–707*, 116–128. https://doi.org/10.1016/j.tecto.2017.04.008

Newman, R. C. (2002). Stress-corrosion cracking mechanisms. In P. Marcus & J. Oudar (Eds.), *Corrosion Mechanisms in Theory and Practice* (pp. 399–450). New York, Basel: Marcel Dekker, Inc. https://doi.org/10.1201/b11020-12

Nichols, T. C. jr. (1975). Deformations associated with relaxation of residual stresses in a sample of Barre Granite from Vermont. *Geological Survey Professional Paper*, *875*.

Nichols, T. C. jr. (1980). Rebound, its nature and effect on engineering works. *Quarterly Journal of Engineering Geology and Hydrogeology*, *13*, 133–152.

Nichols, T. C. jr, & Abel, J. F. (1975). Mobilized residual energy — A factor in rock deformation. *Bulletin of the Association of Engineering Geologists*, *12*(3), 213–225.

Nichols, T. C. jr, & Savage, W. Z. (1976). Rock strain recovery—factor in foundation design. In *Rock Engineering for Foundations and Slopes* (Vol. 1, pp. 34–54). Boulder, Colorado, August 15-18, 1976: American Society of Civil Engineers Specialty Conference Proceedings.

Nicolas, A., Fortin, J., Regnet, J. B., Dimanov, A., & Gúeguen, Y. (2016). Brittle and semi-brittle behaviours of a carbonate rock: Influence of water and temperature. *Geophysical Journal International*, *206*(1), 438–456. https://doi.org/10.1093/gji/ggw154

Nicolas, Adolphe. (1986). *Principles of rock deformation*. Dordrecht, Holland: Reidel Publishing Company.

Noyan, I. C., & Cohen, J. B. (1987). *Residual stresses. Measurement by diffraction and interpretation*. New York, Berlin, Heidelberg, London, Paris, Tokyo: Springer.

Obermann, A., Froment, B., Campillo, M., Larose, E., Planès, T., Valette, B., et al. (2014).

Seismic noise correlations to image structural and mechanical changes associated with the Mw 7.9 2008 Wenchuan earthquake. *Journal of Geophysical Research*, *119*, 3155–3168. https://doi.org/10.1002/2013JB010932

Oesterling, N., Heilbronner, R., Stünitz, H., Barnhoorn, A., & Molli, G. (2007). Strain dependent variation of microstructure and texture in naturally deformed Carrara marble. *Journal of Structural Geology*, *29*(4), 681–696. https://doi.org/10.1016/j.jsg.2006.10.007

Orowan, E. (1944). The fatigue of glass under stress. *Nature*, *154*(3906), 341–43. https://doi.org/10.1038/154341a0

Ozcelik, Y., & Ozguven, A. (2014). Water absorption and drying features of different natural building stones. *Construction and Building Materials*, *63*, 257–270. https://doi.org/10.1016/j.conbuildmat.2014.04.030

Paraskevopoulou, C., Perras, M. A., Diederichs, M. S., Amann, F., Löw, S., Lam, T., & Jensen, M. (2015). Observations for the long-term behaviour of rocks based on laboratory testing. *Engineering Geology*, *216*, 3–8. https://doi.org/10.1016/j.enggeo.2016.11.010

Passchier, C. W., & Trouw, R. A. J. (2005). *Microtectonics* (2nd ed.). Berlin, Heidelberg: Springer.

Peck, L. (1983). Stress corrosion and crack propagation in Sioux quarzite. *Journal of Geophysical Research*, *88*(B6), 5037–5046.

Pedrosa, E. T., Boeck, L., Putnis, C. V., & Putnis, A. (2017). The replacement of a carbonate rock by fluorite: Kinetics and microstructure. *American Mineralogist*, *102*(1), 126–134. https://doi.org/10.2138/am-2017-5725

Pelletier, J. D., & Jerolmack, D. J. (2014). Multiscale bed form interactions and their implications for the abruptness and stability of the downwind dune field margin at White Sands, New Mexico, USA. *Journal of Geophysical Research: Earth Surface*, *119*(11), 2396–2411. https://doi.org/10.1002/2014JF003210

Penck, A. (1905). Glacial features in the surface of the Alps. *The Journal of Geology*, *13*(1), 1–19.

Petley, D. N., Higuchi, T., Petley, D. J., Bulmer, M. H., & Carey, J. (2005). Development of progressive landslide failure in cohesive materials. *Geology*, *33*(3), 201–204. https://doi.org/10.1130/G21147.1

Phillips, J. D. (2003). Sources of nonlinearity and complexity in geomorphic systems. *Progress in Physical Geography*, *27*(1), 1–23. https://doi.org/10.1191/0309133303pp340ra

Phillips, J. D. (2017). Laws, place, history and the interpretation of landforms. *Earth Surface Processes and Landforms*, *42*(2), 347–354. https://doi.org/10.1002/esp.4083

Pintschovius, L. (1992). Macrostresses, microstresses and stress tensors. In M. T. Hutchings & A. D. Krawitz (Eds.), *Measurement of residual and applied stress using neutron diffraction* (NATO ASI S, pp. 115–130). Dordrecht: Kluwer Academic Publishers.

Pirling, T., Bruno, G., & Withers, P. J. (2006). SALSA-A new instrument for strain imaging in engineering materials and components. *Materials Science and Engineering*, *437*(1), 139–144. https://doi.org/10.1016/j.msea.2006.04.083

Platt, J. P., & De Bresser, J. H. P. (2017). Stress dependence of microstructures in experimentally deformed calcite. *Journal of Structural Geology*, *105*(June), 80–87. https://doi.org/10.1016/j.jsg.2017.10.012

Pollet-Villard, M., Daval, D., Ackerer, P., Saldi, G. D., Wild, B., Knauss, K. G., & Fritz, B. (2016). Does crystallographic anisotropy prevent the conventional treatment of aqueous mineral reactivity? A case study based on K-feldspar dissolution kinetics. *Geochimica et Cosmochimica Acta*, *190*, 294–308. https://doi.org/10.1016/j.gca.2016.07.007

Potyondy, D. O. (2007). Simulating stress corrosion with a bonded-particle model for rock. *International Journal of Rock Mechanics and Mining Sciences*, *44*(5), 677–691. https://doi.org/10.1016/j.ijrmms.2006.10.002

Prasicek, G., Larsen, I. J., & Montgomery, D. R. (2015). Tectonic control on the persistence of glacially sculpted topography. *Nature Communications*, *6*(8028). https://doi.org/10.1038/ncomms9028

Preisig, G., Eberhardt, E., Smithyman, M., Preh, A., & Bonzanigo, L. (2016). Hydromechanical rock mass fatigue in deep-seated landslides accompanying seasonal variations in pore pressures. *Rock Mechanics and Rock Engineering*, *49*(6), 2333–2351. https://doi.org/10.1007/s00603-016-0912-5

Putnis, A. (2014). Why mineral interfaces matter. *Science*, *343*, 1441–1442. https://doi.org/10.1126/science.1250884

Ramsay, J. G. (1967). *Folding and fracturing of rock*. New York, San Francisco, London: McGraw-Hill Inc.

Rao, K. V. K., Naidu, S. V. N., & Murthy, K. S. (1968). Precision lattice parameters and thermal expansion of calcite. *Journal of Physics and Chemistry of Solids*, *29*, 245–248.

Rayleigh, Lord. (1934). The bending of marble. *Proceedings of the Royal Society of London. Series A*, *144*, 266–279.

Rehbinder, P. A., & Shchukin, E. D. (1972). Surface phenomena in solids during deformation and fracture processes. *Progress in Surface Science*, *3*(2), 97–188.

Reid, M. E., & Iverson, R. M. (1992). Gravity-Driven Groundwater Flow and Slope Failure Potential. *Water Resources Research*, *28*(3), 939–950.

Renard, F., Røyne, A., & Putnis, C. V. (2019). Timescales of interface-coupled dissolution-precipitation reactions on carbonates. *Geoscience Frontiers*, *10*(1), 17–27. https://doi.org/10.1016/j.gsf.2018.02.013

Resende, L., & Martin, J. B. (1984). A progressive damage “continuum” model for granular materials. *Computer Methods in Applied Mechanics and Engineering*, *42*, 1–18.

Richard, D., Ferrand, M., & Kearley, G. J. (1996). Analysis and visualisation of neutron-scattering data. *Journal of Neutron Research*, *4*, 33–39. https://doi.org/10.1080/10238169608200065

Richardson, L., & Adams St. Pierre, E. (2018). Writing, a method of inquiry. In N. K. Denzin & Y. S. Lincoln (Eds.), *The Sage handbook of qualitative research* (5th ed., pp. 818–838). Thousand Oaks, CA, USA: Sage.

Řihošek, J., Bruthans, J., Masin, D., Filippi, M., Carling, G. T., & Schweigstillová, J. (2016). Gravity-induced stress as a factor reducing decay of sandstone monuments in Petra, Jordan. *Journal of Cultural Heritage*, *19*(9), 415–425. https://doi.org/10.1016/j.culher.2015.10.004

Risnes, R., Madland, M. V, Hole, M., & Kwabiah, N. K. (2005). Water weakening of chalk - mechanical effects of water-glycol mixtures. *Journal of Petroleum Science and Engineering*, *48*(1–2), 21–36. https://doi.org/http://dx.doi.org/10.1016/j.petrol.2005.04.004

Ritchie, R. O. (2011). The conflicts between strength and toughness. *Nature Materials*, *10*(11), 817–822. https://doi.org/10.1038/nmat3115

Rostom, F., Røyne, A., Dysthe, D. K., & Renard, F. (2013). Effect of fluid salinity on subcritical crack propagation in calcite. *Tectonophysics*, *583*, 66–75. https://doi.org/10.1016/j.tecto.2012.10.023

Rouyet, L., Kristensen, L., Derron, M. H., Michoud, C., Blikra, L. H., Jaboyedoff, M., & Lauknes, T. R. (2017). Evidence of rock slope breathing using ground-based InSAR. *Geomorphology*, *289*, 152–169. https://doi.org/10.1016/j.geomorph.2016.07.005

Roy, S. G., Koons, P. O., Upton, P., & Tucker, G. E. (2016). Dynamic links among rock damage, erosion, and strain during orogenesis. *Geology*, *44*(7), 583–586. https://doi.org/10.1130/G37753.1

Røyne, A., Jamtveit, B., Mathiesen, J., & Malthe-Sørenssen, A. (2008). Controls on rock weathering rates by reaction-induced hierarchical fracturing. *Earth and Planetary Science Letters*, *275*(3–4), 364–369. https://doi.org/10.1016/j.epsl.2008.08.035

Røyne, A., Meakin, P., Malthe-Sørenssen, A., Jamtveit, B., & Dysthe, D. K. (2011). Crack propagation driven by crystal growth. *Europhysics Letters*, *96*(2), 24003. https://doi.org/10.1209/0295-5075/96/24003

Røyne, A., Bisschop, J., & Dysthe, D. K. (2011). Experimental investigation of surface energy and subcritical crack growth in calcite. *Journal of Geophysical Research*, *116*(B4), 1–10. https://doi.org/10.1029/2010JB008033

Røyne, A., Dalby, K. N., & Hassenkam, T. (2015). Repulsive hydration forces between calcite surfaces and their effect on the brittle strength of calcite-bearing rocks. *Geophysical Research Letters*, *42*(12), 4786–4794. https://doi.org/10.1002/2015GL064365

Ruedrich, J., Bartelsen, T., Dohrmann, R., & Siegesmund, S. (2011). Moisture expansion as a deterioration factor for sandstone used in buildings. *Environmental Earth Sciences*, *63*(7), 1545–1564. https://doi.org/10.1007/s12665-010-0767-0

Ruiz-Agudo, E., & Putnis, C. V. (2012). Direct observations of mineral fluid reactions using atomic force microscopy: the specific example of calcite. *Mineralogical Magazine*, *76*(1), 227–253. https://doi.org/10.1180/minmag.2012.076.1.227

Ruiz-Agudo, E., King, H. E., Patiño-López, L. D., Putnis, C. V., Geisler, T., Rodriguez-Navarro, C., & Putnis, A. (2016). Control of silicate weathering by interface-coupled dissolution-precipitation processes at the mineral-solution interface. *Geology*, *44*(7), 567–570. https://doi.org/10.1130/G37856.1

Rutter, E. H. (1972). The influence of interstitial water on the rheological behaviour of calcite rocks. *Tectonophysics*, *14*(1), 13–33. https://doi.org/10.1016/0040-1951(72)90003-0

Rutter, E. H. (1974). The influence of temperature, strain rate and interstitial water in the experimental deformation of calcite rocks. *Tectonophysics*, *22*(3–4), 311–334. https://doi.org/10.1016/0040-1951(74)90089-4

Sadananda, K., Solanki, K. N., & Vasudevan, A. K. (2017). Subcritical crack growth and crack tip driving forces in relation to material resistance. *Corrosion Reviews*, *35*(4–5), 251–265. https://doi.org/10.1515/corrrev-2017-0034

Sadler, P. M., & Jerolmack, D. J. (2015). Scaling laws for aggradation, denudation and progradation rates: the case for time-scale invariance at sediment sources and sinks. *Geological Society, London, Special Publications*, *404*(1), 69–88.

https://doi.org/10.1144/SP404.7

Samsu, A., Cruden, A. R., Micklethwaite, S., Grose, L., & Vollgger, S. A. (2020). Scale matters: The influence of structural inheritance on fracture patterns. *Journal of Structural Geology*, *130*(October 2019), 103896. https://doi.org/10.1016/j.jsg.2019.103896

Santhanam, A. T., & Gupta, Y. P. (1968). Cleavage surface energy of calcite. *International Journal of Rock Mechanics and Mining Sciences & Geomechanics Abstracts*, *5*(3), 253–259. Retrieved from http://www.sciencedirect.com/science/article/B6V4V-482GH4M-9H/2/880c7ddb38124a39e83f0609692d597d

Savage, W. Z. (1978). The development of residual stress in cooling rock bodies. *Geophysical Research Letters*, *5*(8), 633–636. https://doi.org/10.1029/GL005i008p00633

Savage, W. Z., & Swolfs, H. S. (1986). Tectonic and gravitational stress in long symmetric ridges and valleys. *Journal of Geophysical Research*, *91*(B3), 3677–3685. https://doi.org/10.1029/JB091iB03p03677

Scheffzük, C., Siegesmund, S., & Koch, A. (2004). Strain investigations on calcite marbles using neutron time-of-flight diffraction. *Environmental Geology*, *46*(3–4), 468–476. https://doi.org/10.1007/s00254-004-1048-6

Scheffzük, C., Siegesmund, S., Nikolayev, D. I., & Hoffmann, A. (2007). Texture, spatial and orientation dependence of internal strains in marble: a key to understanding the bowing of marble panels? In R. Prikryl & B. J. Smith (Eds.), *Building Stone Decay: From Diagnosis to Conservation* (Geological, Vol. 271, pp. 237–249). London: Geological Society, London,. https://doi.org/10.1144/GSL.SP.2007.271.01.23

Scheidegger, A. E. (1979). The principle of antagonism in the earth's evolution. *Tectonophysics*, *55*(3–4), T7–T10. https://doi.org/10.1016/0040-1951(79)90177-X

Scheidegger, A. E. (1984). A review of recent work on mass movements on slopes and on rock falls. *Earth-Science Reviews*, *21*(4), 225–249. https://doi.org/10.1016/0012-8252(84)90054-0

Scheidegger, A. E. (1998). Tectonic predesign of mass movements, with examples from the Chinese Himalaya. *Geomorphology*, *26*(1–3), 37–46. https://doi.org/10.1016/S0169-555X(98)00050-6

Scheidegger, A. E. (2004). *Morphotectonics*. Berlin, Heidelberg, New York: Springer.

Scheidegger, A. E., & Ai, N. S. (1986). Tectonic processes and geomorphological design. *Tectonophysics*, *126*(2–4), 285–300. https://doi.org/10.1016/0040-1951(86)90234-9

Schmidt, K. M., & Montgomery, D. R. (1995). Limits to relief. *Science*, *270*, 617–620. https://doi.org/10.1126/science.270.5236.617

Schofield, P. F., Covey-Crump, S. J., Stretton, I. C., Daymond, M. R., Knight, K. S., & Holloway, R. F. (2003). Using neutron diffraction measurements to characterize the mechanical properties of polymineralic rocks. *Mineralogical Magazine*, *67*(5), 967–987. https://doi.org/10.1180/0026461036750138

Schofield, P. F., Covey-Crump, S. J., Daymond, M. R., Stretton, I. C., Knight, K. S., & Holloway, R. F. (2006). Methodology and recent developments for using neutron diffraction to characterize the mechanical properties of rocks. *Physica B: Condensed Matter*, *385–386*, 938–941. https://doi.org/10.1016/j.physb.2006.05.277

Schott, J., Brantley, S. L., Crerar, D. A., Guy, C., Borcsik, M., & Willaime, C. (1989). Dissolution kinetics of strained calcite. *Geochimica et Cosmochimica Acta*, *53*(2), 373–382. https://doi.org/10.1016/0016-7037(89)90389-X

Schubnel, A., Walker, E., Thompson, B. D., Fortin, J., Guéguen, Y., & Young, R. P. (2006). Transient creep, aseismic damage and slow failure in Carrara marble deformed across the brittle-ductile transition. *Geophysical Research Letters*, *33*(17), 1–6. https://doi.org/10.1029/2006GL026619

Schumm, S. A. (1979). Geomorphic thresholds: the concept and its applications. *Transactions of the Institute of British Geographers*, *4*(4), 485–515.

Scott, D. N., & Wohl, E. E. (2018). Bedrock Fracture Influences on Geomorphic Process and Form Across Process Domains and Scales. *Earth Surface Processes and Landforms*. https://doi.org/10.1002/esp.4473

Sekine, K., & Hayashi, K. (2009). Residual stress measurements on a quartz vein: A constraint on paleostress magnitude. *Journal of Geophysical Research: Solid Earth*, *114*(1), 1–16. https://doi.org/10.1029/2007JB005295

Shobe, C. M., Hancock, G. S., Eppes, M.-C., & Small, E. E. (2017). Field evidence for the influence of weathering on rock erodibility and channel form in bedrock rivers. *Earth Surface Processes and Landforms*, *42*, 1997–2012. https://doi.org/10.1002/esp.4163

Shushakova, V., Fuller, E. R., & Siegesmund, S. (2013). Microcracking in calcite and dolomite marble: Microstructural influences and effects on properties. *Environmental Earth Sciences*, *69*(4), 1263–1279. https://doi.org/10.1007/s12665-012-1995-2

Siegesmund, S., Weiss, T., & Tschegg, E. K. (2000). Control of marble weathering by thermal expansion and rock fabrics. In *Proceedings of the 9th International Congress on deterioration and conservation of stone, Venice June 19-24, 2000* (pp. 205–213).

Siegesmund, S., Ruedrich, J., & Koch, A. (2008). Marble bowing: Comparative studies of three different public building facades. *Environmental Geology*, *56*(3–4), 473–494. https://doi.org/10.1007/s00254-008-1307-z

Siegesmund, S., Mosch, S., Scheffzük, C., & Nikolayev, D. I. (2008). The bowing potential of granitic rocks: Rock fabrics, thermal properties and residual strain. *Environmental Geology*, *55*(7), 1437–1448. https://doi.org/10.1007/s00254-007-1094-y

Silberberg, A., & Hennenberg, M. (1984). Relaxation of stored mechanical stress along chemical reaction pathways. *Nature*, *312*, 746–748.

Sjöberg, E. L., & Rickard, D. T. (1984). Temperature dependence of calcite dissolution kinetics between 1 and 62°C at pH 2.7 to 8.4 in aqueous solutions. *Geochimica et Cosmochimica Acta*, *48*(3), 485–493. https://doi.org/10.1016/0016-7037(84)90276-X

Sklar, L. S., Riebe, C. S., Marshall, J. A., Genetti, J., Leclere, S., Lukens, C. L., & Merces, V. (2017). The problem of predicting the size distribution of sediment supplied by hillslopes to rivers. *Geomorphology*, *277*, 31–49. https://doi.org/10.1016/j.geomorph.2016.05.005

Slim, M., Perron, J. T., Martel, S. J., & Singha, K. (2015). Topographic stress and rock fracture: A two-dimensional numerical model for arbitrary topography and preliminary comparison with borehole observations. *Earth Surface Processes and Landforms*, *40*(4), 512–529. https://doi.org/10.1002/esp.3646

Smith, B. J., Whalley, W. B., & Warke, P. A. (1999). Uplift, erosion and stability: perspectives on long-term landscape development. *Geological Society Special Publications*, *162*, 284. https://doi.org/10.1177/030913330002400321

Snieder, R., & Larose, E. (2013). Extracting Earth's Elastic Wave Response from Noise Measurements. *Annual Review of Earth and Planetary Sciences*, *41*(1), 183–206. https://doi.org/10.1146/annurev-earth-050212-123936

Sorace, S. (1996). Long-term tensile and bending strength of natural building stones. *Materials and Structures*, *29*(7), 426–435. https://doi.org/10.1007/BF02485993

St.Clair, J., Moon, S., Holbrook, W. S., Perron, J. T., Riebe, C. S., Martel, S. J., et al. (2015). Geophysical imaging reveals topographic stress control of bedrock weathering. *Science*, *350*(6260), 534–538. https://doi.org/10.1126/science.aab2210

Stead, D., & Wolter, A. (2015). A critical review of rock slope failure mechanisms: The importance of structural geology. *Journal of Structural Geology*, *74*, 1–23. https://doi.org/10.1016/j.jsg.2015.02.002

Stipp, S. L. (1999). Toward a conceptual model of the calcite surface: Hydration, hydrolysis, and surface potential. *Geochimica et Cosmochimica Acta*, *63*(19–20), 3121–3131. https://doi.org/10.1016/S0016-7037(99)00239-2

Stipp, S. L., & Hochella, M. F. (1991). Structure and bonding environments at the calcite surface as observed with X-ray photoelectron spectroscopy (XPS) and low energy electron diffraction (LEED). *Geochimica et Cosmochimica Acta*, *55*(6), 1723–1736. https://doi.org/10.1016/0016-7037(91)90142-R

Stipp, S. L., Eggleston, C. M., & Nielsen, B. S. (1994). Calcite surface structure observed at microtopographic and molecular scales with atomic force microscopy (AFM). *Geochimica et Cosmochimica Acta*, *58*(14), 3023–3033. https://doi.org/10.1016/0016-7037(94)90176-7

Strahler, A. N. (1952). Dynamic basis of geomorphology. *Bulletin of the Geological Society of America*, *63*, 923–938.

Sturgul, J. R. (1967). A complex variable technique to study notch-effects in geodynamics. *Pure and Applied Geophysics*, *68*(3), 66–82.

Sturgul, J. R., & Scheidegger, A. E. (1967). Some applications of elastic notch theory to problems of geodynamics. *Pure and Applied Geophysics*, *68*(3), 49–65.

Swanson, P. L. (1984). Subcritical crack growth and other time- and environment-dependent behavior in crustal rocks. *Journal of Geophysical Research*, *89*(B6), 4137–4152. https://doi.org/Doi 10.1029/Jb089ib06p04137

Terzaghi, K. (1943). *Theoretical soil mechanics*. London: Chapman and Hall.

Terzaghi, K. (1962). Stability of steep slopes on hard unweathered rock. *Géotechnique*, *12*(4), 251–270.

Timoshenko, S. P., & Goodier, J. N. (1970). *Theory of Elasticity* (3rd ed.). New York: McGraw-Hill Inc.

Toffolo, M. B., Ricci, G., Caneve, L., & Kaplan-Ashiri, I. (2019). Luminescence reveals variations in local structural order of calcium carbonate polymorphs formed by different mechanisms. *Scientific Reports*, *9*(1), 1–15. https://doi.org/10.1038/s41598-019-52587-7

Toribio, J. (1998). Residual stress effects in stress corrosion cracking. *Journal of Materials Engineering and Performance*. https://doi.org/10.1361/105994998770347891

Toribio, J., Kharin, V., Vergara, D., Blanco, J. A., & Ballesteros, J. G. (2007). Influence of residual stresses and strains generated by cold drawing on hydrogen embrittlement of prestressing steels. *Corrosion Science*, *49*(9), 3557–3569. https://doi.org/10.1016/j.corsci.2007.03.027

Traskin, V. Y. (2009). Rehbinder effect in tectonophysics. *Izvestiya, Physics of the Solid Earth*, *45*(11), 22–33. https://doi.org/10.1134/S1069351309110032

Ungár, T. (1998). Strain broadening caused by dislocations. *Materials Science Forum*, *278–281*, 151–157. https://doi.org/https://doi.org/10.4028/www.scientific.net/MSF.278-281.151

Upton, P., Koons, P. O., & Roy, S. G. (2018). Rock failure and erosion of a fault damage zone as a function of rock properties: Alpine Fault at Waikukupa River. *New Zealand Journal of Geology and Geophysics*, *61*(3), 367–375. https://doi.org/10.1080/00288306.2018.1430592

Vajdova, V., Baud, P., Wu, L., & Wong, T. fong. (2012). Micromechanics of inelastic compaction in two allochemical limestones. *Journal of Structural Geology*, *43*, 100–117. https://doi.org/10.1016/j.jsg.2012.07.006

Varnes, D. J., & Lee, F. T. (1972). Hypothesis of mobilization of residual stress in rock. *Geological Society Of America Bulletin*, *83*(September), 2863–2866.

Velbel, M. A. (1993). Constancy of silicate-mineral weathering-rate ratios between natural and experimental weathering: implications for hydrologic control of differences in absolute rates. *Chemical Geology*, *105*(1–3), 89–99. https://doi.org/10.1016/0009-2541(93)90120-8

Ventura, G., Vinciguerra, S., Moretti, S., Meredith, P. G., Heap, M. J., Baud, P., et al. (2010). Understanding slow deformation before dynamic failure. In T. Beer (Ed.), *Geophysical Hazards* (pp. 229–247). Dordrecht, Holland: Springer. https://doi.org/10.1007/978-90-481-3236-2

Viles, H. A. (2005). Can stone decay be chaotic? In A. V. Turkington (Ed.), *Stone decay in the architectural environment* (Geological, pp. 11–16).

Viles, H. A. (2013). Linking weathering and rock slope instability: Non-linear perspectives. *Earth Surface Processes and Landforms*, *38*(1), 62–70. https://doi.org/10.1002/esp.3294

Vincent-Dospital, T., Toussaint, R., Santucci, S., Vanel, L., Bonamy, D., Hattali, L., et al. (2020). To creep or to snap ? How induced heat governs the brittleness of matter. In *EGU General Assembly 2020, Online, 4–8 May 2020* (pp. EGU2020-19084). EGU General Assembly.

Violay, M., Nielsen, S., Spagnuolo, E., Cinti, D., Di Toro, G., & Di Stefano, G. (2013). Pore fluid in experimental calcite-bearing faults: abrupt weakening and geochemical signature of co-seismic processes. *Earth and Planetary Science Letters*, *361*, 74–84. https://doi.org/10.1016/j.epsl.2012.11.021

Violay, M., Nielsen, S., Gibert, B., Spagnuolo, E., Cavallo, A., Azais, P., et al. (2014). Effect of water on the frictional behavior of cohesive rocks during earthquakes. *Geology*, *42*(1), 27–30. https://doi.org/10.1130/G34916.1

Voight, B. (1966a). Correlation of large horizontal stresses in rock masses with tectonics and denudation. In *Internat. Soc. Rock Mechanics Cong., 1st, Lisbon* (pp. 49–56).

Voight, B. (1966b). Residual stresses in rocks. In *Internat. Soc. Rock Mechanics Cong., 1st, Lisbon* (pp. 45–50). Bertrand: International Society for Rock Mechanics.

Voigtländer, A., & Krautblatter, M. (2017). Breaking rocks made easy: subcritical processes and tectonic predesign. In *Geophysical Research Abstracts* (Vol. 19, pp. EGU2017-16469). EGU General Assembly.

Voigtländer, A., Scandroglio, R., & Krautblatter, M. (2014). *Ermittlung geotechnischer Felsparameter des Kitzsteinhorner Kalkglimmerschiefers*. München.

Voigtländer, A., Leith, K., & Krautblatter, M. (2017a). Constraining the physics of subcritiacl

crack growth in Carrara Marble using neutron diffraction techniques. In *Geological Society of America Abstracts with Programs* (Vol. 49, pp. 212–11). The Geological Society of America. https://doi.org/10.1130/abs/2017AM-296203

Voigtländer, A., Leith, K., & Krautblatter, M. (2017b). Time to failure - progression of joints by subcritical crack growth and stress corrosion cracking in quartzite. In *Progressive rock failure conference, 5–9 June 2017* (pp. 96–100). Monte Verità, Switzerland: ISRM.

Voigtländer, A., Leith, K., & Krautblatter, M. (2018). Subcritical crack growth and progressive failure in Carrara marble under wet and dry conditions. *Journal of Geophysical Research: Solid Earth*, *123*, 3780–3798. https://doi.org/10.1029/2017JB014956

Wan, K.-T., Lathabai, S., & Lawn, B. R. (1990). Crack velocity functions and thresholds in brittle solids. *Journal of the European Ceramic Society*, *6*(4), 259–268. https://doi.org/https://doi.org/10.1016/0955-2219(90)90053-I

Watt, J. P., & Peselnick, L. (1980). Clarification of the Hashin-Shtrikman bounds on the effective elastic moduli of polycrystals with hexagonal, trigonal, and tetragonal symmetries. *Journal of Applied Physics*, *51*(3), 1525–1531. https://doi.org/10.1063/1.327804

Weinberger, R., Eyal, Y., & Mortimer, N. (2010). Formation of systematic joints in metamorphic rocks due to release of residual elastic strain energy, Otago Schist, New Zealand. *Journal of Structural Geology*, *32*(3), 288–305. https://doi.org/10.1016/j.jsg.2009.12.003

Weiss, T., Siegesmund, S., Kirchner, D., & Sippel, J. (2004). Insolation weathering and hygric dilatation: Two competitive factors in stone degradation. *Environmental Geology*, *46*(3–4), 402–413. https://doi.org/10.1007/s00254-004-1041-0

Whalley, W. B. (1974). The mechanics of high magnitude, low frequency rock failure and its importance in a mountainous area. *Geographical Papers Reading*, *27*, 1–48.

Whalley, W. B. (1987). Mechanisms, materials and classification in Geomorphology explanation. In M. J. Clark, K. J. Gregory, & A. M. Gurnell (Eds.), *Horizons in Physical Geography* (pp. 86–103). London: Palgrave. https://doi.org/https://doi.org/10.1007/978-1-349-18944-1_6

Whalley, W. B., Douglas, G. R., & McGreevy, J. P. (1982). Crack propagation and associated weathering in igneous rocks. *Zeitschrift Für Geomorphologie*, *26*(1), 33–54.

Wheeler, J. (2018). The effects of stress on reactions in the Earth: Sometimes rather mean, usually normal, always important. *Journal of Metamorphic Geology*, *36*(4), 439–461. https://doi.org/10.1111/jmg.12299

White, A. F., & Brantley, S. L. (2003). The effect of time on the weathering of silicate minerals: why do weathering rates differ in the laboratory and field? *Chemical Geology*, *202*(3–4), 479–506. https://doi.org/10.1016/j.chemgeo.2003.03.001

Wiederhorn, S. M., & Bolz, L. H. (1970). Stress corrosion and static fatigue of glass. *Journal of the American Ceramic Society*, *53*(10), 543–548. Retrieved from http://www.blackwell-synergy.com/doi/abs/10.1111/j.1151-2916.1970.tb15962.x

Winkler, E. M. (1975). *Stone: properties, durability in man's environment* (2nd ed.). New York: Springer.

Winkler, E. M. (1996). Properties of marble as building veneer. *International Journal of Rock Mechanics and Mining Sciences & Geomechanics Abstracts*, *33*(2), 215–218.

Withers, P. J. (2007). Residual stress and its role in failure. *Reports on Progress in Physics*, *70*(12), 2211–2264. https://doi.org/10.1088/0034-4885/70/12/R04

Withers, P. J. (2015). Fracture mechanics by three-dimensional crack-tip synchrotron X-ray microscopy. *Philosophical Transactions of the Royal Society of London. Series A*, *373*, 20130157. https://doi.org/10.1098/rsta.2013.0157

Withers, P. J., & Bhadeshia, H. K. D. H. (2001a). Residual stress. Part 1 – Measurement techniques. *Materials Science and Technology*, *17*, 355–365. https://doi.org/10.1179/026708301101509980

Withers, P. J., & Bhadeshia, H. K. D. H. (2001b). Residual stress. Part 2 – Nature and origins. *Materials Science and Technology*, *17*(4), 366–375. https://doi.org/10.1179/026708301101510087

Wolman, M. G., & Miller, J. P. (1960). Magnitude and frequency of forces in geomorphic processes. *The Journal of Geology*, *68*(1), 54–74.

Wong, L. N. Y., Maruvanchery, V., & Liu, G. (2016). Water effects on rock strength and stiffness degradation. *Acta Geotechnica*, *11*(4), 713–737. https://doi.org/10.1007/s11440-015-0407-7

Yatsu, E. (1966). *Rock control in Geomorphology*. Tokyo: Sozosha.

Yatsu, E. (1992). To make geomorphology more scientific. *Transactions Japanese Geomorphological Union*, *13*(2), 87–124.

Yerro, A., Pinyol, N. M., & Alonso, E. E. (2016). Internal progressive failure in deep-seated landslides. *Rock Mechanics and Rock Engineering*, *49*(6), 2317–2332. https://doi.org/10.1007/s00603-015-0888-6

Yu, F., & Hunt, A. G. (2017). Damköhler Number Input to Transport-Limited Chemical Weathering Calculations. *ACS Earth and Space Chemistry*, *1*(1), 30–38. https://doi.org/10.1021/acsearthspacechem.6b00007

Zang, A., & Berckhemer, H. (1989). Residual stress features in drill cores. *Geophysical Journal International*, *99*(3), 621–626. https://doi.org/10.1111/j.1365-246X.1989.tb02046.x

Zang, A., & Stephansson, O. (2010). *Stress field of earth's crust*. Berlin, Heidelberg, New York: Springer. https://doi.org/10.1007/978-1-4020-8444-7

Zang, A., Wagner, C. F., Christian, F., Stanchits, S., & Dresen, G. (2000). Fracture process zone in granite. *Journal of Geophysical Research*, *105*(B10), 23651–23661. Retrieved from http://onlinelibrary.wiley.com/doi/10.1029/2000JB900239/full

Zhang, D., Pathegama Gamage, R., Perera, M., Zhang, C., & Wanniarachchi, W. (2017). Influence of water saturation on the mechanical behaviour of low-permeability reservoir rocks. *Energies*, *10*(2), 236. https://doi.org/10.3390/en10020236

Zoback, M. Lou. (1992). First- and second-order patterns of stress in the lithosphere: The World Stress Map project. *Journal of Geophysical Research*, *97*(B8), 11703–11728.

Supplement 1 – Scientific Publication I

Supporting Information for Chapter 4.1

Subcritical crack growth and progressive failure in Carrara marble under wet and dry conditions

Anne Voigtländer, Kerry Leith and Michael Krautblatter

Introduction

This supporting information provides the supplementary figures and tables for the main article. We provide supplementary information on the crystallographic preferred orientation (CPO) of the used Carrara marble, a numerical model to define the dimension of the tested samples and additional details of the fracture path in the thin section of sample M4.

S1 Crystallographic preferred orientation measurements

To discern the influence of the marble rock fabric (foliations), especially (texture) from the microstructural behavior, three oriented slices of an untested Carrara Marble sample M0 where tested with the X-Ray goniometer from Panalytical at the Geoscience Center Göttingen. Three sections of ~ 8mm thickness have been cut from the top, the mid and bottom of an untested Carrara marble beam, grinded and polished. Pole figures of the crystallographic preferred orientations (texture) are calculated from the diffractions patterns acquired by the application of X-Rays and are further quantitatively analyzed. The quantitative texture analysis uses the inversion of the experimental two-dimensional pole figures to generate three dimensional orientation distribution functions (ODF) Resulting pole figures (**Figure S1**) are back calculated and display a sum of three measurement points each. Section position had no influence on texture, thus only the CPO of the first measured section are shown. Plastic deformation within single grains are not resolved as a bulk volume is measured. The crystallographic orientation is axial symmetrical to the c-axis (hkl (001) parallel to (006)), thus exhibits a near random distribution. The intensity of the texture is also minor (random = 1), and ranges between 1.18 and 1.41 (**Figure S1**). The near random crystallographic orientation indicates no geological inherited or induced directional (plastic) deformation, which would influence the microstructural behavior.

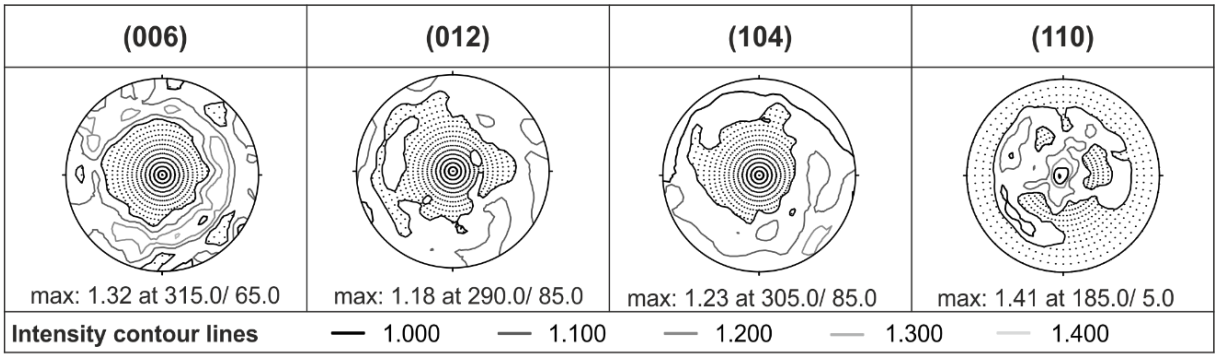

Figure 4.1. S1 Orientation distribution function (ODF) plots of the texture measurements of the top most slice of M0 of hkl (006), (102), (104) and (110) as an equal angle projection of the lower hemisphere. Maximum intensity, with a line spacing of 0.1, and orientations are indicated below the distribution figures.

S2 Numerical model of Carrara marble beams

In order to evaluate the proper dimensions of our samples with the induced stress field of the loading, as well as allowing tensile fractures to propagate without interfering with the compressive stress field, we set up a simple finite element method (FEM) model using RS2 v9 from Rocscience. In order to carefully evaluate the induced elastic stress field, and to some degree the potential for, and effect of brittle failure on the loaded and unloaded samples, we set up from an initial unloaded condition, followed by a stage with the beam hanging under its own weight in the loading frame, then a 55% load stage, 85% load stage. We apply a triangular graded mesh with mean element lengths of 5 mm for the majority of the beam, and 0.5 mm for the region local to the notch. We assume the tensile strength and Young's modulus in the inner zone, local to the notch tip, reduce below that of the outer zone as a result of subcritical crack growth, while the residual tensile strength is slightly below that of the peak in order to approximate the effect of strain localization at the tip of propagating micro-cracks.

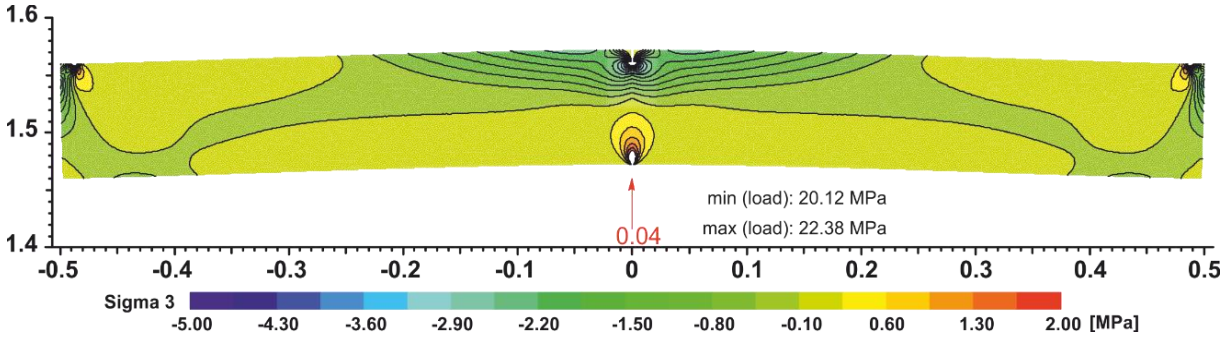

Figure 4.1.S2 FEM model of a 0.1 m thick beam with an applied load of 3.95 kN. The sigma 3 stress field is indicated during loading, where the expression of tensile stresses is negative and compression positive.

Table 4.1.S2 Results of numerical modelling stages of the large Carrara marble beam.

stage	external load	Young's modulus	Poisson's ratio	tensile strength		cohesion		friction angle	Unit weight
				peak	residual	peak	residual		
	kN/m²	***GPa***		***MPa***	***MPa***				***Kg/m²***
1	*0*	*30*	*0.21*	*50*	*10*	*100*	*100*	*35*	*0*
2	25.6	30	0.21	50	10	100	100	35	2650
3	39.5	30	0.21	50	10	100	100	35	2650

S3 Detailed fracture path of M4

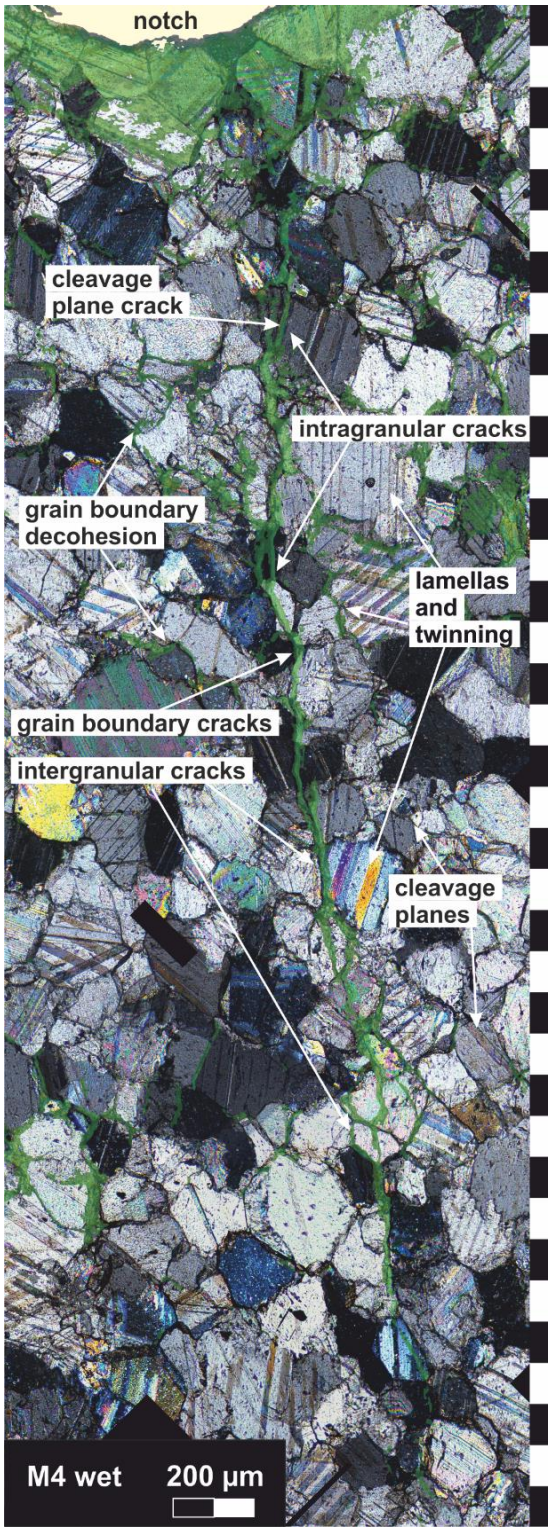

Figure 4.1.S3 Cross-polarized thin section close-up (1.3 x 3.7 mm) of the fracture below the saw-cut notch in sample M4. The fracture path predominantly follows grain boundaries but also dissects single grains partly following cleavage planes or lamella. Neon-green-colored persistent discontinuities are derived from the fluorescent dyed images.

Supplement 2 – Scientific Publication II

Supporting Information for Chapter 4.2

Constraining internal states in progressive rock failure of Carrara marble by measuring residual strains with neutron diffraction

Anne Voigtländer, Kerry Leith, Jens M. Walter and Micahel Krautblatter

Introduction

Complementary **Figure 4.2.S1** of the crystallographic preferred orientation (CPO) of the Carrara marble reference sample M0.

Complementary **Figures 4.2.S2** and **4.2.S3** of the neutron diffraction measurements of residual crystal lattice strains to characterize reference sample M0 in detail.

Supplementary Information 1 provides details on intragranular residual microstrains. We report the results of the peak shape metric full-width at half maximum (FWHM) of the intact reference sample M0 (**Figure 4.2.S4**) and the pretested samples M2, M4, and M5 (**Figure 4.2.S5, 4.2.S6)**. Due to the instrument specifications of SALSA on intergranular residual strains, the FWHM estimates have been viewed as subsidiary. Also, due to a lack of a true strain-free FWHM, an initial intracrystallite strain state could not be determined. We therefore reference the peak broadening or narrowing with respect to the mean FWHM of sample M0. Results are discussed in regard to their potential of the discussion line presented in the main article.

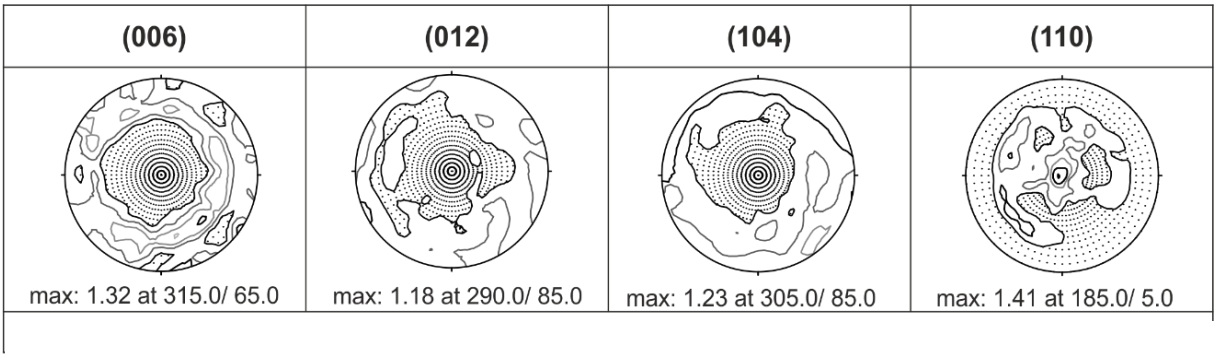

Figure 4.2.S1 Orientation distribution function (ODF) plots of the texture measurements of the top most slice of M0 of hkl (006), (102), (104) and (110) as an equal angle projection of the lower hemisphere. Maximum intensity, with a line spacing of 0.1, and orientations are indicated below the distribution figures.

To discern the influence of the marble rock fabric (foliations), especially (texture) from the microstructural behavior and possible distortions of the neutron diffraction patterns, three oriented slices of an untested Carrara marble sample M0 were tested with the X-Ray goniometer from Panalytical at the Geoscience Center Göttingen. Three sections of ~ 8mm thickness have been cut from the top, the mid and bottom of an untested Carrara marble beam, grinded and polished. Pole figures of the crystallographic preferred orientations (texture) are calculated from the diffraction patterns acquired by the application of X-Rays and are further quantitatively analyzed. The quantitative texture analysis uses the inversion of the experimental two-dimensional pole figures to generate three dimensional orientation distribution functions (ODF)

Resulting pole figures (**Figure 4.2.S1**) are back calculated and display a sum of three measurement points each. Section position had no influence on texture, thus only the CPO of the first measured section are shown. Plastic deformation within single grains are not resolved as a bulk volume is measured. The crystallographic orientation is axial symmetrical to the c-axis (hkl (001) parallel to (006)), thus exhibits a near random distribution. The intensity of the texture is minor, ranging between 1.18 and 1.41 (random = 1, **Figure 4.1.S1**). The near random crystallographic orientation indicates no geological inherited or induced directional (plastic) deformation, which would influence the microstructural behavior or the residual strain measurements.

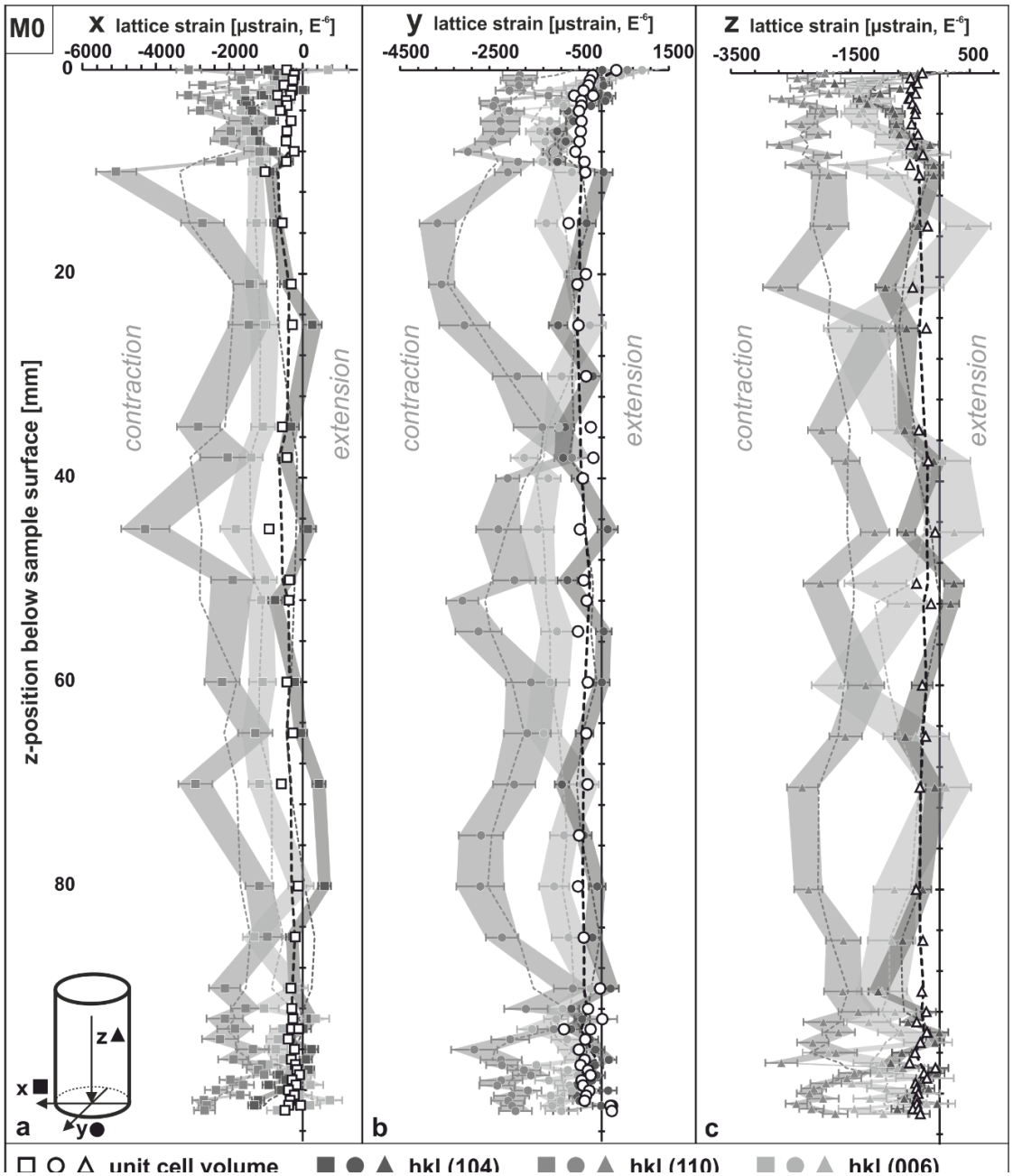

Figure S4.2.S2 Intergranular residual lattice strain state of sample M0 in x-, y- and z-direction along the vertical measured gradient. Note that the unit cell volume strain is more or less constant in all spatial directions (black symbols with a three point running average in dashed lines). The measured single crystal plane strains are given in grey, with their error bounds.

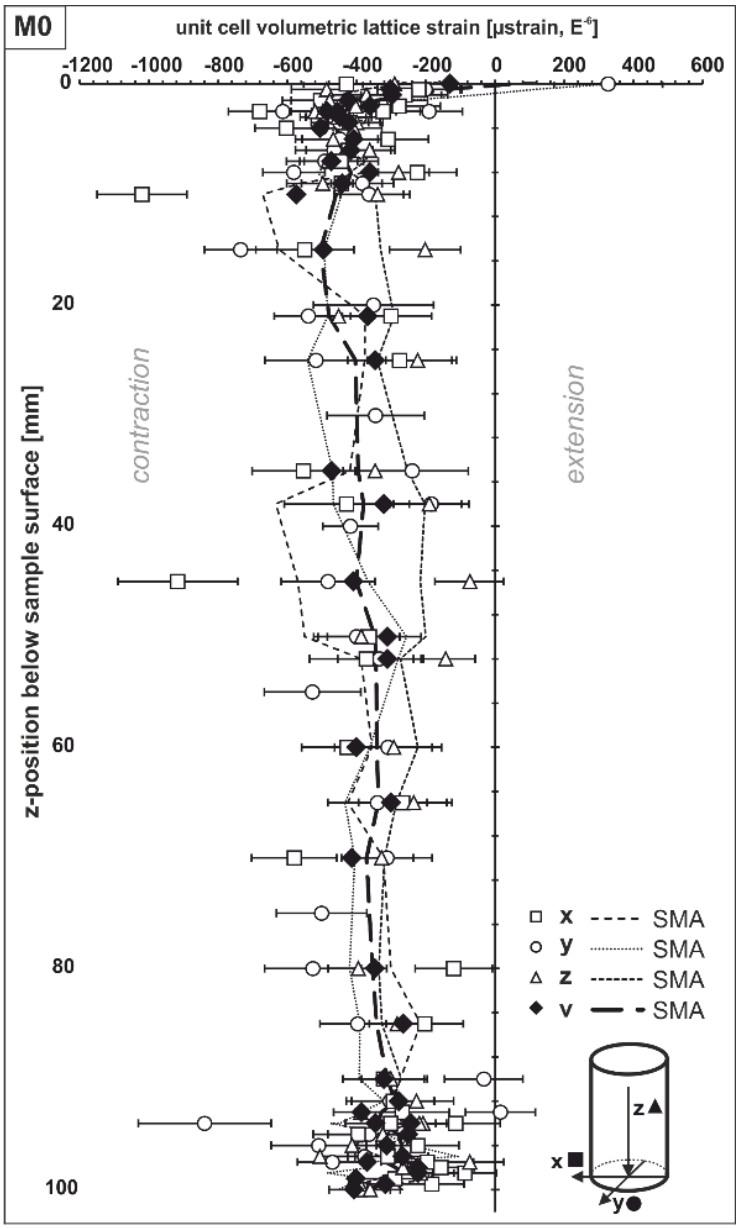

Figure 4.2.S3 Unit cell volumetric lattice strain state of sample M0 in x-, y- and z-direction along the vertical measured gradient in z. The volumetric residual strain given by v = $(\varepsilon_x + \varepsilon_y + \varepsilon_z)/3$, in the black full diamond symbol, shows contractional lattice strains throughout the measured vertical gradient. Three point running averages (SMA) in dashed lines.

Supplementary Information 1

Neutron diffraction measurements were conducted at the SALSA strain diffractometer at the Institute Laue-Langevin (ILL), Grenoble, France which is specified on the determination of the diffraction peak position (Pirling et al., 2006). Additional distortions of lattice planes, by plastic deformation within grains and crystallites can result in changes in the dispersion of the reflected neutrons. Within the diffraction spectra this affects the peak shape metric, e.g., the full-width at half maximum (FWHM). In reference to an undistorted sample, a deviatory broadening of the FWHM indicates an increase in the intracrystallite strains, while a narrowing indicates a relaxation of those strains (Noyan & Cohen, 1987; Withers & Bhadeshia, 2001a). This type of microstrain is termed intracrystallite or intragranular strain. As those metrics are

not primarily assessed and measurement errors are high, this data has been viewed as subsidiary. The general pattern of the intracrystallite strains can provide useful insights to plastic deformation. Due to the different causes of intergranular and intracrystallite residual strains, damage zones of the induced damage with predominant intergranular alterations can be delimited, and variance of the FWHMs could constrain the extent of plastic zones within the samples. It is a gradual distinction because intergranular and intracrystallite strains are derived from the same diffraction peaks, they influence each other, i.e., a peak width change is also a subsumed effect of the peak position and vice versa (Ungár, 1998).

Due to the lack of an undistorted reference sample we use the deviatory changes in the peak full-width at half maximum metric (FWHM) in reference to the mean FWHM of M0 as an indicator for intracystallite residual strains (**Figure 4.2.S3**). We compared the peak metric variation in pretested samples and report the deviatory changes for the FWHMs of crystallographic planes in $\{10\bar{1}4\}$ and in $\{1\bar{1}20\}$, which showed the lowest and greatest magnitude of deviation from the reference FWHM, respectively (**Figure 4.2.S4**).

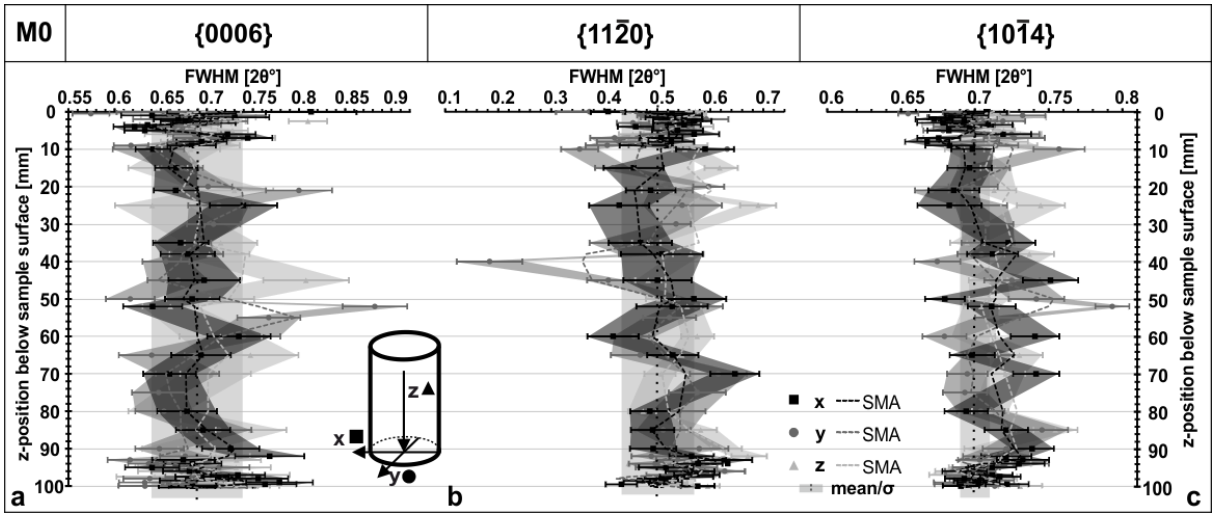

Figure 4.2.S3 Full-width at half maximum (FWHM) of M0 in crystallographic planes **a** {0006}, **b** $\{1\bar{1}20\}$ and **c** $\{10\bar{1}4\}$. Data points with error bars in the three spatial directions are indicated by different symbols and shading, the three point running average (SMA) in dashed lines. The overall mean is given as a vertical dotted line and the standard deviation in a grey block.

An exception of peak broadening in crystal planes $\{10\bar{1}4\}$, exceeding the bounds of the standard deviation of the reference in the x-direction, is observed in sample M4 at around 16 mm (in z), thus near the visible crack tip (**Figure 4.2.S4**). The coefficient of variation of FWHM in the measured crystal planes of the wet-tested samples, M2 and M4 is overall greater than the dry-tested sample M5 (**Figure 4.2.S4**). Deviatory FWHM of M5 is generally confined within the bounds of the standard deviation of the reference FWHM of M0, of the measured crystal planes, whereas in the wet samples this behavior is observed below the neutral axis (**Figure 4.2.S5**).

Deviatory peak broadening and narrowing of the FWHM in crystallographic planes {0006} and in $\{1\bar{1}20\}$ display opposing behavior in the x-direction, which experienced the highest deviatory stress during the pretest. For example, while a peak broadening in crystal planes {0006}, a narrowing in $\{1\bar{1}20\}$ is observed at the notch tip in sample M5 and M2 (in z,

Figure 4.2.S5 a-b, d-e). Similar for sample M4, where crystal planes {0006} show a narrowing in the first ~10 mm below the notch tip, and a broadening at a depth of ~16-26 mm, while a near opposite pattern is observed in $\{1\bar{1}20\}$ (**Figure 4.2.S5g-h**).

The vertical extent of the plastic zone exceeds the damage zone, delimited by the intergranular residual strains. Especially in the wet samples the vertical section within which strain broadening or narrowing is observed is very distinct. Intracrystalline deformation seems to be enhanced in the presence of water. The effect of the plastic deformation exceeding the damage zone and possible conditioning effect for progressive fracture propagation should be investigated further.

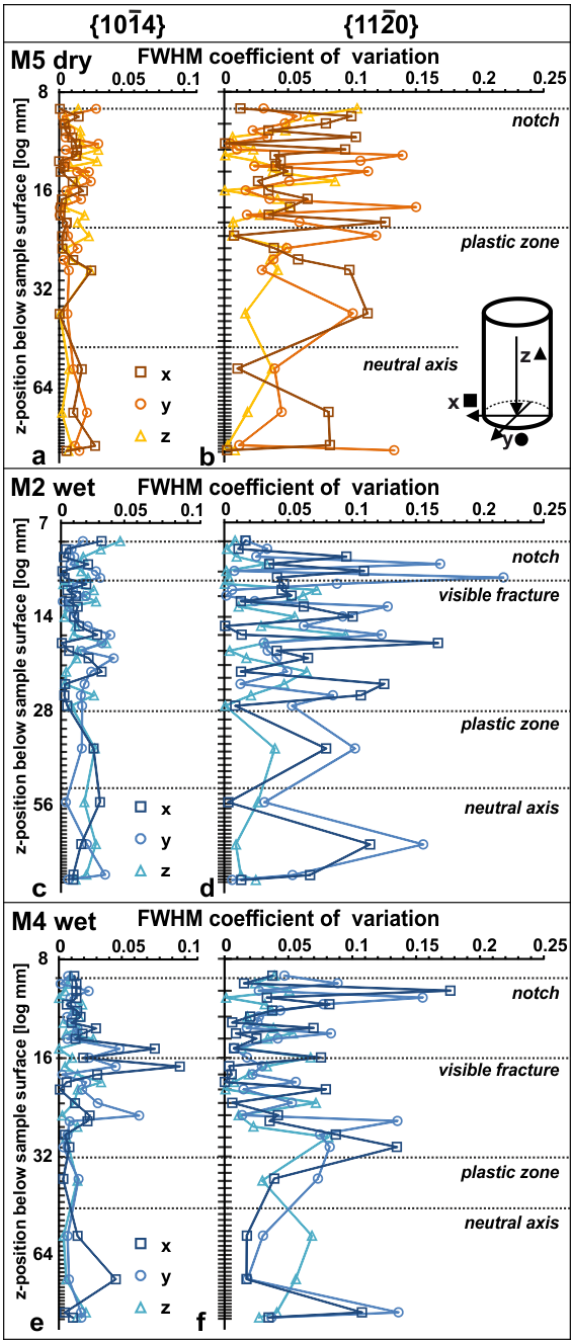

Figure 4.2.S4 Coefficient of variation of the FWHM in reference to mean FWHM of M0 of crystallographic planes {10$\bar{1}$4}, and {1$\bar{1}$20} of samples M5 (a-b), M2 (c-d) and M4 (e-f). The spatial directions are indicated by color and symbol. Notch and visible fracture extent are inferred from thin section images. The extent of the plastic zone is discussed in the text.

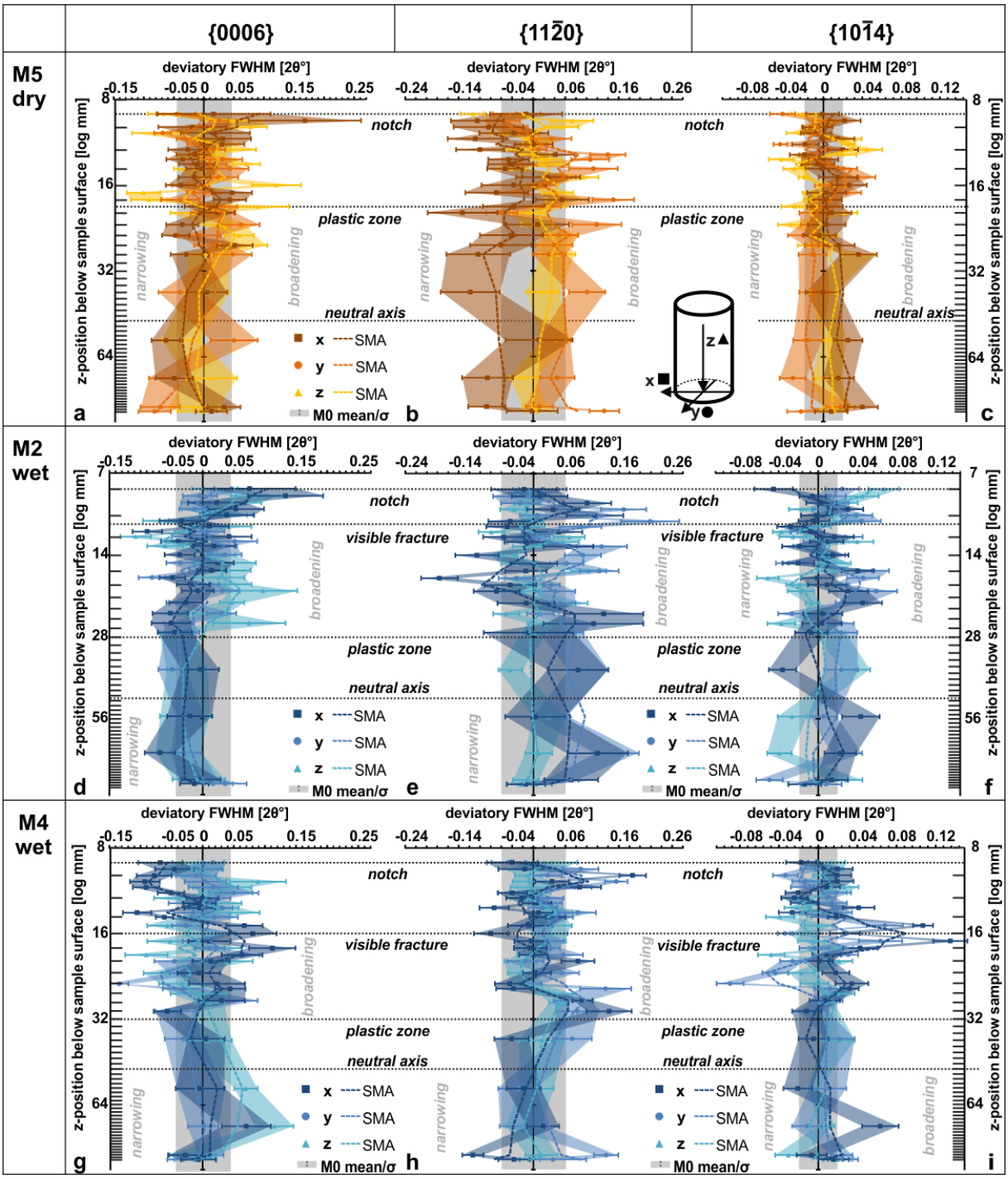

Figure 4.2.S4 Deviatory full-width at half maximum (FWHM) in reference to the mean FWHM of M0 of crystallographic planes {0006}, {11$\bar{2}$0}, and {10$\bar{1}$4} of samples M5 (**a-c**), M2 (**d-f**) and M4 (**g-i**). Deviatory peak broadening indicates an introduction, narrowing a relaxation of intracrystallite residual strains. The spatial direction is indicated by color and symbol. Deviations are given with their error bounds and a three-point running average in dashed lines (SMA). Note the vertical grey bound gives the standard deviation of FWHM of M0. Vertical extent (in z) of the notch and visible fracture are inferred from thin section images. The delimitation of the extent of the plastic zone is discussed in the text.

BREAKING ROCKS MADE EASY: subcritical processes and tectonic predesign

The simple material-form-process triangle framework of geomorphology.

Form changes either due to an increase in driving forces (A) or a decrease in resisting forces (B).

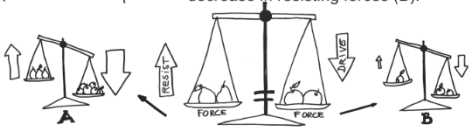

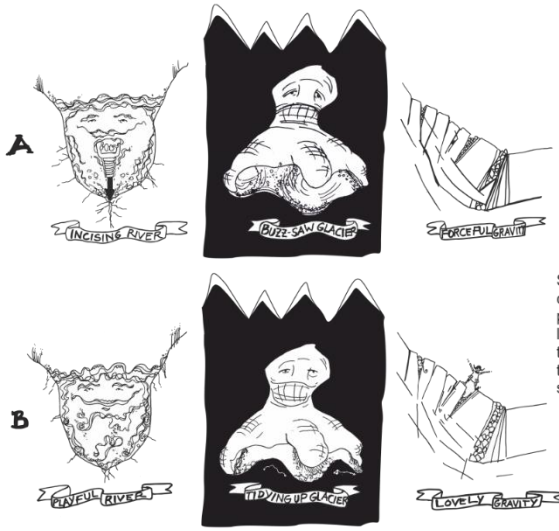

A (upper triplet): Persistent geomorphological imaginaries of the primacy of erosional processes, where rivers forcefully incise and glacier buzz-sawing their bed or gravity pushes rocks apart. Its exaggerated antipode in **B** (lower triplet), where rivers simply juggling sediments, glaciers clean up valleys and gravity provides a lovely place to be.

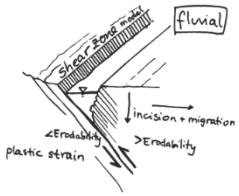

Rivers incise where erodability is lower which reinforces the plastic strain in a shear zone (after Roy et al., 2016)

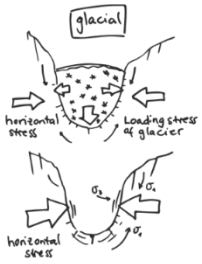

Stress fields with and without a valley glacier, where differential topographic stresses evolve which exceed the microfracture threshold (after Leith et al. 2014).

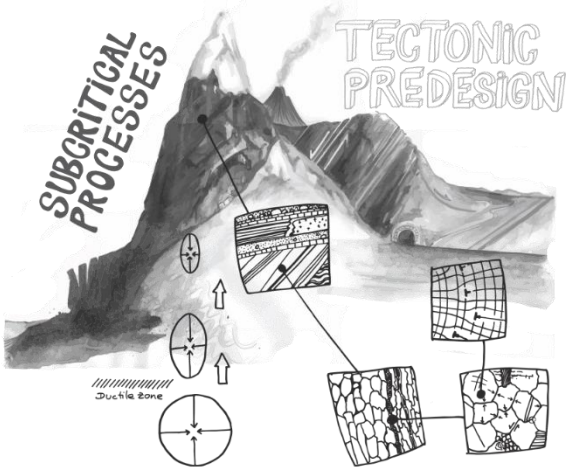

Subcritical processes and tectonic predesign both root in the same stress control perspective. Tectonic predesign provides a concept of the active and passive stress fields, which can provide the circumstances for subcritical stress levels to be sufficient for subcritical processes to fracture, erode and transport the material, which in turn influences the stress fields. The combination and their stress control also offer a conceptual bridging of spatial and temporal scales.

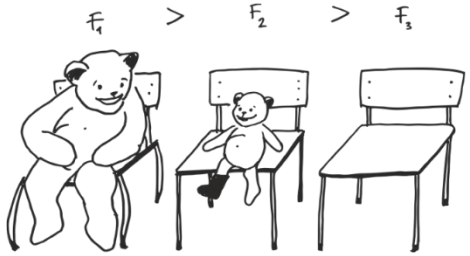

External (bear) forces (F) can alter the internal stress state of the form (chair). The internal stress state (forms or chairs are quite stable, strong and in static equilibrium by themselves) responds to these external forces with deformation or damage, but also poses a feedback control on the magnitude of force needed to move the chair, i.e. erode the form.

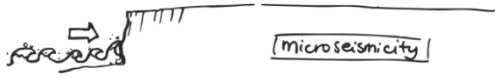

Does subcritical dynamic loading and unloading of cliffs by wave action, thus microseismicity decrease rock strength, at which rate and how?

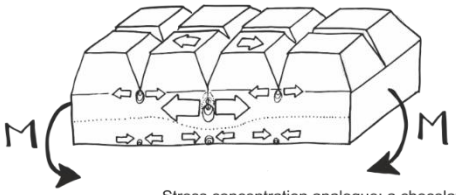

Stress concentration analogue: a chocolate bar. Due to bending force M, tensile stresses concentrate at the notch tips and eases the breaking apart. Luckily the chocolate or landscape is only locally affected and the remainder stays intact.

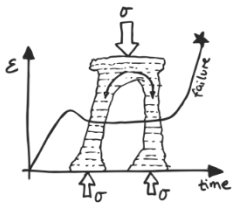

Time-dependent material response to stress. At some time stress might be strengthening or already weakening the material. Is there an optimal amount of stress for a certain form and how long does it persist?

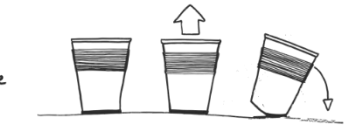

The efficiency of a force also depends on the mode and direction it is applied in, e.g. plucking, flaking or cracking. This mechanical control is readily imaged if your cup is glued to a table (by mistake). If you simply tried to pull it off, a major or critical force is needed. If you tear it off step by step, subcritical stress levels are sufficient and can even be reduced as the detached area or crack lengthens, to remove it.

Dividing becomes even easier if pre-existing flaws, interfaces and microcracks are constituent of the microstructure, just like perforations of paper have made daily routines easier.

Anisotropy and heterogeneities are ubiquitous material properties in geomaterials. They highly matter if referenced to applied stresses. To picture this, imagine a random movie scene where a car (mass, m = 1500 kg) speeds up (speed, v = 150 km/h) and bursts through a safety glass window of a bank (compressive strength ~ 900 MPa and flexural strength ~ 90 MPa). Speeding towards the window the car has an impulse (P = m*v), over an impact time of t ~ 0.5 s, and thus exerts a force (F = P/t) over an impact area (~1000 x 10 mm = 10000 mm2), thus a stress of 12.5 MPa on the glass. Compared to the strength of safety glass, the beetle car would look like a smashed bug on the windscreen. Parallel to the window, a scratch or nudge would be sufficient to shatter the glass.

Supplement Material to Voigtländer & Krautblatter (2018)